ACTA PROTOZOOLOGICA

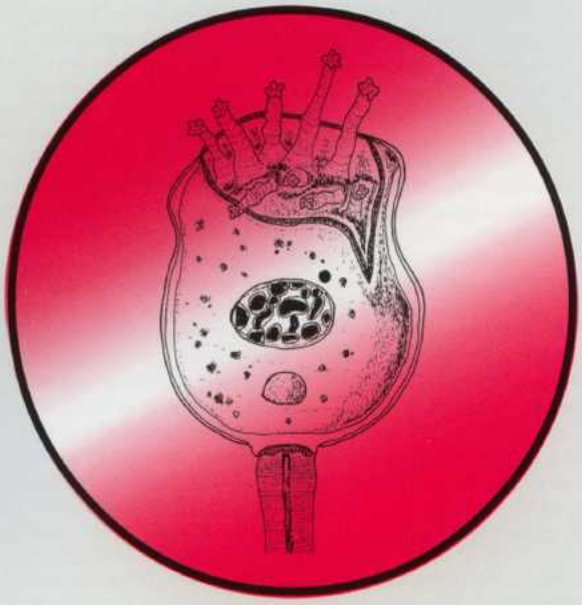

NENCKI INSTITUTE OF EXPERIMENTAL BIOLOGY
WARSAW, POLAND
2003
VOLUME 42 NUMBER 4
ISSN 0065-1583

Polish Academy of Sciences
Nencki Institute of Experimental Biology
and
Polish Society of Cell Biology

ACTA PROTOZOOLOGICA
International Journal on Protistology

ACTA PROTOZOOLOGICA appears quarterly.

The price (including Air Mail postage) of subscription to *Acta Protozoologica* at 2004 is: US $ 180.- by institutions and US $ 120.- by individual subscribers. Limited numbers of back volumes at reduced rate are available. Terms of payment: check, money order or payment to be made to the Nencki Institute of Experimental Biology account: 91 1060 0076 0000-4010 5000 1074 at BPH PBK S. A. III O/Warszawa, Poland. For the matters regarding *Acta Protozoologica*, contact Editor, Nencki Institute of Experimental Biology, ul. Pasteura 3, 02-093 Warszawa, Poland; Fax: (4822) 822 53 42; E-mail: jurek@ameba.nencki.gov.pl For more information see Web page **http://www.nencki.gov.pl/ap.htm**

Front cover: Fernandez-Leborans G., Hanamura Y. and Nagasaki K. (2002) A new suctorian, *Flectacineta isopodensis* (Protozoa: Ciliophora) epibiont on marine isopods from Hokkaido (Northern Japan). *Acta Protozool.* **41:** 79-84

This publication is supported by the State Committee for Scientific Research

Desktop processing: Justyna Osmulska, Information Technology Unit of the Nencki Institute
Printed at the MARBIS, ul. Poniatowskiego 1
05-070 Sulejówek, Poland

Acta Protozool. (2003) 42: 259 - 267

ACTA
PROTOZOOLOGICA

Nitric Oxide Production and Thermoregulation in *Paramecium caudatum*

Gary M. MALVIN[1], Nathan CECAVA[1] and Leif D. NELIN[1,2]

[1]Vascular Physiology Group, University of New Mexico Health Sciences Center Albuquerque, New Mexico; [2]Center for Developmental Pharmacology and Toxicology Columbus Children's Research Institute and Department of Pediatrics, The Ohio State University, Columbus, Ohio, USA

Summary. We investigated nitric oxide (NO) production in *Paramecium caudatum*, and the role of NO production in population growth in culture and thermoregulation. Nitrite (NO_2^-) concentration in media containing *P. caudatum* [6350 ± 390 (SD) paramecia/ml] was 2.37 ± 0.53 µM after 6 h, compared to 0.16 ± 0.06 µM in media alone ($p<0.005$), and the NO synthase (NOS) inhibitor, N^{ω}-nitro-L-arginine methylester (L-NAME), reduced [NO_2^-] to 0.81 ± 0.24 µM ($p<0.02$). Media containing *P. caudatum* produced [^{3}H]L-citrulline from [^{3}H]L-arginine, and the [^{3}H]L-citrulline production was inhibited by L-NAME. Addition of A23187, a calcium ionophore, to the media resulted in greater [NO_2^-] (1.49 ± 0.28 µM with no A23187, 2.51 ± 0.23 µM with 0.1 µM A23187 added, $p<0.05$). Western blot analysis revealed a 155 kDa protein that reacted with mouse NOS1 antibody. Paramecia concentration increased from 51 ± 9 per ml on day 0 to 943 ± 53 per ml on day 7. L-NAME decreased paramecia concentration at day 7 (0.1 mM, 720 ± 70 per ml; 1.0 mM, 761 ± 49 per ml; and 10 mM, 132 ± 32 per ml; $p<0.05$ compared to control for all 3 concentrations). In a thermal gradient, *P. caudatum* selected an environmental temperature (Ts) of 32.9 ± 0.3°C, addition of 10 mM L-NAME reduced Ts to 24.3 ± 0.3°C ($p<0.05$). These data suggest that *P. caudatum* produce NO *via* a calcium dependent NOS similar to mammalian NOS1, and inhibition of NO production reduced paramecia number in culture and decreased Ts.

Key words: calcium ionophore, environmental temperature, nitric oxide synthase, nitrite, selected temperature, thermal gradient.

Abbreviations: D-NAME - N^{ω}-nitro-D-arginine methylester, L-NAME - N^{ω}-nitro-L-arginine methylester, NO - nitric oxide, NO_2^- - nitrites, NOS - nitric oxide synthase, SNAP - S-nitroso-N-acetylpencillamine, Ts - selected temperature.

INTRODUCTION

Nitric oxide synthase (NOS) was first described in macrophages and endothelial cells isolated from mammals (Nathan 1992). NOS metabolizes L-arginine to NO and L-citrulline. Mammals have three isoforms of NOS; NOS1 and NOS3 are constitutively expressed and are calcium dependent, while NOS2 expression is up-regulated by stimuli including, inflammation, flow and environmental stress. NOS activity can be competitively inhibited using analogs of L-arginine such as N^{ω}-nitro-L-arginine methylester (L-NAME) (Nelin *et al.* 1996). Since its description in mammals, NOS has been described in invertebrates (Regulski and Tully 1995, Nighorn *et al.* 1998, Luckhart and Rosenberg 1999), and recently NOS has been described in Protists (Basu *et al.* 1997,

Address for correspondence: Leif D. Nelin, Section of Neonatology, 700 Children's Drive, Columbus, Ohio 43205, USA; Fax: +1 614 722 45 41; E-mail: nelinl@pediatrics.ohio-state.edu

Tao *et al.* 1997, Goldstein *et al.* 2000, Piacenza *et al.* 2001). Paramecia express several targets of NO, including guanylyl cyclase, potassium channels and voltage-gated calcium channels (Thiele and Schultz 1981, Preston *et al.* 1992, Prajer *et al.* 1997, Imada and Oosawa 1999, Linder *et al.* 1999). Although, NOS appears to be widespread among taxa, its function in Protists remains unclear. In this study we examined NO production and the possible physiologic effects of its inhibition in *P. caudatum*.

We first assessed whether *P. caudatum* produce NO. NO is highly reactive and therefore short-lived in oxygenated media (Nathan 1992, Nelin *et al.* 1996). Therefore, we measured nitrite (NO_2^-) concentration, the stable end product of NO oxidation, in the media after a 6 h incubation period. To further confirm that the NO_2^- was due to NOS activity we also measured the conversion of [^{3}H]L-arginine to [^{3}H]L-citrulline. The effects of L-NAME and the calcium ionophore A23187 on [NO_2^-] were also determined.

Thermoregulation is a basic physiologic process that is widespread among taxa (Wood and Malvin 1992). Although, paramecia have only limited internal means to thermoregulate, they and other ectotherms actively select an environmental temperature (Ts) that best supports their physiological processes (Malvin and Wood 1992, Malvin *et al.* 1994, Malvin 1998). Ectotherms can thermoregulate with considerable precision (Vaughn *et al.* 1974, Wood and Malvin 1992). Adaptive changes in thermoregulatory "set-point" in ectotherms include response to infection and hypoxia. For example, in a thermal gradient, infection increases Ts (Kluger 1991), and hypoxia decreases Ts (Malvin and Wood 1992, Malvin *et al.* 1994). The increase in Ts in response to infection aids in immunological function and survival (Kluger *et al.* 1975); while the decrease in Ts in response to hypoxia decreases metabolic needs and improves survival (Malvin and Wood 1992, Malvin *et al.* 1994). Thermoregulation in *P. caudatum* was first described by Mendelssohn (1895) who demonstrated that *P. caudatum* accumulate around their Ts in a thermal gradient. Jennings (1906) demonstrated that *P. caudatum* actively avoided temperatures above and below their Ts. In a thermal gradient, it has been demonstrated that paramecia change swimming direction more frequently when moving away from Ts than when moving toward Ts (Nakaoka and Oosawa 1977). The cellular mechanisms responsible for the changes in swimming direction, or avoiding reactions, have been found to involve membrane depolarization leading to activation of voltage-gated Ca^{2+} channels (Hennessey *et al.* 1983, Imada and Oosawa 1999). The precise mechanisms leading to this thermoregulatory response in *P. caudatum* remains unknown (Malvin 1998). Since temperature selection in *P. caudatum* involves ciliary motion, and ciliary motion involves activation of guanylate cyclase and calcium channels (Erxleben *et al.*1997, Schultz *et al.* 1997, Malvin 1998), and in mammalian cells, NO activates soluble guanylate cyclase and calcium channels (Clementi 1998), we hypothesized that *P. caudatum* produces NO, which is involved in the thermoregulatory responses of *P. caudatum*. To determine the role of NO production in thermoregulation, the effect of L-NAME, and its non-active stereoisomer D-NAME, and the NO donor S-nitroso-N-acetylpencillamine (SNAP) on selected temperature (Ts) were studied in *P. caudatum* in a thermal gradient.

MATERIALS AND METHODS

Organisms. *Paramecium caudatum* (Carolina Biological Supply, Burlington, NC) were cultured as described previously (Malvin and Wood 1992, Malvin *et al.* 1994, Malvin 1998). Briefly, *P. caudatum* were cultured at 19-21°C in cerophyl media (Sigma Chemicals, St Louis, MO) inoculated with *Enterobacter aerogenes*. *P. caudatum* in mid-log phase growth were isolated by filtration (5 µm pore size) and then centrifuged at 100 *g* for 10 min, and washed three times in fresh cerophyl media before experimentation.

Nitrite measurement. The samples of medium were assayed for NO_2^- using a chemiluminescence analyzer (Sievers Instruments, Boulder, CO) as previously described (Nelin *et al.* 2001). The samples were injected into a reaction chamber containing NaI in 1N acetic acid through which a steady stream of N_2 gas flowed. The NaI mixture reduced NO_2^- to NO and the stream of N_2 gas carried the NO gas into the chemiluminescence analyzer. $NaNO_2$ (Sigma Chemicals, St Louis, MO) was used for a standard curve.

Production of [^{3}H]L-citrulline. To determine if the nitrites measured above represented NO produced from NOS, we measured the production of [^{3}H]L-citrulline from [^{3}H]L-arginine in similar experimental conditions. In other words, we did not strictly measure NOS activity in these paramecia, but rather measured the appearance in the medium of the NO co-product, L-citrulline to further demonstrate that *P caudatum* produce NO *via* NOS. Paramecia were concentrated to ~6500/ml in a final volume of fresh cerophyl medium of 25 ml in a 50 ml test tube. Then L-[2,3,4,5-^{3}H]arginine monohydrochloride (25 µCi; specific activity 59 Ci/mmol; Amersham Life Sciences, Arlington Heights, IL) was added to the medium. After 1 h, 3 ml of cell suspension was removed and centrifuged at 500 *g* for 5 min. Then 2 ml of the supernatant was passed over a Dowex

AG50W-X8 (Na^+ form) column. [^{3}H]L-citrulline was eluted with 2 ml of distilled water. The radioactivity was measured using a liquid scintillation counter.

Western blots. Basu *et al.* (1997) and Goldstein *et al.* (2000) found that *Leishmania donovani* and *Trypanosoma cruzi*, respectively, express a protein that cross-reacts with mammalian NOS1 on Western blots. Therefore, Western blots were done on *P caudatum* protein as previously described (Nelin *et al*. 2001). Paramecia were concentrated to ~15000/ml by filtration and centrifugation, and then centrifuged at 1500 *g* for 5 min at room temperature. The pellet containing the paramecia was then resuspended in 2 ml of sonication buffer (pH 7.5) containing 0.32 M sucrose, 10 mM Tris HCl, 1 mM EDTA, 1 mM dithiothreitol, 0.01 mg/ml aprotinin, 0.01 mg/ml leupeptin, 0.01 mg/ml soybean trypsin inhibitor and 0.1 mM phenylmethylsulfonyl fluoride (PMSF). The paramecia were then sonicated for 10 s. The paramecia protein extracts were centrifuged at 1500 *g* at 4°C for 10 min to remove cellular debris. The protein was resolved by sodium dodecyl sulfate-polyacrylamide gel electrophoresis with 10% acrylamide. In addition to samples, each gel included molecular weight standards (Bio-Rad) and purified NOS1, NOS2 and NOS3 (Transduction Laboratories) standards. The separated proteins were transferred to PVDF membranes and stained with Coomassie brilliant blue to confirm equal protein loading in all lanes. Membranes were blocked overnight with 5% nonfat milk in 20 mM Tris-HCl, 50 mM NaCl (pH 7.5) buffer. The blot was incubated for 4 h with a mouse monoclonal antibody specific for NOS1 (1:1500), NOS2 (1:1000) or NOS3 (1:2500) (Transduction Laboratories) in TBS with 0.02% NaN_3. Immunochemical labeling was achieved by incubation for 2 h with biotinylated goat anti-mouse IgG (1:5000) (Bio-Rad) followed by chemiluminescence labeling (Amersham ECL detection assay). NOS1, NOS2 or NOS3 protein bands were detected by exposure to chemiluminescence-sensitive film. Protein concentrations of samples were determined by the Bradford method.

***Paramecium caudatum* population growth in culture.** *P. caudatum* were washed and placed in fresh Erlenmeyer flasks containing cerophyl medium. Then the number of paramecia per ml was determined by counting the number of paramecia in 20, 50-µl aliquots of media treated with 20-µl of 1 mM NiCl under a stereo microscope. NiCl inhibited ciliary motion, facilitating cell counting. Paramecia were counted daily for seven days.

***Paramecium caudatum* temperature selection (Ts).** Ts was determined as previously described (Malvin and Wood 1992, Malvin *et al.* 1994, Malvin 1998). Briefly, *P. caudatum* were washed and resuspended in cerophyl medium at a concentration of 100 per ml. One ml of the suspension was placed in a plexiglass aquatic thermal gradient (80 mm x 4 mm x 2 mm). The thermal gradient was cooled at one end by a copper tube beneath the gradient carrying chilled polyethylene glycol, and was warmed using heating tape at the other end. Sixteen thermal couples were placed 5 mm apart along the gradient for measuring temperature. A microscope was positioned above the gradient to visualize the paramecia in the gradient, and the magnified images were recorded by video microscopy. One hour after the paramecia were added to the thermal gradient, the distribution of Ts values was determined by video recording for 10 s at each of the 16 gradient positions containing a thermocouple. From the tapes the number of paramecia at each location was determined. Thermocouple temperatures were recorded immediately before videotaping. The temperature at each thermocouple is shown in Fig. 1.

Experimental protocols

Nitric oxide production. To determine if paramecia produce NO, *P. caudatum* were isolated as described above and concentrated (6350 ± 390 per ml). In the first set of experiments, the final volume of medium was 4 ml. Paramecia were incubated for 6 h in either cerophyl medium or cerophyl medium with 1 mM L-NAME. Cerophyl medium without paramecia, and cerophyl medium without paramecia but with 1 mM L-NAME were also incubated at room temperature for 6 h. 400-µl of cell suspension was then removed and centrifuged at 500 *g* for 5 min to remove paramecia, and the supernatant was assayed for NO_2^- as described above. In a second set of experiments, the final volume of medium was 25 ml. Paramecia were incubated at room temperature in either cerophyl medium or cerophyl medium containing 1 mM L-NAME. Cerophyl medium without paramecia was also incubated at room temperature. After 1 h 3 ml of the cell suspension was removed and processed for [^{3}H]L-citrulline measurement as described above. In a third set of experiments, to determine the calcium sensitivity of paramecium NO production, cells were incubated for 6 h in cerophyl medium or cerophyl medium with either 0.01 µM A23187 (Sigma Chemicals, St Louis, MO) or 0.1 µM A23187. Then 400 µl of the cell suspensions were removed and centrifuged at 500 *g* for 5 min to remove paramecia, and the supernatant was assayed for NO_2^-.

To determine if *P. caudatum* contains a protein that cross-reacts with mammalian NOS1 antibody Western blot analysis was done. *P. caudatum* were isolated and concentrated to ~15000 per ml in a final cell suspension volume of 8 ml. Four cultures of *P. caudatum* were then processed as described above for Western blot analysis for NOS1, NOS2 or NOS3.

NO production and *P. caudatum* population growth in culture. To determine the effect of blocking NO production on population growth in culture, *P. caudatum* were isolated as described above and placed in fresh cerophyl medium [50 ± 9 (SD) paramecia per ml]. The paramecia concentration was determined daily for 7 days as described above in cerophyl medium, cerophyl medium with 0.1, 1.0 or 10 mM L-NAME, or in cerophyl medium with 0.1, 1.0 or 10 mM D-NAME.

NO and selected temperature in *P. caudatum*. Finally, to determine the effect of blocking NO production on Ts, Ts was determined for paramecia in cerophyl medium (control), cerophyl medium with either 1 or 10 mM L-NAME, or in cerophyl medium with either 1 or 10 mM D-NAME. In addition, to determine if the L-NAME effect was due to inhibition of NO production, Ts was determined for paramecia in cerophyl medium (control), cerophyl medium with 10 mM L-NAME and either 0, 1, 10 or 100 µM of the NO donor S-nitroso-N-acetylpencillamine (SNAP). Finally, to determine the effect of SNAP on Ts, Ts was determined for paramecia in cerophyl medium (control), or cerophyl medium with 1, 10 or 100 µM SNAP added. In our laboratory, the control Ts varied ~10% depending on the conditions, i.e. the temperature in the laboratory, the time of season, etc. Therefore in the studies examining Ts in different experimental conditions, each control and experimental condition was carried out in random order and on the same day.

Statistics. Data are shown as mean ± SE unless otherwise specified. Groups were compared using one-way analysis of variance (ANOVA). Differences between groups were identified using a Newman-Keuls post-hoc test. A p-value of <0.05 was used to determine statistical significance.

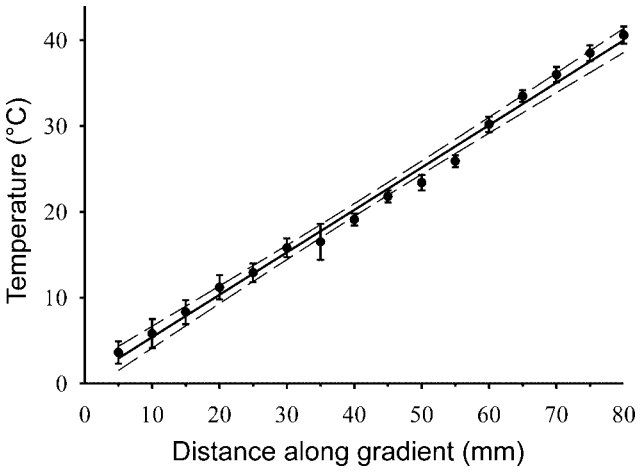

Fig. 1. Temperature range of aquatic thermal gradient. The temperatures (°C) at each of the 16 thermocouples along the 80 mm length of the aquatic thermal gradient (mean ± SD). The solid line is the linear regression fit of the data, and the dashed line is the 95% confidence intervals, $y = 0.49x + 0.44$, $r^2 = 0.99$.

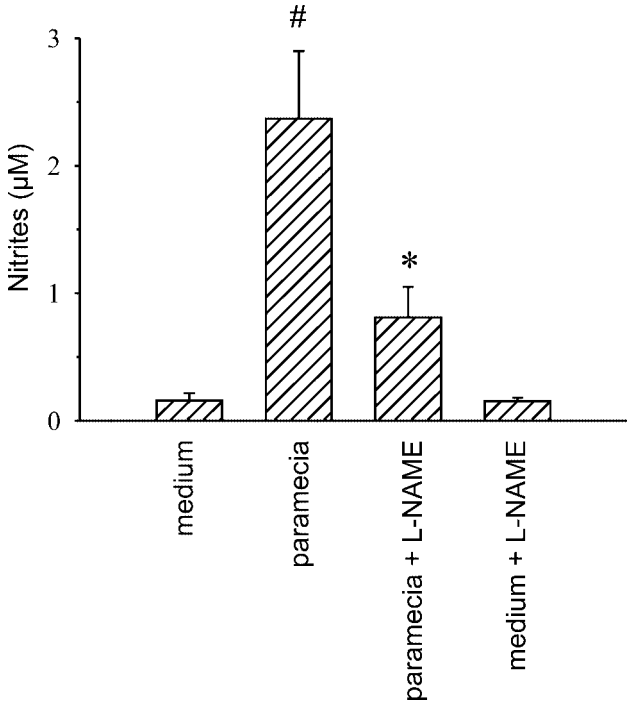

Fig. 2. Paramecia and production of nitrites. Paramecia produced NO as measured by nitrite concentration [NO_2^-] in the medium after a 6 h incubation, and NO production was inhibited by L-NAME. The first bar is cerophyl medium without paramecia (n = 6), the second bar is cerophyl medium with ~6500 paramecia/ml (n = 6), the third bar is cerophyl medium with paramecia (~6500 paramecia/ml) and 1 mM L-NAME added (n = 6) and the fourth bar is cerophyl medium without paramecia with 1 mM L-NAME added (n = 6). Note that L-NAME had no effect on [NO_2^-] in the medium. # signifies paramecium different from medium, $p<0.005$. * signifies paramecium + L-NAME different from both paramecium and medium, $p<0.05$.

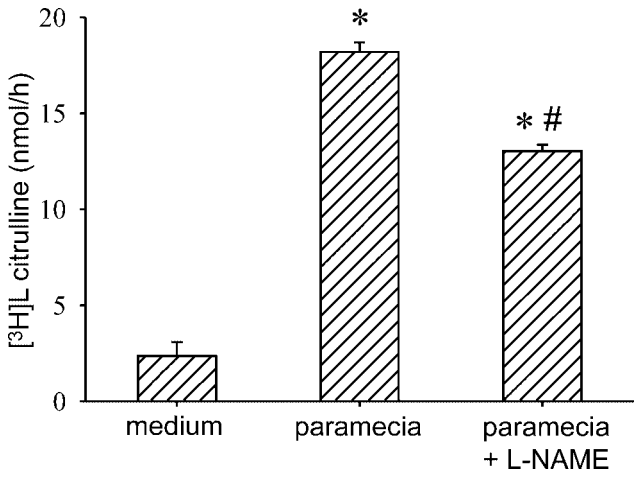

Fig. 3. Paramecia and L-citrulline production. Paramecia produced NO as measured by [^{3}H]L-citrulline production from [^{3}H]L-arginine, and the production of [^{3}H]L-citrulline was inhibited by L-NAME. [^{3}H]L-citrulline production 1 h after adding [^{3}H]L-arginine to 25 ml of cerophyl medium containing ~6500 paramecia/ml. The first bar is cerophyl medium without paramecia (n = 4), the second bar is cerophyl medium with ~6500 paramecia/ml (n = 4), and the third bar is cerophyl medium with paramecia (~6500 paramecia/ml) and 1 mM L-NAME added (n = 4). * different from medium, $p<0.001$. # paramecia + L-NAME different from paramecia, $p<0.005$.

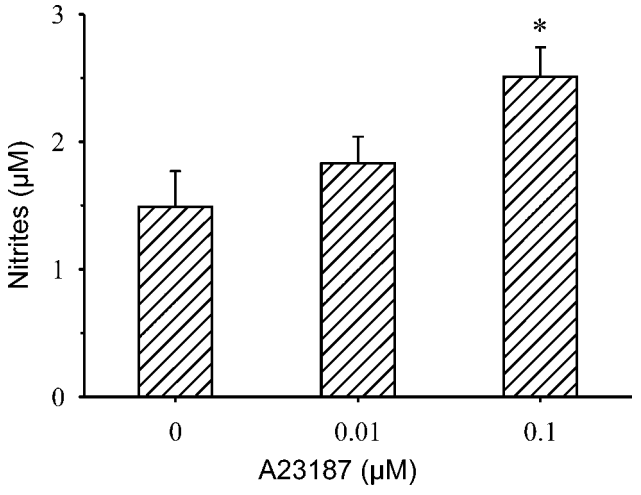

Fig. 4. Paramecia NO production was calcium sensitive. The bars are the [NO_2^-] after a 6 h incubation in cerophyl medium with ~6500 paramecia/ml containing either 0 (n = 6), 0.01 (n = 8) or 0.10 (n = 8) µM A23187. * signifies 0.10 µM different from both 0 µM and 0.01 µM, $p<0.05$.

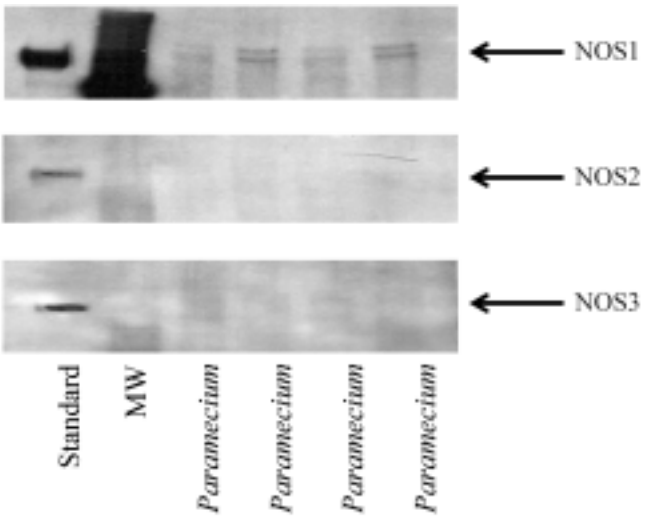

Fig. 5. Paramecia protein cross-reacts with mammalian NOS1. The top blot demonstrates that *P. caudatum* had a protein that cross-reacted with mammalian NOS1 antibody, but not mammalian NOS2 (middle blot) or NOS3 (bottom blot) antibodies. The first lane in each blot is the standard (NOS1, NOS2 or NOS3, respectively), the second lane is the molecular weight (MW) marker shown in the NOS1 blot, and the next 4 lanes in all three blots are paramecia protein extract.

RESULTS

Nitric oxide production. Nitrite concentration in medium containing paramecia was much higher than in medium alone (Fig. 2). This demonstrates that *P. caudatum* produced the majority of the NO_2^- in the medium. The mean medium [NO_2^-] concentration of 2.37 µM suggests that a single paramecium produces NO at ~60 femtomoles per h. L-NAME (1 mM) reduced mean medium NO_2^- concentration, although the medium [NO_2^-] was still greater than in medium without paramecia, and L-NAME had no effect on medium [NO_2^-] since medium + L-NAME was not different from medium alone (Fig. 2). [^{3}H]L-citrulline production in medium containing paramecia was much higher than in medium alone (Fig. 3). L-NAME (1 mM) reduced mean medium [^{3}H]L-citrulline production, although the medium [^{3}H]L-citrulline production was still greater than in medium without paramecia (Fig. 3).The mean medium [^{3}H]L-citrulline production of 18.20 nmol/h suggests that a single paramecium produces NO at ~120 femtomoles per h. The appearance of [^{3}H]L-citrulline in medium alone without added paramecia, may represent [^{3}H]L-arg that passed through the column as a function of the L-arg binding efficiency of the column. The binding efficiency of columns in our laboratory are ~95%. Thus, both methods, NO_2^- and [^{3}H]L-citrulline, give good agreement for NO production rates in paramecium, and the fact that measurement of 2 different products of NOS by 2 different methods resulted in similar results demonstrates that *P. caudatum* produces NO from NOS. Furthermore, these results demonstrate the utility of the measurement of medium NO_2^- concentration as a marker of NO production, and the ability of L-NAME to inhibit NO production by *P. caudatum*.

Nitric oxide production by *P. caudatum* was calcium sensitive (Fig. 4). Addition of the calcium ionophore, A23187 significantly increased medium [NO_2^-] by *P. caudatum* at the highest dose tested (0.1 µM A23187). Furthermore, *P. caudatum* contain a protein that cross-reacts with mammalian NOS1 on Western blotting, but not with mammalian NOS2 or NOS3 (Fig. 5).

NO production and *P. caudatum* population growth in culture. Figure 6A is the mean 7 day growth curve for *P. caudatum* in cerophyl medium in our laboratory. The concentration of paramecia per ml increased from 51 ± 9 to 943 ± 53 in seven days. The majority of the increase in paramecia number occurred between days 2 and 5. Figure 6B is the mean 7 day growth curve for paramecia in cerophyl medium with 0.1 mM L-NAME or D-NAME added, Fig. 6C is the mean 7 day growth curve for paramecia in cerophyl medium with 1.0 mM L-NAME or D-NAME added, and Fig. 6D is the mean 7 day growth curve for paramecia in cerophyl medium with 10 mM L-NAME or D-NAME added. Paramecia concentrations were not different between L-NAME and D-NAME at the same concentration on days 1 through 5 (Fig. 6). However, on day 7 L-NAME treated cultures had fewer paramecia than did D-NAME treated cultures (Fig. 6). The 10 mM concentration of D-NAME had a small effect on paramecia number on day 7, however the effect of 10 mM L-NAME was much greater than that of D-NAME on paramecia number (Fig. 6D).

NO and selected temperature in *P. caudatum*. The addition of 1 mM of either L-NAME or D-NAME had no significant effect on Ts (Fig. 7A). However, the addition of 10 mM L-NAME to the medium reduced Ts (Fig. 7A). The addition of 10 mM D-NAME to the medium also reduced Ts. However, the Ts of the 10 mM D-NAME treated *P. caudatum* was greater than Ts of the 10 mM L-NAME treated paramecia (Fig. 7A). When the NO donor, SNAP, was added to the medium containing 10 mM L-NAME there was a dose-dependent increase in Ts, although the Ts at 100 µM SNAP remained less than the Ts without added L-NAME and

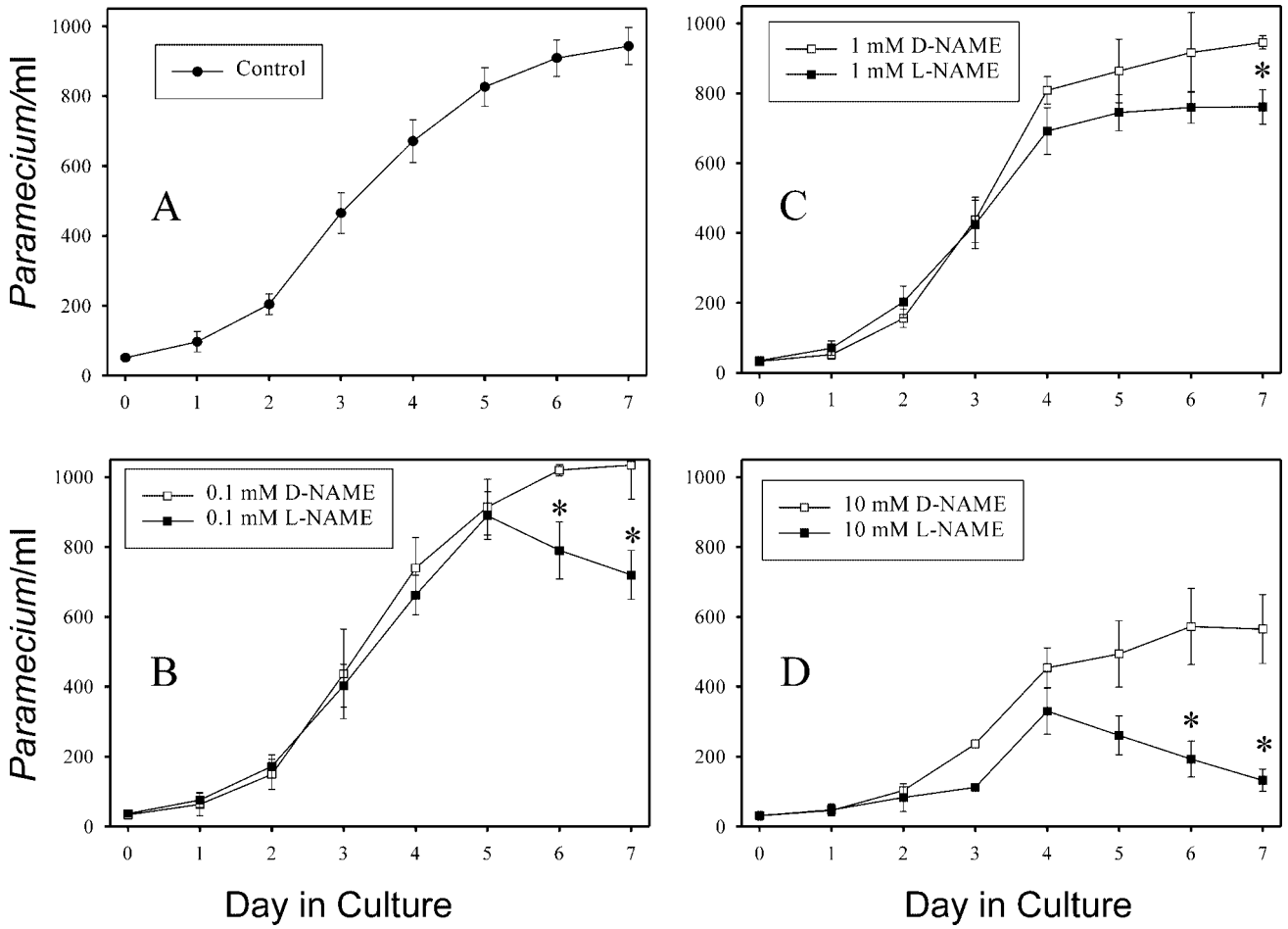

Fig. 6. L-NAME decreased the number of paramecia in culture. Inhibiting NO production with L-NAME resulted in a dose-dependent decrease in number of paramecia in culture. Panel 6A is the paramecia concentration (per ml) during the 7 day culture period (n = 11). **Panel 6B** is the paramecia concentration during the 7 day culture period with either 0.1 mM L-NAME (black squares; n = 6) or D-NAME (opened squares; n = 5) added to the medium. **Panel 6C** is the paramecia concentration during the 7 day culture period with either 1 mM L-NAME (black squares; n = 6) or D-NAME (opened squares; n = 5) added to the medium. **Panel 6D** is the paramecia concentration during the 7 day culture period with either 10 mM L-NAME (black squares; n = 4) or D-NAME (opened squares; n = 4) added to the medium. * signifies L-NAME different from D-NAME, $p<0.05$.

SNAP (Fig. 7B). Interestingly, the addition of SNAP alone to cerophyl medium resulted in a small reduction in Ts, which did not appear to be dose-dependent (Fig. 7C).

DISCUSSION

The main findings of this study were that: (1) *P. caudatum* produced NO, and the NO production was inhibited by L-NAME, (2) inhibiting NO production reduced the number of paramecia after 7 days of culture, and (3) inhibiting NO production altered thermoregulation, as evidenced by a reduction in selected temperature by *P. caudatum*. These data support our hypothesis and demonstrate for the first time that *P. caudatum* produce NO, and that this NO production is physiologically important to *P. caudatum*.

Paramecium caudatum NO production was inhibited by the L-arginine analogue, L-NAME, and was sensitive to the calcium ionophore, A23187. This suggests that *P. caudatum* produced NO from L-arginine by a calcium sensitive NO synthase. A role for L-arginine in NO production is confirmed in this study by the ability of *P. caudatum* to produced [^{3}H]L-citrulline from [^{3}H]L-arginine, by an L-NAME inhibitable process. Recently, similar findings have been described in *Trypanosoma cruzi* (Piacenza 2001) and *Dictyostelium discoideum* (Tao 1997). Thus, our results are consistent

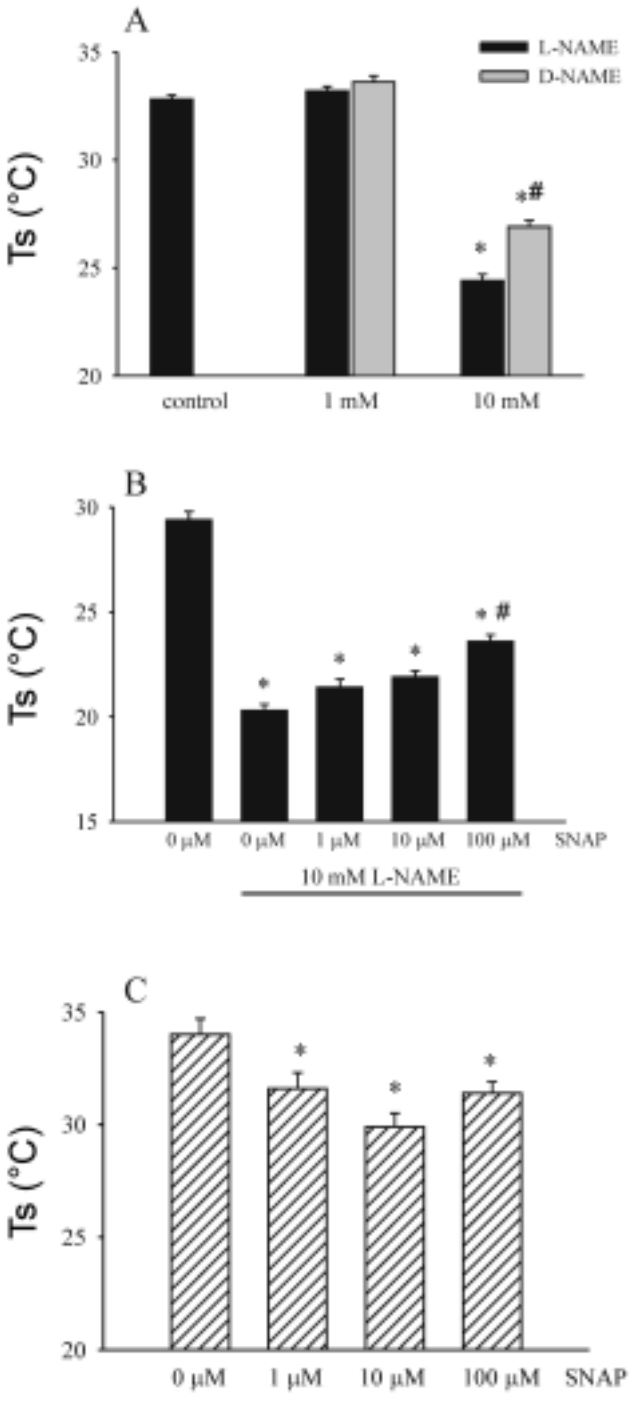

Fig. 7. Panel A. L-NAME reduced Ts. Inhibiting NO production with L-NAME resulted in a reduction in the selected temperature (Ts). The first bar is the Ts for paramecia in cerophyl medium (control; n = 4), the second set of bars is the Ts for paramecia in cerophyl medium with either 1 mM L-NAME (black bar; n = 6) or D-NAME (gray bar; n = 3) added, and the third set of bars is the Ts for paramecia in cerophyl medium with either 10 mM L-NAME (black bar; n = 5) or D-NAME (gray bar; n = 6) added. * signifies different from control, $p<0.01$. # signifies different from 10 mM L-NAME, $p<0.05$. **Panel B.** SNAP attenuated the L-NAME-induced reduction in Ts. The addition of the NO donor, SNAP, to cerophyl medium containing 10 mM L-NAME resulted in an increase in Ts. The first bar is the Ts for paramecia in cerophyl medium (0 µM; n = 5), the next four bars are the Ts for paramecia in cerophyl medium with 10 mM L-NAME and 0 (n = 5), 1 (n = 5), 10 (n = 5) or 100 (n = 5) µM SNAP added, respectively. * signifies different from control, $p<0.01$. # signifies different from previous SNAP concentration, $p<0.05$. **Panel C.** SNAP reduced Ts. The addition of SNAP alone to cerophyl medium resulted in a small reduction in Ts. The first bar is the Ts for paramecia in cerophyl medium (control; n = 5), the next 3 bars are the Ts for paramecia in cerophyl medium with 1 (n = 5), 10 (n = 5) or 100 (n = 5) µM SNAP added, respectively. * signifies different from control, $p<0.05$.

with the finding that Protists have a NO synthase, which oxidizes L-arginine to NO and L-citrulline. Furthermore, we found that a 155 kDa protein derived from *P. caudatum* reacted with an antibody against mammalian NOS1 but not with antibodies against mammalian NOS2 or NOS3. *Leishmania donovani* have a protein that reacts with mammalian NOS1 (Basu *et al.* 1997), and a polyclonal antibody against mammalian NOS1 has been utilized to determine the location of *Trypansoma cruzi* nitric oxide synthase (Goldstein *et al.* 2000). Thus, taken together these results suggest that Protists contain an NO synthase that is similar to mammalian NOS1.

Paramecia express many of the proteins necessary for NOS activity and NO effects. For example, paramecia express calmodulin (Chan *et al.* 1999). In mammals, the best characterized target for NO is guanylate cyclase, and NO activates guanylate cyclase to increase cyclic guanosine monophosphate (cGMP) production (Nathan 1992). In insects, the presence of soluble guanylyl cyclase in the nervous system has been used to infer the function of insect NOS (Nighorn *et al.* 1998). Paramecia have guanylyl cyclase in their cilia, although it is a particulate guanylyl cyclase (Linder *et al.* 1999). In mammalian cells, it has been demonstrated that NO also activates voltage-gated calcium channels to increase the influx of calcium (Clementi 1998). Paramecia also have voltage-gated calcium channels in their cilia (Thiele and Schultz 1981, Preston *et al.* 1992, Schultz *et al.* 1997), and cilia are involved in thermoregulatory behavior (Tominaga and Naitoh 1992, Imada and Oosawa 1999). Thus, one possible role for NO production in *P. caudatum* may be involvement in ciliary function and thermoregulation.

We found that inhibition of NO production reduced Ts by ~30%, or ~9°C in *P. caudatum*, and that this response could be partially reversed by administration of exogenous NO during inhibition of NO production. We know of no studies examining the role of NO production in

temperature regulation in *P. caudatum*, however NO has been found to be important in the central thermoregulatory response in mammals (Steiner and Branco 2002). For example, in rats inhibiting NO production with L-NAME resulted in a reduction in body temperature, whereas administration of D-NAME had no effect on body temperature (DePaula *et al.* 2000, Nakano *et al.* 2001). It is of interest to note that when we administered the NO donor, SNAP, alone there was also a reduction in Ts by ~5% or 2°C, which was much smaller than with NO inhibition. This finding is compatible with studies in mammals, wherein administration of SNAP caused either no significant change in body temperature (Eriksson *et al.* 1997) or a slight decrease in body temperature (Mathai *et al.* 1997). Thus, it may be that the influence of exogenous NO on Ts may be dependent on the starting Ts, i.e. if the starting Ts is low, as in the L-NAME treated paramecia, then exogenous NO will raise Ts. On the other hand, if the starting Ts is closer to the normal range, then exogenous NO may cause a slight reduction in Ts.

Inhibition of NO production with L-NAME resulted in a dose-dependent decrease in the number of paramecia at 7 days in culture. Since calcium oscillations have been implicated in cell division (Prajer *et al.* 1997), and NO activates voltage-gated Ca^{2+} channels (Clementi 1998), one might speculate that inhibition of NO production affects the population of *P. caudatum* in the culture flask by decreasing these Ca^{2+} oscillations, and thereby decreasing the number of cell divisions. However, Fig. 6 shows that the paramecia increased in number normally until approximately day 5 in 0.1 and 1 mM L-NAME, then paramecia number began to fall when compared to control paramecia number. One possible explanation for this is that inhibition of NO production increased paramecia death. The addition of 10 mM D-NAME decreased paramecia number suggesting that a change in osmolality or pH may have contributed to the reduction in paramecia number in the culture flasks with the highest concentrations of NAME (either stereoisomer). However, 10 mM L-NAME reduced paramecia number to a greater extent than did 10 mM D-NAME, demonstrating that even at the highest concentrations of L-NAME and D-NAME employed in these studies, L-NAME-induced inhibition of NO production decreased paramecia number in culture. Again, Fig. 6D suggests that the number of paramecia in the 10 mM D-NAME and 10 mM L-NAME cultures increased at approximately the same rate for the first 4 days and then in the L-NAME treated group paramecia numbers began to fall. This is consistent with the concept that inhibiting NO production hastened cell death. Alternatively, NO inhibition may have interfered with later fission, as has been observed in aging paramecia (Smith-Sonnenborn 1981), resulting in more rapid decline in paramecium number in the L-NAME treated cells. Thus, inhibition of NO production clearly decreased the number of paramecia in culture, although further studies will be needed to elucidate the exact mechanism of the decreased number of paramecia in culture.

In summary, this study demonstrates that NO_2^- accumulated in the media containing paramecia, and that the NO_2^- accumulation was inhibited by L-NAME and was calcium sensitive. Confirmation that the changes in $[NO_2^-]$ reflected changes in NO production by NOS in *P. caudatum* comes from the finding that [^{3}H]L-arginine was converted to [^{3}H]L-citrulline, in a process that was inhibited by L-NAME. Paramecia had a protein that cross-reacted with mouse NOS1 antibody, but not with mouse NOS2 or NOS3 antibody. Inhibition of NO production resulted in reduced numbers of paramecia after 7 days in culture. Finally, inhibition of NO production resulted in a reduced selected temperature for paramecia in a thermal gradient. Thus, these data demonstrate for the first time that *P. caudatum* produce NO, that *P. caudatum* NO production is calcium dependent, and that NO production by *P. caudatum* is involved in basic physiologic processes including population growth in culture and thermoregulation.

Acknowledgements. The authors wish to thank Heather Nash and Kelly Billings for excellent technical support. The authors would also like to thank Professor Benjimen Walker for discussions regarding experimental design and data interpretation.

REFERENCES

Basu N. K., Kole L., Ghosh A., Das P. K. (1997) Isolation of a nitric oxide synthase from the protozoan parasite, *Leishmania donovani*. *FEMS Microbiol. Letts.* **156:** 43-47

Chan C. W., Saimi Y., Kung C. (1999) A new multigene family encoding calcium-dependent calmodulin-binding membrane proteins of *Paramecium tetraurelia*. *Gene* **231:** 21-32

Clementi E. (1998) Role of nitric oxide and its intracellular signaling pathways in the control of Ca^{2+} homeostasis. *Biochem. Pharmacol.* **55:** 713-718

DePaula D., Steiner A. A., Branco L. G. S. (2000) The nitric oxide pathway is an important modulator of stress-induced fever in rats. *Physiol. Behav.* **70:** 505-511

Eriksson S., Hjelmqvist H., Keil R., Gerstberger R. (1997) Central application of a nitric oxide donor activates heat defense in the rabbit. *Brain Res.* **774:** 269-273

Erxleben C., Klauke N., Flotenmeyer M., Blanchard M. P., Braun C., Plattner H. (1997) Microdomain Ca^{2+} activation during exocytosis in paramecium cells. Superposition of local subplasmalemmal calcium store activation by local Ca^{2+} influx. *J. Cell Biol.* **136:** 597-607

Goldstein J., Paveto C., Lopez-Costa J. J., Pereira C., Alonso G., Torres H. N., Flawia M. M. (2000) Immuno and cytochemical localization of *Trypansoma cruzi* nitric oxide synthase. *Biocell* **24:** 217-222

Hennessey T. M., Saimi Y., Kung C. (1983) A heat-induced depolarization of *Paramecium* and its relationship to thermal avoidance behavior. *J. Comp. Physiol.* **153:** 39-46

Imada C., Oosawa Y. (1999) Thermoreception of *Paramecium*: different Ca^{2+} channels were activated by heating and cooling. *J. Mem. Biol.* **168:** 283-287

Jennings H. S. (1906) Behavior of the Lower Organisms. Columbia University Press, New York

Kluger M. J. (1991) Fever: role of pyrogens and cryogens. *Physiol. Rev.* **71:** 93-127

Kluger M. J. Ringler D. H., Anver M. R. (1975) Fever and survival. *Science* **188:** 166-168

Linder J. U., Engel P., Reimer A., Kruger T., Plattner H., Schultz A., Schultz J. E. (1999) Guanylyl cyclases with the topology of mammalian adenylyl cyclases and an N-terminal P-type ATPase-like domain in paramecium, tetrahymena and plasmodium. *EMBO J.* **18:** 4222-4232

Luckhart S., Rosenberg R. (1999) Gene structure and polymorphism of an invertebrate nitric oxide synthase gene. *Gene* **232:** 25-34

Malvin G. M. (1998) Theromregulatory changes by hypoxia: Lessons from the paramecium. *Clin. Exper. Pharmacol. Physiol.* **25:** 165-169

Malvin G. M., Wood S. C. (1992) Behavioral hypothermia and survival of hypoxic protozoans *Paramecium caudatum*. *Science* **255:** 1423-1425

Malvin G. M., Havlen P., Baldwin C. (1994) Interactions between cellular respiration and thermoregulation in the paramecium. *Am. J. Physiol. Regulatory Integrative Comp. Physiol.* **36:** R349-R352

Mathai M. L., Hjelmqvist H., Keil R., Gerstberger R. (1997) Nitric oxide increases cutaneous and respiratory heat dissipation in conscious rabbits. *Am. J. Physiol. Regulatory Integrative Comp. Physiol.* **272:** R1691-R1697

Mendelssohn M. (1895) Über den thermotropismus einzelliger organismen. *Pflügers Arch. Ges. Physiol.* **60:** 1-27

Nakano H., Lee S. D., Ray A. D., Krasney J. A., Farkas G. A. (2001) Role of nitric oxide in thermoregulation and hypoxic ventilatory response in obese Zucker rats. *Am. J. Respi.r Crit. Care Med.* **164:** 437-442

Nakaoka Y., Oosawa F. (1977) Temperature-sensitive behavior of *Paramecium caudatum*. *J Protozool* **24:** 575-580

Nathan C. (1992) Nitric oxide as a secretory product of mammalian cells. *FASEB J.* **6:** 3051-3064

Nelin L. D., Thomas C. J., Dawson C. A. (1996) The effect of hypoxia on nitric oxide production in the neonatal pig lung. *Am. J. Physiol. Heart Circ. Physiol.* **41:** H8-H14

Nelin L. D., Nash H. E., Chicoine L. G. (2001) Cytokine treatment increases arginine metabolism and uptake in bovine pulmonary arterial endothelial cells. *Am. J. Physiol. Lung Cell Mol. Physiol.* **281:** L1232-L1239

Nighorn A., Gibson N. J., Rivers D. M., Hildebrand J. G., Morton D. B. (1998) The nitric oxide-cGMP pathway may mediate communication between sensory afferents and projection neurons in the antennal lobe of *Manduca sexta*. *J. Neurosci.* **18:** 7244-7255

Piacenza L., Peluffo G., Radi R. (2001) L-arginine-dependent suppression of apoptosis in *Trypanosoma cruzi*: contribution of the nitric oxide and polyamine pathways. *Proc. Natl. Acad. Sci. USA* **98:** 7301-7306

Prajer M., Fleury A., Laurent M. (1997) Dynamics of calcium regulation in paramecium and possible morphogenetic implication. *J. Cell Science* **110:** 529-535

Preston R. R., Saimi Y., Kung C. (1992) Calcium current activated upon hyperpolarization of *Paramecium tetraurelia*. *J. Gen. Physiol.* **100:** 233-251

Regulski M., Tully T. (1995) Molecular and biochemical characterization of dNOS: a dorsophila Ca^{2+}/calmodulin-dependent nitric oxide synthase. *Proc. Nat. Acad. Sci. USA* **92:** 9072-9076

Schultz J. E., Guo Y., Kleefeld G., Volkel H. (1997) Hyperpolarization- and depolarization-activated Ca^{2+} currents in Paramecium trigger behavioral changes and cGMP formation independently. *J. Membr. Biol.* **156:** 251-259

Smith-Sonnenborn J. (1981) Genetics and aging in Protozoa. *Inter. Rev. Cytol.* **73:** 319-354

Steiner A. A., Branco L. G. S. (2002) Hypoxia-induced anapyrexia: implications and putative mediators. *Annu. Rev. Physiol.* **64:** 263-288

Tao Y. P., Misko T. P., Howlett A. C., Klein C. (1997) Nitric oxide, an endogenous regulator of *Dictyostelium discoideum* differentiation. *Development* **124:** 3587-3595

Thiele J., Schultz J. E. (1981) Ciliary membrane vesicles of paramecium contain the voltage-sensitive calcium channel. *Proc. Nat. Acad. Sci. USA* **78:** 3688-3691

Tominaga T., Naitoh Y. (1992) Membrane potential responses to thermal stimulation and the control of thermoaccumulation in *Paramecium caudatum*. *J. Exp. Biol.* **164:** 39-53

Vaughn L. K., Bernheim H. A., Kluger M. J. (1974) Fever in *Dipsosaurus dorsalis*. *Nature* **252:** 473-474

Wood S. C., Malvin G. M. (1992) Behavioral hypothermia: an adaptive stress response. In: Physiological Adaptations in Vertebrates, (Eds. S. C. Wood, R. E. Weber, A. R. Hargens and R. W. Millard) Marcel Dekker, New York, Basel, Hong Kong, 295-312

Received on 3rd March, 2003; revised version on 24th June, 2003; accepted on 11th July, 2003

Acta Protozool. (2003) 42: 269 - 276

ACTA
PROTOZOOLOGICA

Effect of Essential Oil of *Ocimum gratissimum* on the Trypanosomatid *Herpetomonas samuelpessoai*

Fabíola Barbieri HOLETZ[1], Tânia UEDA-NAKAMURA[3], Benedito Prado Dias FILHO[3], Diógenes Aparício Garcia CORTEZ[2], José Andrés MORGADO-DÍAZ[4] and Celso Vataru NAKAMURA[3]

[1]Estudante de Pós-graduação em Ciências Farmacêuticas; [2]Departamento de Farmácia e Farmacologia; [3]Departamento de Análises Clínicas, Universidade Estadual de Maringá, Maringá, Paraná; [4]Divisão de Biologia Celular, Instituto Nacional do Câncer, Rio de Janeiro, RJ Brazil

Summary. In this study, we reported the effect of the essential oil of *Ocimum gratissimum* on *Herpetomonas samuelpessoai*, a non-pathogenic trypanosomatid. Parasites were grown at 28 or 37°C, in a chemically defined or a complex medium, containing essential oil obtained from *Ocimum gratissimum.* At concentrations from 20 to 250 µg/ml, the essential oil, progressively inhibited the protozoan growth. The IC_{50}, in defined and complex media, at 28°C were 100 and 91 µg/ml, respectively. Cells cultivated in chemically defined medium were more sensitive to essential oil at concentration of 50, 62.5 and 100 µg/ml in relation to those cultured in complex medium at 37°C. In addition, ultrastructural and enzymatic alterations of the trypanosomatid were also evaluated. *H. samuelpessoai* exposed to 100 µg/ml of essential oil, in chemically defined medium at 28°C for 72 h, presented considerable ultrastructural alteration, mainly at mitochondrial level, as showed by transmission electron microscopy. Furthermore, cells cultivated in the presence of 100 µg/ml of essential oil showed a decrease of activity of the succinate cytochrome *c* reductase enzyme, a typical mitochondrion marker, as compared to untreated cells.

Key words: *Herpetomonas samuelpessoai*, medicinal plants, *Ocimum gratissimum*, ultrastructure.

INTRODUCTION

During the last century the practice of herbalism has become mainstream throughout the world. In spite of the great advances observed in modern medicine, plants still make an important contribution to health care. This is due in part to the recognition of the value of traditional medical systems, particularly of Asian origin, and the identification of medicinal plants from indigenous pharmacopoeias, which have significant healing power. Medicinal plants are distributed worldwide, but they are most abundant in tropical countries (Calixto 2000, Lewis 2001). In Brazil, around 80,000 species of higher plants were described, which offer enormous prospects for discovering new compounds with therapeutic properties.

Among all families of the plant kingdom, members of the Lamiaceae have been used for centuries in folk medicine. *Ocimum gratissimum* L. (Lamiaceae), commonly known as "alfavaca", is naturally used in the treatment of different diseases, e.g., upper respiratory tract infections, diarrhea, headache, fever, ophthalmic

Address correspondence to: Celso Vataru Nakamura, Departamento de Análises Clínicas, Universidade Estadual de Maringá; Avenida Colombo, 5790; BR-87020-900, Maringá, PR, Brazil; Fax: +55 44 261-4490; E-mail: cvnakamura@uem.br

and skin diseases, and pneumonia (Corrêa 1932, Onajobi 1986, Ilori *et al*. 1996). The *Ocimum* oil is also active against several species of bacteria (*Escherichia coli, Shigella, Salmonella* and *Proteus*) and fungi (*Trichophyton rubrum* and *T. mentagrophytes*) (El-Said *et al*. 1969, Begum *et al*. 1993, Nwosu and Okafor 1995, Nakamura *et al*. 1999, Orafidiya *et al*. 2000). Various sister species of *O. gratissimum*, e.g., *O. viride* Linn, *O. suave* Linn, *O. basilicum* Linn and *O. canum* Sims, have been reported for their numerous medicinal uses (Mshana *et al*. 2000).

Diseases caused by protozoa are responsible for mortality in tropical and subtropical countries. At the moment, the number of drugs available for the treatment of human and animal trypanosomiasis, amoebiasis, leishmaniasis, and malaria are limited. Considering the side effects and the resistance that pathogenic protozoan builds against these drugs, more attention should be given to the extracts and biologically active compounds which are isolated from plant species commonly used in herbal medicine (Essawi and Srour 2000).

Protozoa of the Trypanosomatidae family comprise a large number of species, some of which are agents of important illnesses, such as leishmaniasis, Chagas' disease and African trypanosomiasis. In addition, other non-pathogenic trypanosomatids have emerged as important models for the study of basic biological processes, including RNA editing and *trans*-splicing, organization of extranuclear DNA, antigenic variation, etc (De Souza and Motta 1999). *Herpetomonas samuelpessoai* is a non-pathogenic trypanosomatid that shares important antigens with *Trypanosoma cruzi*, the agent of Chagas' disease (Souza *et al*. 1974). *H. samuelpessoai* can be easily cultivated in a defined medium at 28°C and 37°C, and can induce a humoral and cell-mediated immune response (Roitman *et al.* 1972). Several Brazilian researcher groups have used this parasite as a model to study the biology of trypanosomatids. So, it may be suitable as a model for screening new trypanocidal drugs.

A previous screening of crude extracts of plants used in traditional medicine showed that the essential oil of *O. gratissimum* inhibited the growth of *H. samuelpessoai* (Holetz *et al*. 2002), however a detailed study of this natural product has not been carried out. In the present study we reported the effect of the essential oil from *O. gratissimum* on growth, viability, ultrastructural and biochemical alterations of *H. samuelpessoai* cultivated in defined or complex medium at 28°C and 37°C.

MATERIALS AND METHODS

Plant material. *Ocimum gratissimum* was collected in Maringá, Paraná, Brazil, identified, and a voucher no. HUM 9.613 is deposited at the Maringá State University Herbarium. Fresh leaves from the plant were cut into pieces and subjected to steam distillation. The distillate was then extracted with petroleum ether, which was removed carefully, and the essential oil was obtained. The oil was then stored at -20°C until needed.

Preparation of stock solutions. The stock solution (10 mg/ml) of essential oil from *O. gratissimum* was made in a chemically defined medium (Roitman *et al*. 1972). For this purpose, initially the essential oil was diluted in 2% Tween 80. From the stock solution, dilutions were made to obtain 250, 150, 125, 100, 62.5, 50, and 20 µg/ml. The stock solution of Eugenol (Biodinâmica Química e Farmacêutica Ltda) was prepared in a similar way, just considering its density (1.0664 g/ml) (Budavari *et al*. 1989). Benznidazole (N-benzyl-2-nitro-1-imidazolacetamide - Roche Pharmaceuticals, Rio de Janeiro, Brazil) was used as reference drug. Both stock solutions of Eugenol and Benznidazole were prepared in the defined medium.

Microorganism. *Herpetomonas samuelpessoai* (ATCC 30252) was maintained by weekly transfers in a chemically defined medium (Roitman *et al*. 1972) and distributed in 5 ml volumes in screw-capped tubes. Cells were grown at 28°C for 48 h and cultures were kept at 4°C.

Antiprotozoan activity. For experiment *H. samuelpessoai* was incubated in defined or complex medium (Roitman *et al*. 1972) containing different concentrations of essential oil, which were added only once to the cultures. Cells were grown in 13 x 100 mm tubes containing 1 ml of defined medium and the start inoculum consisted of the protozoan in logarithmic growth phase (1 x 10^6 cells/ml). After 24, 48, 72 and 96 h at 28°C or 37°C, the cell growth was estimated by counting in a haemocytometer (Improved Double Neubauer). As negative controls, defined medium alone and defined medium plus 2% Tween 80, were used. All experiments were performed in triplicate and the results expressed as log number cells/ml and as percentage of the growth inhibition at 72 h.

Viability assay. In order to evaluate the viability of the protozoa treated with essential oil, each solution was added to eppendorfs containing 1 x 10^7 cells in logarithmic growth phase. Immediately after the addition of the essential oil (time zero) and after 1, 2, 3, 6 and 24 h at 28°C, equal volumes (25 µl) of protozoan suspension and 0.4% erythrosine B were mixed and the cell viability was quantified by light microscopy. The preparations were made in duplicate and the percentage of viability was determined by counting at least 300 cells (Hodgkinson *et al*. 1980).

Light microscopy. To evaluate the morphologic changes induced by the essential oil of *O. gratis*simum in *H. samuelpessoai*, cells treated with 100 µg/ml of the oil in defined medium during 72 h, were collected by centrifugation, smear-dried onto slides, fixed in methanol and stained for light microscopy using the "Panótico Rápido LB" stain (Laborclin Prod. Lab. Ltda., Pinhais, Paraná State, Brazil). Images were obtained using an optic microscope Olympus CBA coupled to an Image Pro-Plus program, version 4.0 (Media Cybertennics).

Ultrastructural analysis. *Herpetomonas samuelpessoai* treated with 100, 125 or 150 µg/ml of the essential oil, 2% Tween 80 or

medium alone, at 28°C were collected by centrifugation in intervals of 24 h and for a period up to 96 h, washed in PBS and fixed with 2.5% glutaraldehyde in 0.1 M sodium cacodylate buffer, pH 7.2, containing 1.0 mM $CaCl_2$ at 4°C. Cells were then washed three times with 0.1 M sodium cacodylate buffer and postfixed for 1 h at room temperature in 1% osmium tetroxide plus 0.8% potassium ferricyanide and 5 mM $CaCl_2$. After rinsing, cells were dehydrated in acetone, incubated in an acetone-epon mixture (2:1, 1:1, 1:2) and embedded in Epon resin. Ultrathin sections obtained in a Reichert Ultracut E ultramicrotome were stained with uranyl acetate and lead citrate and observed in a Zeiss CEM - 900 electron microscope.

Biochemical analysis. Cells treated with 100 µg/ml essential oil and untreated cells were incubated at 28°C for 72 h, and harvested by centrifugation at 3000 *g* for 10 min in a refrigerated centrifuge Sorvall Super 21 (SL50T Rotor). Then, they were washed three times in PBS (pH 7.2), resuspended in a hypotonic solution (Tris-HCl 10 mM) containing a cocktail of protease inhibitors (antipain, aprotinin, leupeptin and pepstatin - 10 µg/ml each) and disrupted by sonication with 20 cycles of 2 s with 1 s rest between cycles on ice using an Ultrasonic Processor (CV 33 Model). The cell disruption was monitored with light microscope. Protein concentration was determined by Bio-Rad protein assay, using bovine serum albumin as a standard and following the manufacturer's instructions.

Succinate cytochrome *c* reductase activity was measured according to Masters *et al*. (1967). The reaction mixture contained 0.2 M phosphate buffer pH 7.4; 0.003 M EDTA pH 7.4; 0.6 M succinic acid adjusted to pH 7.4 with NaOH; 0.001 M cytochrome *c*. The specific activity was measured at 30°C, by following the reduction of cytochrome *c* at 550 nm.

RESULTS

A dose-dependent antiprotozoan effect of the essential oil of *O. gratissimum* is shown in Fig. 1. It was possible to observe an inhibitory effect of the essential oil on the cell growth when cells were treated with a high concentration of the drug in defined and complex media. The IC_{50} (50% inhibitory concentration) in both media at 28°C were 100 and 91 µg/ml, respectively. Eugenol inhibited *H. samuelpessoai* growth at the same concentration of essential oil and Benznidazole did not induce a representative inhibition in defined medium at 28°C. Tween 80, the dilution agent, and Petrolatum oil used as indifferent oil, showed no effect on the protozoa growth (data not shown). The effects of the essential oil on growth of *H. samuelpessoai* cultivated in defined or complex medium for 72 h, at 28°C or 37°C are shown in Table 1. It is possible to observe in this Table that the composition of the culture medium did not interfere with the growth inhibition of the flagellate when incubated at 28°C. On the other hand, *H. samuelpessoai* cultivated at 37°C in defined medium containing 50, 62.5 and 100 µg/ml of essential oil was inhibited more efficiently

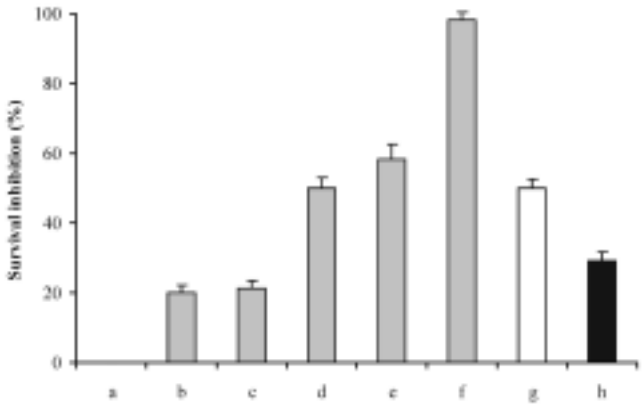

Fig. 1. Effect of essential oil from *O. gratissimum* (a - f); eugenol (g) and benznidazole (h) on growth inhibition of *Herpetomonas samuelpessoai* in defined medium at 28°C by 72 h. **a** - 20 µg/ml; **b** - 50 µg/ml; **c** - 62.5 µg/ml, **d** - 100 µg/ml; **e** - 125 µg/ml; **f** - 150 µg/ml; **g** - 100 µg/ml; h - 100 µg/ml. Results from three experiments in duplicate are shown as percentages of growth inhibition ± standard deviations.

Table 1. Effect of essential oil from *O. gratissimum* on growth of *Herpetomonas samuelpessoai* cultivated in defined and complex media at 28°C and 37°C, during 72 h.

	Protozoan growth inhibition (%)			
Concentration of essential oil (µg/ml)	Chemically defined medium		Complex medium	
	28°C	37°C	28°C	37°C
250	99.3	97.3	99.2	98.0
150	98.1	96.7	98.7	98.1
125	58.2	96.9	57.5	98.1
100	50.0	96.3	56.0	74.3
62.5	21.5	72.1	30.8	49.0
50	20.0	74.0	25.0	30.0
20	0.0	21.0	0.0	20.0

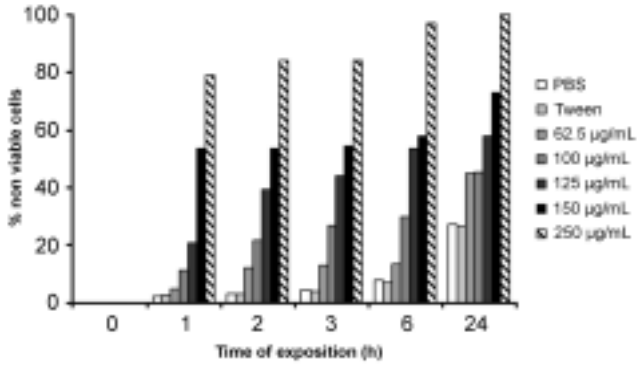

Fig. 2. Effect of essential oil on viability of *Herpetomonas samuelpessoai.*

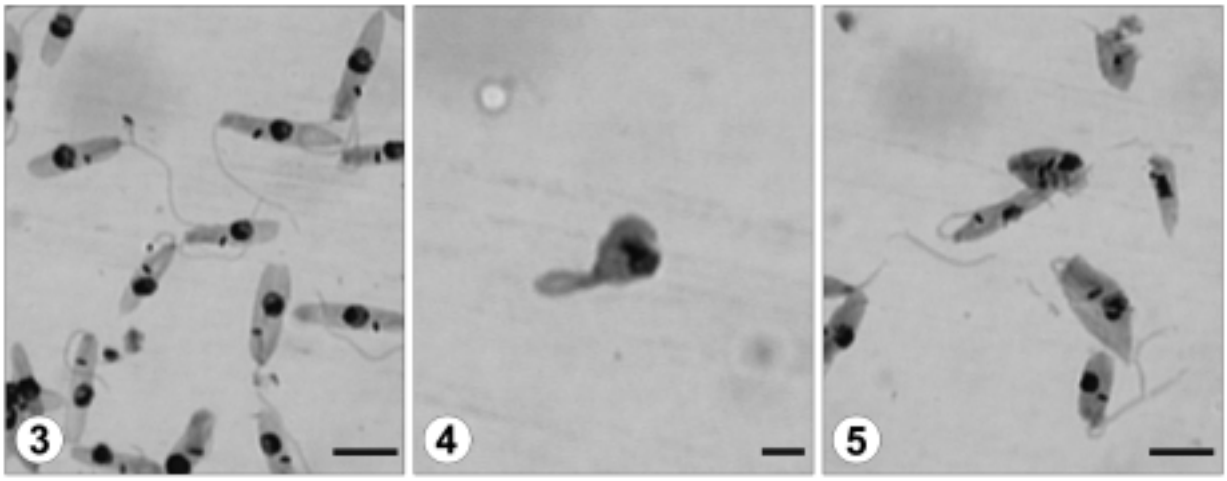

Figs 3-5. Light microscopy of *Herpetomonas samuelpessoai* cultivated in defined medium in the presence of essential oil during 72 h at 28°C; **3** - control; **4, 5** - 100 µg/ml. Scale bar 5 µm.

than when cultivated in complex medium. The inhibitory activity of the essential oil was increased at 37°C in both culture media used.

Viability of treated and control cells were assessed by the dye exclusion test. The percentage of non-viable cells, obtained by exposition of the protozoan to different concentrations of essential oil, is shown in Fig. 2. Treatment with 150 and 250 µg/ml of essential oil, in the first hour, reduced the parasite viability in 53.5% and 78.5% respectively. Low concentration of the drug did not interfere with the viability of protozoa. After 6 h of treatment, at concentration of 125, 150, and 250 µg/ml, lethality were 53.5, 58, and 97%, respectively. Morphologic alterations, such as cellular volume increase and irregular shape of the cells grown in chemically defined medium for 72 h containing 100 µg/ml of essential oil, were also observed (Figs 3-5).

In order to determine ultrastructural changes in the *H. samuelpessoai* treated with 100 µg/ml essential oil, electron microscopy analysis was carried out. It was possible to observe a considerable swelling of the mitochondrion, showing the inner mitochondrial membrane altered with a significant increase of the number of cristae and in some cells the mitochondrial matrix became less electron dense (Fig. 7). Concentric membranes within the flagellar pocket were also seen (Fig. 8). Similar alterations were observed when cells were cultured using eugenol (Fig. 9), which represent 67% of the composition of the essential oil, as demonstrated by Nakamura *et al.* (1999). These ultrastructural changes were not observed in cells cultured in the presence of Tween 80 (not shown) and in untreated cells, which showed a mitochondrion with well-distinguished membranes and a dense matrix (Fig. 6). In order to verify the activity of succinate cytochrome *c* reductase, an enzyme related to metabolism of this organelle, enzymatic assays were performed. The enzymatic activity of treated cells with the essential oil (2.0 ± 0.36 nmol/min/mg of protein) decreased about 5- fold in relation to untreated cells (9.7 ± 1.82 nmol/min/mg of protein).

DISCUSSION

Several species and varieties of plants of the genus *Ocimum* have been reported to yield oil of diverse nature, commonly known as basilic oils. Craveiro *et al.* (1981) reported some chemical components usually found in the essences of these plants, such as: eugenol, linalool, methyl cinnamate, camphor and thymol. It has been demonstrated that the eugenol isolated from *O. gratissimum* presents antibacterial (Nakamura *et al.* 1999) and antihelmintic activity (Pessoa *et al.* 2002). In the present study, when the IC_{50} of essential oil and eugenol in *H. samuelpessoai* were compared, a similar antiprotozoan activity was observed. Since eugenol is the principal constituent of the essential oil, this result suggests that it could be responsible for this effect.

Herpetomonas samuelpessoai can be easily cultivated in defined medium (free of macromolecules) showing its ability to synthesize macromolecules, for instance lipids, from compounds with low molecular weight. Silva and Oliveira (1985) reported that

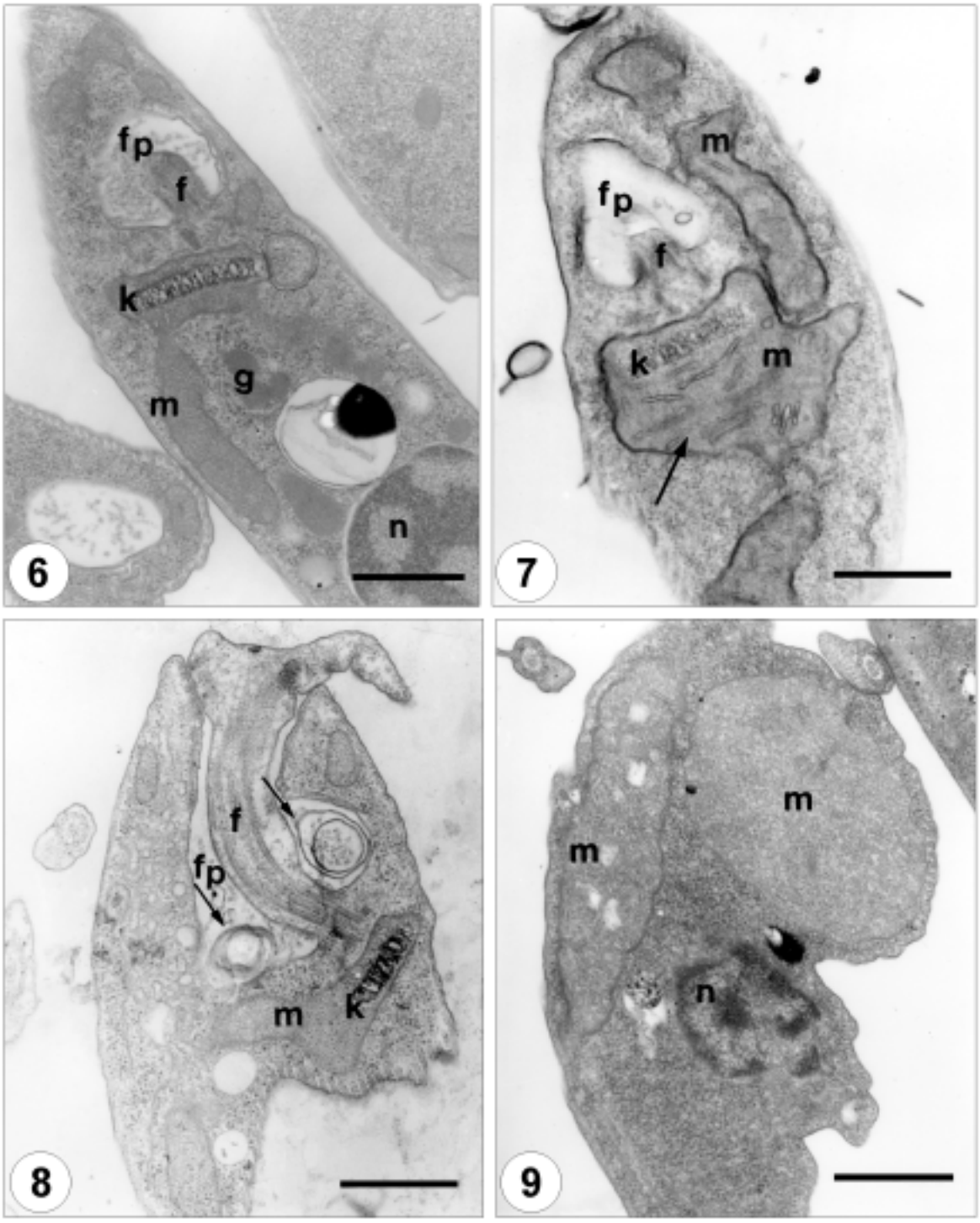

Figs 6-9. Transmission electron microscopy of *Herpetomonas samuelpessoai* cultivated in defined medium with essential oil at 28°C for 72 h; **6** - control; **7, 8** - 100 µg/ml; **9** - 100 µg/ml of eugenol. Arrows showed swelling mitochondria (Fig. 7) and concentric membranes within flagellar pocket (Fig. 8). f - flagellum; fp - flagellar pocket; g - glycosome; k - kinetoplast; m - mitochondria; n - nucleus. Scale bar 1 µm.

H. samuelpessoai presents lower levels of lipids when cultivated in defined medium at 28°C and this difference is more evident in total sterol content. Rodrigues *et al.* (2002) suggested that ergosterol and its analogs are essential to the maintenance and organization of the mitochondrial membrane in trypanosomatids. Furthermore, it is well known that the cell membrane fluidity is highly dependent on the lipid composition. On the other hand, temperature increases causes disorganization of the hydrophobic portion of the fat acids chains present in the membrane increasing the fluidity of this structure (Granner 1990). It was reported that the lipid composition of the cell membrane changes drastically depending on the temperature and culture conditions in *H. samuelpessoai*. Fagundes *et al.* (1980) verified a substantial increase of the total lipids when these protozoa were incubated at 37°C suggesting a balanced reposition of membrane components necessary for the maintenance of the functionality of this structure. In addition, when this flagellate was cultivated in defined medium a decrease in stearic acid content was observed (Pinto *et al.* 1982). Thus, in the present study the medium constitution and incubation temperature may be the adjuvant factors, responsible for the action of the essential oil as antiprotozan agent.

Benznidazole is a drug used for the treatment of the Chagas' disease, which is caused by *Trypanosoma cruzi.* Considering that *H. samuelpessoai* belong to the same family, we used this drug to compare the effect of the essential oil. Yong *et al.* (2000) reported values of IC_{50} of benznidazole to the *T. cruzi* strains Dm_{28C} resistant and sensitive, of 6 and 5 µM, respectively. In the present study, culture of *H. samuelpessoai* in chemically defined medium at 28°C, were inhibited in 31% with concentration of 384 µM of benznidazole. As IC_{50} could not be determined even at 3840 µM, it is possible that *H. samuelpessoai* is naturally resistant to this compound.

Viability assay showed that cells treated with high concentrations of the essential oil caused more than 50% of cell death in the first hour of incubation. Similar results were obtained in lower concentrations of the oil after 24 h of treatment. These results were confirmed through the growth curves of the protozoa where high concentrations of the essential oil inhibited more than 95% of the growth.

Morphological alterations of *H. samuelpessoai* were observed after treatment with the essential oil, as seen by light microscopy. At ultrastructural level it was possible to observe significant alteration at the mitochondrion, such as a remarkable swelling and some modifications in the inner membrane like disorganization and increase of the number of cristae. We do not have an explanation to the exact mechanism involved in these alterations. However similar results have been reported in other trypanosomatids; for instance, Delorenzi *et al.* (2001), reported mitochondrial alterations when promastigote and amastigote forms of *Leishmania amazonensis* were treated with a purified indole alkaloid, obtained from the crude extract of stem of *Peschiera australis* (Apocinaceae). Analog alterations were observed in this organelle in promastigote forms of *L. amazonensis* when submitted to the treatment with a purified chalcone of *Piper anduncum* (Torre-Santos *et al.* 1999). Rodrigues *et al.* (2002) reported that the treatment of *L. amazonensis* with 22,26 - azasterol, an inhibitor of ergosterol synthesis, induced a marked alteration in the inner mitochondrial membrane, with the formation of elaborated and complex structures. Other studies reported similar alterations in epimastigote and amastigote forms of *T. cruzi* treated with different compounds (Lazardi *et al.* 1991).

Due to these ultrastructural alterations at the mitochondrion, the activity of a well-known marker enzyme involved in the respiratory chain, the enzyme succinate cytochrome *c* reductase, was evaluated. Cells treated with essential oil of *O. gratissimum* showed a decreasing in enzymatic activity as compared with control cells. Some studies have shown that the lincochalcone A, an oxygenated chalcone, showed a potent antimalarial and antileishmanial activity. This compound also altered the mitochondrial morphology and inhibited the activity of the mitochondrial dehydrogenase (Chen *et al.* 1994, Zhai *et al.* 1995). Recently these authors investigated the action mechanism of this chalcone focusing the respiratory chain of *L. major* and *L. donovani.* The authors showed that several important enzymes of the electron-transport systems were inhibited, including the enzyme succinate cytochrome *c* reductase (Chen *et al.* 2001).

In conclusion, the study of the medicinal plant effect on the trypanosomatid *H. samuelpessoai* here reported demonstrates the utility of this flagellate as a biologic model in the evaluation of cellular alterations induced by drugs. This model is capable of mimic events that happen in pathogenic microorganisms as *T. cruzi*, *Leishmania* sp., *T. brucei* and even in phytopathogenic

trypanosomatid. The results obtained with the essential oil of *O. gratissimum* open perspectives to find more effective drugs of vegetal origin, less toxic and available for low socioeconomic population in the treatment of these diseases.

Acknowledgements. This study was supported through grants of the Conselho Nacional de Desenvolvimento Científico e Tecnológico-CNPq, Capacitação de Aperfeiçoamento de Pessoal de Nível Superior CAPES, and Programa de Pós-graduação em Ciências Farmacêuticas da Universidade Estadual de Maringá.

REFERENCES

Begum J., Yusuf M., Chowdhury U., Wahab M. A. (1993) Studies on essential oils for their antibacterial and antifungal properties. Part 1. Preliminary screening of 35 essential oils. *J. Sci. Ind. Res*. **28:** 25-34

Budavari S., O'Neil M., Smith A., Heckelman P. E. (Eds.). (1989) The Merck Index: An Encyclopedia of Chemicals, Drugs, and Biologicals. Merck & CO., Rahway

Calixto J. B. (2000) Efficacy, safety, quality control, marketing and regulatory guidelines for herbal medicines (phytotherapeutic agents). *Braz. J. Med. Biol. Res*. **33:** 179-189

Chen M., Theander T. G., Christensen S. B., Hviid L., Zhai L., Kharazmi A. (1994) Lincochalcone A, a new antimalarial agent, inhibits in vitro growth of the human malaria parasite *Plasmodium falciparum* and protects mice from *P. yoelii* infection. *Antimicrob. Agents Chemother.* **38:** 1470-1475

Chen M., Zhai L., Christensen S. B., Theander T. G., Kharazmi A. (2001) Inhibition of fumarate reductase in *Leishmania major* and *L. donovani* by chalcones. *Antimicrob. Agents Chemother.* **45:** 2023-2029

Corrêa M. P. (1932) Dicionário das plantas úteis do Brasil. IBDF, Rio de Janeiro

Craveiro A. A., Fernandes A. G., Andrade C. H. S., Matos F. J. A., Alencar W. J. (1981) Óleos essenciais de plantas do Nordeste, Imprensa Universitária, Universidade Federal do Ceará, Fortaleza

Delorenzi J. C., Attias M., Gattas C. R., Andrade C. R., Pinto A. C., Henriques A. T., Bou-Habib D. C., Saraiva E. M. B. (2001) Antileishmanial activity of an indole alkaloid from *Peschiera australis. Antimicrob. Agents Chemother.* **45:** 1349-1354

De-Souza W., Motta M. C. M. (1999) Endosymbiosis in protozoa of the Trypanosomatidae family. *Fems Microbiol. Lett*. **173:** 1-8

El-Said F., Sofowora E. A., Malcolm S. A., Hofer A. (1969) An investigation into the efficacy of *Ocimum gratissimum* as used in Nigerian native medicine. *Planta Medica*. **17:** 195-200

Essawi T., Srour M. (2000) Screening of some Palestinian medicinal plants for antibacterial activity. *J. Ethnopharmacol*. **70:** 343-349

Fagundes L. J. M., Angluster J., Gilbert B., Roitman I. (1980) Synthesis of sterols in *Herpetomonas samuelpessoai*: Influence of growth conditions. *J. Protozool*. **27:** 238-241

Granner D. K. (1990) Membranas: Estrutura, Arranjo e Função. In: Harper: Bioquímica (Eds. R. K. Murray, P. A. Mayes and V. W. Rodwell). Atheneu, São Paulo, **42:** 454-472

Hodgkinson V. H., Herman R., Semprevivo L. (1980) *Leishmania donovani*: Correlation among assays of amastigote viability. *Exp. Parasitol*. **50:** 397-408

Holetz F. B., Ueda-Nakamura T., Dias-Filho B. P., Cortez D. A. C, Mello J. C. P., Nakamura C. V. (2002) Effect of plant extracts used in folk medicine on cell growth and differentiation of *Herpetomonas samuelpessoai* (Kinetoplastida, Trypanosomatidae) cultivated in defined medium. *Acta Scientiarum*. **24:** 657-662

Ilori M., Sheteolu A. O., Omonibgehin E. A., Adeneye A. A. (1996) Antidiarrhoeal activities of *Ocimum gratissimum* (Lamiaceae). *J Diarrhoeal Dis Res*. **14:** 283-285

Lazardi K.; Urbina J. A.; De Souza W. (1991) Ultrastructural alterations induced by ICI 195,739, a bis-triazole derivate with strong antiproliferative action against *Trypanosoma* (*Schizotrypanun*) *cruzi*. *Antimicrob. Agents Chemother.* **35:** 736-740

Lewis E. M. (2001) Should we be concerned about herbal remedies. *J. Ethnopharmacol.* **75:** 141-164

Masters B. S., Willians C. H. Jr, Kamin H. (1967) The preparation and properties of microsomal TPNH-cytochrome *c* reductase from pig liver. In: Methods in Enzymology (Eds. R. W. Estrabrook and M. E. Pullman). Academic Press, New York **10:** 565-573

Mshana N. R., Abbiw D. K., Addae-mensah I., Adjanohoun E., Ahyi M. R. A., Enow-Orock E. G., Gbile Z. O., Noamesi B. K., Odei M. A., Adunlami H., Oteng-Yeboah A. A., Sarpong K., Sofowora A., Tackie A. N. (2000) Traditional Medicine and Pharmacopoeia. Contribution to the Revision of Ethnobotanical and Floristic Studies in Ghana. Scientific, Technical and Research Commission of the Organization of African Unity

Nakamura C. V., Nakamura T. U., Bando E., Melo A. F. N., Cortez D. A. G., Dias Filho B. P. (1999) Antibacterial activity of *Ocimum gratissimum* L. essential oil. *Mem. Inst. Oswaldo Cruz*. **94:** 675-678

Nwosu M. O., Okafor J. I. (1995) Preliminary studies of the antifungal activities of some medicinal plants against *Basidiobolus* and some other pathogenic fungi. *Mycoses*. **38:** 191-195

Onajobi F. D. (1986) Smooth muscle contracting lipid soluble principles in chromatographic fractions of *Ocimum gratissimum. J. Ethnopharmacol*. **18:** 3-11

Orafidiya O. O., Elujoba A. A., Iwalewa F. O., Okeke I. N. (2000) Evaluation of antidiarrhoeal properties of *Ocimum gratissimum* volatile oil and its activity against enteroagregative *Escherichia coli. Pharm. Pharmacol. Lett.* **10:** 9-12

Pessoa L. M., Morais S. M., Bevilaqua C. M. L., Luciano J. H. S. (2002) Anthelmintic activity of essential oil of *Ocimum gratissimum* Linn. and eugenol against *Haemonchus contortus. Vet. Parasitol*. **109:** 59-63

Pinto A. S., Pinto A. C., De Souza W., Angluster J. (1982) Fatty acid composition in *Herpetomonas samuelpessoai*: influence of growth conditions. *Comp. Biochem. Physiol*. **73b:** 351-356

Rodrigues J. C. F., Attias M., Rodriguez C., Urbina J. A., De Souza W. (2002) Ultrastructural and biochemical alterations induced by 22,26-azasterol, a $\Delta^{24(25)}$-sterol methyltransferase inhibitor, on promastigote and amastigote forms of *Leishmania amazonensis. Antimicrob. Agents Chemother.* **46:** 487-499

Roitman C., Roitman I., Azevedo H. P. (1972) Growth of an insect Trypanosomatid at 37°C in a defined medium. *J. Protozool*. **19:** 346-349

Silva R., Oliveira M. M. (1985) Investigations on phospholipids of *Herpetomonas samuelpessoai*: influence of growth conditions. *Comp. Biochem. Physiol.* **82b:** 173-177

Souza M. C., Reis A. P., Silva W. D., Brener Z. (1974) Mechanism of acquired immunity induced by "*Leptomonas pessoai"* against *Trypanosoma cruzi* in mice. *J. Protozool.* **21:** 579-584

Torres-Santos E. C., Moreira D. L., Kaplan M. A. C., Meirelles M. N., Rossi-Bergmann B. (1999) Selective effect of 2', 6'-dihydroxy-4'-methoxylchalcone isolated from *Piper aduncum* on *Leishmania amazonensis*. *Antimicrob. Agents Chemother.* **43:** 1234-1241

Yong V., Schmitz V., Vannier-Santos M. A., Lima A. P. C. A., Lalmanach G., Juliano L., Gauthier F., Scharfstein J. (2000) Altered expression of cruzipain and a cathepsin B-like target in a *Trypanosoma cruzi* cell line displaying resistance to synthetic inhibitors of cysteine-proteinases. *Mol. Biochem. Parasitol.* **109:** 47-59

Zhai L., Blom J., Chen M., Christensen S. B., Kharazmi A. (1995) The antileishmanial agent lincochalcone a interferes with the function of parasite mitochondria. *Antimicrob. Agents Chemother.* **39:** 2742-2748

Received on 4th April, 2003; revised version on 16 th June, 2003; accepted on 14th July, 2003

Acta Protozool. (2003) 42: 277 - 285

ACTA
PROTOZOOLOGICA

Phosphatidylinositol 3-kinase-like Activity in *Tetrahymena*. Effects of Wortmannin and LY 294002

Péter KOVÁCS[1] and Éva PÁLLINGER[2]

[1]Department of Genetics, Cell- and Immunobiology, Semmelweis University; [2]Molecular Immunological Research Group, Hungarian Academy of Sciences, Budapest, Hungary

Summary. Insulin has many different effects on *Tetrahymena*, as e.g. on the glucose uptake, cell division, survival, phosholipase D activity and insulin production. PI 3-kinase is one of the key enzymes in the action of insulin. Thus it was supposed that similarly to the higher eukaryotes, PI 3-kinase activity plays fundamental role in the insulin action also in *Tetrahymena*. Here we report that PI 3-kinase-like activity is immunoprecipitated from *Tetrahymena* cell lysate with anti-IRS 1 and anti-p85 antibodies. Both immunoprecipitates contain higher PI 3-kinase activity from lysate of insulin treated cells than the lysate of untreated ones. *In vivo* treatments with PI 3-kinase inhibitors wortmannin (100-500 nM) and LY 294002 (10-20 µM) elevated the PI 3-kinase activity in the IRS 1-antibody precipitable material, while in anti-p85 antibody precipitate this activity was lower than in the controls. *In vitro*, wortmannin proved to be an effective PI 3-kinase inhibitor. Immunostaining revealed that p85 immunoreactivity localized to the cortex of cells, while IRS 1 localized cytoplasmically. *In vivo* treatments with both PI 3-kinase inhibitors elevated the amount of IRS 1, while p85 immunoreactivity was increased only after wortmannin treatments. Both PI 3-kinase inhibitors reduced the F-actin content of cells. Wortmannin caused a forward cytoplasmic stream, which translocate the nucleus towards cytopharynx. These treatments inhibited the phagocytotic activity significantly. On the basis of the results, we propose that in *Tetrahymena* a PI 3-kinase like activity is functioning; the ability of both PI 3-kinase inhibitors and insulin to influence the synthesis or association of subunits of PI 3-kinase, and to influence F-actin remodelling and F-actin dependent processes (e.g. phagocytosis) indicate the supposed activity of PI 3-kinase in *Tetrahymena*.

Key words: IRS 1, LY 294002, PI 3-kinase, phagocytosis, signalling, *Tetrahymena*, wortmannin.

INTRODUCTION

Phosphatidylinositol (PtdIns), the basic building block for the intracellular inositol lipids in eukaryotic cells, consists of D-*myo*-inositol-1-phosphate (Ins1P) linked *via* its phosphate group to diacylglycerol. The inositol head group of PtdIns has five free hydroxyl groups, as many as three of which (except 2 and 6 position) have been found to be phosphorylated in cells, in different combination. PtdIns and its phosphorylated derivatives (phosphoinositides, PIs) all reside in membranes and are substrates for kinases (Vanhaesbroeck *et al.* 2001).

Phosphatidylinositol 3-kinase (PI 3-kinase) transfers the terminal phosphate of ATP to the D-3 position of PtdIns, PtdIns-4-monophoshate, or PtdIns-4,

Address for correspondence: Péter Kovács, 1445 Budapest, Nagyvárad tér 4, POB 370, Hungary; Fax: (36-1) 303-6968; E-mail: kovpet@dgci.sote.hu

5-bisphosphate to yield the products PtdIns-3-P, PtdIns-3,4-bisphosphate, or PtdIns-3,4,5-trisphosphate, respectively (Fruman *et al.* 1998). These PIs are not in the pathway for hormone-stimulated inositol 1,4, 5 trisphosphate production and are not substrates for PtdIns-specific phospholipase C enzymes (Serunian *et al.* 1989). PI 3-kinase has a heterodimeric structure, consisting of a regulatory 85 kD (p85) subunit and a catalytic 110 kD (p110) subunit. In addition two distinct forms of p85 subunit have been described: p85α and p85β (Otsu *et al.* 1991). The isoforms of PI 3-kinases can be divided into three classes. All PI 3-kinase catalytic subunits share a homologous region that consists of a catalytic core domain (HR1) linked to PI kinase homology domain (HR2) and a C2 domain. *In vitro*, class I PI 3-kinases can utilize PtdIns, PtdIns-4-P and PtdIns-4,5-P_2 as substrates. In cells, however, their preformed substrate appears to be PtdIns-4,5-P_2 (Vanhaesbroeck *et al.* 2001). The 3-phosphorylated inositol lipids (3-PIs) fulfil roles as second messengers by interacting with the lipid binding domains of a variety of cellular proteins. 3-PIs have been shown to impinge on many different aspects of cell biology, including vesicle trafficking, growth, DNA synthesis, regulation of apoptosis and cytoskeletal changes (Vanhaesbroeck *et al.* 2001). PI 3-kinase acts as a direct biochemical link between its phosphorylated products and a number of proteins containing intrinsic or associated tyrosine kinase activities, including the receptor for PDGF (Whitman *et al.* 1987), or insulin (Endemann *et al.* 1990). N-terminal SH2 domain of PI 3-kinase associates e.g. with insulin receptor substrate 1 (IRS 1), after insulin treatment of liver and muscle cells 10 to 20 fold increase in PI 3-kinase activity was immunoprecipitated with anti-IRS1-antibody (Folli *et al.* 1992).

The unicellular *Tetrahymena pyriformis* has receptors for signal molecules (e.g. hormones) and can respond to them (Csaba 1994). It utilizes many signalling pathways analogous to those of mammalian cells e.g. the inositol phospholipids (Kovács and Csaba 1990a), and provides evidence for the activity of enzymes such as PLA_2, PLC and PLD, which play important roles in the generation of second messengers (Kovács and Csaba 1997, 1999; Kovács *et al.* 1997).

Insulin has many different effects on *Tetrahymena*. Insulin is one of the hormones produced by *Tetrahymena* (LeRoith *et al.* 1980) as well as being recognized by its receptors (Kovács and Csaba 1990b). Exogenously administered insulin promotes glucose uptake by *Tetrahymena* (Csaba and Lantos 1975) and increases its cell division capacity (Hegyesi and Csaba 1997). It was found that insulin altered the protein composition in ciliary membrane extracts (Christopher and Sundermann 1995); the new proteins may be candidates for cellular activities in insulin imprinting, in which phenomenon *Tetrahymena* cells memorize their first encounter with insulin and then alter their sensitivity to these molecules (Csaba 1980). Insulin at micro- and nanomolar levels activates the survival and proliferation of *Tetrahymena* (Christensen *et al.* 1996, 1998). On the basis of the above-mentioned facts it is presumable that also in *Tetrahymena* PI 3-kinase is functioning properly, similarly to that of the higher eukaryotic cells.

In this study, the presence and activity of PI 3-kinase in *Tetrahymena* was examined. We investigated the possibility that PI 3-kinase is activated by insulin treatment in this unicellular organism. Effective inhibitors of PI 3-kinase may help to define the role of PI 3-kinase and its products in these cells. To study whether PI 3-kinase inhibitors wortmannin and LY294002 act on the different - presumably PI 3-kinase-dependent - physiological phenomena of *Tetrahymena*, we investigated the immunoprecipitable PI 3-kinase activity, the localization and amount of p85 and IRS 1, the phagocytotic activity and the cytoskeletal system in this ciliate organism in the presence of these inhibitors.

MATERIALS AND METHODS

Materials. Antibodies against IRS 1, p85α, acetylated tubulin, FITC-labelled anti rabbit and anti-mouse IgG, wortmannin, LY294002, FITC-labelled Con A, TRITC-labelled phalloidin, daunorubicin, protein A - agarose, chromatographic phospholipid and inositol phospholipid standards, and tryptone were obtained from Sigma (St. Louis, MO. USA). Silica gel G TLC aluminium sheets were obtained from Merck (Darmstadt, Germany). [γ-^{32}P]-ATP (specific activity 30 TBq/mM) was purchased from Institute of Isotope Kft. (Budapest, Hungary). Yeast extract was obtained from Oxoid (Unipath, Basingstoke, UK). Insulin Semilente MC is a product of Novo (Copenhagen, Denmark). All other chemicals used were of analytical grade available from commercial sources.

***Tetrahymena* cultures**. In the experiments, *T. pyriformis* GL strain was tested in the logarithmic phase of growth. The cells were cultivated at 28°C in 0.1 % yeast extract containing 1 % tryptone medium. Before the experiments the cells were washed with fresh culture medium and were resuspended at a concentration of 5×10^4 cells ml^{-1}.

Enzymatic assay for PI 3-kinase. **Preparation of cell lysates**. *Tetrahymena* cells were treated with 500 nM wortmannin, 20 μM LY 294002, or 10^{-6} M insulin for 1 h at 28°C. Untreated cells served as controls. After three washings with fresh culture medium, the cells were lysed in lysis buffer (1 % Triton X 100, 150 mM NaCl, 10 mM

Tris pH 7.4, 1 mM EDTA, 1 mM EGTA, 0.2 mM Na_3VO_4, 0.2 mM PMSF, 0.5 % Nonidet NP-40, 10 µg/ml aprotinin) for 60 min at 4°C with constant agitation. The lysates were centrifuged (10 000 x g, 4°C for 15 min). The supernatant (total cell lysate) were frozen at -80°C. (In the case of measurement of *in vitro* PI 3-kinase activity to the lysate of insulin treated cells 500 nM wortmannin were added.)

Immunoprecipitation with anti IRS 1- and anti p85- antibodies. The lysates [50 µl, 100 µg protein (measured the absorbance at 280 nm)] were incubated with either anti-IRS 1 antibody (15 µl, 5 µg) or anti-p85α antibody (15 µl, 5 µg) for 1 h and then for 30 min with 10 µl 50 % protein A - agarose at 4°C. The immunoprecipitates were washed three times with PBS/ 1% NP-40, twice with 0.5 mM LiCl/ 100 mM Tris HCl, pH 7.6, and twice with 10 mM Tris-HCl, pH 7.4/ 100 mM NaCl/ 1 mM EDTA.

Assay of PI 3-kinase activity in immunoprecipitates. PI 3-kinase activity was measured by *in vitro* phosphorylation of phosphatidylinositol (PtdIns). The pellets of immunoprecipitates were resuspended in 50 µl of 10 mM Tris (pH 7.4) containing 100 mM NaCl and 1 mM EDTA. To each pellet 10 µl of 100 mM $MgCl_2$ and 10 µl of PtdIns (2 µg/ml; sonicated in 10 mM Tris with 1 mM EDTA) were added. The reaction was started by the addition of 10 µl of 440 µM ATP containing 30 µCi of [γ-^{32}P]-ATP. After 15 min at room temperature with constant shaking, the reaction was stopped by the addition of 20 µl 8 N HCl and 160 µl of $CHCl_3$: methanol [1 : 1]. The samples were centrifuged, and the organic phase was applied to a silica gel TLC plate coated with 1 % potassium oxalate. In order to separate the highly phosphorylated phosphatidylinositols from the non-specific radioactivity remaining at the origin of the TLC plate, the plates were developed in 1-propanol/ 2 M acetic acid - 63 : 35 (v/v). After development, 0.5 cm strips were cut from the chromatogram and transferred into scintillation vials, and the radioactivity was measured by liquid scintillation counting. The individual inositol phospholipids were identified by a parallel run of authentic standards. The experiments were carried out in triplicate.

Confocal scanning laser microscopic (CSLM) analysis of *Tetrahymena* cells labelled with monoclonal anti-acetylated tubulin, anti-IRS 1, anti-p85a and TRITC-phalloidin. To localize tubulin containing structures, wortmannin (100, 500 and 1000 nM; 1 h) - treated, and untreated (control) cells were fixed in 4 % paraformaldehyde dissolved in PBS, pH 7.2. After washing with wash buffer (WB; - 0.1 % BSA in 20 mM Tris-HCl; 0.9 % NaCl; 0.05 % Tween 20, pH 8.2) the cells were incubated with monoclonal anti-acetylated tubulin antibody diluted 1 : 500 with antibody (AB) buffer (1 % BSA in 20 mM Tris-HCl, 0.9 % NaCl, 0.05 % Tween 20; pH 8.2) for 45 min at room temperature. After three washings with WB the anti-tubulin antibody treated cells were incubated with FITC-labelled anti-mouse goat IgG (diluted to 1 : 500 with AB buffer) for 45 min at room temperature. After the immunocytochemical labelling - to localize the nucleus - the cells were treated with daunorubicin (0.01 mg/ml, dissolved in PBS) for 10 min. After this incubation, the cells were washed four times with WB, and were mounted onto microscopic slides. The mounted cells were analyzed in a Bio-Rad MRC 1024 confocal scanning laser microscope (CSLM) equipped a krypton/ argon mixed gas laser as a light source. Excitation carried out with the 480 nm line (for FITC) and 530 nm (for daunorubicin) from the laser.

In the case of localization of the binding of anti-p85 and anti-IRS 1-antobodies the *Tetrahymena* cultures were treated with 500 nM wortmannin, 20 µM LY 294002 or 1 µM insulin for 60 min. After three washings with WB, the cells were treated as above. Both antibodies were diluted with AB to 1 : 500. The secondary antibody (FITC-labelled anti- rabbit goat IgG) was diluted with AB to 1 : 750.

To localize F-actin, 500 nM wortmannin- and 20 µM LY 294002-treated cells were fixed (in 4% paraformaldehyde dissolved in PBS, pH 7.2) and incubated with 0.1 µM TRITC-phalloidin (diluted in AB) for 30 min. After three washings with AB, the cells were mounted onto microscope slides and analysed in CSLM.

Flow-cytometric (FACS) analysis of the binding of anti-p85- and anti-IRS 1 antibodies to *Tetrahymena*. *Tetrahymena* populations were treated with 500 nM wortmannin, 20 µM LY 294002 or 1 µM insulin for 60 min. Untreated cells served as controls. After treatments, the cells were fixed in 4 % paraformaldehyde dissolved in PBS, pH 7.2. After washing with WB, the cells were incubated with anti-p85 or anti-IRS 1 - antibody diluted 1 : 300 with AB for 45 min at room temperature. After three washings with WB, the cells were incubated with FITC-labelled anti-rabbit IgG for 45 min at room temperature. After these incubations, the cells were washed four times with WB. To determine the non-specific binding of secondary antibodies the primary antibodies were omitted as absolute controls. The measurement of fluorescence intensity was done in a FACS Calibur flow cytometer (Beckton Dickinson, San Jose, USA), using 10^4 cells for each measurement. For the measurement and analysis a CellQuest 3.1 program was used. During the evaluation, cell populations had been separated on the basis of size defined by „gating". In the identical cell populations, the FITC-labelled second antibody content inside the cells was measured. The evaluation of the results was done by the comparison of percentage changes of geometric mean channel values to the control groups. Each experiment was repeated three times.

Analysis of the phagocytotic activity. *Tetrahymena* populations were treated with wortmannin (100 or 500 nM) or LY 294002 (10 or 20 µM) in the presence of FITC-labelled Con A (0.01 mg/ml, dissolved in fresh culture medium). Untreated cells served as controls. Samples were taken after 5, 15 and 30 min. The cells were fixed in 4 % paraformaldehyde solution (in pH 7.2 PBS), washed in two changes of PBS, and the number of fluorescent food vacuoles was quantified by a Zeiss Fluoval fluorescent microscope. In each sample, 100 cells were counted. The experiments were carried out in triplicate.

Statistical treatment of the data. Student's *t*-test was used for the evaluation of all data, with $p<0.05$ accepted as the level of statistical significance.

RESULTS

Assay of PI 3-kinase activity. Upon *in vivo* addition of both PI 3-kinase inhibitors (wortmannin and LY 294002) and insulin to *Tetrahymena* cells, a marked increase was observed in anti-IRS 1- immunoprecipitable PI 3-kinase activity, measured by PtdIns as substrate (Fig. 1). The results indicate that 1 µM insulin activates the appearance of PI 3-kinase in *Tetrahymena* lysate significantly. In this experiment, 500 nM wortmannin was shown to be nearly as effective as 1 µM insulin. LY 294002 was only ~ 30 % as effect as wortmannin

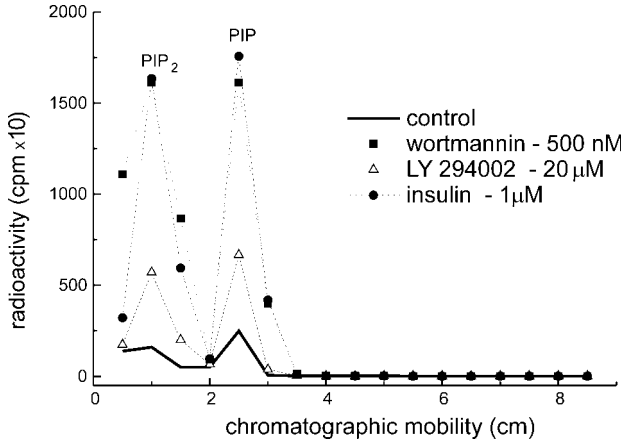

Fig. 1. Anti-IRS 1-immunoprecipitated PI 3-kinase activity of control (untreated); *in vivo* wortmannin (500 nm); LY 294002 (20 μM) and insulin (1 μM) treated *Tetrahymena*. Incorporation of [γ-^{32}P] ATP into the inositol phospholipids. The labelled lipids were extracted, separated by TLC and measured by liquid scintillation counting. The experiments were done in triplicate with a representative experiment shown.

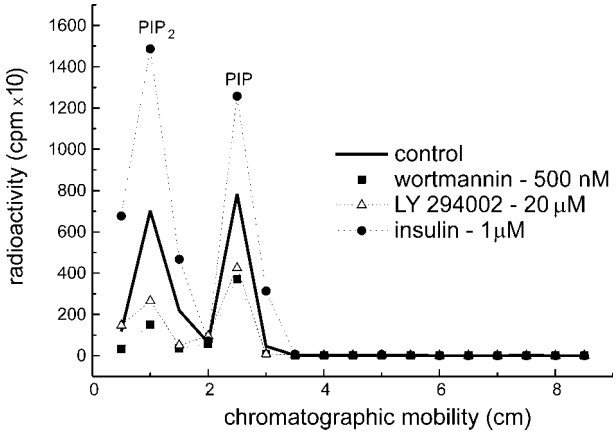

Fig. 2. Anti-p85 immunoprecipitated PI 3-kinase activity of control (untreated); *in vivo* wortmannin (500 nm); LY 294002 (20 μM) and insulin (1 μM) treated *Tetrahymena*. Incorporation of [γ-^{32}P] ATP into the inositol phospholipids. The labelled lipids were extracted, separated by TLC and measured by liquid scintillation counting. The experiments were done in triplicate with a representative experiment shown.

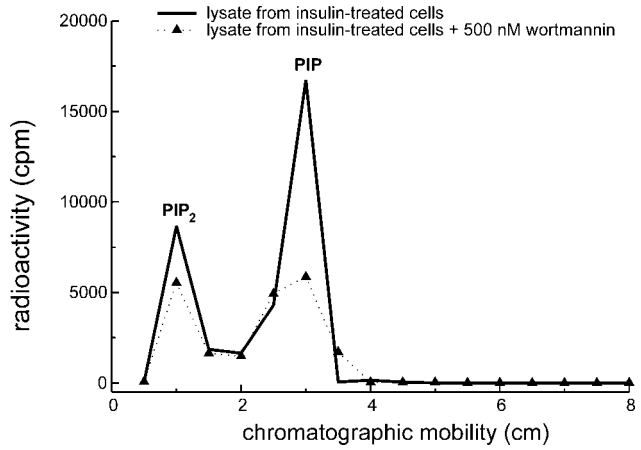

Fig. 3. *In vitro* inhibition of anti-IRS 1-immunoprecipitated PI 3-kinase activity of lysate of insulin (1 μM) treated *Tetrahymena* with 500 nM wortmannin. The experiments were done in triplicate with a representative experiment shown.

stimulating the IRS 1-antibody immunoprecipitable PI 3-kinase activity. The ability of the anti-p85 antibody to immunoprecipitate the PI 3-kinase was different compared to the anti-IRS 1. Upon addition of insulin, a marked increase was observed, but in contrast with IRS 1-immunoprecipitation, both PI 3-kinase inhibitors decreased the activity of this enzyme in the *Tetrahymena* lysate (Fig. 2).

The activity of PI 3-kinase in the lysate of insulin treated cells *in vitro* was inhibited with 500 nM wortmannin. The amount of ^{32}P-labeled PtInsP decreased significantly, while the amount of labelled $PtInsP_2$ decreased to a lesser degree (Fig. 3).

Localization of IRS 1 and p85. p85 immunoreactivity was localized in the cortex of *Tetrahymena* revealed by confocal images (Figs 4 a-d). The ciliary basal bodies (in the basal body cages) and the oral apparatus were strongly labelled with p85 antibody. Treatments with insulin and both PI 3-kinase inhibitors resulted in a significant increase of the labelling of cortical elements. In each experiment the wortmannin treatment influenced the localization of the macronucleus: the nucleus was localized forwards, near or around the cytopharynx (Figs 4, 6-8).

Immunostaining of the IRS 1 was diffusely punctuated, it was localized in the cytosol and in the oral apparatus; the cortical structures remained unlabeled (Figs 4 e-h). The localization and pattern of both immunoreactivity remained similar after the PI 3-kinase inhibitor treatments, but in the amount of labelling arose differences. These differences are clearly visible in the FACS measurements.

Measurement of binding of p85- and IRS 1-antibodies to the *Tetrahymena* by FACS. In accordance with PI 3-kinase activity measurements, on the basis of the FACS measurements, the IRS 1-immunore-

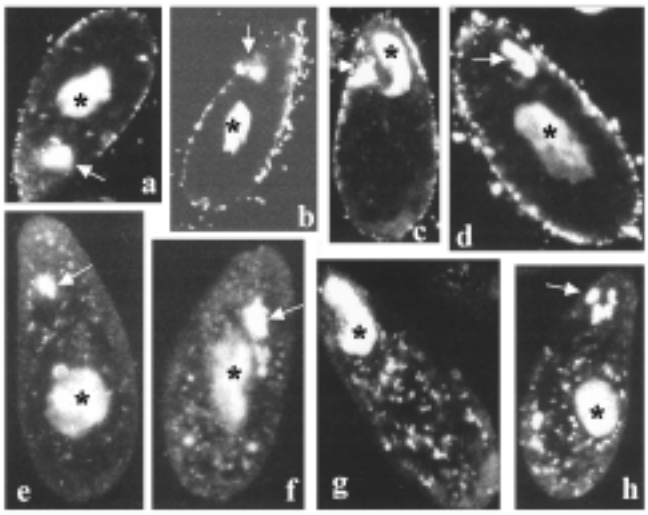

Fig. 4. Localization of p85 - (a-d) and IRS 1-antibody (e-h) in *Tetrahymena* demonstrated by FITC-labelled anti rabbit goat IgG. **a, e** - untreated (control) cells; **b, f** - 1 μM insulin treated cells; **c, g** - 500 nM wortmannin treated cells; **d, h** - 20 μM LY294002 treated cells. Confocal scanning laser microscopic pictures. Magnification x950. Asterisk - nucleus (labelled with daunorubicin); arrows - oral apparatus.

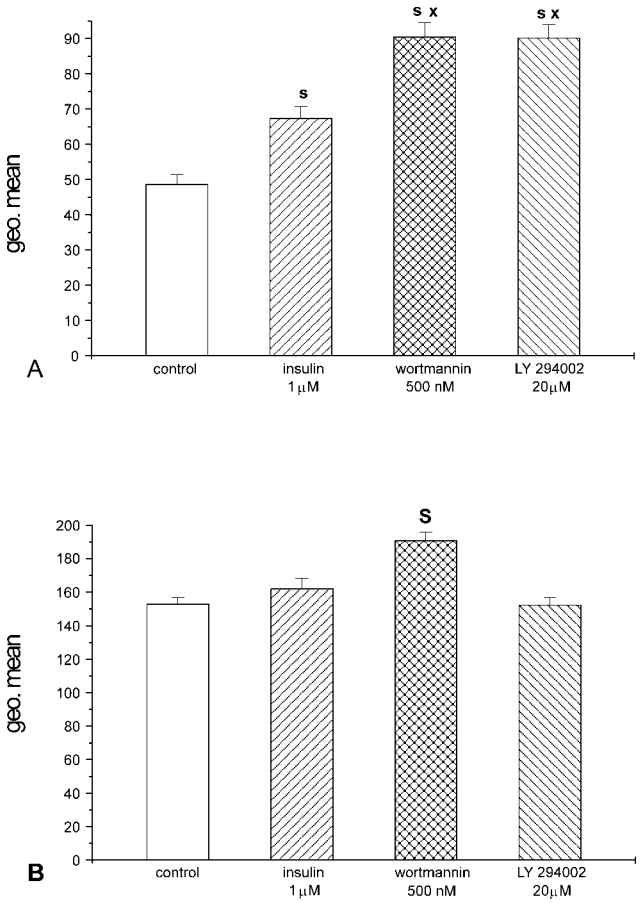

Figs 5. A, B. Flow cytometric analysis of the binding of anti-IRS 1- (**A**) and anti-p85 (**B**) antibody to the untreated; *in vivo* wortmannin (500 nm); LY 294002 (20 μM) and insulin (1 μM) treated *Tetrahymena*. The data represent the mean (±SD) derived from three separated experiments. S - $p<0.01$ to the controls; X - $p<0.01$ to the insulin treated cells.

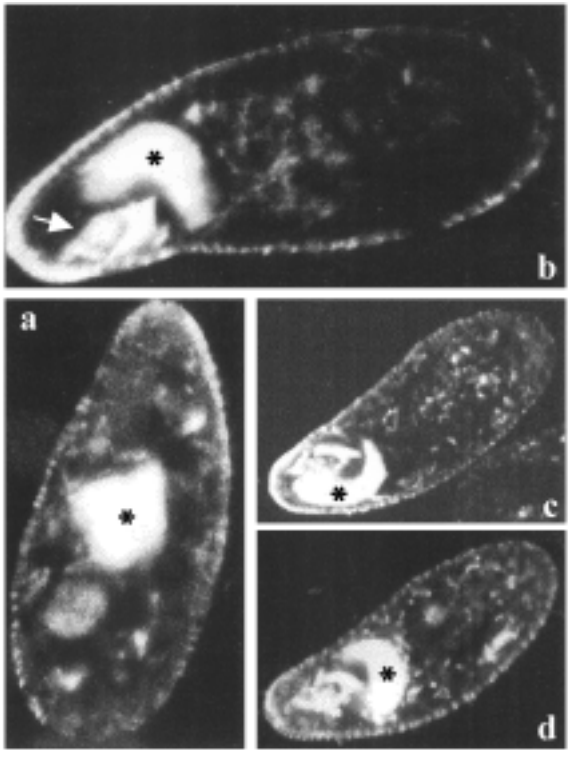

Fig. 6. Confocal scanning laser microscopic pictures of control (**a**) and 500 nM wortmannin treated cells (**b-d**). Binding of anti-acetylated tubulin antibody to the tubulin containing structures, and daunorubicin to the nuclei of *Tetrahymena*. Asterisk - nucleus (labelled with daunorubicin). arrow - oral apparatus. Magnification a - x1100; b - x1300; c, d - x850.

activity was significantly higher in the wortmannin, LY294002 and insulin treated cells than in the controls. In addition, in the wortmannin and LY 294002 treated groups further increase appeared compared with the insulin treated ones (Fig. 5 A). In the case of p85-antibody only the wortmannin treatment caused significantly higher labelling compared to the controls (Fig. 5 B).

The effect of wortmannin on the microtubular system of *Tetrahymena* cytoskeleton. After treatments with both PI 3-kinase inhibitors, no visible changes were observed in the anti-acetylated tubulin-antibody binding. The basal body cages and the components of

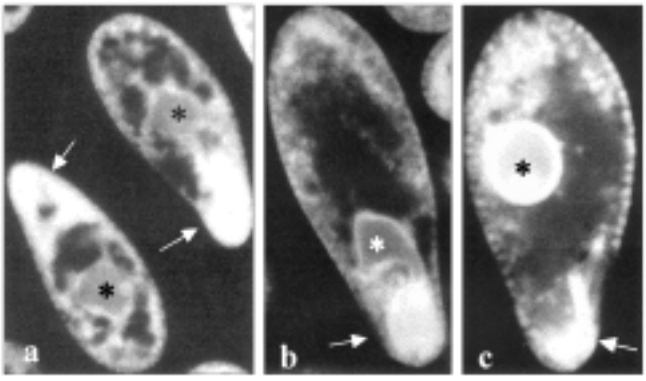

Fig. 7. Binding of TRITC-phalloidin to the F-actin containing structures of untreated (**a**), 500 nM wortmannin (**b**) and 20 µM LY 294002 (**c**) treated *Tetrahymena*. Asterisk - nucleus (labelled with daunorubicin); arrows - oral apparatus. Confocal scanning laser microscopic pictures. Magnification a - x850; b, c - x1100.

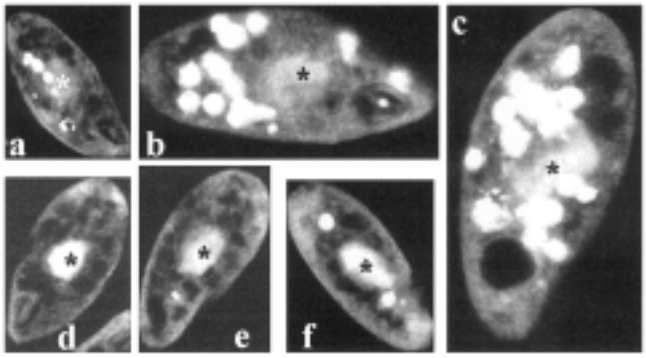

Fig. **9.** Phagocytotic activity of control (**a-c**), 10 µM (d-f) LY 294002 treated *Tetrahymena*. Incubation with FITC-Con A for 5 min (**a, d**); 15 min (b, e) and 30 min (c, f). Confocal scanning laser microscopic pictures. Asterisk - nucleus (labelled with daunorubicin). Magnification x850.

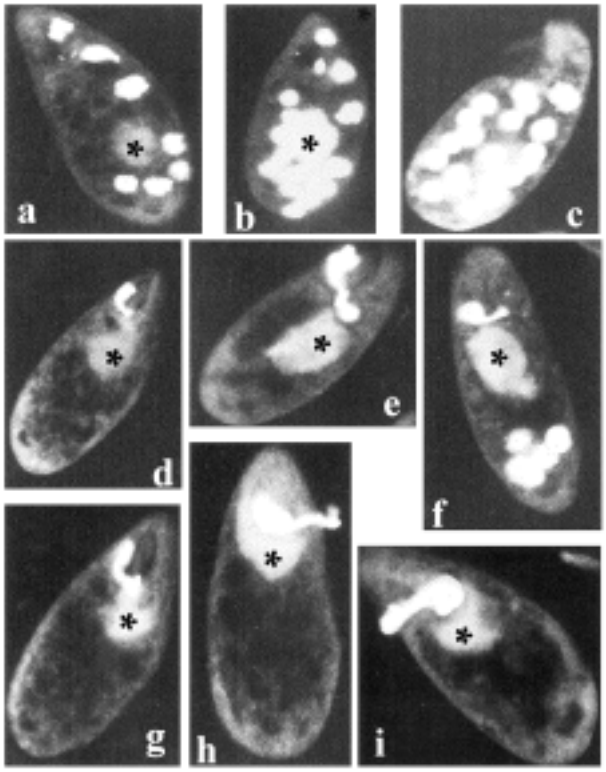

Fig. 8. Phagocytotic activity of control (**a-c**), 100 nM (**d-f**) and 500 nM (**g-i**) wortmannin treated *Tetrahymena*. Incubation with FITC-Con A for 5 min (a, d, g); 15 min (b, e, h) and 30 min (c, f, i). Confocal scanning laser microscopic pictures. Asterisk - nucleus (labelled with daunorubicin). Magnification x850.

oral apparatus (undulating membrane and adoral membranelles) were strongly labelled in each concentration of wortmannin used. These pictures clearly show the translocation of the nucleus to the cytopharynx (Fig. 6). In contrast, the other PI 3-kinase inhibitor LY 294002, failed to alter the position of nucleus.

The effect of wortmannin and LY 294002 on the localization of F-actin. In contrast to tubulin, the pattern of localization of F-actin was different in the treated cells, compared to the controls, revealed by TRITC-phalloidin labelling. In the control cells, the basal body cages and the elements of oral apparatus were strongly labelled with TRITC-phalloidin, and also in the cytoplasm, mostly around the food vacuoles and nucleus, considerable amount of labelling was visible (Fig. 7 a). After wortmannin treatments, the internal part of the cells was free from the F-actin, but these treatments did not alter the labelling of basal body cages and the oral apparatus with phalloidin (Fig. 7 b). After LY 294002 treatment, the cytoplasmic F-actin content was limited to the caudal part of the cells, but these treatments also did not alter the labelling of cortical structures and oral apparatus. The strong nuclear fluorescence was remarkable (Fig. 7 c).

Effect of wortmannin and LY 294002 on the phagocytotic activity of *Tetrahymena*. The food vacuoles were labelled strongly with FITC-labelled Con A; thus the vacuoles were easily counted in fluorescent microscope. The phagocytotic activity was inhibited considerably by both wortmannin concentrations (100 and 500 nM) (Table 1). During wortmannin treatments, the cavity of cytopharynx was markedly labelled with FITC-Con A, and the labelled material often was hanging out from the cytopharynx. In presence of wortmannin,

Table 1. Phagocytotic activity of control, wortmannin (100 and 500 nM) and LY 294002 (10 and 20 μM) treated *Tetrahymena*. The data represent the mean (±SD) derived from three separated experiments. **a** - labelling only in the cytopharynx; **b** - very small vacuoles under the cytopharynx. **c** - p<0,01 to the controls.

	5 min	15 min	30 min
control	6.3 ± 0.49	13.4 ± 1.34	18.3 ± 1.76
wortmannin 100 nM	**a**	**a**	4.7 ± 0.51**c**
wortmannin 500 nM	**a**	**a**	**a**
LY 294002 10 μM	1.6 ± 0.2**c**	2.3 ± 0.4**c**	4.9 ± 0.37**c**
LY 294002 20 μM	0	1.4 ± 0.22**bc**	2.1 ± 0.29**c**

food vacuoles were perceptibly separate with difficulty from the cytopharynx-membrane (Fig. 8). LY 294002 treatments also inhibited significantly the formation of food vacuoles (Table 1), the separated vacuoles were often very small, but did not affect the labelling of cytopharynx, as wortmannin did (Fig. 9).

DISCUSSION

Although phosphatidylinositol (PtdIns) represents only a small percentage of total cellular phospholipids, it plays a crucial role in signal transduction as the precursor of several second messenger molecules. The products of different PI-kinases, among others the 3-phosphorylated inositol lipids produced by PI 3-kinases, fulfil roles as second messengers by interacting with the lipid-binding domains of a variety of cellular proteins. Similarly to the higher eukaryotic cells, the ciliated unicellular organism *Tetrahymena* also contains PtdIns, which participates in its signalling mechanism (Kovács and Csaba 1990a).

Insulin has many different effects on *Tetrahymena*, influencing glucose uptake (Csaba and Lantos 1975), cell division (Hegyesi and Csaba 1997), survival (Christensen *et al.* 1996, 1998), phosholipase D activity (Kovács *et al.* 1996), insulin production (Csaba *et al.* 1999) and on the alteration of the protein composition in ciliary membrane extracts (Christopher and Sundermann 1995). Thus we supposed that also in *Tetrahymena* a PI 3-kinase like activity is functioning properly, one of the key enzymes in the action of insulin. In the present study, the presence, localization and activity of PI 3-kinase and the effects of PI 3-kinase inhibitors wortmannin and LY 294002 on different physiological phenomena of *Tetrahymena* were investigated.

Wortmannin and LY 294002 are structurally unrelated, cell-permeable compounds. Wortmannin binds covalently to the PI 3-kinase catalytic subunit, whereas LY 294002 is a competitive inhibitor of ATP binding-site (Vlahos *et al.* 1994). Probably these different properties lead to the divergences in the effects of PI 3-kinase inhibitors on *Tetrahymena*.

In most cell types, insulin stimulates tyrosine phosphorylation of insulin receptor substrate 1 (IRS 1). IRS 1 contains 14 potential tyrosine phosphorylation sites; the tyrosine phosphorylation generates docking sites for several SH2-containing proteins (White 1998). Among these, the predominant partner seems to be the p85 regulatory subunit of the PI 3-kinase. This enzyme is stimulated by a number of growth factors, including insulin, insulin-like growth factor and EGF (Rudermann *et al.* 1990).

In the present experiments using IRS 1- and p85 antibodies immunoprecipitable PI 3-kinase activity was found in *Tetrahymena* (Figs 1-3). These activities have been stimulated significantly with *in vivo* insulin treatment (Figs 1, 2). *In vivo* administration of wortmannin and LY 294002 caused also alterations in the immunoprecipitable PI 3-kinase activity. In case of IRS-1- antibody-precipitated material both PI 3-kinase inhibitors elevated the activity significantly (albeit the LY 294002 resulted in a lower value of this activity). It seems to be very difficult to explain the stimulatory effect of these molecules in the light of their inhibitory effects in mammalian cells. One of the possible explanations is that these treatments induce an enzyme-and/or IRS 1-overproduction in *Tetrahymena*; the higher amount of these molecules enables these organisms to carry out the appropriate functions. In contrast with IRS 1-antibody precipitation, lysate of both inhibitor-treated cells contained less PI 3-kinase activity in the anti-p85 immunoprecipitate than the controls. Similarities were found also in the FACS measurements: the binding of anti-IRS 1 antibody to the insulin, wortmannin and LY 294002-treated cells was significantly higher than to the controls, while the binding of p85 antibody was significantly higher only in the wortmannin-treated cells. These phenomena can derive also from the SH2-domain of p85 regulatory subunit of PI 3-kinase. If the complete enzyme has internal SH2-domain, it is capable to bind to the IRS 1; thus if the p85 regulatory and p110 catalytic subunits are associated, with IRS 1-antibody can immunoprecipitate higher PI 3-kinase activity; whereas p85 antibody can detect without respect to the association of this subunit (or integrity of SH2 domains of p85). In

accordance with these premises, in *Tetrahymena* the above mentioned treatments in all probability influence the association of subunits of PI 3-kinase, and leave the amount of synthesized molecules nearly unchanged. Another additional possibilities can be considered to approach this problem: (a) PI 3-kinase of *Tetrahymena* may not follow mechanisms of action described for mammalian enzymes; (b) phosphorylation and dephosphorylation of IRS-1 occurring likely in a response to insulin and PI 3-kinase inhibitors may change its reactivity with antibodies affecting its immunoprecipitation and intensity of its fluorescence.

In vitro, wortmannin seems to be a potent PI 3-kinase inhibitor: it strongly inhibits PI 3-kinase activity in the lysate of insulin-stimulated *Tetrahymena* (Fig. 3). This means that *in vivo* and *in vitro* methods can produce divergent results, as it was demonstrated earlier by us in other systems of *Tetrahymena* (Kovács and Csaba 1999).

To investigate the role of PI 3-kinase activity in the function of cytoskeleton and membrane-traffic dependent processes (e.g. phagocytosis), phagocytotic activity (formation of food vacuoles) was measured in wortmannin and LY 294002 treated cells (Table 1).

In *Tetrahymena* which has a more or less fixed cell surface area, because of the presence of a pellicle, endocytosis cannot occur by an invagination of the cell membrane. In this case, new membrane must be incorporated into the cytopharyngeal membrane to provide the limiting membrane for a new food vacuole. The source of the food vacuolar membrane may be newly synthesized, or recycling-membrane vesicles derived from older food vacuoles or from the Golgi complex (Nilsson 1979). Both possibilities require an intensive membrane-flow - mostly from caudal part of the cell towards cytopharynx. On the basis of experimental results obtained by using of different drugs it may be concluded that actin microfilaments play an important role in the formation of food vacuoles and in the membrane recycling processes (Nilsson 1979).

In connection with endocytosis, a variety of phosphoinositide functions have been discovered. In this process, phosphoinositides provide signals for targeting vesicles to specific fusion sites for membrane trafficking and have crucial roles in cytoskeletal reorganization (Takenawa and Itoh 2001).

In contrast to tubulin (where no visible changes appeared after treatments with both PI 3-kinase inhibitors), in the pattern and localization of F-actin revealed differences in the untreated and PI 3-kinase-inhibitor treated cells. The cortex contains F-actin also in the treated cells, whereas these treatments were accompanied by dramatic deficit in a subset of F-actin enriched structures in the inner part of cytoplasm (Fig. 7). This finding suggests that these treatments influence the remodelling of actin cytoskeleton by changing PI levels. In these cells the position of nucleus became irregular: the nucleus localized near or around the cytopharynx (Fig. 6). In wortmannin-treated cells the mechanism that allows cells maintain the normal localization of organelles, was significantly impaired. Perceptibly, a cytoplasmic stream pushed the nucleus forward. Also the inhibited phagocytosis refers to this stream. This phenomenon is maybe due to the localization of nucleus near or around the cytopharynx, which obstructs the traffic of food vacuoles. The FITC-labelled Con A binds to the content of food vacuoles of *Tetrahymena*. In wortmannin-treated cells the FITC-labelled Con A sometimes hanged out from the cavity of cytopharynx, indicating the forward stream of cytoplasmic elements (Fig. 8).

Treatments with LY 294002 also inhibit phagocytotic activity of *Tetrahymena* significantly, notwithstanding in these cells we did not find alterations in the localization of nucleus, and also the formation of food vacuoles seems to be normal, but the number and size of vacuoles became restricted (Fig. 9). These phenomena refer to the different effect of the wortmannin and LY 294002; this latter exerts its effect on the cytoskeleton probably through some other means than wortmannin.

The PI 3-kinase localization is limited to the cortical structures of *Tetrahymena*, such as basal body cages and the oral apparatus. PI 3-kinase associates with γ and α tubulin. After stimulation the cells with some growth factors and insulin, PI 3-kinase associates also with γ-tubulin (Kapeller *et al.* 1995). Presumably the cortical labelling of *Tetrahymena* with p85 antibody - on the basis of this phenomenon - is due to the γ-tubulin content of basal bodies; γ-tubulin is permanently associated with basal bodies in ciliates (Liang *et al.* 1996) (Figs 4 a-d). Another possibility for the cortical localization of p85 antibody is that this subunit has an inter-SH2 domain, which binds to PtdIns-4, 5. This property may provide a mechanism for concentrating PI 3-kinase at membranes rich in these lipids (Fruman *et al.* 1998).

The localization of IRS 1 is not limited to the cortex; the labelling with IRS 1-antibody was restricted to the oral apparatus and spot-like manner in the cytoplasm (Figs 4 e-h). Localization of both antigen (p85 and IRS 1) is unchanged after PI 3-kinase-inhibitor and

insulin treatments, while the amount of immunoreactive materials was changed.

From the results of the present experiments several conclusions can be drawn: (a) in *Tetrahymena* a PI 3-kinase-like activity functions; a material with PI 3-kinase activity can be immunoprecipitated with p85 and IRS 1-antibodies; (b) *in vivo* treatments with PI 3-kinase inhibitors and insulin alter the amount or activity of this enzyme; (c) *in vitro* this activity can be inhibited with wortmannin; (d) inhibitors of PI 3-kinase activity (wortmannin and LY 294002) and insulin alter the immunoreactivity of p85 and IRS 1-antibodies of *Tetrahymena*; (e) treatments with inhibitors decreased the amount of F-actin, inhibited the mechanism which allows the cells maintain the normal position of organelles, and inhibited the phagocytotic activity.

Acknowledgement. Contract/grant sponsors: National Research Found; contract/grant number: OTKA-T-037303 and Scientific Research Council, Ministry of Health, Hungary; contract/grant number:213/2000.

REFERENCES

Christensen S. T., Quie H., Kemp K., Rasmussen L. (1996) Insulin produces a biphasic response in *Tetrahymena thermophila* by stimulating cell survival and activating cell proliferation in two separate concentration intervals. *Cell Biol. Int.* **20:** 437-444

Christensen S. T., Leick V., Rasmussen L., Wheatley D. N. (1998) Signaling in unicellular eukaryotes. *Int. Rev. Cytol.* **177:** 181-253

Christopher G. K., Sundermann C. A. (1995) Isolation and partial characterization of the insulin binding site in *Tetrahymena pyriformis*. *Tissue Cell* **27:** 585-589

Csaba G. (1980) Phylogeny and ontogeny of hormone receptors: the selection theory of receptor formation and hormonal imprinting. *Biol. Rev.* **55:** 47-63

Csaba G. (1994) Phylogeny and ontogeny of chemical signalling: origin and development of hormone receptors. *Int. Rev. Cytol.* **155:** 1-48

Csaba G., Lantos T. (1975) Effect of insulin on the glucose uptake in Protozoa. *Experientia* **31:** 107-109

Csaba G., Gaál A., Kovács P., Simon G. (1999) Prolonged elevation of insulin content in the unicellular *Tetrahymena* after insulin treatment: induction of insulin production or storage? *Cell Biochem. Funct.* **17:** 165-173

Endemann G., Yonezawa K., Roth R. A. (1990) Phosphatidylinositol kinase or an associated protein is a substrate for the insulin receptor tyrosine kinase. *J. Biol. Chem.* **265:** 396-400

Folli F., Saad M. J. A., Backer J. M., Kahn C. R. (1992) Insulin stimulation of phosphatidylinositol 3-kinase activity and association with insulin receptor substrate 1 in liver and muscle the intact rat. *J. Biol. Chem.* **267:** 22171-22177

Fruman D. A., Meyers R. E., Cantley L. C. (1998) Phosphoinositide kinases. *Annu. Rev. Biochem.* **67:** 481-508

Hegyesi H., Csaba G. (1997) Time and concentration-dependence of the growth-promoting activity of insulin and histamine in *Tetrahymena*. Application of the MTT-method for the determination of cell proliferation in a protozoan model. *Cell Biol. Int.* **21:** 289-293

Kapeller R., Toker A., Cantley L. C., Carpenter C. L. (1995) Phosphoinositide 3-kinase binds constitutively to alpha/beta-tubulin and binds to gamma-tubulin in response to insulin. *J. Biol. Chem.* **270:** 25985-25991

Kovács P., Csaba G. (1990a) Involvement of phosphatidylinositol (PI) system in the mechanism of hormonal imprinting. *Biochem. Biophys. Res. Commun.* **170:** 119-126

Kovács P., Csaba G. (1990b) Evidence of the receptor nature of the binding sites induced in *Tetrahymena* by insulin treatment. A quantitative cytofluorimetric technique for the study of binding kinetics. *Cell Biochem. Funct.* **8:** 49-56

Kovács P., Csaba G. (1997) PLA_2 activity in *Tetrahymena pyriformis*. Effects of inhibitors and stimulators. *J. Lipid Mediat. Cell Signal* **15:** 223-247

Kovács P., Csaba G. (1999) Fluorimetric analysis of phosopholipase activity in *Tetrahymena pyriformis* GL. *Biosci. Rep.* **19:** 81-87

Kovács P., Csaba G., Ito Y., Nozawa Y. (1996) Effect of insulin on the phospholipase-D activity of untreated and insulin-pretreated (hormonally imprinted) *Tetrahymena. Biochem. Biophys. Res. Commun.* **222:** 359-361

Kovács P., Csaba G., Nakashima S., Nozawa Y. (1997) Phospholipase D activity in the *Tetrahymena pyriformis*. *Cell Biochem. Funct.* **15:** 53-60

LeRoith D., Schiloach J., Roth J., Lesniak M. A. (1980) Evolutionary origins of vertebrate hormones: substances similar to mammalian insulin are native to unicellular eukaryotes. *Proc. Natl. Acad. Sci. USA* **77:** 6184-6186

Liang A., Ruiz F., Heckmann K., Klotz C., Tollon Y., Beisson J., Wright M. (1996) Gamma-tubulin is permanently associated with basal bodies in ciliates. *Eur. J. Cell Biol.* **70:** 331-338

Nilsson J. R. (1979) Phagotrophy in *Tetrahymena*. In: Biochemistry and Physiology of Protozoa. Second Edition, Vol. 2. Academic Press, New York, 339-379

Otsu M., Hiles I., Gout I., Fry M. J., Ruiz-Larrea F., Panayotou G., Thompson A., Dhand R., Hsuan J., Totty N. (1991) Characterization of two 85 kD proteins that associate with receptor tyrosine kinases, middle-T/pp60c-src complexes, and PI 3-kinase. *Cell* **65:** 91-104

Rudermann B. N., Kapeller R., White M. F., Cantley L. C. (1990) Activation of phosphatidylinositol 3-kinase by insulin. *Proc. Natl. Acad. Sci. USA* **87:** 1411-1415

Serunian L. A., Haber M. T., Fukui T., Kim J. W., Rhee S. G., Lowenstein J. M., Cantley L. C. (1989) Phosphoinositides produced by phosphatidylinositol 3-kinase are poor substrates for phospholipases C from rat liver and bovine brain. *J. Biol. Chem.* **264:** 17809-17815

Takenawa T., Itoh T. (2001) Phosphoinositides, key molecules for regulation of actin cytoskeletal organization and membrane traffic from the plasma membrane. *Biochim. Biophys. Acta* **1533:** 190-206

Vanhaesbroeck B., Leevers S. J., Ahmadi K., Timms J., Katso R., Driscoll P. C., Woscholski R., Parker P. J., Waterfield M. D. (2001) Synthesis and function of 3-phosphorylated inositol lipids. *Annu. Rev. Biochem.* **70:** 535-602

Vlahos C. J., Matter W. F., Hui K. Y., Brown R. F. (1994) A specific inhibitor of phosphatidylinositol 3-kinase, 2-(4-morpholinyl)-8-phenyl-4H-1-benzopyran-4-one (LY294002). *J. Biol. Chem.* **269:** 5241-5248

White M. F. (1998) The IRS-signalling system: a network of docking proteins that mediate insulin action. *Mol. Cell Biochem.* **182:** 3-11

Whitman M., Kaplan D., Roberts T., Cantley L. C. (1987) Evidence for two distinct phosphatidylinositol kinases in fibroblasts. Implications for cellular regulation. *Bichem. J.* **247:** 165-174

Received on 4th March, 2003; revised on 22nd July, 2003; accepted on 24th July, 2003

Acta Protozool. (2003) 42: 287 - 307

ACTA
PROTOZOOLOGICA

Phylogenetic Position and Ultrastructure of Two *Dermocystidium* Species (Ichthyosporea) from the Common Perch (*Perca fluviatilis*)

Marketta PEKKARINEN[1], Jiří LOM[2], Colleen A. MURPHY[3], Mark A. RAGAN[4] and Iva DYKOVÁ[2]

[1]Department of Biosciences, Division of Animal Physiology, University of Helsinki, Finland; [2]Institute of Parasitology, Academy of Sciences of the Czech Republic, České Budějovice, Czech Republic; [3]Institute for Marine Biosciences, National Research Council of Canada, Halifax, Nova Scotia, Canada; [4]Institute for Molecular Bioscience, University of Queensland, Brisbane, Australia

Summary. Sequences of small-subunit rRNA genes were determined for *Dermocystidium percae* and a new *Dermocystidium* species established as *D. fennicum* sp. n. from perch in Finland. On the basis of alignment and phylogenetic analysis both species were placed in the *Dermocystidium-Rhinosporidium* clade within Ichthyosporea, *D. fennicum* as a specific sister taxon to *D. salmonis,* and *D. percae* in a clade different from *D. fennicum*. The ultrastructures of both species well agree with the characteristics approved within Ichthyosporea: walled spores produce uniflagellate zoospores lacking a collar or cortical alveoli. The two *Dermocystidium* species resemble *Rhinosporidium seeberi* (as described by light microscope), a member of the nearest relative genus, but differ in that in *R. seeberi* plasmodia have thousands of nuclei discernible, endospores are discharged through a pore in the wall of the sporangium, and zoospores have not been revealed. The plasmodial stages of both *Dermocystidium* species have a most unusual behaviour of nuclei, although we do not actually know how the nuclei transform during the development. Early stages have an ordinary nucleus with double, fenestrated envelope. In middle-aged plasmodia ordinary nuclei seem to be totally absent or are only seldom discernible until prior to sporogony, when rather numerous nuclei again reappear. Meanwhile single-membrane vacuoles with coarsely granular content, or complicated membranous systems were discernible. Ordinary nuclei may be re-formed within these vacuoles or systems. In *D. percae* small canaliculi and in *D. fennicum* minute vesicles may aid the nucleus-cytoplasm interchange of matter before formation of double-membrane-enveloped nuclei. *Dermocystidium* represents a unique case when a stage of the life cycle of an eukaryote lacks a typical nucleus.

Key words: *Dermocystidium percae*, *D. fennicum* sp. n., development, Ichthyosporea, *Perca fluviatilis*, phylogenetic position, ultrastructure.

INTRODUCTION

The phylogenetic position and composition of the genus *Dermocystidium* Perez, 1908 have long been unclear. Ragan *et al*. (1996) included phylogenetic analysis in their study and assigned the genus in a group called the DRIPs clade (*Dermocystidium*, rosette agent, *Ichthyophonus*, *Psorospermium*), near the dichotomy of animals and fungi. Ragan *et al*. (1996) examined two representatives of *Dermocystidium*, *Dermocystidium* sp. from brook trout and *D. salmonis* Davis, 1947 from chinook salmon in their study. Later, Herr *et al*. (1999), when studying the phylogenetic affinities of *Rhinospo-*

Address for correspondence: Jiří Lom and Iva Dyková, Institute of Parasitology, Academy of Sciences of the Czech Republic, Branišovská 31, 370 05 České Budějovice, Czech Republic; E-mail: jlom@paru.cas.cz, iva@paru.cas.cz

ridium seeberi, a pathogen of humans and animals, established a new clade called Mesomycetozoa for *Rhinosporidium* and the former DRIPs.

Herr *et al*. (1999) were perhaps unaware of the work of Cavalier-Smith (1998) who in his discussion on probable evolution of Animalia and Fungi from Choanozoa erected for the former DRIPs clade a new class Ichthyosporea, which thus has a priority over Mesomycetozoa, and included it in the subphylum Choanozoa. He chose the name Ichthyosporea for the class because these organisms producing unicellular walled spores infect mostly fish. The walls of the trophic stages lack chitin. If zoospores are present, they are uniflagellate, without a collar or cortical alveoli. The new class included two orders, Dermocystida and Ichthyophonida. Cavalier-Smith (1998) assumed that the members of Dermocystida have flat mitochondrial cristae and those in Ichthyophonida have tubulovesicular cristae. Vacuoles with contents of different density, lipid globules and inclusion bodies are common in Ichthyosporea (see references to description of different species in the Discussion).

Lom and Dyková (1992) defined the description of the genus *Dermocystidium*, dividing the known species into three groups according to their morphology and types of infection. At that time about 20 species were known, mostly thanks to light microscope observation. Knowledge of the life cycle was incomplete and their phylogenetic position was enigmatic. To group 1 (e.g., *D. branchiale* Léger, 1914) were assigned walled multinuclear plasmodia (cysts) formed usually in the skin or gills of fish. These plasmodia divide to form round spores with a solid refractile body. In group 2 (e.g., *D. koi* Hoshina and Sahara, 1950), thick-walled hyphae are formed, and the spores are of variable size. The species in group 3 (*D. macrophagi* van de Moer, Manier and Bouix, 1987) cause visceral infections, a large thick-walled plasmodium is absent and the spores have a large central vacuole instead of an inclusion.

A member of the first group, *D. percae* Reichenbach-Klinke, 1950, described from the skin of the common perch, *Perca fluviatilis* L., has, since its original description in Germany (Reichenbach-Klinke 1950), been found in perch in the Czech Republic (Ergens and Lom 1970), in the former USSR (Pronin 1976) and in Estonia and Finland (Pekkarinen and Lotman 2003). Pronin (1976) and Pekkarinen and Lotman (2003) recorded two morphological types of cysts; Pronin assigned both to the same species *D. percae*, while Pekkarinen and Lotman assigned one type to *D. percae* and the other to an unnamed species *Dermocystidium* sp. The developmental cycles of both vicarious species include walled plasmodium stages, formation of spores from the plasmodium, and ultimately formation of numerous zoospores from each spore (Pekkarinen and Lotman 2003). The two species differ only slightly in morphology from each other in the different shape of the plasmodial cysts and the different thickness of the cyst wall. Moreover, they have different site preferences in the host. The fine structure of the plasmodium, its subsequent developmental stages and nuclear structure remain unknown.

This study presents an outline of the ultrastructure of the sequential stages of both species, and particularly tries to solve the puzzle of the plasmodium nucleus: on the basis of light microscope studies by Pekkarinen and Lotman (2003) it was thought that the nucleus of the young plasmodium later changes to a reticulate structure containing chromatin clumps. The molecular analysis included in this study aims to shed more light on the relationships and position of these organisms in the phylogenetic tree of the Ichthyosporea and to solve the mutual relationship of both *Dermocystidium* species.

MATERIALS AND METHODS

Collecting and management of the fish. The common perch were caught in two lakes in Finland, Lake Hirvijärvi in southern Finland and Lake Juurusvesi in central Finland. Infected fins were removed and refrigerated until preparation. Material from several years was used in the study.

The cysts for 18S rDNA analysis originated from perches collected in Lake Hirvijärvi in the summer of 2000. One large cyst with spores of *Dermocystidium* sp. was used, and several cysts of *D. percae* from a few individual perch were pooled for the sample. These latter cysts also contained pre-spore stages. The cysts were purified from host tissue, put in a very small amount of dilute NaCl, and frozen. The samples were packed with dry ice for the courier transportation to Canada (Institute for Marine Biosciences, Halifax, Nova Scotia). The samples did not thaw during the transport.

In order to find early stages of *D. percae*, an experimental infection was carried out in August 2001. 0-group perch were collected from inshore areas of lake Hirvijärvi and acclimated to aquarium conditions (tap water 20-23°C) for a few days. The fish were fed with aquarium fish food (chironomid and mosquito larvae), and most of the water in both test and control aquaria was replaced with aged tap water at least once a day. Cysts of *D. percae* were removed from perch fins in early August, put in tap water in small Petri dishes (at about 22-25°C) for 5 days (only two cysts produced zoospores). In mid-August the contents of the already ruptured cysts were mixed with the food offered to the 0-group test fish. The zoospore culture was repeated with new cysts (for 2 days), and the products were

mixed in part with the fish food and in part with the water in the test aquarium on August 18. After two weeks the test and control fishes were put into flowing, charcoal-filtered tap water (14-17°C) (the same feeding was continued). The experiment ended on October 23, 2001. For zoospore studies lower incubation temperatures were also used (10 and 15-17°C).

Amplification and sequencing of 18S rDNAs. Spores of *Dermocystidium* sp. and *D. percae* were collected by centrifugation, and DNA was extracted using the Y-DER yeast extraction reagent kit (Pierce). The gene encoding nuclear small-subunit (18S) ribosomal RNA was amplified using universal primers GO1 and GO7 (Saunders and Kraft) and the rTth DNA Polymerase XL kit (Perkin Elmer). Amplification conditions were: hot start (AmpliWax PCR Gem50 beads: (Perkin Elmer) at 94°C for 2 min; 16 cycles of denaturation at 94°C for 15 s, reannealing at 65°C for 4 min, then 12 cycles with the same denaturation conditions but extending the reannealing step by 15 s per cycle; finally 72°C for 10 min before cooling to 4°C.

A 1-µl aliquot was removed and placed into a new amplification reaction under the same conditions, except that the reannealing step was conducted at 52°C. Gel electrophoresis of the products showed a single clean amplicon in each case. Primers and reagents were removed on a Centricon-100 column, and amplicons were sequenced directly on an ABI 377 (Applied Biosystems) using the ABI Prism Big Dye Terminator Cycle Sequencing Ready reaction kit and standard 18S rDNA primers (Saunders and Kraft 1994).

The amplicon from *Dermocystidium* sp. sequenced smoothly, but that from *D. percae* showed overlaid signals indicative of a heterogeneous product. Therefore the amplicon was cloned into PCR 2.1 vector (Invitrogen) and colonies for individual DNA preparation and sequencing were selected.

Alignment and phylogenetic analyses. rDNA sequences were aligned visually with others from the Ichthyophonales (see legend to Fig. 1), taking secondary structure (Gutell 2002) into account as necessary. Ambiguous nucleotides (N, R, Y) at positions where all other nucleotides at that position in an alignment were identical were reassigned to agree with the others. A small number of positions (columns) that could not be securely aligned, or were mostly empty (e.g. extreme 5' and 3' termini), were removed prior to phylogenetic analysis, yielding a 25 species x 1811 position matrix. Bayesian trees were inferred using MRBAYES 2.0 (Huelsenbeck and Ronquist 2001, Huelsenbeck *et al*. 2001) under a general time-reversible model (Yang 1994), using a discrete (8-category) approximation to a continuous Γ model of nucleotide substitution rates across sites (Yang 1993) and Markov chain temperature initialized at 0.2000. In most analyses eight Markov chains were propagated for 50000 Markov-chain generations; burnin was conservatively set at 1000 generations. For other phylogenetic methods we used programs in PHYLIP 3.6a2.1 (Felsenstein 2002).

Sequences. For explanation, see legend to Fig. 1.

Electron microscopy. The parasites were fixed either *in situ* in fish fins or separately, or embedded in nonfish tissue or gelatin. The pre-fixatives used were 2.5-3 % phosphate-buffered (0.1M, pH 7.2) glutaraldehyde (usually), 4% buffered formaldehyde, or formaldehyde-glutaraldehyde or formaldehyde-glutaraldehyde-picric acid mixtures. The 1% buffered osmium tetroxide fixation was sometimes used alone. The excess pre-fixative was washed off from the samples with the phosphate buffer, and the samples were treated with 1% OsO_4 in the phosphate buffer, dehydrated with an ethanol series and embedded in Epoxy resin. Ultrathin sections from the samples were stained with uranyl acetate and lead citrate. The subsequent osmification-embedding protocol, final sectioning and the subsequent staining of the sections were made with the help of the staff of the EM unit, Institute of Biotechnology, University of Helsinki. The sections were examined and photographed in the same unit with a Jeol 1200EX electron microscope. Some prefixed or already embedded samples were examined with a Jeol 1010 electron microscope in the Institute of Parasitology of the Academy of Sciences of the Czech Republic in České Budějovice.

RESULTS

18S rRNA genes of the new *Dermocystidium* sp. and *D. percae*

Sequence determination. Amplified rDNAs of lengths 1812 (*Dermocystidium* sp.) and 1857-1865 (*D. percae*) were recovered and sequenced. One clone of *D. percae* had to be re-amplified (using inset primers) prior to sequencing, yielding only 1792 nucleotides. The additional length in the *D. percae* sequences results from 19 insertions of 1 to 13 nucleotides each. Accession numbers, gi numbers and other information for these ten new sequences are presented in Table 1. No introns were found.

The 9 sequences recovered from the bacterial clones expressing 18S rDNA of *D. percae* differ among themselves in 52 positions (~2.8%), with the greatest pairwise difference being 33 positions (1.77%). By fitting the *D. percae* SSU-rDNA to an established secondary structure model (Gutell 2002) we identified the type of structural region in which these differences occur. Among the 24 differences occurring in only one of these nine sequences, 6 are internal to a stem region; 4 expand a

Table 1. Nuclear small-subunit ribosomal RNA genes as recovered in *Dermocystidium.*

Species or clone	Length (nt)	Accession no.	gi number
D. percae 1	1853	AF533941	28629202
D. percae 4	1865	AF533942	28629203
D. percae 5	1863	AF533943	28629204
D. percae 6	1861	AF533944	28629205
D. percae 9	1792	AF533945	28629206
D. percae 33	1857	AF533946	28629207
D. percae 34	1863	AF533947	28629208
D. percae 35	1863	AF533948	28629209
D. percae 52	1862	AF533949	28629210
D. fennicum sp. n.	1812	AF533950	28629211

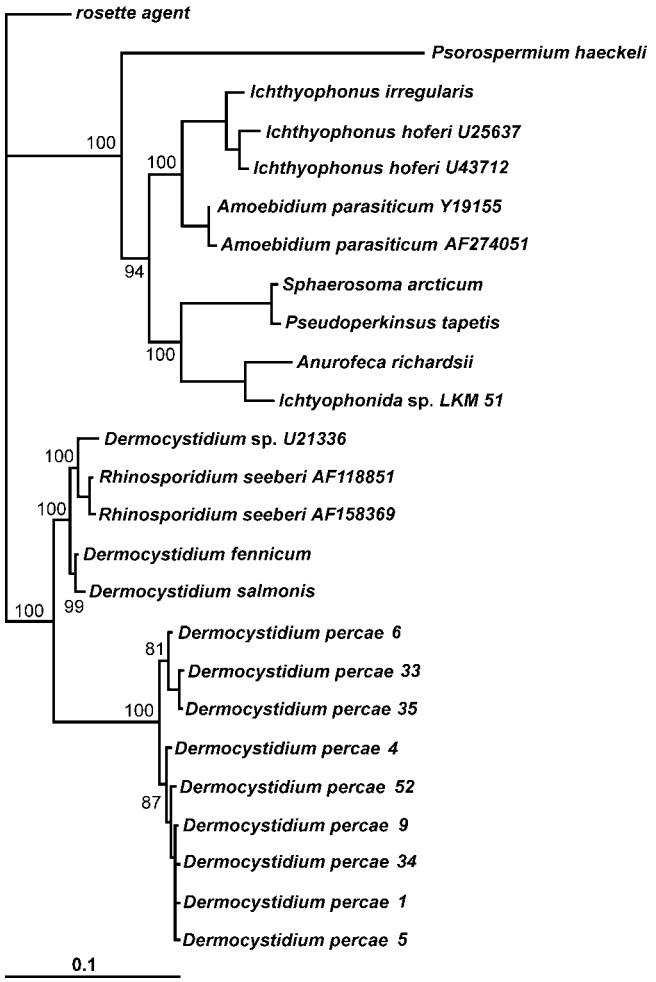

Fig. 1. Bayesian phylogenetic tree relating SSU rDNA sequences of *Dermocystidium fennicum*, *D. percae* and other members of Ichthyosporea (*Amoebidium parasiticum* Y19155, gi:10432427 and AF274051, gi: 9964066; *Anurofeca richardsi* AF070445, gi:4322029; *Dermocystidium percae* clones 1, 4, 5, 6, 9, 33, 34, 35 and 52, this paper; *Dermocystidium salmonis* U21337, gi:857457; *Dermocystidium fennicum*, this paper; *Dermocystidium* sp. U21336, gi:857456; *Ichthyophonida* sp. LKM51, AJ130859, gi:3894141; *Ichthyophonus hoferi* U25637, gi:1002422 and U43712, gi:1542965; *Ichthyophonus irregularis* AF232303, gi:7769642; *Pseudoperkinsus tapetis* AF192386, gi:6288975; *Psorospermium haeckeli* U33180, gi:1143192; *Rhinosporidium seeberi* AF118851, gi:6538786 and AF158369, gi:7110146; rosette agent of chinook salmon L29455, gi:1000847; *Sphaerosoma arcticum* Y16260, gi:4995786).

loop or bulge at the end of a stem; 9 occur in a loop, bulge, sequence end or other unpaired region; and 5 are in the poorly structured region between positions *ca* 654 and 913. Of the 28 differences common to two or more of the *D. percae* clones, 13 are internal to a stem; 1 expands a bulge; 11 occur in a loop or bulge; and 3 are in the above-mentioned poorly structured region. Transitions and transversions are almost equally balanced.

The variations internal to stem regions are of particular note. Among the 9 unpaired variations internal to a stem, only 2 would obviously weaken the between-strands interaction, and hence might be candidates for PCR errors; 3 seem likely to strengthen the interaction (taking the other *Dermocystidium* species as outgroups). Of the 13 shared variations, 8 exist in co-varying pairs; 3 pairs maintain a Watson-Crick or other energetically favourable base pair, while the other avoids an energetically favourable base pair. Co-variation in a highly structured region strongly implies that the corresponding SSU rRNA is being maintained under selection. These co-variations, plus 12 other shared differences, tend to divide the 9 clones into two groups (clones 6, 33 and 35 *vs* the others).

Alignment and phylogenetic analysis. The unrooted tree recovered Bayesian analysis of our 25 x 1811-alignment matrix is shown in Fig. 1. Trees very similar in all significant respects were recovered following neighbour-joining and parsimony analyses (results not shown).

Dermocystidium percae ultrastructure

Figure 2 shows the typical elongated cyst shape of *Dermocystidium percae* observed in perch fins.

Early stages. The earliest stages of *D. percae* observed were intracellular (Fig. 3) and circular in transverse section with a diameter of 2.4 μm (Fig. 4). They had vacuolated cytoplasm with numerous ribosomes and a large, slightly eccentric nucleus with a nucleolus and double-membrane envelope. The parasite cell was bounded with a trilaminar envelope about 20 nm thick covered with a fuzzy cell coat about 80 nm thick (Fig. 5). What can be interpreted as a slightly more advanced stage, about 2.7 μm in diameter, had an electron dense wall about 170 nm thick; the trilaminar envelope could no longer be discerned. The cytoplasm showed RER cisternae, and in addition to small vacuoles, there were also larger ones with granular and formed inclusions. In stages of about 5.2 μm in diameter, the dense wall, about 220 nm thick, seemed very compact and the parasite was surrounded by an empty space (Fig. 6).

In stages in transition to a larger plasmodium, about 15 μm in diameter, the cyst wall was about 0.5 to 1.0 μm in thickness, already with numerous fine outer projections (Fig. 7). The wall was differentiated into a denser outer layer and a less dense, thicker inner layer. These

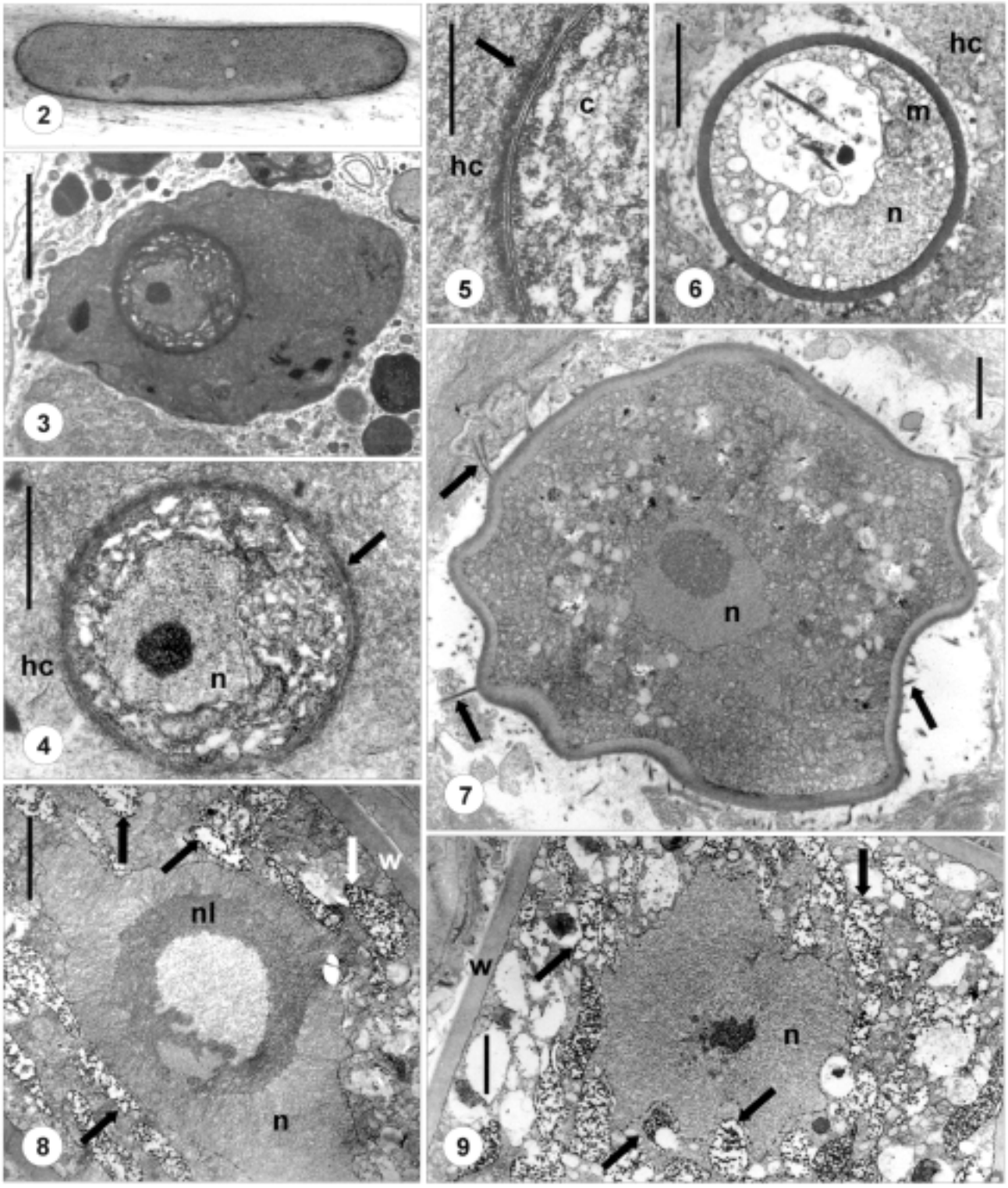

Figs 2-9. *Dermocystidium percae*. **2 -** a cyst from perch fin, actual length is 580 μm; **3** - intracellularly located early stage; **4** - the stage from Fig. 3, enlarged, arrow indicates the cell envelope; **5** - cross section of the cell envelope of the preceding stage; arrow indicates the fuzzy cell coat; **6** - a slightly more advanced stage encased with a thick wall; **7** - growing young plasmodium; arrows indicates the fine projections of the wall; **8** - part of a growing plasmodium with a huge nucleus and a hollow, large nucleolus, arrows indicates vacuoles with dense granules; **9** - part of a growing plasmodium with a nucleus with short projections; some of the vacuoles with dense granules (arrows) are lodged between them. c - parasite cytoplasm, hc - host cell cytoplasm, m - mitochondria, n - nucleus, nl - nucleolus, w - plasmodium wall. Scale bars - 0.5 μm (5); 1 μm (4); 2 μm (3, 6-9).

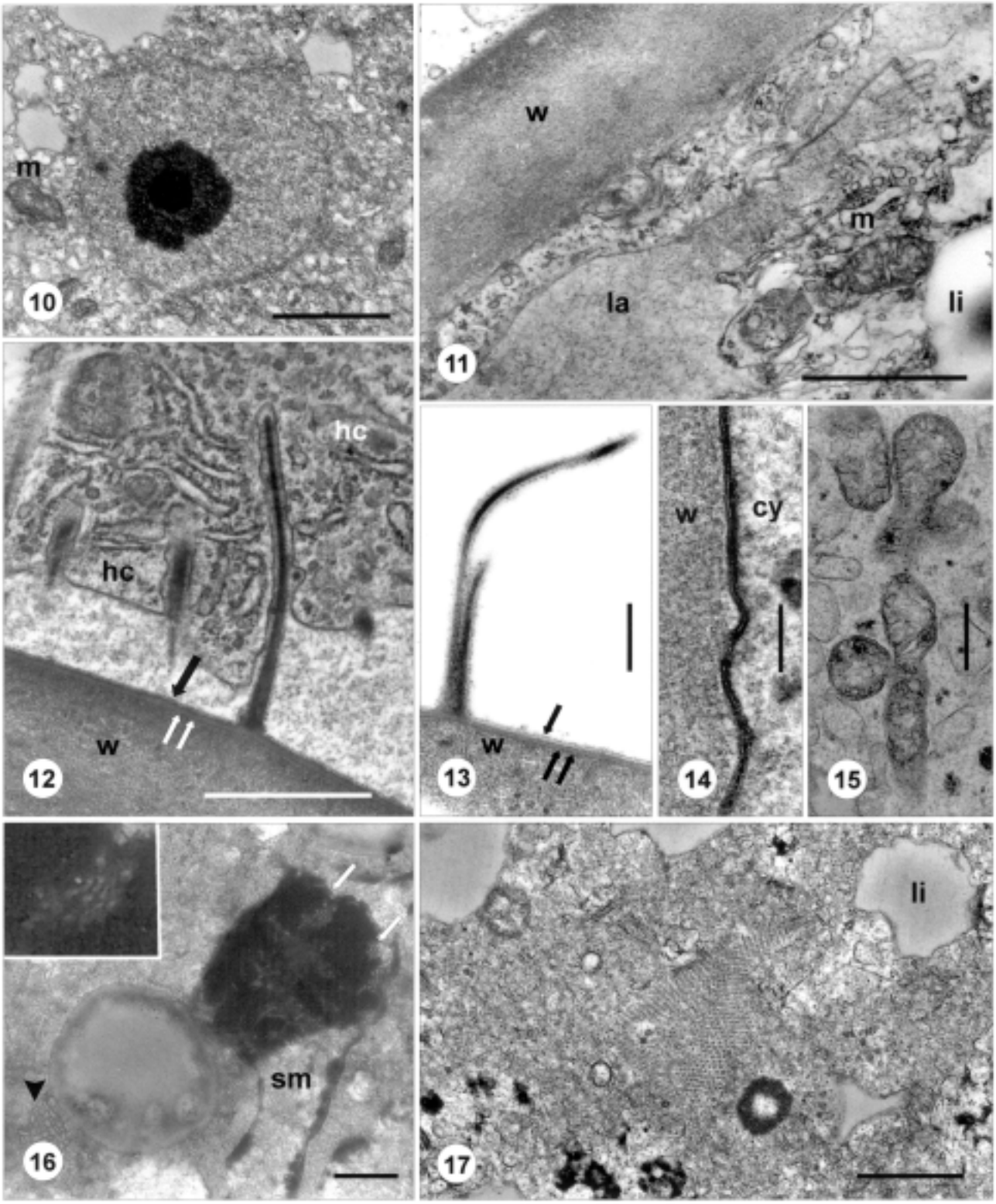

Figs 10-17. *Dermocystidium percae*. **10** - a normal nucleus in a young plasmodium; **11** - a branched, single membrane-bound lacuna with finely granular content; **12** - plasmodium wall with its homogeneous outer layer (white double arrows) covered by fine surface coat (arrow); **13** - a villus branched near the surface of the wall; arrow - surface coat, double arrow - outer homogeneous layer of the wall ; **14** - the dense lamina lining the inner face of the plasmodium wall; **15** - mitochondria in the cytoplasm; **16** - smooth-membrane envelope (sm) containing dense substance with small tubules (arrows, enlarged in the inset); at left, a multivesicular body-like structure (arrowhead); **17** - bundle of small fibrils in the plasmodia. cy - plasmodium cytoplasm, hc - host cell, la - membrane-bound lacuna, li - lipid inclusion, m - mitochondrion, w - plasmodium wall. Scale bars - 100 nm (14); 0.4 μm (13), 0.5 μm (15, 16); 1 μm (11, 12, 17); 2 μm (10).

stages had a large nucleus with finely granular nucleoplasm and a sizeable eccentric nucleolus. The cytoplasm was replete with small vacuoles; also small lipid vacuoles appeared, absent in previous early stages and constituting later a common feature of more developed plasmodia.

In apparently more advanced plasmodia, there were vacuoles with coarsely granular, dark, chromatin-like material (Figs 8, 9). It is difficult to put observed plasmodia in sequential developmental order; referring to the wall thickness, the plasmodia in Figs 8 and 9 may perhaps be stages following that in Fig. 7. In these plasmodia the central nucleus is quite large (8 to 12 μm) with centrally situated, sometimes hollow large nucleolus (5.5 μm) such as in Fig. 7; fine chromatin strands run radially from this central darker area to the nuclear envelope (Fig. 8). The nuclear envelope is normal, equipped with pores. The vacuoles with dark granules, which become quite numerous, are slightly reminiscent of prophase nuclei were it not for their small size and their single-membrane envelope. In some of these bodies, the dense particles adhered to the membrane, as chromatin particles would do in a nucleus. The vacuoles were sometimes situated between short extensions of the nucleus (Fig. 9). Later on, only occasionally could small normal nuclei be observed in the plasmodia (Fig. 10). Similar vacuoles with coarsely granular matter could also be found in plasmodia without any nuclei. We also found plasmodia where even the coarse granule-containing vacuoles were absent. Instead, branched membranous lacunae with finely granular content could sometimes be seen (Fig. 11).

Developing and developed plasmodia. The cyst wall of the middle-aged plasmodium was a compact, finely granulo-fibrillar structure ranging between 1.5 to 4 μm (rarely 6 μm) in thickness (Figs 11, 12). The outer face of the wall formed a homogeneous layer about 30 nm thick. This was covered by a fine granular surface coat, which also covered the villi-like protrusions or spikes, which reached a length of about 2.5 μm (Fig. 12). The villi were sunk into the surrounding host cells, the cell membrane of which provided an additional membrane for the villi. Some of the villi branched near their base, forming a bifurcate structure (Fig. 13). The inner face of the wall was lined with a dense lamina approximately 10 μm thick, with the structure of a unit membrane (Fig. 14). The plasmodium abutted on the wall; there were no villi or projection extending towards the wall.

The diversity and variety of plasmodium structure can hardly be described in full. What was most striking, however, is that there was no trace of a regular nucleus. The nuclei were easily visible only at the early stage of development and then at the stage preceding sporoblast formation, when numerous small nuclei reappeared.

According to the stage of its development, the organelles within the plasmodium were mitochondria (Fig. 15), Golgi bodies comprising several cisternae only, most varied vesicles with lucent or finely granular content, ribosomes, cisternae of endoplasmic reticulum, glycogen granules arranged in rosettes and numerous lipid vacuoles; these organelles varied in size and number. Faintly dense lipid vacuoles were always present, of different size and number. Mitochondria had flat, plate-like cristae, in some the cristae were less conspicuous but there was a central dense body or a few granules. Structures reminiscent of multivesicular bodies were sometimes observed (Fig. 16). Bundles of fibrils or crystal-like structures in the plasmodia were rarely observed (Fig. 17).

In the cytoplasm of plasmodia without detectable nuclei there were smooth membranes, sometimes folded and convoluted in a complicated way. A similar membranous system was observed to form a single-membrane envelope containing chromatin-like material (Fig. 16). Dark matter formed spindle-shaped or irregular concentrations along the inner sides of the membranes (Figs 16, 18-20). At the ends, and sometimes at the centres, of the membranous extensions there were also concentrations of dark matter (Figs 16, 19). Interestingly, there were small tubules (about 30 to 40 nm in diameter) in the dark matter or in the finely granular matrix in the extensions (Figs 16, 18-20).

Before the onset of sporogenesis, occasional nuclei could be seen. In some plasmodia, small, single-membrane vacuoles with granular matter (as in younger plasmodia, see Figs 8, 9) were observed. In some vacuoles the granular matter was condensing, or alternatively the dark matter of the extensions (described previously) may have been dispersing (Figs 20, 21). The previously mentioned tubules were still visible among the dark matter. It is tempting to believe that the typical heterochromatin was then composed from the dark or granular matter (Figs 22, 23). Membranes from the cytoplasm may form the outer layer of the envelope of the re-organised nucleus.

The lipid droplets were largest before sporogenesis, about 4 μm in diameter; later the droplets began to

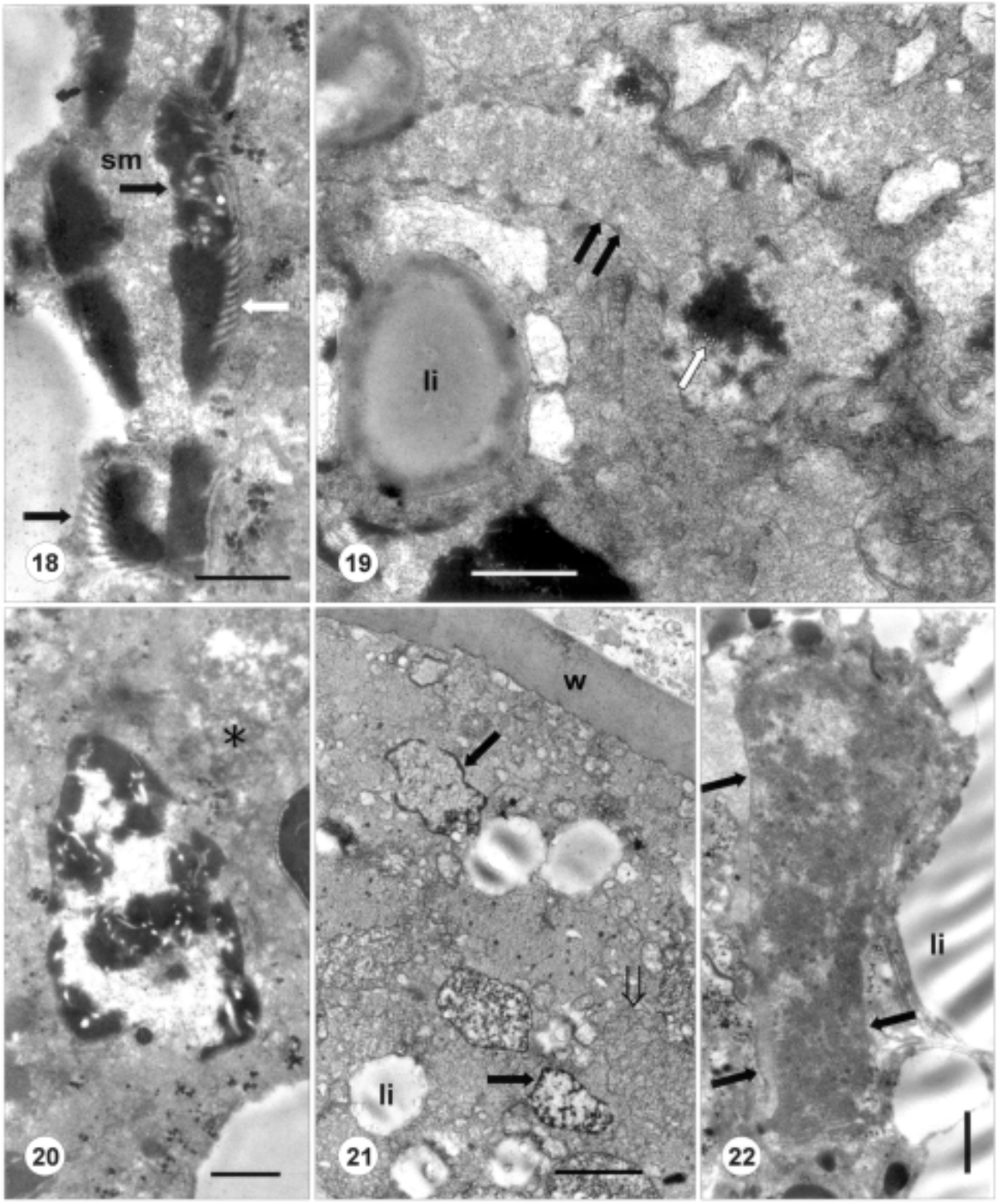

Figs 18-22. *Dermocystidium percae*, grown plasmodia. **18** - dense matter within a space delimited by a smooth membrane with small tubules (arrows); **19, 20** - smooth membrane envelopes (double arrow in Fig. 19) containing dense, chromatin-like material with small tubuli (white arrow in Fig. 19) in a lucent or finely granular matrix, asterisk - granular matter; **21** - single membrane vacuoles with coarsely (arrows) or finely granular substance (hollow arrow); **22** - a single membrane-bound envelope, probably the precursor of the new nucleus, filled with moderately dense granulation; arrows indicates the envelope wall. li - lipid inclusion, sm - matter within a space, w - plasmodium wall. Scale bars - 0.4 μm (18); 0.5 μm (19, 20, 22); 2 μm (21).

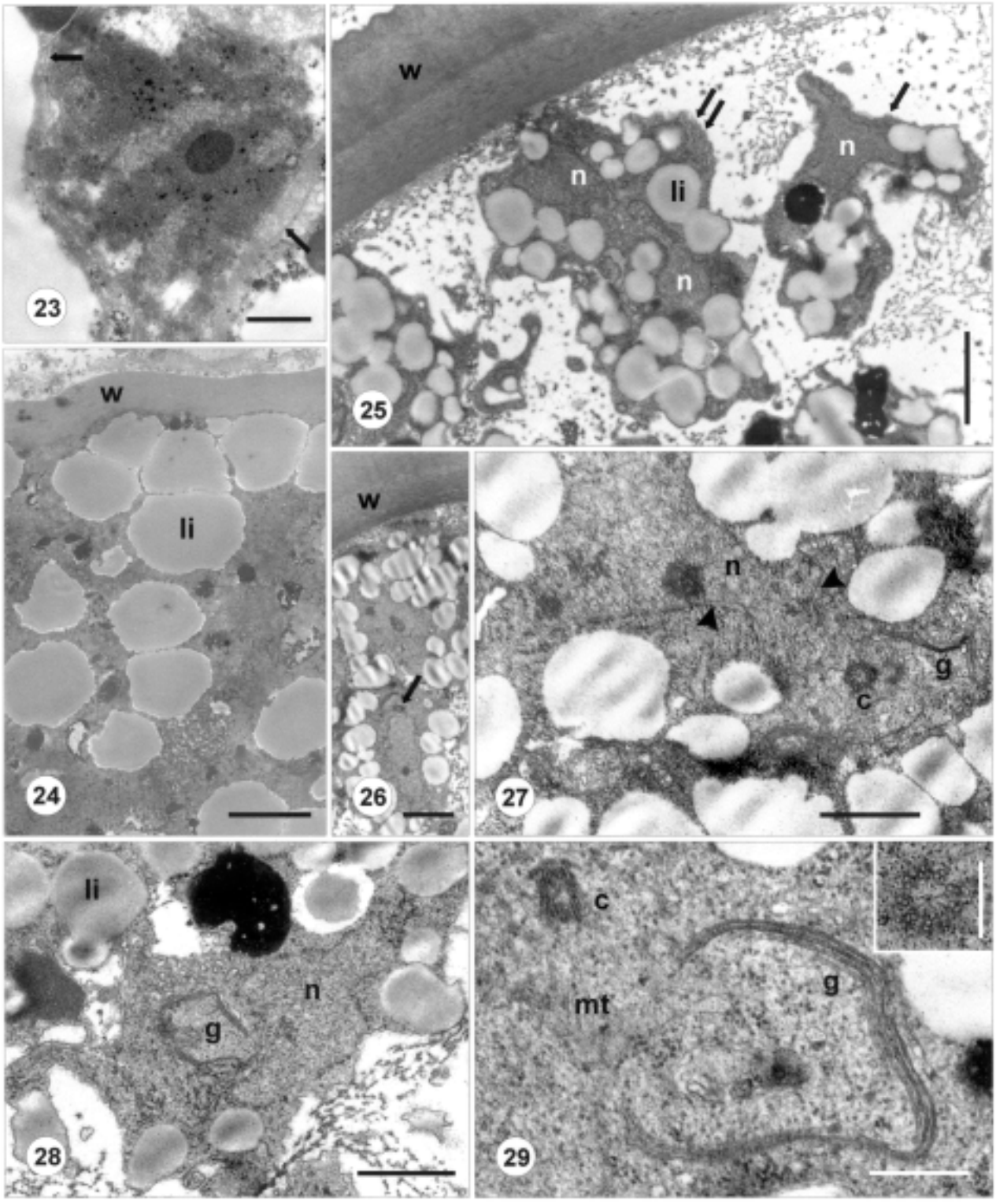

Figs. 23-29. *Dermocystidium percae*, mature and presporogonic plasmodia. **23** - a single membrane-bound structure (arrows indicate the envelope) with granular content of variable density; a possible precursor of the new nucleus; **24** - part of the periphery of the presporogonic plasmodium with a mass of large lipid droplets; **25** - the plasmodium fragmenting to form sporoblast mother cells with two nuclei (double arrow) which divide to produce sporoblasts (arrow); the wall is now two-layered; **26** - part of the periphery of the fragmenting plasmodium which is seen in more detail in Fig. 27; arrow points at the centriole; **27** - formation of sporoblasts, with a new nucleus with envelope marked by arrowheads; **28** - sporoblast formation with nucleus and Golgi; **29** - cells forming sporoblasts: centriole next to Golgi; inset, upper right - transverse section through a centriole, bar - 0.2 µm. c - centriole, g - Golgi, li - lipid droplets, mt - microtubules, n - nucleus, w - plasmodium wall. Scale bars - 0.5 µm (23, 29); 1 µm (27, 28); 2 µm (25, 26); 4 µm (24).

divide. They were sometimes seen to group together (Fig. 24). Small ruptures as signs of future plasmotomy were seen in the plasmodium.

Sporogenesis. At about the time when sporoblasts were being formed within the plasmodium, the wall differentiated into two layers, the outer slightly more lucent and the inner more dense with interspersed dense, comma-like structures (Fig. 25).

The plasmodium fragmented into smaller parts (Figs 25, 26). The nuclei formed in the late stage of the plasmodium did not represent the final number of the sporoblasts, since the segmentation of the plasmodia produced sporoblast mother cells which divided to form sporoblasts (Fig. 25). The nuclei of the sporoblast mother cells ("sporonts") and sporoblasts were irregular in shape, with a small nucleolus and hardly visible chromatin; they became centres for a small amount of cytoplasm, surrounded or even penetrated by lipid droplets. These small lipid vacuoles originated from the preceding large plasmodial vacuoles and still continued dividing to be ultimately about 0.5 to 1 μm in diameter, sometimes appearing quite lucent.

During the division producing sporoblasts, the nuclear envelope, or at least most of it, persisted. Centrioles were often visible at this stage (Figs 26, 27), and a prominent, cup-shaped Golgi body was seen in the vicinity of the centriole (Fig. 29). Microtubules were found near the centriole and near the nuclear envelope. Numerous lucent vesicles were seen at the cis-side of many Golgi bodies, and it seemed as if the vesicles and some cisternae were in the vicinity of electron dense concretions (Fig. 28).

Sporoblasts, 4 to 6 μm in diameter, were separated from each other by a foamy matrix (Fig. 30). The outside of the nuclear membrane in sporoblasts was covered by ribosomes and there were some RER cisternae in the cytoplasm. There were indistinct mitochondria and scarce glycogen granules. Roundish bodies of dark or lighter matter were distributed to the sporoblasts possibly from the plasmodium. An apparently primordial stage of the typical large spore inclusion could be observed in some nascent spores (Fig. 31). The growing inclusion in sporoblasts was light when observed with the electron microscope, sometimes with darker flecks or concentric rings at the centre. As the spore matures, the inclusion becomes denser.

Spores. In young spores the nucleus was indistinct and irregular in contour (Fig. 32), in older spores it was roundish and more easily visible and had a distinct nucleolus. The cytoplasm was laden with glycogen rosettes. The slightly eccentrically located inclusion body, about 4 to 7.5 μm in diameter had a moderately dense matrix and a much darker, irregular rim (Fig. 33). The dark rim apparently engulfed the glycogen and some bulges of the inclusion could be seen. Cisternae and vesicles of the Golgi body or endoplasmic reticulum may be involved in modification of the central inclusion body.

The size of mature spores was approximately 6 to 8 μm. Spore age and mode of fixation affect the size of spores; spores kept in water sometimes increased in size from 6-7 μm to more than 10 μm. The spores (Fig. 34) had an indistinctly visible cell membrane, covered by a rather electron lucent wall of fibrous or lamellar appearance, approximately 40 nm thick, and a surface coat made up of rough granules (Figs 32, 33). The inclusion was moderately dense, sometimes, probably in what were older spores, with up to 6 faintly dense concentric layers (Fig. 36). Lipid vacuoles at the periphery of the spore, next to the inclusion, were 0.5 to 1 μm in diameter; some, even in young spores, displayed crumpled lamellae and may have lost some of their content (Fig. 35). The number of lipid vacuoles may decrease in older spores. The cytoplasm contained scarce mitochondria and cisternae probably of Golgi nature. In older spores glycogen rosettes were scarcer but there were numerous ribosomes.

Zoosporogenesis. The spores, when incubated in water, divided to form zoospores. The process began with an increase in size of the nucleus (Fig. 37). The inclusion became lighter showing concentric rings or flecks, its size was reduced until it almost disappeared. The nucleus moved to the centre of the cell and became irregular in shape (Fig. 38). Many small electron dense globules appeared in the cytoplasm, some with an electron lucent centre; the globules may arise from fragmentation of the central inclusion. Sometimes small tubuli surrounded a globule (Fig. 39). There were ribosomes, small vacuoles and/or lipid droplets and small mitochondria in the cytoplasm.

As the nucleus moved to the cell centre, the cytoplasm begun to detach from the spore wall (Fig. 38). The margin of the cell showed small villi. The cell then divided into two halves, then into four cells (Fig. 40) and the division proceeded until a cell group (a rosette) of developing zoospores was formed (Figs 41, 42). Dark inclusions were then scarce but lipid-like droplets were

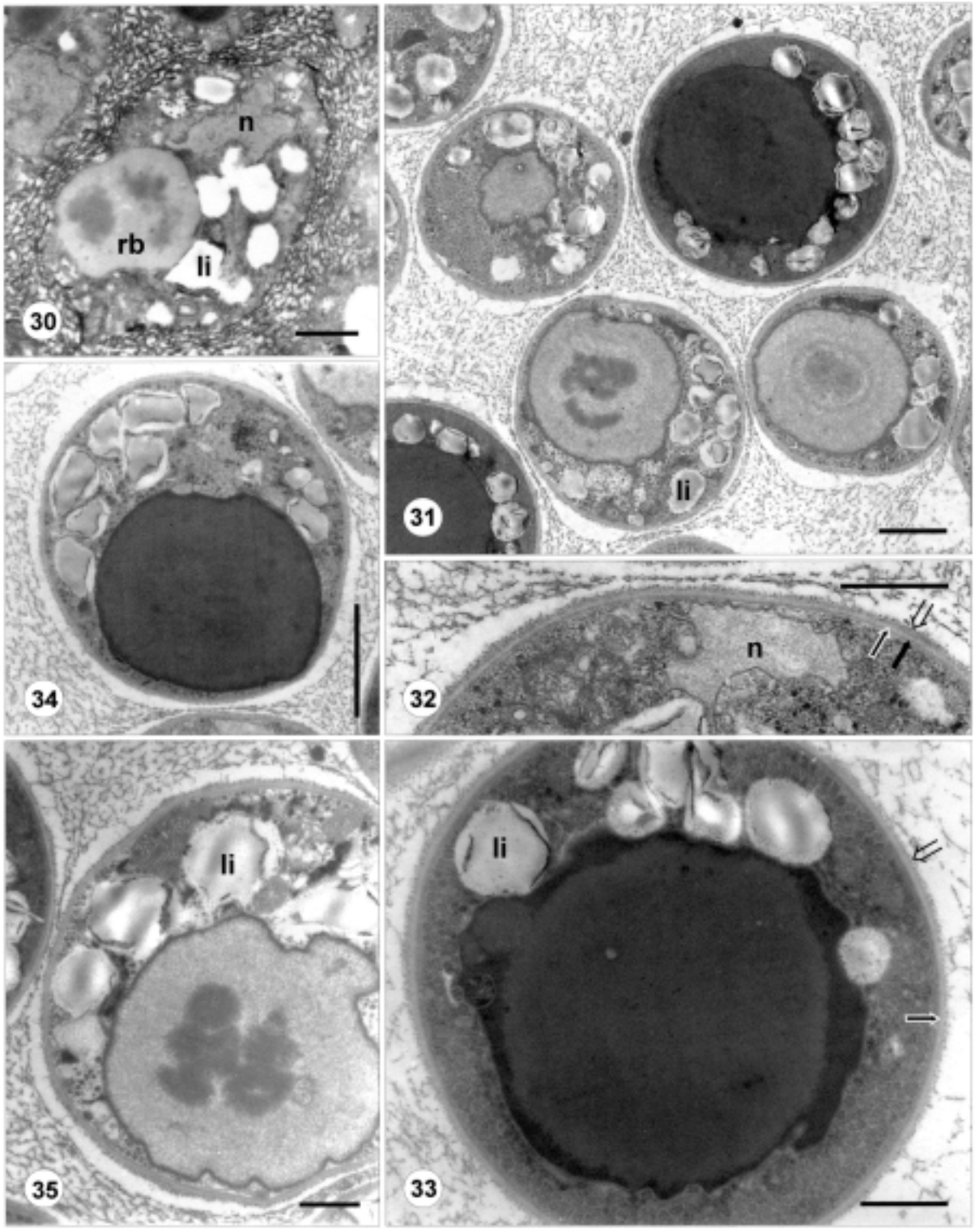

Figs 30-35. *Dermocystidium percae*, sporogenesis. **30** - sporoblast separated from the others by a foamy matrix; rounded body, possibly a precursor of the large spore inclusion; **31** - a group of one mature (upper right) and several young spores with the large central inclusions; all are embedded in a foamy matrix; **32** - section through the periphery of a young spore; black arrow marks the cell membrane, white-lined arrow the lucent spore wall, hollow arrow marks the surface coat. **33** - spore, note the irregular rim of the central inclusion, denser than the inclusion itself; white-lined arrow points at the wall of the spore, hollow arrow at the surface coat; **34** - another mature spore with distinctly eccentric inclusion; **35** - young spore with immature inclusion, reminiscent of the rounded body of Fig. 30, with lipid vacuoles displaying crumpled lamellae. The mitochondrion at left of the lipid inclusion is exceptional in having tubular cristae. n - nucleus, li - lipid vacuole or inclusion, rb - rounded body. Scale bars - 1 µm (30-33, 35); 2 µm (31); 3 µm (34).

present. The zoospore cells had irregular contours, nuclei, and a few mitochondria with flat cristae (Fig. 42). An inclusion which appeared grey, with a denser core, developed in each cell (Figs 41, 42). The flagellum developed before the zoospores were separated.

Mature zoospores. The inclusion body - possibly proteinaceous in nature (Figs 43, 44, 47) - usually had a dense core, and one side of the inclusion was also denser; this side consisted of thin lamellae, possibly of crystallised matter. The single, posterior flagellum (Fig. 44) of the zoospore originated in the vicinity of the inclusion body (Fig. 43). The nucleus was in intimate contact with the single, large mitochondrion. The latter had basically plate-like cristae - sometimes reminiscent of annulate lamellae (Figs 45, 46) and a fairly dense matrix with some granules. At the cell margin beside the inclusion there was a rumposome-like structure (Figs 44, 47).

The basal body of the single posterior flagellum was located near the inclusion body. Below this basal body, and at a right angle to it, there was a non-functional centriole (Fig. 48). At least one microtubule extended anteriorly below the cell membrane from the vicinity of the basal body and the non-functional centriole. A rhizoplast with transverse striae ran from the vicinity of the non-functional centriole and its associated dark bands between the cell margin and the inclusion body (Figs 49, 50, 62).

Zoospores then escaped from the spore envelope, which was left empty behind.

Dermocystidium fennicum sp. n. ultrastructure

Plasmodium stage. The plasmodium cysts (Fig. 51) were roundish, oval or dumb-bell-shaped. The cyst wall was about 4 to 7 μm thick; the outer, homogeneous layer was less electron dense (Fig. 52). The villi on the surface did not exceed 1.5 μm in length.

A common feature of the plasmodia was the abundance of more or less lucent lipid vacuoles. There were numerous smooth and rough membranes and free ribosomes and glycogen rosettes. Mitochondria with plate-like or somewhat swollen cristae were sometimes seen.

As in *D. percae*, in most plasmodia no nucleus could be detected. Small nuclei with a distinct nucleolus were only occasionally seen. Spaces delimited by single membranes with finely granular content found in some plasmodia might possibly represent nuclear structures. In some, possibly older plasmodia similar spaces also included larger and smaller concentrations of dense matter (Figs 53, 54). Prior to plasmotomy, nuclei may be formed at the sites of such concentrations. Nuclei possibly arose first by condensation of a nucleolus and then the chromatin matter around it (Fig. 55).

The developing nucleus had a single membrane with irregular chromatin concentrations on its inner side. Nucleolus-like structures could often be seen (Fig. 53). Small vesicles (50 to 150 nm) were seen near the condensing chromatin (Fig. 54). The nuclear envelope then acquired an outer membrane (Fig. 56); in this figure the double envelope at the right side of the nucleus is clearly seen.

Sporogony and spores. Sporoblasts were formed as the result of plasmotomy, and were almost identical to those of *D. percae*: the glycogen rosettes were perhaps more numerous. The transformation of sporoblasts to spores was also similar. In young spores a darker rim of the central inclusion seemed to engulf glycogen. In the cytoplasm of mature spores of *D. fennicum* glycogen appeared more plentiful (Fig. 57) than in mature spores of *D. percae*.

Zoosporogony and zoospores. The pre-division and division processes of the *D. fennicum* spore did not differ from those of *D. percae* (Fig. 58). The zoospore stage had a large mitochondrion with fairly dense matrix, which contained many dense granules. When the cristae could be discerned, they were lamellar in structure (Fig. 59). The nucleus partially enveloped the mitochondrion. The zoospores had a large glycogen reserve, a lipid droplet and sometimes, in the organisms freed from spore envelopes, a groove or pit could be seen (Fig. 60).

The flagellated zoospores were possibly of short duration, at least when incubated at higher temperatures (23-25°C); flagella were never found still attached to the bodies. Remains of an inclusion were seen being discharged from the body (Fig. 61).

DISCUSSION

Phylogenetic position of *Dermocystidium fennicum* and *D. percae* within Ichthyosporea

In the unrooted phylogenetic tree shown in Fig. 1 the rosette agent is displayed as the outgroup, it is suggested that for ease of interpretation, a root should be visualised joining at the midpoint of the long left-hand vertical edge. The 18S rDNA of rosette agent can be resolved, with high bootstrap support, as the most-basal branch within the Ichthyosporea. Our Bayesian phylogenetic analysis resolves two groups with 100% posterior probability

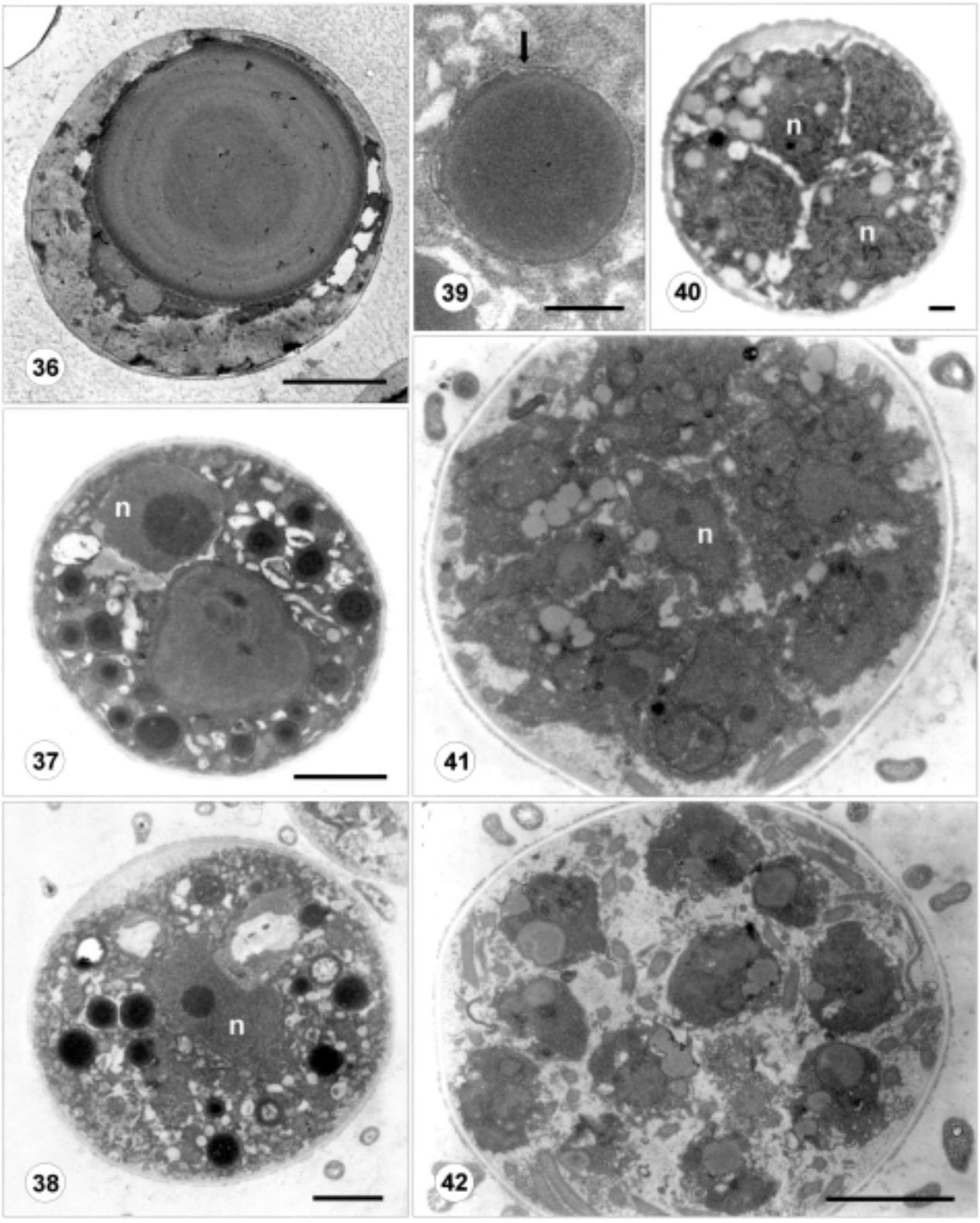

Figs 36-42. *Dermocystidium percae*, spores and zoosporogenesis. **36** - an old spore in which lipid and glycogen reserves became scarce, with distinct concentric layers in the inclusion; **37** - first phase of zoosporogenesis with enlarged nucleus of the spore; note the appearance of dense globules in the cytoplasm; **38** - next step of sporogenesis; the central inclusion has almost vanished; **39** - one of the dense globules from Fig. 38 enlarged; arrow points at the tubuli at the periphery of the globule; **40** - the spore has divided into four cells; **41** - a rosette of daughter cells within the old spore wall; **42** - old spore wall with developing zoospores inside it. n - nucleus. Scale bars - 0.5 μm (39, 40); 1 μm (38); 2 μm (36, 37, 41, 42).

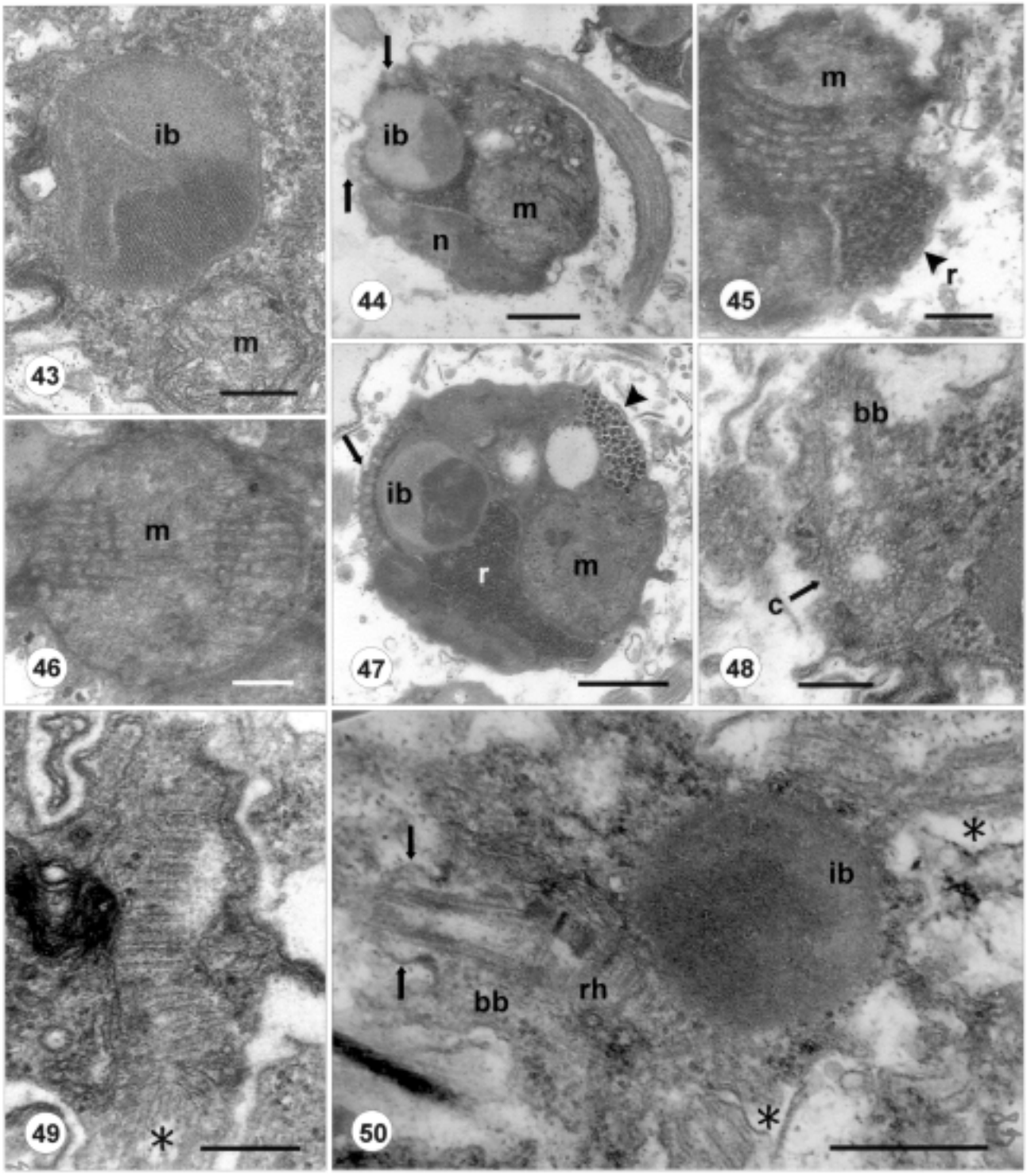

Figs 43-50. Details of zoospore structures in *Dermocystidium percae*. **43** - inclusion body of the zoospore, part of it revealing a densely striated structure; **44** - the zoospore with its single, posteriorly curved flagellum; arrows point at the rumposome-like structure; **45, 46** - mitochondria with diverse structures of cristae. **47** - section through the zoospore; next to the inclusion there is the rumposome-like structure (arrow); arrowhead points at glycogen rosettes. **48** - basal body of the zoospore flagellum; beneath it is the barren (non-functional) centriole; **49** - transversely striated rhizoplast, associated with the basal body of the flagellum (asterisk); **50** - basal body with the flagellum extending through the cell membrane (arrows) and its associated rhizoplast; asterisks - flagella of neighbouring zoospores. bb - basal body, c - centriole, ib - inclusion body, m - mitochondrion, n - nucleus, r - ribosomes, rh - rhizoplast. Scale bars - 0.2 µm (43, 45, 46, 49); 0.4 µm (44, 48, 50); 0.5 µm (47).

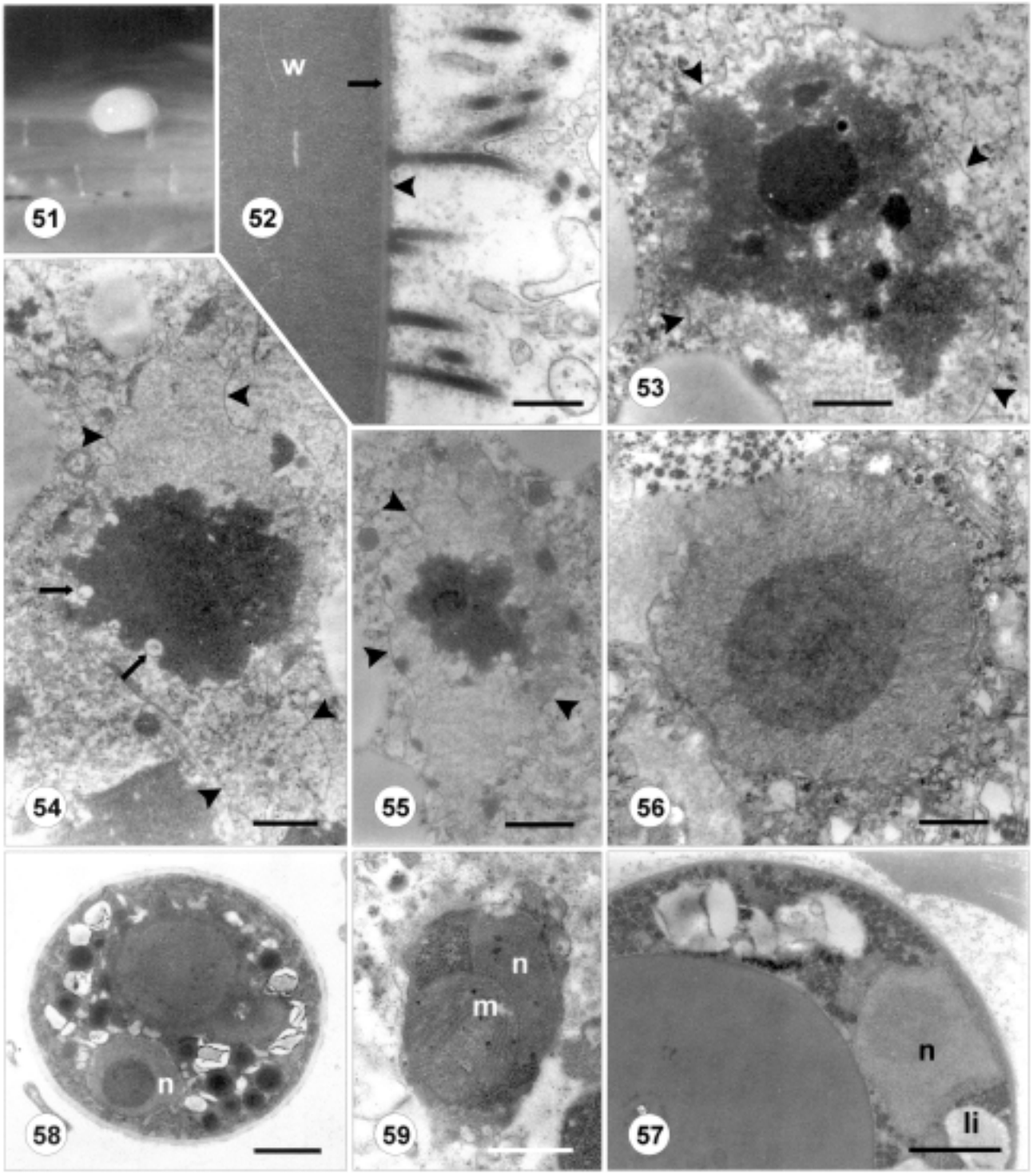

Figs 51-59. *Dermocystidium fennicum* sp. n. **51** - a cyst on the surface of the gills, actual size is 360 μm; **52** - the cyst wall and the villi; arrow points at the outer homogeneous layer of the wall; arrowhead points at the surface coat; **53-55** - single membrane-bound structures with (chromatin-like) concentrates of dense matter, possible precursors of (presporogonic) nuclei; arrowheads point at the delimiting membranes, arrows at vesicles wedged in the margin of the dense substance; **56** - a presporogonic nucleus with double envelope. **57** - a sector of mature spore with the inclusion, mass of glycogen, nucleus and lipid inclusion; **58** - spore in the early phase of zoosporogenesis with reduced inclusion, dense globules, lipid globules and growing nucleus; **59** - a mitochondrion of the preceding stage. li - lipid inclusion, m - mitochondrion, n - nucleus, w - cyst wall. Scale bars - 0.4 μm (54); 0.5 μm (52, 53, 55, 59); 1 μm (57, 58); 2 μm (58).

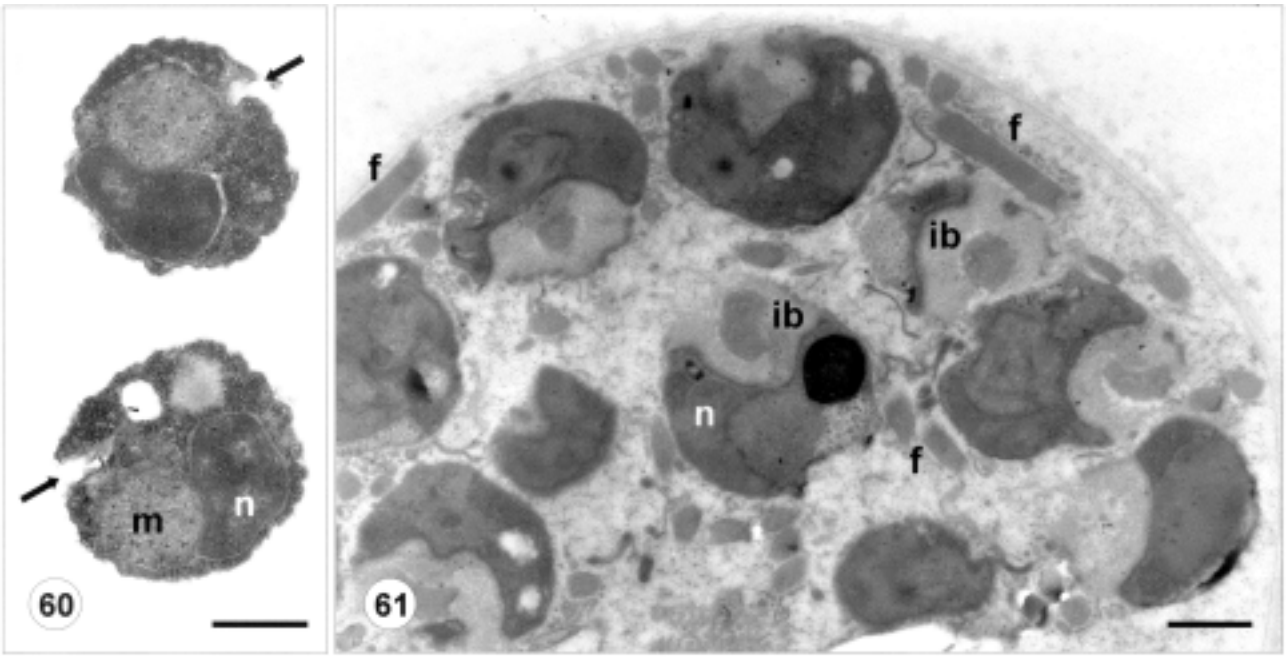

Figs 60, 61. *Dermocystidium fennicum* sp. n. **60** - zoospores escaped from spore walls with a pit (arrow) in their cell; **61** - zoospores discharging their inclusion bodies. ib - inclusion bodies, f - flagellum, m - mitochondrion, n - nucleus. Scale bars - 0.5 μm (60, 61).

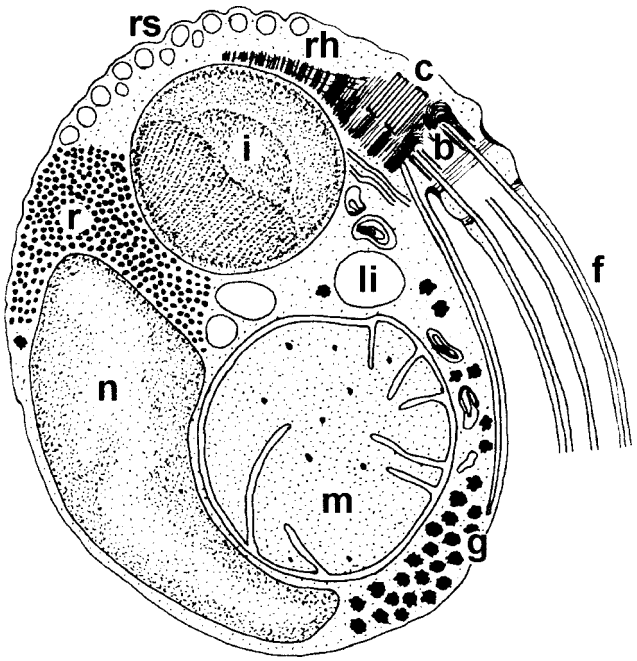

Fig. 62. A drawing of the site of the flagellar basal body and associated structures in *Dermocystidium percae* zoospore. b - basal body, c - non-functional centriole, f - flagellum, g - glycogen rosettes, i - inclusion body, li - lipid inclusion, m - mitochondrium, n - nucleus, r -ribosomes, rh - rhizoplast, rs - rumposome.

within the Ichthyosporea. In trees that also contain sequences from organisms other than Ichthyosporea (e.g., Benny and O'Donnell 2000, Figueras *et al*. 2000, Rand *et al*. 2000, Ustinova *et al*. 2000), ichthyosporean SSU rDNAs are resolved into two clades, one consisting of rDNAs of *Dermocystidium* species and *Rhinosporidium seeberi*, the other with rDNAs of *Amoebidium parasiticum*, *Anurofeca richardsi*, *Ichthyophonida* sp. LKM51, *Ichthyophonus* sp., *Pseudoperkinsus tapetis*, *Psorospermium haeckeli* and *Sphaerosoma arcticum*.

Sequences from both *Dermocystidium* isolates reported here group securely within the *Dermocystidium-Rhinosporidium* clade. The SSU rDNA of the new *Dermocystidium fennicum* described here is resolved, with 99% posterior probability, as a specific sister-group with that of *D. salmonis*. Based on SSU rDNA sequences, our new *D. fennicum* is not specifically related to the *Dermocystidium* sp. studied by Ragan *et al*. (1996), which by contrast groups with 100% posterior probability with several isolates of *R. seeberi*.

Sequences from the nine *D. percae* clones are resolved into a single group with 100% posterior probability. Within *D. percae*, clones 6, 33 and 35 are resolved separately (see above - Fig. 1). To answer the

possibility whether different sequences of clones of *D. percae* might reflect expression in different life history stages, one could carry out RT-PCR studies which will demonstrate whether the different sequences reflect pseudogenes or are really expressed. This could, however, raise enormous technical challenges. First, one would have to separate different life-history stages in amounts that allow RT-PCR. RT-PCR is typically done from poly(A)-mRNA, but the primary transcript that contains SSU-rDNA is a large RNA and (even assuming that it is polyadenylated in the first place) standard RT-PCR could not read far enough in from the 5' end to reach the SSU coding region. Special PCR techniques might help (or might not). This is why the close sequence analysis of variants has been included. Most variants show evidence of being under selection, which would not be the case if they were pseudogenes. Thus these are probably not pseudogenes.

Given our experimental design, we cannot distinguish whether these results indicate that the rDNAs of *D. percae* are microheterogeneous, or that our biomass contained very closely related organismal variants (e.g. subspecies). Several cysts from a few host fish individuals were included in the sample. If these sequences reflect microheterogeneity within a unitary species, it would be interesting to examine whether the different sequences are differentially expressed throughout the life history of *D. percae.*

The possible occurrence of subspecies in *D. percae* will be addressed in future.

Classification of *Dermocystidium* species from the perch

Pekkarinen and Lotman (2003) suggested that two different *Dermocystidium* species occurred in perch in Finland. Both developed independently. In the same light microscope study, the species differed in their cyst shape, thickness of their cyst wall and in microhabitat preference of the cysts on the fish surface. At the ultrastructural level, the two species do not differ much. Restructuring of the plasmodial nuclei may, however, be slightly different. Summary of all observed differences, including those in the SSU rDNAs, justifies considering the species as separate. We propose therefore to establish a new species, *Dermocystidium fennicum* sp. n. with the following differences from *D. percae*:

- the cyst formed by the plasmodium of *D. fennicum* is roundish, more rarely oval or dumb-bell shaped compared to the elongate-cylindrical shape of *D. percae*;

- the cysts of *D. fennicum* are situated on the skin of the head region and bases of the fins, while *D. percae* forms cysts in the skin of the fins. *D. fennicum* favours the dorsal fin, while *D. percae* does not. (Only in O-group fish may cysts of *D. percae* be formed anywhere in the skin).

- the wall of *D. fennicum* is 4 to 7 μm thick, compared with 1.5 to 4, rarely 6 μm in *D. percae*.

- within the *Rhinosporidium - Dermocystidium* clade, *D. fennicum* is a sister taxon with *D. salmonis*, while *D. percae* forms a sub-clade of its own.

Specimens of *D. fennicum* are deposited in the collection of the Institute of Parasitology in České Budějovice under the numbers H-PH-073, 074, 075, 076.

Comparison with other *Dermocystidium* species and ichthyosporeans

Throughout this paper, we have used the traditional term "cyst" for the *Dermocystidium* plasmodium with its thick wall, although the term "sporocyst" as used by Vogt and Rug (1999) for the same stage in *Psorospermium* would be more convenient.

Until now, three cyst-forming *Dermocystidium* species have been studied with the electron microscope. Wootten and McVicar (1982) presented a few electron micrographs of the cyst wall and a micrograph of the spore of *D. anguillae* Spangenberg, 1978. Olson *et al*. (1991) reported the formation of uniflagellated zoospores within discharged spores of *D. salmonis* Davis, 1947. Lotman *et al*. (2000) investigated the fine structure of *D. cyprini* Červinka and Lom, 1974. All are principally gill parasites, and *D. salmonis* and *D. cyprini* have been described to produce infective uniflagellate zoospores. In *D. cyprini* zoosporulation may take place in compartments and in *D. salmonis* it takes place in the spore envelope. Thus *D. fennicum* and *D. percae* resemble *D. salmonis* in this respect. The cyst development of *D. salmonis* is, however, very rapid; Olson *et al*. (1991) did not describe any plasmodial stages, and the immature spores developed in an experimental infection did not resemble the sporoblasts described in this study. The ultrastructure of *D. salmonis* needs further study.

The cyst-forming dermocystidia are quite varied morphologically, reflecting the diversity of members of the whole group of Ichthyosporea; this applies especially to the cyst wall. In *D. cyprini* it differs from that in perch dermocystidia; there is an only 0.1 μm thick dense layer, from which thin tubular villi extend and which is subtended by a layer with dense granules and a

granulofibrillar layer, the whole being about 3 µm across. In *D. salmonis* the cyst wall (as calculated from the photomicrograph) is about 0.3 µm thick, whilst in *D. granulosum*, according to light microscope observations of Sterba and Naumann (1970), it is multilayered and 4 to 5 µm thick. Only in *D. cyprini* has the cyst cytoplasm been investigated (Lotman *et al*. 2000), but it includes normal nuclei and lacks the unusual vacuoles with dense material, found in perch dermocystidia.

Flagellated cells exist both among choanoflagellates and chytrids and in having them, dermocystidia reflect their position near the early branching of the animal and fungal lines. The *Dermocystidium* zoospores show structures of Chytridiomycetes; they have a single, posterior flagellum. The zoospores of *D. percae* even seem to have a rumposome-like structure. The rumposome is a honeycomb-like structure of unknown function usually near a lipid globule in some Chytridiomycetes (Barr and Hartmann 1976, Lange and Olson 1979). In *D. percae* the structure was, however, associated with the possibly proteinaceous inclusion. Some Chytridiomycetes also have a striated fibrous rhizoplast projecting inside the zoospore body from the basal body of the flagellum; striated flagellar roots or rootlets, rhizoplasts, are also known in animal cilia and flagella, too (e.g., Tyler 1984).

The rhizoplast of the *D. percae* zoospore is different from that of *D. cyprini* zoospores in having a less dense striation. In both *D. percae* and *D. cyprini* zoospores the non-functional centriole seems to be at a right angle to the functional kinetosome. The flagellar roots of *D. fennicum* and *D. salmonis* have not been described.

The shape of mitochondrial cristae has often been thought to serve as a guide to the phylogenetic position of organisms. Animals and true fungi generally have flat mitochondrial cristae, while the Mesozoa and what is now considered to be the Protozoa have tubulovesicular cristae. The DRIPs clade introduced by Ragan *et al*. (1996) and widened later to Ichthyosporea by Cavalier-Smith (1998), forms a basal branch near animals and fungi. It was thought that within the Ichthyosporea *Ichthyophonus* and other representatives of the group have tubulovesicular cristae, and the members of the *Dermocystidium-Rhinosporidium* group have flat cristae. The hypothesis seems to be true among the *Dermocystidium* species studied: i.e., *Dermocystidium* sp. from brook trout (Ragan *et al.* 1996), *D. cyprini* from carp (Lotman *et al*. 2000) and *D. percae* and *D. fennicum* from perch (this study). The mitochondrial cristae of *Rhinosporidium seeberi* were first described as flat (Herr *et al*. 1999) and later as tubulovesicular (Fredricks *et al*. 2000). Fredricks *et al*.(2000) explain this discrepancy by possibly different methods of preparation or by different developmental stages of the parasite. In the *Ichthyophonus-Psorospermium* clade, *Ichthyophonus hoferi* has tubulovesicular cristae (Spanggaard *et al*. 1996, Rahimian 1998), and *Pseudoperkinsus tapetis* has vesicular cristae (J. Lom, unpublished observation), whereas *Amoebidium parasiticum* has mostly flat cristae (Whistler and Fuller 1968). The mitochondrial cristae in Ichthyosporea evidently do not unambiguously follow the phylogenetic grouping. The rosette agent, in the most basal branch of Ichthyosporea in our study, has plate-like mitochondrial cristae (according to micrographs presented by Arkush *et al*. (1998) and Harrell *et al*. (1986)).

The crayfish parasite *Psorospermiun haeckeli*, and the ectosymbiont of arthropod *Amoebidium parasiticum* very clearly differ in morphology from *Dermocystidium* species. *P. haeckeli* and its genetically diverse forms (Rug and Vogt 1995, Bangyeekhun *et al*. 2001) are best known at the oval sporocyst stage. The wall of the organism is composed of plates (Nylund *et al*. 1983), which distinguishes it form the other ichthyosporeans. *A. parasiticum* reproduces either by nonmotile sporangiospores or by amoebae (Ustinova *et al*. 2000). Uniquely, thalli of *A. parasiticum* are attached externally to a host by an acellular holdfast (Benny and O'Donnell 2000). Figueras *et al*. (2000) included *Perkinsus atlanticus*-like organisms, with the proposed name *Pseudoperkinsus tapetis*, from carpet shell clams in northwestern Spain to the DRIPs clade. It is not certain that the *Perkinsus atlanticus* described by Azevedo (1989) from Portugal is an identical organism. Two flagella and an ultrastructure typical of apicomplexans formed in the zoospores of *Perkinsus atlanticus* sensu Azevedo refer to the Perkinsea in the Alveolata.

Anurofeca richardsi, parasitic in the gut of tadpoles, described by Beebee (1991), Wong and Beebee (1994) and Baker *et al*. (1999), and the intracellular, cell cluster-forming parasites in salmonids, *viz.*, rosette agent, described e.g., by Harrell *et al*. (1986) and Arkush *et al*. (1998), may not differ very much from *Dermocystidium* species. The daughter cells in dividing forms of *A. richardsi* and of the rosette agent are walled in contrast to developing zoospores of *D. percae*, which, at least in experimental culture, we have found to be irregular in contour and naked.

Ichthyophonus hoferi, occurring in many fish species, includes, as is typical of ichthyosporeans, vacuoles of varying density and also lipid-like bodies (Paperna 1986, Spanggaard *et al*. 1996, Rand 1994). Active spores of *I. hoferi* described by Rahimian (1998) show some similarity to the plasmodial cysts of *D. percae*. Viewed at a low magnification, the ground cytoplasm of the spore (plasmodium) has a network of fibre-like cords, and dense bodies (cf. Fig. 10 in Rahimian 1998 and Fig. 2h in Pekkarinen and Lotman (2003)). Nuclei were, however, easily seen in *I. hoferi* and could be a few or several hundred in number. The organism was divided into units containing from one to a few nuclei accompanied by cytoplasmic material, just as was the case in *D. percae*, and *D. fennicum*. No flagella were described in *I. hoferi*. Hyphae-like structures of *I. hoferi* (Ruggieri *et al*. 1970) and thalli of *I. irregularis* (Rand 1994) suggest a closeness to fungi. There is one report where aseptate hyphae of a *Dermocystidium* species have been described (Dyková and Lom 1992): in koi carp, spores of *D. koi* developed in subcutaneous hyphae. Production of hyphae-like structures thus occurs rarely in both groups of the Ichthyosporea (*Ichthyophonus* group and *Dermocystidium-Rhinosporidium* group).

There have been a few cases of visceral and systemic infections in salmonid fish by an intracellular parasite identified as a *Dermocystidium* species. It was found mainly in the visceral cavity (McVicar and Wootten 1980), or in melanomacrophages (Hedrick *et al*. 1989); or it induced systemic infections (van de Moer *et al.* 1987, Nash *et al*. 1989). These organisms and the rosette agent are fairly similar in structure in that the daughter individuals are produced by segmentation within the common wall. The infection by rosette agent can ultimately result in host cell death (Arkush *et al*. 1998). The agent can cause limited nodules in different organs or systemic dispersion of the organisms with minimal host inflammatory cell response.

Rhinosporidium seeberi produces thick-walled spherical structures containing protein spherules and lipid globules (see Ashworth (1923) for references). At variance with our *Dermocystidium* species, *R. seeberi* clearly acquires numerous nuclei during its development. A pore appears in the wall of the 'sporangium' and the organism then discharges 12000 to 16000 endospores (Ashworth 1923, Herr *et al*. 2000), which in the host tissue mature again into endosporulating sporangia. Flagellated zoospores of *R. seeberi* have not been discovered. However, there has been a debate about discharge of 'sporules' or 'sporozoites' from the spores (see Ashworth (1923) for references). The parasite causes tumor-like growths in the nose or nasopharynx of humans and animals, mostly in the tropics. Fredricks *et al*. (2000) hypothesise that *R. seeberi*´s natural hosts are fish or other aquatic animals, and humans acquire infection when they come into contact with water containing these fish and their parasites.

Nuclear cycle of *Dermocystidium*

The young cell of *D. percae* had an ordinary, fairly large nucleus, with a large nucleolus and double, fenestrated envelope. As the cell grew in size, the nucleus sent out short extensions, but these nuclei later disappeared. Possible mitotic events in young stages remained obscure. The growing cell soon became intercellular and ended up as a plasmodium 1 to 2 mm in length (Pekkarinen and Lotman 2003). Strangely, in medium-size plasmodia, odd enough, a typical nucleus could not be seen. The branched lacunae in the medium-sized plasmodia of *D. percae* and *D. fennicum* could be suggested as a vicarious, nucleus-like structure. In a related species of the *Dermocystidium*-clade, *Rhinosporidium seeberi,* Ashworth (1923) summarized the structures of the earliest stages as evident from the previous studies by Seeber, Minchin, Fantham, Beattie, and others (see Ashworth (1923) for references): "The youngest parasite is oval, round, irregular, or even amoeboid, with vesicular nucleus containing nucleolus. It soon becomes a multinucleate plasmodium, but the mode of division of the nucleus has not been ascertained". The first nuclear spindle was visible in plasmodia 50 to 60 μm in diameter (Ashworth 1923). Later (mitotic) nuclear divisions were thought to be synchronous and rapid, 'for the nuclei being found in the "resting" condition in the stages described between two to one hundred and thirty-two nuclei'. No actual mitoses were seen from the telophase of the first division until after the seventh division. In our *Dermocystidium* species, numerous nuclei did not reappear until before division of the advanced plasmodium. Mitoses occurred in the prespore stages. Centrioles were frequently seen outside the nuclei and at least most of the nuclear envelope seemed to persist. In *R. seeberi* the centrioles of the later nuclear spindles were intranuclear and the nuclear envelopes disappeared during the mitosis (Ashworth 1923). In *D. percae,* Golgi bodies were prominent and were sometimes associated with the centriole and microtubules.

The events of the nuclear cycle of *D. percae* and *D. fennicum* are open to speculation. The chromosomal DNA obviously goes through a period of cryptic existence, after which it is reorganised in typical eukaryotic nuclei. During the cryptic stage it is most probably associated with the dark substance seen in single-membrane bound vacuoles or spaces.

We failed to find similar cases among protists or other lower eukaryotes. Among the protists revealing striking changes in their nuclear cycle are many radiolarians in which the nuclei show cyclic polyploidy, undergoing polyploidization at some stages and depolyploidization at other stages of life cycle (Raikov 1982). The polyploid chromatin may not stain with usual DNA-stains. Radiolarians such as *Thalassicolla spumida* possess a very large polyploid nucleus (called primary nucleus) which is apparently unable to divide in two and they therefore reproduce by sporogenesis. The primary nucleus first breaks up into large fragments that continue to divide and initiate many secondary nuclei. The secondary nuclei form zoospore nuclei after more mitotic divisions. The presence of numerous secondary nuclei is of short duration in this case (Raikov 1982). A figure (Fig. 68b) in Raikov (1982, after Hollande and Enjumet (1953)) depicting fragments originating in *T. spumida* after its nucleus was broken into pieces resembles to some extent the vacuoles and lacunae with dark material in growing plasmodia of *D. percae.* In a related radiolarian, *Thalassophyta sanguinolenta,* the structure of the primary nucleus changes before the beginning of sporogenesis. A homogeneous intranuclear centrosphere appears in the centre of the nucleus and all the chromosomes radially converge on this sphere. Nucleolar ribonucleoprotein is extruded into cytoplasm as sacculiform outpockets and breaks down before the beginning of the sporogenesis (Raikov 1982). A large nucleolus (centrosphere?) with lighter core was seen in this paper in a young stage of *D. percae*. Nevertheless, the similarities between nuclear cycle stages of radiolarians and dermocystidia may be just superficial since none of these stages was proven to lack a true nuclear envelope.

The chemical nature of the granular contents of certain vacuoles (Figs 9, 21) in *Dermocystidium* plasmodia is not known (chromatin, ribonucleoprotein?). Some of the vacuoles with dark material could be the origins of true secondary nuclei. The vacuoles have small canaliculi among the electron dense matter, which may serve to increase the exchange of materials with cytoplasm. In the nuclei of *D. fennicum* in the present study the vesicles released from the condensing centre of the future nucleus may also perform the same function. The large concretions in the growing *D. percae* plasmodium (Pekkarinen and Lotman 2003) may be fragments of the nucleolus or centrosphere of the primary nucleus.

REFERENCES

Arkush K. D., Frasca S., Jr., Hedrick R. P. (1998). Pathology associated with the rosette agent, a systemic protist infecting salmonid fishes. *J. Aquat. Anim. Health* **10:** 1-11

Ashworth J. H. (1923). On *Rhinosporidium seeberi* (Wernicke, 1903), with special reference to its sporulation and affinities. *Trans. R. Soc. Edin.* **53 (II:No 16):** 301-342

Azevedo C. (1989). Fine structure of *Perkinsus atlanticus* n. sp. (Apicomplexa, Perkinsea) parasite of the clam *Ruditapes decussatus* from Portugal. *J. Parasitol.* **75:** 627-635

Baker G. C., Beebee T. J. C., Ragan M. A. (1999). *Prototheca richardsi*, a pathogen of anuran larvae, is related to a clade of protistan parasites near the animal-fungal divergence. *Microbiology* **145:** 1777-1784

Bangyeekhun E., Ryynänen H. J., Henttonen P., Huner J. V., Cerenius L., Söderhäll K. (2001). Sequence analysis of the ribosomal internal transcribed spacer DNA of the crayfish parasite *Psorospermium haeckeli. Dis. Aquat. Org.* **46:** 217-222

Barr D. J. S., Hartmann V. E. (1976). Zoospore ultrastructure of three *Chytridium* species and *Rhizoclasmatium globosum*. *Can. J. Bot.* **54:** 2000-2013

Beebee T. J. C. (1991). Purification of an agent causing growth inhibition in anuran larvae and its identification as a unicellular unpigmented alga. *Can. J. Zool.* **69:** 2146-2153

Benny G. L., O'Donnell K. (2000) *Amoebidium parasiticum* is a protozoan, not a trichomycete. *Mycologia* **92:** 1133-1137

Cavalier-Smith T. (1998) Neomonada and the origin of animals and fungi. In: Evolutionary Relationships Among Protozoa. (Eds. G. H. Coombs, K. Vickerman, M. A. Sleigh, A. Warren) Kluwer Academic Publishers, Dordrecht, Boston, London, 375-407

Dyková I., Lom J. (1992) New evidence of fungal nature of *Dermocystidium koi* Hoshina and Sahara, 1950. *J. Appl. Ichthyol.* **8:** 180-185

Ergens R., Lom J. (1970) Původci parasitárních nemocí ryb. (Causative agents of parasitic fish diseases). Academia, Praha

Felsenstein J. (2002) PHYLIP home page. http://evolution.genetics.washington.edu/phylip.html

Figueras A., Lorenzo G., Ordas M. C., Gouy M., Novoa B. (2000) Sequence of the small subunit ribosomal RNA gene of *Pseudoperkinsus atlanticus*-like isolated from carpet shell clam in Galicia, Spain. *Mar. Biotechnol.* **2:** 419-428

Fredricks D. N., Jolley J. A., Lepp P. W., Kosek J. C., Relman D. A. (2000) *Rhinosporidium seeberi*: a human pathogen from novel group of aquatic protistan parasites. *Emerg. Infect. Diseases* **6:** 273-282

Gutell R. R. (2002) Comparative RNA web site. http://www.rna.icmb.utexas.edu/

Harrell L.W., Elston R. A., Scott T. M., Wilkinson M. T. (1986). A significant new systemic disease of net-pen reared chinook salmon (*Oncorhynchus tshawytscha*) brood stock. *Aquaculture* **55:** 249-262

Hedrick R. P., Friedman C. S., Modin J. (1989). Systemic infection in Atlantic salmon *Salmo salar* with a *Dermocystidium*-like species. *Dis. Aquat. Org.* **7:** 171-177

Herr R. A., Ajello L., Taylor J. W., Arseculeratne S. N., Mendoza L. (1999). Phylogenetic analysis of *Rhinosporidium seeberi's* 18S small-subunit ribosomal DNA groups this pathogen among members of the protoctistan Mesomycetozoa clade. *J. Clin. Microbiol.* **37:** 2750-2754

Hollande A., Enjumet M. (1953) Contribution à l´étude biologique des Sphaerocollides (Radiolaires collodaires polycyttaires) et de leurs parasites. Partie I. Thalassicolidae, Physematidae,

Thalassophysidae. *Ann. Sci. Nat., Zool.,* 11e Série XVI 1953, 99-183

Huelsenbeck J. P., Ronquist F. (2001) MRBAYES: Bayesian inference of phylogenetic trees. *Bioinformatics* **17:** 754-755

Huelsenbeck J. P., Ronquist F., Nielsen R., Bollback J. P. (2001) Bayesian inference of phylogeny and its impact on evolutionary biology. *Science* **294:** 2310-2314

Lange L., Olson L. (1979) The uniflagellate Phycomycete zoospore. *Dansk Botanisk Arkiv* **33:** 2: 95

Lom J., Dyková I. (1992) Protozoan parasites of fishes. Developments in Aquaculture and Fisheries Science, 26. Elsevier, Amsterdam, London, New York, Tokyo

Lotman K., Pekkarinen M., Kasesalu J. (2000) Morphological observations on the life cycle of *Dermocystidium cyprini* Červinka and Lom, 1974, parasitic in carps (*Cyprinus carpio*). *Acta Protozool.* **39:** 125-134

McVicar A. H., Wootten R. (1980) Disease in farmed juvenile Atlantic salmon caused by *Dermocystidium* sp. In: Fish Diseases, (Ed. W. Ahne) Springer, Berlin 165-173

Nash G., Southgate P., Richards R. H. (1989) A systemic protozoal disease of cultured salmonids. *J. Fish Dis.* **12:** 157-173

Olson R. E., Dungan C. F., Holt R. A. (1991) Water-borne transmission of *Dermocystidium salmonis* in the laboratory. *Dis. Aquat. Org.* **12:** 41-48

Nylund V., Westman K., Lounatmaa K. (1983) Ultrastructure and taxonomic position of the crayfish parasite *Psorospermium haeckeli* Hilgendorf. *Freshwater Crayfish* **5:** 307-314.

Paperna I. (1986) *Ichthyophonus* infection in grey mullets from Southern Africa: histopathological and ultrastructural study. *Dis. Aquat. Org*. **1:** 89-97

Pekkarinen M., Lotman K. (2003) Occurrence and life cycles of *Dermocystidium* species (Mesomycetozoa) in the perch (*Perca fluviatilis*) and ruff (*Gymnocephalus cernuus*) (Pisces: Perciformes) in Finland and Estonia. *J. Nat. Hist*. **37:** 1155-1172

Pronin N. M. (1976) Distribution of *Dermocystidium percae* in the lakes of Trans-Baikallen, and some aspects of epizootiology and aethiology of young perch's dermocystidiosis. In Bolezni i Parazity Ryb: Sverdlovsk, 104-117 (in Russian, English summary)

Ragan M. A., Goggin C. L., Cawthorn R. J., Cerenius L., Jamieson A. V .D., Plourde S. M., Rand T. G., Söderhäll K., Gutell R. R. (1996) A novel clade of protistan parasites near the animal-fungal divergence. *Proc. Natl Acad. Sci. USA* **93:** 11907-11912

Rahimian H. (1998) Pathology and morphology of *Ichthyophonus hoferi* in naturally infected fishes off the Swedish west coast. *Dis. Aquat. Org.* **34:** 109-123

Raikov I.G. (1982) The Protozoan Nucleus. Morphology and Evolution. (Translated from the Russian). Springer-Verlag, Wien

Rand T. G. (1994) An unusual form of *Ichthyophonus hoferi* (Ichthyophonales: Ichthyophonaceae) from yellowtail flounder *Limanda ferruginea* from the Nova Scotia shelf. *Dis. Aquat. Org.* **18:** 21-28

Rand T. G., White K., Cannone J. J., Gutell R. R., Murphy C. A., Ragan M. A. (2000) *Ichthyophonus irregularis* sp. nov. from the yellowtail flounder *Limanda ferruginea* from the Nova Scotia shelf. *Dis. Aquat. Org.* **41:** 31-36

Reichenbach-Klinke H.-H. (1950) Der Entwicklungskreis der Dermocystidien sowie Beschreibung einer neuen Haplosporidienart *Dermocystidium percae* n. sp. *Verh. Deutsch. Zool. 2-6 August 1949 in Mainz*: 126-132

Rug M., Vogt G. (1995) Histology and histochemistry of developing and mature spores of two morphotypes of "*Psorospermium haeckeli*". *Freshwater Crayfish* **10:** 374-384

Ruggieri G. D., Nigrelli R. F., Powles P. M., Garnell D. G. (1970) Epizootics in yellow tail flounder, *Limanda ferruginea* Storer in the Western North Atlantic caused by *Ichthyophonus*, an ubiquitous parasitic fungus. *Zoologica*, N.Y. **55:** 57-62

Saunders G. W., Kraft G. T. (1994) Small-subunit rRNA gene sequences from representatives of selected families of the Gigartinales and Rhodymeniales (Rhodophyta). I. Evidence for the Plocamiales ord. nov. *Can. J. Bot.* **72:** 1250-1263

Spanggaard B., Skouboe P., Rossen L., Taylor J. W. (1996). Phylogenetic relationships of the intercellular fish pathogen *Ichthyophonus hoferi* and fungi, choanoflagellates and the rosette agent. *Mar. Biol.* **126:** 109-115

Sterba G., Naumann W. (1970) Untersuchungen über *Dermocystidium granulosum* n.sp. bei *Tetraodon palembangensis* (Bleeker, 1852). *Arch. Protistenk.* **112:** 106-118

Tyler S. (1984) Turbellarian Platyhelminthes. In: Biology of the Integument. I. Invertebrates, (Eds. J. Bereiter-Hahn., A. G. Maltoltsy, K. S. Richards) Springer-Verlag, Berlin, Heidelberg, New York, Tokyo, 112-131

Ustinova I., Krienitz L., Huss V. A. R. (2000) *Hyaloraphidium curvatum* is not a green alga, but a lower fungus; *Amoebidium parasiticum* is not a fungus, but a member of the DRIPs. *Protist* **151:** 253-262

Van de Moer A., Manier J.-F., Bouix G. (1987). Etude ultrastructurale de *Dermocystidium macrophagi* n. sp., parasite intracellulaire de *Salmo gairdneri* Richardson, 1836. *Ann. Sci. Nat., Zool. Paris, 13 Série 1986-1987,* **8:** 143-151

Vogt G., Rug M. (1999) Life stages and tentative life cycle of *Psorospermium haeckeli*, a species of the novel DRIPs clade from the animal-fungal dichotomy. *J. Exp. Zool.* **283:** 31-42

Whistler H. C., Fuller M. S. (1968) Preliminary observations on the holdfast of *Amoebidium parasiticum*. *Mycologia* **60:** 1068-1079

Wong A., Beebee T. (1994) Identification of a unicellular, non-pigmented alga that mediates growth inhibition in anuran tadpoles: a new species of the genus *Prototheca* (Chlorophyceae: Chlorococcales). *Hydrobiologia* **277:** 85-96

Wootten R., McVicar A. H. (1982) *Dermocystidium* from cultured eels, *Anguilla anguilla* L., in Scotland. *J. Fish Dis*. **5:** 215-222

Yang Z. (1993) Maximum likelihood estimation of phylogeny from DNA sequences when substitution rates differ over sites. *Mol. Biol. Evol.* **10:** 1396-1401

Yang Z. (1994) Estimating the pattern of nucleotide substitutions. *J. Mol. Evol.* **39:** 105-111

Received on 15th May, 2003; revised version on 26th August, 2003; accepted on 4th September, 2003

Acta Protozool. (2003) 42: 309 - 315

ACTA
PROTOZOOLOGICA

Long-term Patterns of Occurrence of *Nosema locustae* and *Perezia dichroplusae* (Microsporidia) in Grasshoppers (Orthoptera: Acrididae) of the Pampas, Argentina

Carlos E. LANGE

Scientific Investigations Commission (CIC) of Buenos Aires Province, Center for Parasitological Studies (CEPAVE), La Plata National University (UNLP) and National Research Council (CONICET), La Plata, Argentina

Summary. The long-term (through the years) occurrence of the two known microsporidia parasitizing grasshoppers of the subfamily Melanoplinae in the Pampas of Argentina (vertically transmitted, native *Perezia dichroplusae* and horizontally transmitted, introduced *Nosema locustae*) was monitored at 13 localities from 1995 to 2003. *Nosema locustae* occurred at nine localities, and *P. dichroplusae* at five. There was almost no overlap of occurrence, and mixed infections were not registered. The presence and prevalences (1% to 6.1%) of *P. dichroplusae* were relatively stable over the years in all localities while *N. locustae* alternated years of presence and absence, and prevalences fluctuated markedly from 1.8% up to 41%. On four instances, each at a different locality, unusually high prevalences (epizootics) of *N. locustae* were recorded. Natural epizootics of such magnitudes are not known for *N. locustae* in other regions of the world.

Key words: enzootic, epizootic, horizontal transmission, Melanoplinae, prevalence, vertical transmission.

INTRODUCTION

Two species of microsporidia, *Nosema locustae* Canning and *Perezia dichroplusae* Lange, are known to occur in grasshopper species of the Argentine Pampas. *Nosema locustae*, a pathogen of the adipose tissue with an unusually broad host range (today known to include more than 100 species, both natural and experimental; Brooks 1988, Henry 1990, Lange 2002), was experimentally introduced as a grasshopper biological control agent from North America at several localities between 1978 and 1982, and became established in the western Pampas (Lange and de Wysiecki 1996; Lange 2001, 2002). Recent ultrastructural studies have shown that the morphology and development of *N. locustae* remain essentially the same regardless of the host species involved (Sokolova and Lange 2002). Up to the present, infections by *N. locustae* in the Pampas have been detected in grasshoppers belonging to 16 species,

Address for correspondence: Carlos E. Lange, Scientific Investigations Commission (CIC) of Buenos Aires province, Center for Parasitological Studies (CEPAVE), La Plata National University (UNLP) and National Research Council (CONICET). Calle 2 # 584, La Plata (1900), Argentina; Fax: 54 221 423 2327 ; E-mail: Lange@mail.retina.ar

mostly melanoplines (subfamily Melanoplinae) (Table 1), which include some of the most harmful species for crops and forage (COPR 1982, Lange *et al*. 2003). Although vertical transmission have been shown to occur in *N. locustae* (Henry and Oma 1981, Raina *et al.* 1995), the primary route of transmission is horizontal through ingestion of propagules (spores), a characteristic that, together with its broad host range, was central for its development as a microbial control agent (Henry and Oma 1981, Johnson 1997, Lockwood *et al.* 1999, Lange 2002).

Perezia dichroplusae, a pathogen of the Malpighian tubules, is a native microsporidium of the melanopline grasshopper *Dichroplus elongatus* Giglio - Tos (Lange 1987a, b), normally one of the most common and harmful grasshopper species in the Pampas (Cigliano and Lange 1999, Cigliano *et al.* 2003). All attempts at transmitting *P. dichroplusae* to its natural host and other closely related species have systematically failed (Lange 1989, and unpublished results). Experimental studies have shown that its main mode of transmission is vertical through the female line (matroclinal) and within the egg (transovarial) (Lange 1997).

The purpose of this investigation was to record the long-term presence/absence of the two microsporidia in grasshoppers of the Pampas, trying to establish patterns of occurrence, and relating these to own characteristics of the pathogens.

MATERIALS AND METHODS

The study extended from 1995 to 2003, and included 13 localities of grasshopper collection. All localities but one (Benito Juárez) were in the western Pampas, eight in Buenos Aires province (Benito Juárez, Carhué, Casbas, Coronel Suárez, General Lamadrid, Laprida, Rivadavia, Trenque Lauquen), and five in La Pampa province (Alta Italia, Eduardo Castex, Ojeda, Riglos, Santa Rosa) (Fig. 1). Five of these localities (Casbas, Coronel Suárez, General Lamadrid, Riglos, Santa Rosa) were in close vicinity of five of the original introduction sites of *N. locustae* (Casbas in 1979, Coronel Suárez in 1981, General Lamadrid in 1981, Macachín in 1982, and Santa Rosa in 1982). Sampling was done always by the same two surveyors with sweep nets (diameter: 40 cm; depth: 75 cm; angle of sweep: 180°) along transects in natural grasslands and improved pastures in early February of each year, a time when grasshopper populations of most species are at their peak as young adults or older nymphs (COPR 1982, Lange *et al*. 2003). Larson *et al.* (1999) have shown that sweep sampling provides a fairly accurate estimate of the relative abundance of most grasshopper species. Since *N. locustae* and *P. dichroplusae* cause, as most microsporidia of insects do (Becnel and Andreadis 1999), chronic (i.e., prolonged course of infection) rather than acute diseases (Henry and Oma 1981, Lange 1987b), and most grasshopper species involved in the study are univoltine (only the species of *Baeacris* can be bivoltine) with winter egg diapause (COPR 1982), the time of year when sampling was conducted should provide an acceptable estimate of the yearly occurrence of both pathogens. One site (Carhué) was visited every year, three sites (Riglos, Santa Rosa, Trenque Lauquen) were visited eight years, one site (Benito Juárez) was visited six years, one site (Coronel Suárez) was visited five years, one site (Rivadavia) was visited four years, three sites (Alta Italia, Eduardo Castex, Ojeda) were visited three years, and three sites (Casbas, General Lamadrid, Laprida) were visited twice. For estimating prevalences of *P. dichroplusae*, each sample consisted of all the individuals of *D. elongatus*, the natural host of *P. dichroplusae*, that were captured with three hundred sweeps. Since previous studies (Lange and de Wysiecki 1999, Lange 2003) have shown that argentine melanopline species of grasshoppers have similar susceptibilities to *N. locustae*, for estimating prevalences of this pathogen each sample consisted of all the melanoplines captured in the three hundred sweeps, namely *Baeacris punctulatus* Thunberg, *Baeacris pseudopunctulatus* Ronderos, *Dichroplus conspersus* Bruner, *Dichroplus elongatus*, *Dichroplus maculipennis* Blanchard, *Dichroplus pratensis* Bruner, *Dichroplus vitattus* Bruner, *Leiotettix pulcher* Rehn, *Neopedies brunneri* (Giglio-Tos), *Ronderosia forcipatus* (Rehn), *Scotussa lemniscata* (Stal), and *Scotussa daguerrei* Liebermann. Grasshoppers collected were placed in cages, and immediately taken to the laboratory where they were frozen at -32°C for later examination.

For disease diagnosis, frozen grasshoppers were thawed and examined by the homogenization method as described by Henry *et al*. (1973) or, less frequently, by ventral, longitudinal dissection and examination of tissues and organs as fresh preparations under phase contrast microscopy (x400; x1000) (Undeen and Vávra 1997). When using the homogenization method, trace infections (i.e. observation of only one spore per microscopic field; Henry *et al*. 1973) were not considered, avoiding, in doing so, biases that may occur due to contamination of homogenizers. *Nosema locustae* and *P. dichroplusae* are readily distinguished by several characters in addition to the organs affected. *Nosema locustae* has much larger spores (mean: 5.2 by 2.8 µm) with little variation in size except for some macrospores, developmental stages (meronts, sporonts) are mostly rounded and always with intimately paired nuclei (diplokaryotic), and sporogony is disporoblastic (Figs 2-4) (Canning 1953, Henry and Oma 1981, Sokolova and Lange 2002). Spores of *P. dichroplusae* are much smaller (mean: 3.5 by 1.5 µm) and vary greatly in size, moniliform developmental stages are present (sporogonial plasmodia), and sporogony is polysporoblastic (Figs 5-7) (Lange 1987a).

RESULTS

Nosema locustae occurred in nine out of the 13 sites (Alta Italia, Carhué, Casbas, Eduardo Castex, Riglos, Rivadavia, Ojeda, Santa Rosa, and Trenque Lauquen) while *P. dichroplusae* was present in five sites (Benito Juárez, Carhué, Coronel Suárez, General Lamadrid, and Laprida) (Table 2). The occurrence of both pathogens in a given site was registered only twice (1996, 1997) at one site (Carhué). Mixed infections (i.e. a single grass-

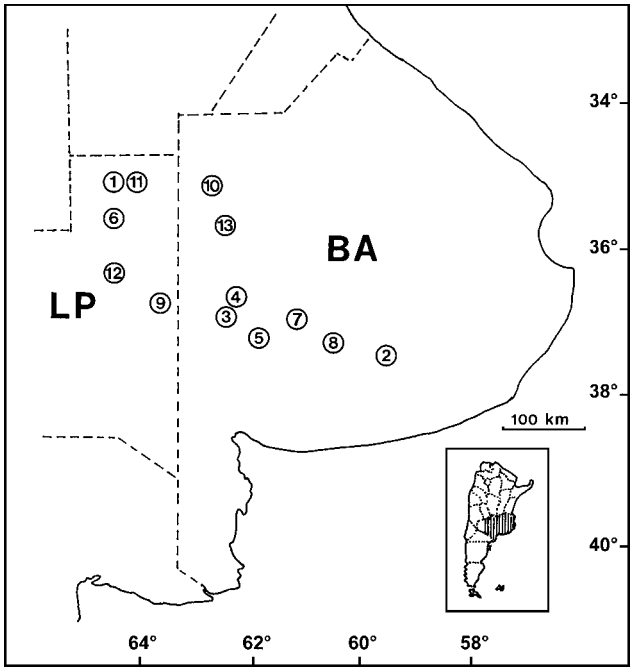

Fig. 1. The 13 sites of grasshopper collection in the Pampas. 1 - Alta Italia, 2 - Benito Juárez, 3 - Carhué, 4 - Casbas, 5 - Coronel Suárez, 6 - Eduardo Castex, 7 - General Lamadrid, 8 - Laprida, 9 - Riglos, 10 - Rivadavia, 11 - Ojeda, 12 - Santa Rosa, 13 - Trenque Lauquen, BA - Buenos Aires province, LP - Pa Pampa province.

Table 1. Species of grasshoppers in which infections of *Nosema locustae* have been found in the western Pampas of Argentina.

Acrididae
Acridinae
Allotruxalis strigata (Bruner)
Euplectrotettix shulzii Bruner
Gomphocerinae
Rhammatocerus pictus (Bruner)
Staurorhectus longicornis Giglio - Tos
Melanoplinae
Baeacris punctulatus (Thunberg)
Baeacris pseudopunctulatus Ronderos
Dichroplus elongatus Giglio - Tos
Dichroplus pratensis Bruner
Dichroplus vitattus Bruner
Leiotettix pulcher Rehn
Neopedies brunneri (Giglio - Tos)
Ronderosia forcipatus Rehn
Scotussa lemniscata (Stal)
Scotussa daguerrei Liebermann
Romaleidae
Romaleinae
Diponthus argentinus Pictet et Saussure
Zoniopoda tarsata (Serville)

hopper individual infected with both pathogens) were never found. In all five sites where *P. dichroplusae* was present, it occurred in all years but one (Coronel Suárez in 2002, albeit the sample size was too small) at fairly stable prevalences that ranged from a minimum of 1% at Benito Juárez in 1995 to a maximum of 6.1% at Carhué in 2001. On the contrary, in all nine sites where *N. locustae* occurred, it alternated years of presence with years of absence (only at Riglos presence was almost permanent). Prevalences of *N. locustae* ranged from a minimum of 1.8% at Trenque Lauquen in 2001 to a maximum of 41% at Riglos in 1996. Aside from Riglos in 1996, there were three other instances where unusually high prevalences of *N. locustae* were detected: 37.5% at Trenque Lauquen in 1996, 21.8% at Rivadavia in 1997, and 20% at Casbas in 2003. The high prevalence registered at Rivadavia in 1997 was followed by three years (1998, 1999, 2002) of absence of *N. locustae* although hosts were still abundant. The high prevalence at Casbas in 2003 was preceded by a year (2002) of absence of *N. locustae* although hosts were relatively abundant.

DISCUSSION

Once a space-time context has been established (in this study, five localities for *P. dichroplusae* and nine for *N. locustae* along two to nine years), the state at which a pathogen occurs in the host population normally fluctuates along a range or continuum with two opposite ends: the enzootic and epizootic states (Fuxa and Tanada 1987). An enzootic disease is usually of low prevalence and is constantly present in the host population while an epizootic disease, on the contrary, is sporadic and limited in duration, and characterized by abrupt changes in prevalence. There are pathogens that tend to occur enzootically, and others that are more prone to vary sharply between states. The long-term occurrence registered for *N. locustae* and *P. dichroplusae* in grasshoppers of the Pampas seems to fit well in this framework. In those localities were *P. dichroplusae* was present, it occurred constantly season after season at relatively low, stable prevalences in what can be considered a typical enzootic state. On the other hand, *N. locustae* exhibited at least four instances in which prevalences that can be considered epizootics (i.e., unusually large number of cases of the disease; Tanada and Kaya 1993) were observed (41 % at Riglos in 1996; 37.5 % at Trenque Lauquen in 1996; 21.8 % at Rivadavia in 1997; 20 % at Casbas in 2003), and several instances of sudden “appearances” or “disappearances” of the

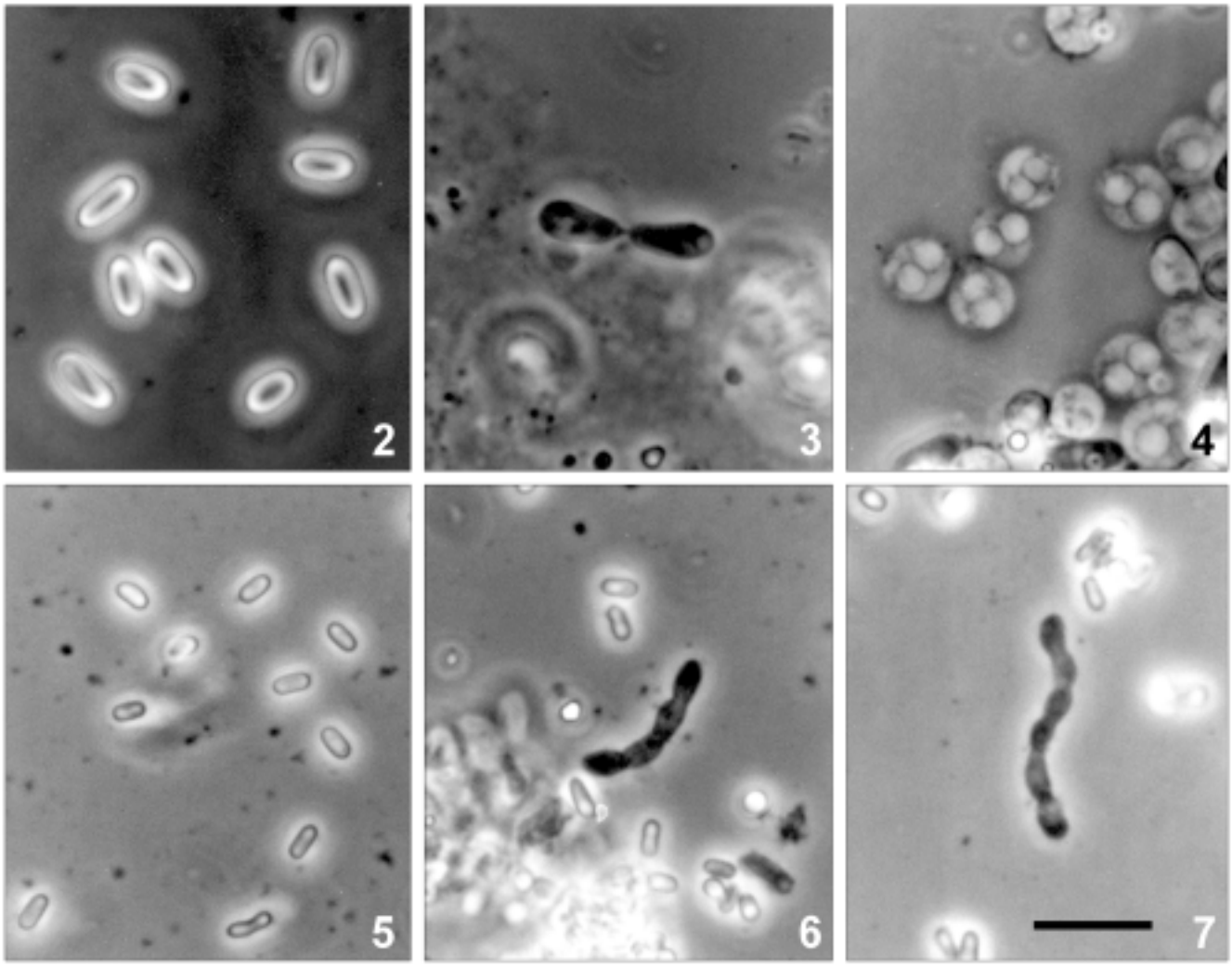

Figs 2-7. Developmental stages and spores of *Nosema locustae* and *Perezia dichroplusae* as fresh preparations under phase contrast microscopy. **2** - mature spores of *N. locustae*, **3** - disporoblastic sporogony of *N. locustae*, **4** - diplokaryotic stages (meronts) of *N. locustae*; **5** - mature spores of *P. dichroplusae*, **6**, **7** - moniliform plasmodia and polysporoblastic sporogony of *P. dichroplusae*. Scale bar 10 µm.

disease in a given locality, most notably at Casbas and Rivadavia, respectively.

Among the many factors that govern the occurrence of an infectious disease in a host population, the ability of the pathogen to be transmitted is of central relevance, and may greatly influence the way the pathogen occurs. In those host-pathogen relationships where horizontal transmission predominates, prevalence typically varies markedly, often culminating in epizootics, while in those relationships where vertical transmission prevails, prevalence is usually maintained in a steady, enzootic state (Andreadis 1987). The predominant transmission routes of *N. locustae* (horizontal) and *P. dichroplusae* (vertical) appear to account for the long-term occurrence that was observed in the Argentine Pampas.

Due to the efficient horizontal transmission that characterizes *N. locustae* (Henry and Oma 1981, Henry 1985, Lange 2003), and the recognized high susceptibility to infection of the melanoplines (Henry 1969, Henry *et al.* 1973, Bomar *et al.* 1993, Lange 2003), the occurrence of the observed epizootics in grasshoppers of the Pampas should probably be considered as an expected phenomenon. However expected, the occurrence of such epizootics are still intriguing. Natural epizootics of *N. locustae* (i.e. those not immediately following its application as a biocontrol agent) of the magnitude

Table 2. Yearly occurrence of *Nosema locustae* in melanopline grasshoppers (top row at each site and year) and *Perezia dichroplusae* in *Dichroplus elongatus* (second row) at 13 sites in the Pampas. The first number indicates prevalence (% of infection) and the one between parenthesis is the sample size (n).

	1995	**1996**	**1997**	**1998**	**1999**	**2000**	**2001**	**2002**	**2003**
A. Italia			2.9 (103) 0 (6)	0 (101) 0 (13)	0 (26) 0 (11)				
B. Juárez	0 (750) 1 (584)				0 (98) 2.8 (71)	0 (329) 1.2 (257)	0 (348) 1.7 (288)	0 (400) 1.3 (318)	0 (340) 2.2 (240)
Carhué	0 (67) 2.2 (90)	2.8 (36) 4 (25)	8 (25) 5.9 (17)	0 (62) 1.3 (74)	0 (44) 3.8 (26)	0 (156) 1.9 (105)	0 (42) 6.1 (33)	0 (47) 4.1 (121)	0 (213) 5.8 (138)
Casbas								0 (97) 0 (15)	20 (190) 0 (8)
C. Suárez		0 (302) 3.4 (156)			0 (257) 3.2 (157)	0 (310) 2.1 (94)		0 (180) 0 (6)	0 (188) 1.7 (59)
E. Castex	4.5 (312) 0 (257)	2.4 (84) 0 (25)	0 (150) 0 (256)						
G. Lamadrid		0 (205) 1.5 (129)				0 (175) 1.2 (87)			
Laprida		0 (371) 2.1 (136)				0 (168) 3.1 (127)			
Riglos	9 (379) 0 (79)	41 (166) 0 (26)	11.4 (44) 0 (25)	11.1 (36) 0 (8)	5.4 (55) 0 (0)	2 (195) 0 (4)		1 (95) 0 (39)	0 (61) 0 (60)
Rivadavia			21.8 (350) 0 (307)	0 (254) 0 (215)	0 (74) 0 (74)			0 (117) 0 (108)	
Ojeda			1.2 (159) 0 (44)	0 (89) 0 (35)	0 (92) 0 (60)				
S. Rosa	0 (274) 0 (104)	3 (269) 0 (96)	8.2 (97) 0 (90)	0 (215) 0 (147)	0 (171) 0 (160)	0 (34) 0 (7)	0 (53) 0 (0)	0 (20) 0 (12)	
T. Lauquen	3.8 (158) 0 (85)	37.5 (40) 0 (22)	15.8 (19) 0 (38)	0 (25) 0 (16)	2.5 (40) 0 (14)	0 (70) 0 (11)	1.8 (55) 0 (16)	0 (45) 0 (29)	

observed in the Pampas are not known in other regions of the world where *N. locustae* is native. In North America, where melanoplines are often numerically dominant in grasshopper communities, prevalences are normally less than 1 % with rare peaks of 2 to 5 % (Henry and Oma 1981, Ewen 1983). In India, prevalences were 1 to 2 %, sporadically reaching 5 % (Raina *et al.* 1987). Almost 10 % has been reported in the South Africa record but the sampled grasshoppers were kept in cages for some time before diagnosis (Whitlock and Brown 1991). Even repeated field applications of *N. locustae* in North America did not result in significant increases of prevalence (Johnson and Dolinsky 1997). Reasons that would explain the occurrence of epizootics of *N. locustae* in the Pampas are not at hand but it should be kept in mind that its introduction resulted in a number of new host-pathogen associations (Hokkanen and Pimentel 1984, Hajek *et al.* 2000) with unpredictable outcomes.

Another intriguing aspect is how *N. locustae* "appears" and "disappears" at a given locality through the seasons. In this sense, persistence and dissemination of

a microsporidian pathogen in host populations is known to be governed by many factors, such as modes of transmission, behavior and movements of hosts and nonhost carriers, and physical agents (Andreadis 1987), and a number of possible scenarios would account for the sudden "appearances" of *N. locustae* in a given locality. In *N. locustae*, the main horizontal route of transmission is complemented by vertical transmission (Henry and Oma 1981, Raina *et al.* 1995), a way that may transfer infection from one season to the following. None of the grasshopper species known to be affected by *N. locustae* in the Pampas is an overwintering species (COPR 1982). Most of the grasshoppers affected in the Pampas have winged adults, and an infected grasshopper still capable of flying may disperse the infection. Among potential nonhost carriers, many insectivorous and opportunistic birds are known to prey on grasshoppers in the general area of establishment of *N. locustae* in the Pampas, notably the Swainson´s hawk, *Buteo swainsoni*, the large flocks of which feed almost exclusively on grasshoppers (Goldstein *et al.* 1999). Physical agents such as wind and water would probably play a very minor role or no role at all in the spread of *N. locustae*. Spores of microsporidia are normally short lived in the environment (Becnel and Andreadis 1999), and Germida *et al.* (1987) found that *N. locustae* spores persisted very poorly in soils, and do not persist at all in vegetation of treated fields.

The absence of *N. locustae* in a locality where it was present in the previous season and where susceptible hosts were still abundant (notably Carhué, Rivadavia and Santa Rosa) remains unexplained. One would expect that as long as reasonable numbers of potential hosts are available, *N. locustae* should be able to persist season after season, especially considering that it has a vertical route of transmission.

Finally, another interesting outcome delivered by the study was that there was almost no geographical overlap between records of the two pathogens. *Perezia dichroplusae* was recorded at the southernmost sites (Benito Juárez, Coronel Suárez, General Lamadrid, Laprida) and *N. locustae* at the western sites (Alta Italia, Casbas, Eduardo Castex, Riglos, Rivadavia, Ojeda, Santa Rosa, Trenque Lauquen). Only at Carhué, and is just two seasons (1996, 1997), there were records of both pathogens in different individuals of *D. elongatus* (i.e., not mixed infections). Considering that some of the introductions of *N. locustae* were made where the southernmost sites are, the possibility that this pathogen did not established there because a native microsporidium (*P. dichroplusae)* was already present can not be ruled out. Antagonistic interactions between *N. locustae* and an undescribed microsporidium have been suggested (Streett and Henry 1984), and Solter *et al.* (2002) have recently demonstrated through experimental work antagonistic interactions for other microsporidia of terrestrial insects.

Acknowledgments. The author is thankful to Dr. María Laura de Wysiecki for her assistance in the field work. This work was supported by CIC, CONICET (PIP 4015/96), and the Orthopterists Society.

REFERENCES

Andreadis T. G. (1987) Transmission. In: Epizootiology of Insect Diseases, (Eds. J. R. Fuxa, Y. Tanada). John Wiley & Sons, New York, 159-176

Becnel J. J., Andreadis T. G. (1999) Microsporidia in insects. In: The Microsporidia and Microsporidiosis, (Eds. M. Wittner, L. M. Weiss). American Society of Microbiology, Washington, D. C., 447-501

Bomar Ch. R., Lockwood J. A., Pomerinke M. A., French J. D. (1993) Multiyear evaluation of the effects of *Nosema locustae* (Microsporidia: Nosematidae) on rangeland grasshoppers (Orthoptera: Acrididae) population density and natural biological controls. *Environ. Entomol.* **22:** 489-497

Brooks W. M. (1988) Entomogenous Protozoa. In: Handbook of Naturally Occurring Pesticides, (Ed. C. M. Ignoffo). CRC Press, Boca Raton, Florida, 1-149

Canning E. U. (1953) A new microsporidium, *Nosema locustae* n. sp., from the fat body of the African migratory locust *Locusta migratoria migratorioides. Parasitology* **43:** 287-290

Cigliano M. M., Lange C. E. (1999) *Dichroplus elongatus*. In: Global Crop Protection Compendium. (Ed. Centre for Agriculture and Biosciences International), Wallingford, UK, (www.cabicompendium.org/cpc)

Cigliano M. M., Torrusio S. E., de Wysiecki M. L. (2003) Grasshopper (Orthoptera: Acridoidea) community composition and temporal variation in the Pampas, Argentina. *J. Orthoptera Res.* **11:** 215-221

COPR (1982) The locust and grasshopper agricultural manual. Centre for Overseas Pest Research, London

Ewen A. B. (1983) Extension of the geographic range of *Nosema locustae* (Microsporidia) in grasshoppers. *Can. Entomol.* **115:** 1049-1050

Fuxa J. R., Tanada Y. (1987) Epidemiological concepts applied to insect epizootiology. In: Epizootiology of Insect Diseases, (Eds. J. R. Fuxa, Y. Tanada). Wiley and Sons, New York, 3-21

Germida J. J., Ewen A. B., Onofriechuk E. E. (1987) *Nosema locustae* Canning (Microsporida) spore populations in treated field soils and resident grasshopper populations. *Can. Entomol.* **119:** 335-360

Goldstein M. I., Lacher T. E., Woodbridge B., Bechard M. J., Canavelli S. B., Zaccagnini M. E., Cobb G. P., Scollon E. J., Tribolet R., Hooper M. J. (1999) Monocrotophos-induced mass mortality of Swainson´s hawks in Argentina, 1995-96. *Ecotoxicology* **8:** 201-214

Hajek A. E., Delalibera I., McManus M. L. (2000) Introduction of exotic pathogens and documentation of their establishment and impact. In: Field Manual of Techniques in Invertebrate Pathology, (Eds. L. A. Lacey, H. K. Kaya). Kluwer Academic Press, Netherlands, 339-369

Henry J. E. (1969) Extension of the host range of *Nosema locustae* in Orthoptera. *Ann. Entomol. Soc. Am.* **62:** 452-453

Henry J. E. (1985) Effect of grasshopper species, cage density, light intensity, and method of inoculation on mass production of *Nosema locustae* (Microsporida: Nosematidae). *J. Econ. Entomol.* **78:** 1245-1250

Henry J. E. (1990) Control of insects by Protozoa. In: New Directions in Biological Control: Alternatives for Suppressing Agricultural Pests and Diseases, (Eds. R. Baker, P. E. Dunn). A. R. Liss, New York, 161-176

Henry J. E. Oma E. A. (1981) Pest control by *Nosema locustae*, a pathogen of grasshoppers and crickets. In: Microbial Control Of Pests and Plant Diseases 1970-1980, (Ed. H. D.Burges). Academic Press, New York, 573-586

Henry J. E., Tiahrt K., Oma E. A. (1973) Importance of timing, spore concentrations, and levels of spore carrier in applications of *Nosema locustae* (Microsporida: Nosematidae) for control of grasshoppers. *J. Invertebr. Pathol.* **21:** 263-272

Hokkanen H. M. T., Pimentel D. (1984) New approach for selecting biological control agents. *Can. Entomol.* **116:** 1109-1121

Johnson D. L. (1997) Nosematidae and other protozoa as agents for control of grasshoppers and locusts: current status and prospects. *Mem. Entomol. Soc. Canada* **171:** 375-389

Johnson D. L., Dolinski M. G. (1997) Attempts to increase the prevalence and severity of infection of grasshoppers with the entomopathogen *Nosema locustae* Canning (Microsporida: Nosematidae) by repeated field application. *Mem. Entomol. Soc. Canada* **171:** 391-400

Lange C. E. (1987a) A new species of *Perezia* (Microsporida: Pereziidae) from the Argentine grasshopper *Dichroplus elongatus* (Orthoptera: Acrididae). *J. Protozool.* **34:** 34-39

Lange C. E. (1987b) Histopathology in the Malpighian tubules of *Dichroplus elongatus* (Orthoptera: Acrididae) infected with *Perezia dichroplusae* (Microspora: Pereziidae). *J. Invertebr. Pathol.* **50:** 146-150

Lange C. E. (1989) Prevalence of *Perezia dichroplusae* (Microspora: Pereziidae) in Argentine Grasshoppers (Orthoptera: Acrididae). *J. Invertebr. Pathol.* **54:** 269-271

Lange C. E. (1997) Transmisión vertical de *Perezia dichroplusae* Lange (Protozoa: Microspora) en su hospedador natural, *Dichroplus elongatus* Giglio-Tos (Orthoptera: Acrididae). *Neotrópica* **43:** 39-42 (in Spanish, English summary).

Lange C. E. (2001) Twenty years after the introductions of *Nosema locustae* for grasshopper control in Argentina: un update. *Metaleptea Special Meeting Issue*, Orthopterists Society, USA, 87

Lange C. E. (2002) El desarrollo de *Nosema locustae* Canning (Microsporidia) para el control biológico de tucuras (Orthoptera: Acridoidea) y las consecuencias de su utilización en la Argentina. *Rev. Soc. Entomol. Arg.* **61:** 1-9 (in Spanish, English summary)

Lange C. E. (2003) Niveles de esporulación experimentales y naturales del agente de biocontrol *Nosema locustae* (Microsporidia) en especies de tucuras y langostas (Orthoptera: Acridoidea) de la Argentina. *Rev. Soc. Entomol. Arg.* **62:** 11-19 (in Spanish, English summary)

Lange C. E., de Wysiecki M. L. (1996) The fate of *Nosema locustae* (Microsporida: Nosematidae) in argentine grasshoppers (Orthoptera: Acrididae). *Biological Control* **7:** 24-29

Lange C. E., de Wysiecki M. L. (1999) Epizootias de *Nosema locustae* (Protozoa: Microspora) en melanoplinos (Orthoptera: Acrididae: Melanoplinae) de Buenos Aires y La Pampa. *Rev. Soc. Entomol. Arg.* **58:** 76-78 (in Spanish, English summary)

Lange C. E., Cigliano M. M., de Wysiecki M. L. (2003) Los acridoideos (Orthoptera: Acridoidea) de importancia económica en la Argentina. En: Barrientos Lozano, L. (Ed.), Los Acridoideos de Importancia Económica en América Latina, Instituto Tecnológico de Ciudad Victoria, Tamaulipas, México, (in press) (in Spanish)

Larson D. P., O´Neill K. M., Kemp W. P. (1999) Evaluation of the accuracy of sweep sampling in determining grasshopper (Orthoptera: Acrididae) community composition. *J. Agricul. Urban Entomol.* **16:** 207-214

Lockwood J. A., Bomar C. R., Ewen A. B. (1999) The history of biological control with *Nosema locustae*: lessons for locusts management. *Insect Sci. Appl.* **19:** 1-17

Raina S. K., Rai M. M., Khurad A. M. (1987) Grasshopper and locust control using microsporidian insecticides. In: Biotechnology in Invertebrate Pathology and Cell Culture, (Ed. K. Maramorosh), Academic Press, New York, 345-365

Raina S. K., Das S., Rai M. M., Khurad A. M. (1995) Transovarial transmission of *Nosema locustae* (Microsporida: Nosematidae) in the Migratory locust *Locusta migratoria migratorioides*. *Parasitol. Res.* **81:** 38-44

Sokolova Y., Lange C. E. (2002) An ultrastructural study of *Nosema locustae* Canning (Microspora) from three species of Acrididae (Orthoptera). *Acta Protozool.* **41:** 221-237

Solter L. F., Siegel J. P., Pilarska D. K., Higgs M. C. (2002) The impact of mixed infection of three species of microsporidia isolated from the gypsy moth, *Lymantria dispar* L. (Lepidoptera: Lymantriidae). *J. Invertebr. Pathol.* **81:** 103-113

Streett D. A., Henry J. E. (1984) Epizootiology of a microsporidium in field populations of *Aulocora elliotti* and *Psoloessa delicatula* (Insecta: Orthoptera). *Can. Entomol.* **116:** 1439-1440

Tanada Y., Kaya H. K. (1993) Insect Pathology. Academic Press, San Diego

Undeen A. H., Vávra J. 1997 Research methods for entomopathogenic Protozoa. In: Manual of Techniques in Insect Pathology, (Ed. L. Lacey), Academic Press, San Diego, 117-151

Whitlock V. H., Brown S. T. (1991) First record for *Nosema locustae* in the Brown locust *Locustana pardalina* in South Africa, and the yield of spores in laboratory bioassays. *J. Invertebr. Pathol.* **58:** 164-167

Received on 19 th May, 2003; revised on 23rd July; accepted on 24th July, 2003

Acta Protozool. (2003) 42: 317 - 324

ACTA
PROTOZOOLOGICA

Genetic Analysis of Forty Isolates of *Acanthamoeba* Group III by Multilocus Isoenzyme Electrophoresis

James A. FLINT[1], Philip J. DOBSON[2] and Bret S. ROBINSON[2]

[1]Caribbean Epidemiology Centre, Part of Spain, Trinidad and Tobago; [2]Australian Water Quality Centre, SA Water Corporation, Bolivar, Australia

Summary. Two clinical and 32 environmental *Acanthamoeba* isolates belonging to Group III were compared with reference strains of *A. culbertsoni*, *A. healyi*, *A. jacobsi*, *A. lenticulata*, *A. royreba* and *A. palestinensis* by multilocus isozyme analysis. Genetically useful data were produced for 21 loci. The two principle clusters corresponded to *A. jacobsi* (20 isolates) and *A. lenticulata* (up to 9 isolates). *A. jacobsi* was the least variable species and was widely distributed, with isolates from Australia, Fiji, Japan, New Guinea, New Zealand and Britain. Most other isolates occurred as single zymodemes, not closely related to each other. No new isolate could be assigned to *A. culbertsoni*, *A. healyi*, or *A. royreba*. A clinical isolate from an Australian GAE case, AC118, was the only 44°C-tolerant isolate not referable to *A. jacobsi* and appears to be a new species.

Key words: *Acanthamoeba* species, biogeography, isozyme analysis.

INTRODUCTION

Acanthamoeba species are small, generally bactiverous amoebae with robust cysts, which occur widely in soil, freshwater and marine environments. While they are undoubtedly freeliving, they are responsible for several distinct human diseases, including granulomatous amoebic encephalitis (GAE), the corneal infection amoebic keratitis and disseminated cutaneous ulcerations (Martinez and Janitsche 1985, Visvesvara and Stehr-Green 1990). *Acanthamoeba* species may also be indirectly significant for health through their ability to harbour and assist in the dissemination of pathogenic bacteria such as *Legionella pneumophila* (Rowbotham 1986, Berk *et al.* 1998).

The genus *Acanthamoeba* includes about 25 nominal species, in three sub-generic groups distinguished on the basis of cyst morphology (Pussard and Pons 1977). Most species were originally described from single strains and few of the descriptions adequately distinguished interspecific differences from intraspecific variation. The morphological characteristics used in many of the descriptions overlap considerably and may vary with culture conditions (Sawyer 1971). New clinical and environmental isolates are therefore difficult to assign to species. In any case, genetic analysis, by isozymes and more recently by 18s rDNA sequencing, has shown that

Address for correspondence: Bret S. Robinson, Australian Water Quality Centre, Private Mail Bag 3, Salisbury, SA 5108, Australia; Fax: 61-8-82590228; E-mail: bret.robinson@sawater.com.au

many of these organisms are not sufficiently distinct to be treated as species (De Jonckheere 1983, Stothard *et al.* 1998). A classification of *Acanthamoeba* species into a series of sequence types (Gast *et al.* 1996, Stothard *et al.* 1998) is growing in acceptance.

In the study reported here, we examined two clinical isolates and 32 environmental isolates of *Acanthamoeba* Group III, using multi locus isoenzyme electrophoresis to compare them with reference strains representing six species or sequence types. By concentrating on a putative subgeneric group and characterising a large number of new isolates, we hoped to discern patterns that have not been apparent in other studies. The following specific questions were addressed: Is genetic diversity discontinuous within *Acanthamoeba* group III, so that the boundaries between species are clear? Is there agreement between isozyme and sequence analysis, particularly regarding the genetic soundness of 'species' represented by the reference strains? Finally, can the clinical and environmental isolates be identified with previously characterised lineages, or do they include new divergent groups?

MATERIALS AND METHODS

Origin and cultivation of strains. All *Acanthamoeba* group III isolates came from the culture collection of the Australian Water Quality Centre, with the reference strains of six currently recognised Group III species acquired originally from the American Type Culture Collection (ATCC). Thirty-two environmental isolates from nine countries were chosen to represent diverse geographic sources and habitats, for comparison with two Australian clinical isolates (Table 1). The type strain of *A. palestinensis*, the species with the lowest temperature tolerance and already known to be divergent from other Group III species, was used as an outgroup.

Isolates were grown initially on non-nutrient agar plates spread with a lawn of penicillin- and streptomycin-sensitive *Escherichia coli* (*NNA/E. coli*) and incubated at 30°C (*A. palestinensis*) or 37°C. To establish axenic cultures, actively growing trophozoites were transferred into 10 ml of Peptone Yeast extract Glucose medium (PYG, ATCC Medium 712) incorporating penicillin and streptomycin to eliminate the *E. coli*, and incubated at the same temperature. For isozyme extracts, amoebae were harvested in late log phase (10^5 to 10^6 cells per ml). Strains that were difficult to grow axenically were enriched on plate cultures by re-spreading with additional *E. coli* and incubating for a further 16-20 h before harvesting.

Temperature tolerance. *NNA/E. coli* plates were inoculated with trophozoites from active cultures and incubated at temperature intervals of one or two degrees between 35°C and 44°C for 48-72 h. The highest temperature at which growth occurred was recorded as the temperature tolerance of the isolate.

Isozyme extracts. Amoebae from plate cultures, suspended in quarter-strength Ringer solution (Oxoid), or from PYG medium were concentrated by centrifugation at 12,000 rcf for 5 min. The pellet was resuspended in an equal volume of homogenising solution (14 mM 2-mercaptoethanol, 120 µM NADP) and subjected to three 0.3 s pulses of sonication (Branson 250 sonicator). Unwanted cell debris was removed by centrifugation for 5 min at 12,000 rcf and the supernatant transferred to haematocrit tubes in 5-10 µl aliquots for storage at -20°C.

Electrophoresis. Enzyme extracts were separated on cellulose acetate gels (Cellogel, Chemetron, Milan, Italy) and stained using a range of conditions found suitable for various enzymes from *Naegleria* species (Table 2; Adams *et al.* 1989, Robinson *et al.* 1992). The resulting zymograms were interpreted in a Mendelian framework. That is, the smallest number of loci consistent with diploidy was assumed, and allelic states were designated in light of the known tertiary structures of particular enzyme families.

Data analysis. The allelic data were converted to a matrix of pairwise differences (% of loci without shared alleles) from which neighbor-joining and UPGMA dendrograms were derived using the PHYLIP package (Felsenstein 2002). A second matrix was calculated for differences weighted to take account of the genetic diversity at each locus (i.e. placing greater weight on less variable loci). The frequency distribution of all pairwise distances (weighted and unweighted) was plotted to aid recognition of any genetic discontinuity that might correspond to species boundaries.

RESULTS

Among the reference strains, only *A. palestinensis* could not grow at least at 40°C (Table 1). The environmetal isolates included a large set that grew at 44°C and others that could not grow above 40°C or 42°C. The strain from the keratitis case grew at 40°C, while the strain from the GAE case could grow at 44°C. Of the 44°C-tolerant isolates, only AC118 would grow in PYG medium. *A. palestinensis* and all 40°C and 42°C-tolerant isolates grew axenically.

Allelic profiles for the 40 *Acanthamoeba* group III isolates are presented in Table 3. The isolates fell into 33 distinguishable zymodemes, with patterns that could be interpreted as heterozygous at 12 of the 21 loci. Two zymodemes consisted of four isolates each (AC088, AC194, AC178, AC201 and AC062, AC085, AC087, AC138) and one of two isolates (AC080, AC229). The relationships among the zymodemes are presented as a neighbor-joining dendrogram (Fig. 1), with the indistinguishable isolates represented by AC088, AC062 and AC080. Twenty replications of the neighbor-joining computation with randomised input order gave dendrograms with identical topology. The UPGMA dendrogram (not shown) was more sensitive to input order, with replicates varying principally in the branching order of the closer relationships within *A. jacobsi* and *A. lenticulata*.

Table 1. *Acanthamoeba* isolates employed in this study.

AWQC No	Genus	Species	TT[a] (°C)	Geographic origin	Habitat	Cross reference
Reference strains						
AC-001	*Acanthamoeba*	*culbertsoni*	40	India	Cell culture contam.	ATCC 30171
AC-005	*Acanthamoeba*	*jacobsi*	44	USA	Marine	ATCC 30732
AC-006	*Acanthamoeba*	*lenticulata*	40	France	Swimming pool	ATCC 30841
AC-014	*Acanthamoeba*	*palestinensis*	35	Israel	Soil	ATCC 30870
AC-020	*Acanthamoeba*	*healyi*	40	USA	Fresh water	ATCC 30866
AC-023	*Acanthamoeba*	*royreba*	42	USA	Cell culture contam.	ATCC 30884
Clinical isolates						
AC-118	*Acanthamoeba*		44	Australia	Clinical (GAE)	
AC-230	*Acanthamoeba*		40	Australia	Clinical (keratitis)	
Environmental isolates						
AC-062	*Acanthamoeba*		44	Australia	Water supply	
AC-080	*Acanthamoeba*		44	Australia	Water supply	
AC-081	*Acanthamoeba*		44	Australia	Sediment	
AC-082	*Acanthamoeba*		44	PNG	Well	
AC-083	*Acanthamoeba*		44	Australia	Sediment	
AC-084	*Acanthamoeba*		44	Australia	Sediment	
AC-085	*Acanthamoeba*		44	Australia	Sediment	
AC-087	*Acanthamoeba*		44	Australia	Water supply	
AC-088	*Acanthamoeba*		44	Australia	Water supply	
AC-089	*Acanthamoeba*		40	Australia	Water supply	
AC-090	*Acanthamoeba*		40	Australia	Soil	
AC-091	*Acanthamoeba*		40	Australia	Soil	
AC-092	*Acanthamoeba*		42	Australia	Soil	
AC-126	*Acanthamoeba*		40	Australia	Air	
AC-137	*Acanthamoeba*		44	Australia	Fresh water	
AC-138	*Acanthamoeba*		44	Australia	Sediment	
AC-140	*Acanthamoeba*		42	Madagascar	Fresh water	
AC-141	*Acanthamoeba*		40	Australia	Airborne dust	
AC-148	*Acanthamoeba*		40	Madagascar	Fresh water	
AC-153	*Acanthamoeba*		40	Madagascar	Fresh water	
AC-159	*Acanthamoeba*		44	Japan	Fresh water	
AC-167	*Acanthamoeba*		40	Bangladesh	Sediment	
AC-168	*Acanthamoeba*		42	Bangladesh	Sediment	
AC-178	*Acanthamoeba*		44	NZ	Sediment	
AC-180	*Acanthamoeba*		40	Bangladesh	Sediment	
AC-181	*Acanthamoeba*		44	Indonesia	Sediment	
AC-194	*Acanthamoeba*		44	UK	Sediment	
AC-201	*Acanthamoeba*		44	Australia	Fresh water	
AC-227	*Acanthamoeba*		44	Fiji	Fresh water	
AC-229	*Acanthamoeba*		44	Australia	Fresh water	
AC-235	*Acanthamoeba*		44	Australia	Sediment	
AC-236	*Acanthamoeba*		40	Australia	Sediment	

[a] - Temperature tolerance

The genetic diversity at individual loci varied from 0.1623 to 0.7034 (Table 4). The frequency distribution of genetic distances was bimodal in nature, whether or not the distance calculations were weighted for the diversity of individual loci (Fig. 2), though a significant number of pairwise comparisons fell in the 'trough' from 20 to 50%. Dendrograms based on weighted distances (not shown) were nearly identical in topology, although some branch lengths were changed.

All 44°C-tolerant environmental isolates cluster closely with the reference strain of *A. jacobsi* (AC005), with fixed differences among the 20 isolates ranging from 0-19% (average 6%). Intraspecific variation was observed at ADH, HK, LAP and ME, while GOT1 ap-

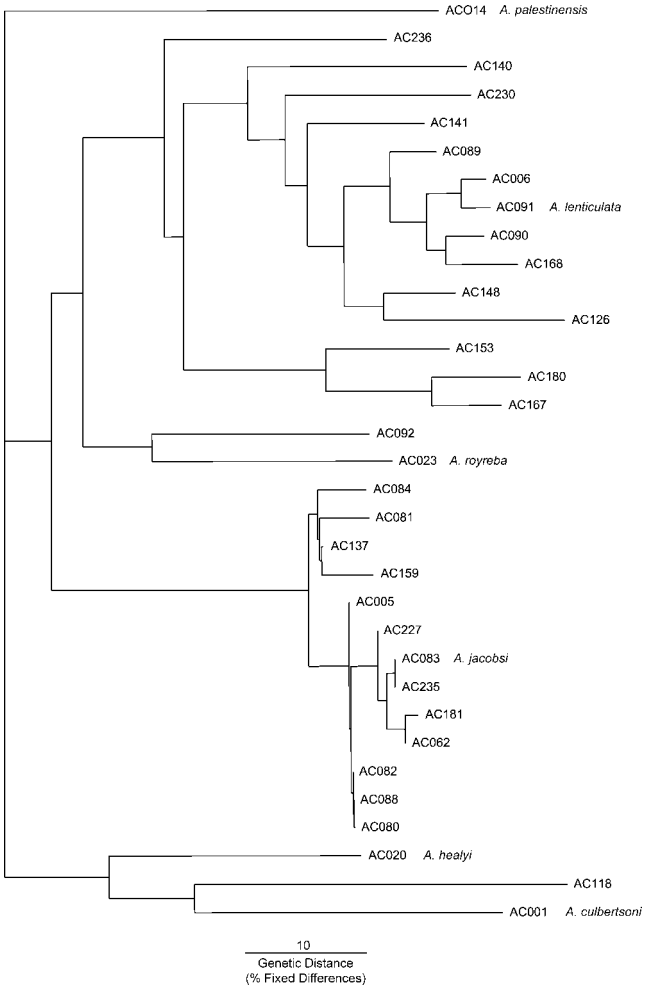

Fig 1. Neighbour-joining tree of genetic relationships among 40 *Acanthamoeba* isolates using isozyme data for 21 loci. 20 replicates of randomised input order gave identical topology.

peared to be universally heterozygous. The only other 44°C-tolerant isolate, the clinical strain AC118, is not closely related to *A. jacobsi*, nor to any other reference strain or environmental isolate.

A looser clustering occurs with *A. lenticulata*, in which four new isolates cluster within 15% of the type strain; further isolates clustered at progressively greater distances, including a discernible sub-group consisting of AC148 and AC126. The only other significant clustering is AC167 with AC180 (14%), then with AC153 (average 28%). The remaining isolates, including reference strains of described species, occur as single zymodemes isolated by distances greater than 40%. The fixed differences among the reference strains, excluding the outgroup *A. palestinensis*, ranged from 55-80% (mean 67%).

DISCUSSION

Relationships among *Acanthamoeba* strains

A number of published studies of *Acanthamoeba* have used isozymes to determine the variation among strains, usually without formal genetic analysis (Tyndall *et al.* 1979, De Jonckheere 1983, Costas and Griffiths 1984, Daggett *et al.* 1985). All but the De Jonckheere study relied strongly on peptidases, esterases and phosphatases, enzymes known to exhibit intraspecific polymorphism in metazoan and other protozoan groups. Not surprisingly, several authors noted the difficulty of recognising affinities within their sets of strains, to the extent that there has been a proposal to abandon the formal binomial nomenclature for this genus (Costas and Griffiths 1984). Other authors have erected new *Acanthamoeba* species partly on the basis of polymorphic isozymes (Sawyer *et al.* 1992, Nerad *et al.* 1995). At least two such 'species' are among those now considered synonyms of better established names, as they fall in the same sequence type (Stothard *et al.* 1998).

By contrast, in the unrelated amoeba genus *Naegleria*, the species-level taxonomy has proved extremely robust. As in *Acanthamoeba*, more than 20 species have been named since pathogenic strains were first isolated in the 1960s, but most species characterisations have included extensive isozyme and/or rDNA sequence data. The most thorough isozyme studies have been extensive in two dimensions (large number of strains and numerous loci) and employed formal genetic interpretation to distinguish polymorphic loci from fixed differences between species (Adams *et al.* 1989, Pernin and Cariou 1989, Robinson *et al.* 1992, Dobson *et al.* 1997). As a consequence, there is almost complete congruence between the clusters recognised on isozyme and sequence criteria.

In the present study, we used the multi-locus approach that has succeeded in studies of *Naegleria* to collect information about the diversity and divergence of strains and the relative scales of intra- and interspecific variation. The analysis suggests that genetic variation among Group III *Acanthamoeba* is at least partly discontinuous. In the dendrogram drawn from the data (Fig. 1), the tight cluster of isolates that group with

Table 2. Enzymes examined and conditions used.

Abbreviation	Enzyme	E.C. No.[a]	Loci scored	Buffer[b]	Run time (min)
Acn	Aconitase	4.2.1.3	1	B	90
Adh	Alcohol dehydrogenase	1.1.1.1	1	A	90
Enol	Enolase	4.2.1.11	1	B	90
Est	Esterase	3.1.1.1	1	C	105
Fdp	Fructose-diphosphatase	3.1.3.11	2	B	90
Gapd	Glycerald-phosphate dehydrogenase	1.2.1.12	1	B	90
Got	Aspartate aminotransferase	2.6.1.1	2	B	90
Gpi	Glucose-phosphate isomerase	5.3.1.9	1	C	120
Hex	Hexosaminidase	3.2.1.30	1	A	120
Hk	Hexokinase	2.7.1.1	1	B	90
Idh	Isocitrate dehydrogenase	1.1.1.42	1	A	120
Lap	Leucine aminopeptidase	3.4.11.1	1	A	75
Mdh	Malate dehydrogenase	1.1.1.37	1	A	105
Me	Malic enzyme	1.1.1.40	1	B	90
Mpi	Mannose-phosphate isomerase	5.3.1.8	1	C	75
Np	Nucleoside phosphorylase	2.4.2.1	1	B	60
PepB	Peptidase Leucine-leucine-leucine	3.4.11/13	1	C	75
6Pgd	6-Phosphogluconate dehydrogenase	1.1.1.44	1	B	90
Pgm	Phosphoglucomutase	5.2.4.2	1	B	75

[a] Enzyme commission number (E.C.)
[b] Running buffers from Richardson *et al.* 1986.

AC005 confirm that *A. jacobsi* is a sound genetic entity, deserving species status. Strains corresponding to *A. lenticulata* cluster less tightly: the four new isolates within 15% of the type strain certainly belong to this species but its boundary is difficult to define with confidence, considering the repeated branching beyond 25% difference. We assign the clinical isolate AC230 tentatively to *A. lenticulata*, to be confirmed by sequence data. Several corneal isolates from North America have been identified as *A. lenticulata* (Visvesvara and Stehr-Green 1990), as have isolates from nasal swabs collected from healthy soldiers in Turkey (De Jonckheere and Michel 1988), in each case by different criteria from those developed in this paper. The new cluster represented by AC153, AC167 and AC180 is also rather poorly defined, since there is no major discontinuity in the internode distances linking it ultimately to *A. lenticulata*.

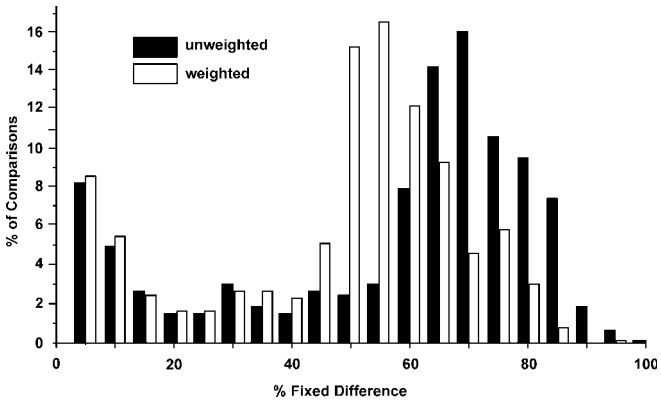

Fig. 2. Frequency distribution of all pairwise genetic distances between *Acanthamoeba* isolates, measured as the percentage of loci without shared alleles. Histograms based on un-weighted distances and on distances weighted using the genetic diversity at each locus.

While the frequency distribution of genetic distances is certainly bimodal (Fig. 2), the low-difference (left-hand) peak is composed almost entirely of interstrain comparisons within *A. jacobsi* and *A. lenticulata*. The high-difference (right-hand) peak is inflated by comparisons among the large number of single, isolated zymodemes and between these and individual strains of the species with multiple representatives. Comparisons in the trough, which is narrowed but not deepened by weighting of individual loci, reflect the continuous branching in some regions of the dendrogram.

In the genus *Naegleria*, all described species for which more than one strain is available cluster in the manner of *A. jacobsi*, as do numerous un-named species (Adams *et al.* 1989, Robinson *et al*. 1992). Internode distances are generally long (greater than 50% difference) and few intermediate relationships have

Table 3. Allelic profiles for *Acanthamoeba* zymodemes.

ZYMODEME	ACN2	ADH	ENOL	EST2	FDP1	FDP2	GAPD	GOT1	GOT2	GPI	HEX	HK	IDH	LAP	MDH	ME	MPI	NP	PEPB	6PGD	PGM
ACO14	cc	dd	—	dd	aa	aa	bb	dd	cc	ee	dd	bb	dd	ff	dd	bb	cc	ee	—	dd	dd
AC001	cc	aa	aa	cc	bb	aa	aa	aa	cc	bb	cc	bc	aa	cc	aa	cc	—	bb	bb	cc	cc
AC006	cc	ee	bb	ee	ee	dd	—	cc	bb	dd	ee	cc	cc	cc	bb	cc	bb	cc	cc	dd	dd
AC020	aa	cc	bb	ee	bb	dd	—	dd	cc	cc	cc	bb	aa	aa	bb	cc	aa	bb	ae	dd	cc
AC126	cc	ee	bb	ee	ee	cc	bb	cc	bb	ff	aa	dd	cc	cc	bb	cc	cc	cc	cc	cc	dd
AC141	dd	cc	bb	ee	ee	dd	—	cc	bb	ee	aa	dd	cc	cc	cc	cc	cc	cc	cc	dd	dd
AC148	dd	ee	bb	ee	ee	bd	bb	cc	bb	ff	cc	dd	cc	cc	dd	cc	cc	cc	cc	bd	dd
AC153	dd	cc	bb	ee	ee	dd	bb	dd	bb	ee	cc	ab	ff	ce	dd	cc	dd	cc	ee	cc	cc
AC167	dd	ee	bb	ee	ee	aa	—	cc	bb	dg	cc	ab	ff	cc	dd	cc	dd	cc	cd	ac	cc
AC180	dd	ee	bb	ee	ee	aa	bb	cc	bb	ff	cc	bb	ff	cc	dd	cc	dd	dd	cc	cc	bb
AC230	bb	cc	bb	ee	ee	dd	—	cc	bb	ee	ee	cc	cc	dd	bb	aa	cc	cc	cc	dd	dd
AC236	bd	cc	bb	dd	ee	dd	bb	bb	bb	dd	cc	dd	ee	ee	cc	cc	dd	dd	cc	dd	dd
AC089	cc	ee	bd	ee	ee	—	bb	cc	bb	dd	ee	bb	cc	cc	cc	cc	cc	cc	cc	dd	dd
AC090	cc	ee	bd	ee	ee	—	—	cc	bb	dd	ee	bb	cc	cc	bb	cc	cc	cc	cc	dd	dd
AC091	cc	ee	bb	ee	ee	dd	bb	cc	bb	dd	ee	cc	cc	dd	bb	cc	bb	cc	cc	dd	dd
AC023	aa	cc	aa	ad	dd	dd	—	aa	bb	dd	aa	dd	bb	ce	cc	dd	aa	aa	df	dd	dd
AC092	dd	dd	bd	dd	—	—	—	bb	—	dd	—	dd	bb	bb	cc	dd	aa	aa	cc	dd	cc
AC140	dd	ee	cc	ee	ee	bd	bb	cc	bb	ff	bb	dd	cf	dd	cc	ee	dd	cc	cc	bd	dd
AC168	cc	ee	bb	ee	ee	dd	—	cc	bb	dd	ee	cc	cc	cc	bb	aa	cc	cc	cc	dd	dd
AC005	bb	ce	dd	ee	cc	dd	bb	bb	ac	ee	cc	bb	bb	cc	cc	ee	bb	aa	dd	dd	—
AC062	bb	ce	dd	ee	cc	dd	bb	bb	ac	ee	cc	cc	bb	cc	cc	ee	bb	aa	dd	dd	bb
AC080	bb	cc	dd	ee	cc	dd	bb	bb	ac	ee	cc	bb	bb	cc	cc	ee	bb	aa	dd	dd	bb
AC081	cc	cc	dd	ee	cc	dd	bb	bb	ac	ee	cc	bb	bb	bd	cc	ee	bb	aa	dd	dd	bb
AC082	bb	ce	dd	ee	cc	dd	bb	bb	ac	ee	cc	bb	bb	cc	cc	ee	bb	aa	dd	dd	bb
AC083	bb	cc	dd	ee	cc	dd	bb	bb	ac	ee	cc	cc	bb	cc	cc	ee	bb	aa	dd	dd	bb
AC084	bb	cc	dd	ee	cc	dd	bb	bb	ac	ee	cc	dd	bb	bd	cc	ee	bb	aa	dd	dd	bb
AC137	bb	ce	dd	ee	cc	dd	bb	bb	ac	ee	cc	bb	bb	bd	cc	ee	bb	aa	dd	dd	bb
AC159	bb	—	dd	ee	cc	dd	bb	bb	ac	ee	cc	bb	bb	dd	cc	dd	bb	aa	dd	dd	bb
AC181	bb	ee	dd	ee	cc	dd	bb	bb	ac	ee	cc	cc	—	cc	cc	ee	bb	aa	dd	dd	bb
AC227	bb	ce	dd	ee	cc	dd	—	bb	ac	ee	cc	bc	bb	cc	cc	ee	bb	aa	dd	dd	bb
AC235	bb	cc	dd	ee	cc	dd	bb	bb	ac	ee	cc	cc	bb	cc	cc	ee	bb	aa	dd	dd	bb
AC088	bb	ce	dd	ee	cc	dd	bb	bb	ac	ee	cc	bb	—	cc	cc	ee	bb	aa	dd	dd	bb

Table 4. Genetic diversity of *Acanthamoeba* Group III isolates at 21 loci.

Locus	No. alleles	Genetic diversity
ACN2	4	0.6876
ADH	5	0.6210
ENOL	4	0.6166
EST2	5	0.3221
FDP1	5	0.6429
FDP2	4	0.3557
GAPD	2	0.1623
GOT1	5	0.6583
GOT2	3	0.6383
GPI	7	0.6606
HEX	5	0.5655
HK	4	0.6937
IDH	6	0.7034
LAP	6	0.6000
MDH	4	0.5949
ME	5	0.6620
MPI	4	0.6885
NP	5	0.6340
PEPB	6	0.6339
6PGD	4	0.3557
PGM	4	0.6548

been observed. Most strains which appeared initially as single, isolated zymodemes proved to be representatives of cohesive clusters, when additional strains were characterised (Robinson *et al*. 1992, Dobson *et al*. 1997). By analogy, isolates in this study that occur as single zymodemes separated by large internode distances could be treated as sole representatives of distinct species, on the criterion of distance alone. Indeed, they include the reference strains of the described species *A. culbertsoni, A. healyi* and *A. royreba*. Whether, on study of additional strains, these species prove to be as cohesive as *Acanthamoeba jacobsi* or as loosely defined as *A. lenticulata* remains to be determined.

Concordance of isozyme and sequence data

There is growing acceptance of a classification that uses the sequence of the 18s rDNA gene to assign *Acanthamoeba* strains to a series of sequence types or ribotypes (currently numbering 14), encompassing most of the reference strains for named species (Gast *et al*. 1996, Stothard *et al*. 1998). For the traditional binomial taxonomy to be reconciled with this classification, many 'species' would become synonyms, but *A. culbertsoni, A. healyi, A. lenticulata* and *A. palestinensis* comprise discrete sequence types. These same strains were also genetically distant from each other in the present study, suggesting that there will be a general concordance of isozyme and rDNA sequence data in *Acanthamoeba*, as there is in *Naegleria*. As a corollary, we predict that other clusters and divergent single zymodemes in our dendrogram will prove to be discrete sequence types. New sequence data for *Acanthamoeba jacobsi* (Hewett *et al*. 2003) fulfill this expectation.

Among the single zymodemes likely to represent new sequence types, the clinical strain AC-118, isolated from a GAE infection (Harwood *et al*. 1988), deserves special mention. A large number of 44°C-tolerant strains were analysed here, in anticipation that an environmental source of this virulent pathogen would be found. Instead, all such isolates were identified unambiguously as *A. jacobsi*. AC-118 appears therefore to represent a new, rare and virulent *Acanthamoeba* species and will be described in detail elsewhere. It seems likely that one of the other single zymodemes will correspond to the recently described sequence type T14, which was not available to us for comparison.

Biogeography and ecology

An interesting debate is developing over the global geographic distribution of protozoan species and their diversity. On one side, Finlay and others argue that the small size of free-living microorganisms, their high numbers and growth potential make opportunities for dispersal to new habitats so frequent that their occurrence should invariably be cosmopolitan (Finlay and Fenchel 1999). Limited opportunities for local speciation would constrain the total number of protozoan species. On the other side, Foissner has described numerous ciliate species from Australia and South America whose distributions appear to correspond with biogeographic regions based on ancient geological events (Foissner 1999). The 'cosmopolitan school' argues that such reports of endemic species reflect a sampling bias, resulting from the intense study of a particular area and sometimes of specialised habitats. The 'endemicity school' argues that in Europe, the ciliate fauna in particular has been so well studied that the apparent absence of certain species is likely to be genuine. It is also argued that reliance on morphological criteria for species identification obscures genuine geographic patterns (De Jonckheere 2002). The two schools differ vastly in their estimates of the total number of protozoan species (Finlay and Fenchel 1999).

The data presented here show that *A. jacobsi* is a widely distributed and rather uniform species, occurring in Asia, Australia, Europe, the Pacific region and in

North America. Strains corresponding closely to *A. lenticulata* occur in Australia and Asia, as well as in Europe and North America. These species clearly fit the cosmopolitan model. Beyond these species, the current study raises questions about the distribution of *A. culbertsoni*, *A. healyi*, *A. royreba* and the species represented by AC118 that will only be answered with further environmental studies. Whichever of these models eventually prevails, it appears from the organisms studied here that the species diversity of *Acanthamoeba* is still not completely described.

Acknowledgments. This study was undertaken by JF in part fulfilment of requirements for the B. Appl. Sci (Environmental Health) at Flinders University, Adelaide. We are grateful to colleagues who collected environmental samples from which some *Acanthamoeba* strains were isolated, including Penny Barnard, Peter Christy, Chandler Fulton and Paul Manning. The clinical strains AC118 and AC230 were referred to us by PathCentre, Perth and St Vincent's Hospital, Melbourne respectively. We thank Paul Monis for help with tree construction.

REFERENCES

Adams M., Andrews, R. H., Robinson, B., Christy, P., Baverstock, P. R., Dobson P. J., Blackler S. J. (1989) A genetic approach to species criteria in the amoeba genus *Naegleria* using allozyme electrophoresis. *Int. J. Parasitol.* **19:** 823-834

Berk S. G., Ting R. S., Turner G. W., Ashburn R. J. (1998) Production of respirable vesicles containing live *Legionella pneumophila* cells by two *Acanthamoeba* spp. *Appl. Environ. Microbiol.* **64:** 279-286

Costas M., Griffiths A. J. (1984) The esterases and acid-phosphatases of *Acanthamoeba* (Amoebida, Acanthamoebidae). *Protistologica* **20:** 33-41

Daggett P.-M., Lipscomb D., Sawyer T. K., Nerad T. A. (1985) A molecular approach to the phylogeny of *Acanthamoeba*. *BioSystems* **18:** 399-405

De Jonckheere J. F. (1983) Isoenzyme and total protein analysis by agarose isoelectric focusing and taxonomy of the genus *Acanthamoeba*. *J. Protozool*. **30:** 701-706

De Jonckheere J. F. (2002) A century of research on the amoeboflagellate genus *Naegleria*. *Acta Protozool*. **41:** 309-342

De Jonckheere J. F., Michel R. (1988) Species identification and virulence of *Acanthamoeba* strains from human nasal mucosa. *Parasitol. Res*. **74:** 314-316

Dobson P. J., Robinson B. S., Rowan-Kelly B. (1997) New thermophilic *Naegleria* species (Heterolobosea: Vahlkampfiidae) from Australia and Asia: allozyme, morphometric and physiological characterisation. *Acta Protozool*. **36:** 261-271

Felsenstein, J. (2002). PHYLIP (Phylogeny Inference Package) version 3.6a3. Department of Genome Sciences, University of Washington

Finlay B. J.,Fenchel T. (1999) Divergent perspectives on protist species richness. *Protist* **150:** 229-233

Foissner W. (1999) Protist diversity: estimates of the near-imponderable. *Protist* **150:** 363-368

Gast R. J., Ledee D. R., Fuerst P. A., Byers T. J. (1996) Subgenus systematics of *Acanthamoeba*: four nuclear 18S rDNA sequence types. *J. Euk. Microbiol*. **43:** 498-504

Harwood C. R., Rich G. E., McAleer R., Cherian G. (1988) Isolation of *Acanthamoeba* from a cerebral absess. *Med. J. Aust*. **148:** 47-49

Hewett M., Robinson B. S., Monis P., Saint C. P. (2003) Identification of a new *Acanthamoeba* 18S rRNA gene sequence type, corresponding to the species *Acanthamoeba jacobsi* Sawyer, Nerad and Visvesvara, 1992 (Lobosea: Acanthamoebidae). *Acta Protozool*. **42:** 325-329

Martinez A. J., Janitsche K. (1985) *Acanthamoeba*, an opportunistic microorganism: a review. *Infection* **13:** 251-256

Nerad T. A., Sawyer T. K., Lewis E. J., McLaughlin S. M. (1995) *Acanthamoeba pearcei* n. sp. (Protozoa: Amoebida) from sewage contaminated sediments. *J. Euk. Microbiol*. **42:** 702-705

Pernin P., Cariou M. L. (1989) Large genetic heterogeneity within amoebas of the species *Naegleria gruberi* and evolutionary affinities to the other species of the genus. *J. Protozool*. **36:** 179-181

Pussard M., Pons R. (1977) Morphologie de la paroi kystique et taxonomie du genre *Acanthamoeba* (Protozoa, Amoebida). *Protistologica* **13:** 557-598

Richardson B. J., Baverstock P. R., Adams M. (1986) Allozyme electrophoresis. A Handbook for Animal Systematics and Population Studies. Academic Press, Sydney

Robinson B. S., Christy P., Hayes S. J., Dobson P. J. (1992) Discontinuous genetic variation among mesophilic *Naegleria* isolates: further evidence that *N. gruberi* is not a single species. *J. Protozool*. **39:** 702-712

Rowbotham T. J. (1986) Current views on the relationships between amoeba, legionellae and man. *Israel J. Med. Sci*. **22:** 678-689.

Sawyer T. K. (1971) *Acanthamoeba griffini*, a new species of marine amoeba. *J. Protozool*. **18:** 650-654

Sawyer T. K., Nerad T. A., Visvesvara G. S. (1992) *Acanthamoeba jacobsi* sp.n. (Protozoa: Acanthamoebidae) from sewage contaminated ocean sediments. *J. Helminthol. Soc. Wash*. **59:** 223-226

Stothard D. R., Schroeder-Dietrich J., Awwad M. H., Gast R. J., Ledee D. R., Rodriguez-Zaragoza S., Dean C. L., Fuerst P. A., Byers T. J. (1998) The evolutionary history of the genus *Acanthamoeba* and the identification of eight new 18S rRNA gene sequence types. *J. Euk. Microbiol*. **45:** 45-54

Tyndall R. L., Willaert E., Stevens A. A. N. (1979) Pathogenic and enzymatic characteristics of *Acanthamoeba* isolated from cultured tumor cells. *Protistologica* **15:** 17-22

Visvesvara G. S., Stehr-Green J. K. (1990) Epidemiology of free-living ameba infections. *J. Protozool*. **37:** 25S-33S

Received on 22nd May, 2003; accepted on 28th August, 2003

Acta Protozool. (2003) 42: 325 - 329

ACTA
PROTOZOOLOGICA

Identification of a New *Acanthamoeba* 18S rRNA Gene Sequence Type, Corresponding to the Species *Acanthamoeba jacobsi* Sawyer, Nerad and Visvesvara, 1992 (Lobosea: Acanthamoebidae)

Melissa K. HEWETT[1,2], Bret S. ROBINSON[1], Paul T. MONIS[1,2] and Christopher P. SAINT[1,2]

[1]Cooperative Research Centre for Water Quality and Treatment, Australian Water Quality Centre, SA Water Corporation, Bolivar; [2]School of Pharmaceutical, Molecular and Biomedical Sciences, University of South Australia, Mawson Lakes, Australia

Summary. Since 1996, a new classification system has been used to assign members of the genus *Acanthamoeba* to different sequence types. This study aimed to place the thermophilic species *Acanthamoeba jacobsi* into the sequence type classification by sequencing part of the 18S rRNA gene for six isolates of this species. Phylogenetic analysis of the sequences showed the six strains to be closely related and confirmed their identification as *A. jacobsi*. This species is well separated from all previously typed *Acanthamoeba* strains, and is allocated to a new sequence type, T15.

Key words: 18S rRNA gene, *Acanthamoeba jacobsi*, sequence type.

INTRODUCTION

The protozoan genus *Acanthamoeba* contains free-living organisms, some of which are clinically significant. Many strains cause the corneal infection *Acanthamoeba* keratitis, while some strains can also cause granulomatous amoebic encephalitis (GAE), a potentially fatal brain infection. Traditionally, identification beyond the genus level of *Acanthamoeba* was based on morphological characteristics. The cyst size and shape, as well as the growth temperature range, allow the Acanthamoebae to be distinguished into three subgeneric groups (Pussard and Pons 1977), encompassing more than 20 nominal species. However, characterisation at the species level has been inconsistent in the past, with several 'type strains' not genetically distinct from earlier-named species and many clinical and environmental isolates now judged to be incorrectly assigned (Stothard *et al.* 1998). A very confused binomial classification has resulted.

More recently, a subgeneric identification system has been described which involves sequence analysis of the 18S rRNA gene to segregate the *Acanthamoeba* strains into sequence types. To date, fourteen separate sequence types have been reported (Gast *et al.* 1996,

Address for correspondence: Bret S. Robinson, Australian Water Quality Centre, Private Mail Bag 3, Salisbury, SA 5108 Australia; Fax: 61 8 82590228; E-mail: bret.robinson@sawater.com.au

Stothard *et al.* 1998, Horn *et al.* 1999, Gast 2001). The largest and most diverse sequence type, T4, contains many of the strains that are infectious to humans, causing keratitis and occasionally GAE.

In this study, 18S rRNA gene sequencing was employed to determine the affinities of six *Acanthamoeba* strains from diverse geographic origins, identified as *Acanthamoeba jacobsi* by isozyme analysis and physiological characteristics.

MATERIALS AND METHODS

Cultures. The *Acanthamoeba* strains that were analysed in this study were the type strain of *A. jacobsi*, ATCC 30732 (AC005 in the culture collection of the Australian Water Quality Centre (AWQC)), isolated from a marine source in the United States of America; and five environmental isolates from the AWQC collection. Strains AC080 (from an Australian water supply), AC194 (fresh water sediment, England) and AC227 (fresh water, Fiji) were selected from an isozyme study (Flint *et al.* 2003) to represent the wide geographic distribution of *A. jacobsi*. AC304 and AC305, which originated from an untreated water system in Australia, were included as they are natural hosts of bacterial endosymbionts (Todd *et al.* 2001) and their responses to temperature suggested that they may also belong to *A. jacobsi*. The cultures were grown at 35°C in 25 cm^2 and 75 cm^2 culture flasks containing 1/4 strength Ringer solution (Oxoid, Hampshire, England) seeded with approximately 10^9 cells/ml *Escherichia coli* (ATCC 11775).

DNA isolation, PCR and sequencing. Amoeba cells were harvested from culture flasks, concentrated by centrifugation, then lysed by treatment with lysozyme and freeze-thawing (using liquid nitrogen and heating to 65°C). The samples were then treated with proteinase K, SDS and RNAse. The DNA was purified using the QIAamp DNA mini kit (Qiagen) according to the manufacturers instructions.

PCR primers CRN5 and 1137 as described by Schroeder *et al.* (2001) were used for amplification of 1475 bp of the 18S rRNA gene. PCR amplifications were performed in 50 µl volumes, containing 20 pmol of each of the primers, 2.5 mM $MgCl_2$, Buffer II, 200 µM deoxynucleoside triphosphates (Promega), 2.5 units of Ampli *Taq* Gold (Applied Biosystems), 5% DMSO and 1-10 ng of template DNA. PCR was carried out using the Perkin Elmer GeneAmp 2400 PCR system. Thermal cycling conditions for the PCR were: 94°C for 10 min; 35 cycles of 94°C for 1 min, 60°C for 1 min, 72°C for 2 min; followed by a final extension at 72°C for 7 min. PCR products were purified using the QIAquick gel extraction kit (Qiagen) according to the manufacturers instructions.

Oligonucleotide primers used for sequencing were: CRN5, 1137, 373, 570C, 892C and 892 (Schroeder *et al.* 2001). DNA was sequenced using the BigDye v2.0 Terminator mix and an automated model 3700 capillary sequencer (Applied Biosystems). Sequences were analysed using SeqMan software (DNASTAR), and homology searches were performed using the BLAST network service on the database of the National Centre for Biotechnology Information.

Phylogenetic analysis. The six *Acanthamoeba* sequences from this study were aligned with 17 published sequences representing all previously characterised *Acanthamoeba* sequence types, and including three representatives of sequence type T4, the most diverse sequence type. Table 1 details the GenBank accession numbers of the *Acanthamoeba* sequences that were analysed, as well as strain details. Sequence alignments were performed using Clustal X version 1.64b software (Thompson *et al.* 1997). Phylogenetic relationships were inferred by neighbour-joining analysis of Kimura two-parameter distance estimates using Mega version 2b3 software (Kumar *et al.* 2000). The data were also analysed by maximum parsimony analysis (heuristic search) using Paup* version 4.0b10 software (Swofford 1998). The robustness of the distance-based and parsimony trees was determined by bootstrap analysis (1,000 replicates).

GenBank accession numbers. The 18S rRNA gene sequences of the six *A. jacobsi* isolates were submitted to the GenBank database with the following accession numbers: AY262360 (AC005); AY262361 (AC080); AY262362 (AC194); AY262363 (AC227); AY262364 (AC304) and AY262365 (AC305).

RESULTS

A portion of the 18S rRNA gene (between 1443 bp and 1475 bp in length) was amplified and sequenced for all six of the *Acanthamoeba* strains studied. This region of the 18S rRNA gene was studied as it has been shown to contain eight segments of variable sequence for members of the genus *Acanthamoeba* (Schroeder *et al.* 2001). Previous studies have differentiated *Acanthamoeba* strains into different sequence types by sequencing the complete 18S rRNA gene, which is between 2,300 and 2,700 bp (Stothard *et al.* 1998). However, the smaller fragment analysed in the current study contains enough information to differentiate all of the sequence types (Schroeder *et al.* 2001).

The neighbour-joining and maximum parsimony analyses (neighbour-joining tree illustrated in Fig. 1) showed that the six *Acanthamoeba* strains AC005, AC080, AC194, AC227, AC304 and AC305 were all closely related to one another, sharing greater than 99.4% sequence similarity (calculation based on the p-distance, Mega version 2b3). The distances between the sequences were very small, much less than the distances between the three representative sequences of the sequence type T4. Therefore, all six of these strains are considered to belong to the same sequence type. As a group, the six *Acanthamoeba* strains were well separated from members of all other sequence types (Fig. 1). The bootstrap support for the *A. jacobsi* group is highly significant, as it shows 100% support with both neighbour-joining and maximum parsimony analysis. The six *A. jacobsi* strains share at most 92.1% sequence similarity with members of the most closely related sequence type, T13, and so the *A. jacobsi* strains can be consid-

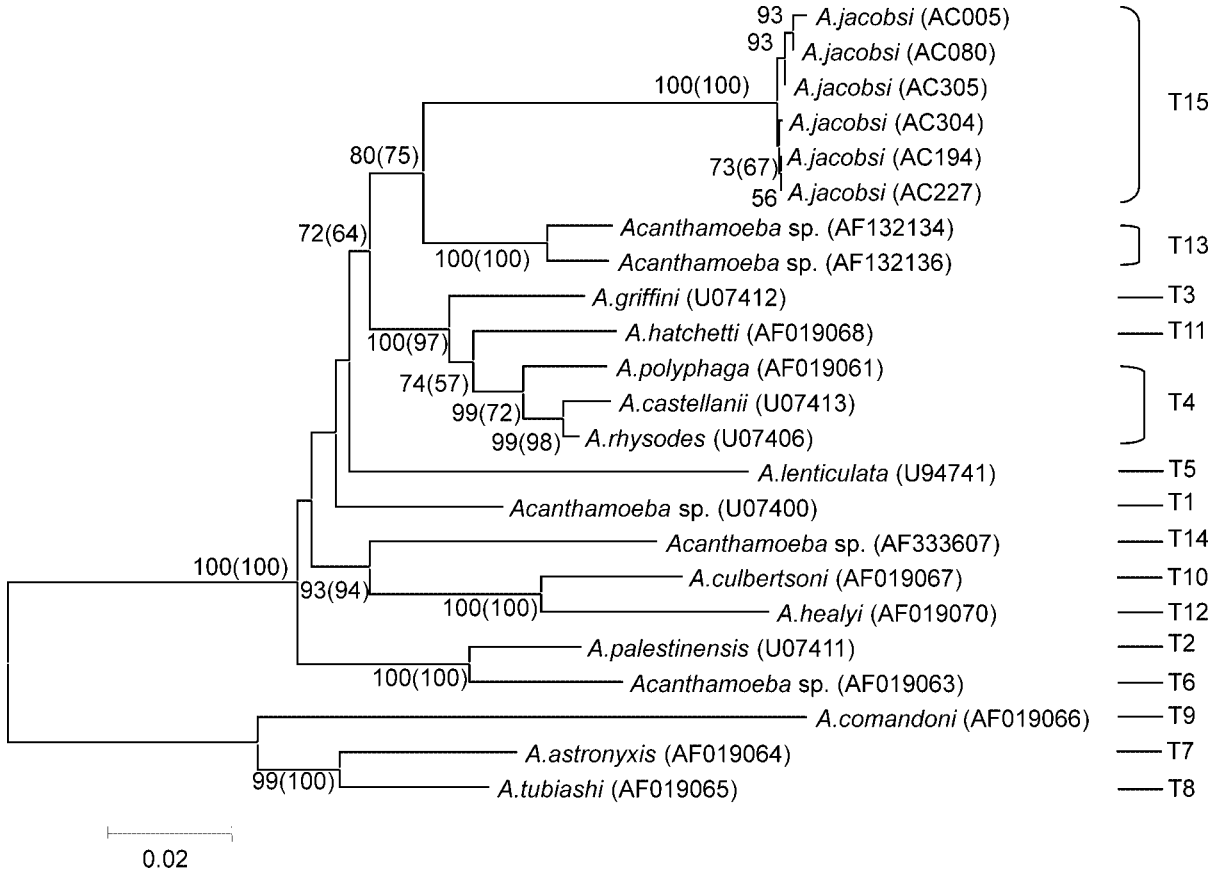

Fig. 1. Neighbour-joining tree showing the position of six *A. jacobsi* isolates (AC005, AC080, AC194, AC227, AC304, AC305) in relation to representatives of the other *Acanthamoeba* sequence types, based on their 18S rRNA gene sequences. Numbers on branch points depict the percent occurrence of a given branch during 1,000 bootstrap replicates. Numbers in brackets are bootstrap values based on maximum parsimony analysis, with 1,000 replicates. Values below 50 are not shown.

ered a new sequence type. We therefore propose the new sequence type T15, which corresponds to the species *A. jacobsi*.

DISCUSSION

The assignment of *Acanthamoeba* species to a series of 18S rRNA gene sequence types is gaining wide acceptance as a genetically-sound classification system and corresponds partially with the existing binomial taxonomy (Stothard *et al.* 1998). However, it does not yet encompass all previously described species. In particular, *A. jacobsi* is a widely distributed thermophilic species for which sequence data have not previously been published.

In this study, comparison of a substantial part of the 18S rRNA gene confirmed that the *Acanthamoeba* strains AC080, AC167, AC227, AC304 and AC305, are closely related to *A. jacobsi* AC005, consistent with their isozyme profiles, growth temperature range and cyst morphology (Flint *et al.* 2003). Furthermore, the *A. jacobsi* strains are distinctly separated from members of the existing sequence types, with high bootstrap support (Fig. 1). The degree of sequence uniformity among the six strains and their divergence from other Acanthamoebae represent strong agreement with the isozyme analysis (Flint *et al.* 2003). We conclude therefore that *A. jacobsi* is a sound genetic entity and a new sequence type.

Previous analysis of the 18S rRNA gene of *Acanthamoeba* strains by Gast *et al*. (1996) and Stothard *et al*. (1998) identified twelve discrete sequence types, T1-T12. Horn *et al*. (1999) described two additional sequence types, T13 and T14, corresponding to the strains *Acanthamoeba* sp. UWC9 and *Acanthamoeba*

Table 1. *Acanthamoeba* strains analysed in this study

Sequence type	Species classification	Strain identification	GenBank accession number	Reference (GenBank sequence)
T1	*Acanthamoeba* sp.	CDC:0981:V006	U07400	Gast *et al.* 1996
T2	*A. palestinensis*	ATCC:30870	U07411	Gast *et al.* 1996
T3	*A. griffini*	ATCC:30731	U07412	Gast *et al.* 1996
T4	*A. castellanii*	ATCC:50374	U07413	Gast *et al.* 1996
T4	*A. polyphaga*	ATCC:30871	AF019061	Stothard *et al.* 1998
T4	*A. rhysodes*	ATCC:50368	U07406	Gast *et al.* 1996
T5	*A. lenticulata*	ATCC:30841	U94741	Stothard *et al.* 1998
T6	*Acanthamoeba* sp.	ATCC:50708	AF019063	Stothard *et al.* 1998
T7	*A. astronyxis*	ATCC:30137	AF019064	Stothard *et al.* 1998
T8	*A. tubiashi*	ATCC:30867	AF019065	Stothard *et al.* 1998
T9	*A. comandoni*	ATCC:30135	AF019066	Stothard *et al.* 1998
T10	*A. culbertsoni*	ATCC:30171	AF019067	Stothard *et al.* 1998
T11	*A. hatchetti*	Sawyer:NMFS	AF019068	Stothard *et al.* 1998
T12	*A. healyi*	CDC1283:V013	AF019070	Stothard *et al.* 1998
T13	*Acanthamoeba* sp.	Horn:UWC9	AF132134	Horn *et al.* 1999
T13	*Acanthamoeba* sp.	Horn:UWE39	AF132136	Horn *et al.* 1999
T14	*Acanthamoeba* sp.	Gast:PN15	AF333607	Gast 2001
T15	*A. jacobsi*	ATCC:30732 (AWQC:AC005)	AY262360	This study
T15	*A. jacobsi*	AWQC:AC080	AY262361	This study
T15	*A. jacobsi*	AWQC:AC194	AY262362	This study
T15	*A. jacobsi*	AWQC:AC227	AY262363	This study
T15	*A. jacobsi*	AWQC:AC304	AY262364	This study
T15	*A. jacobsi*	AWQC:AC305	AY262365	This study

sp. UWE39 respectively. Subsequently Gast (2001) described a new sequence type, also named T14, which included the near identical strains *Acanthamoeba* sp. PN13 and *Acanthamoeba* sp. PN15. In the current study, the sequences of *Acanthamoeba* sp. UWC9, *Acanthamoeba* sp. UWE39 and *Acanthamoeba* sp. PN15 (obtained from GenBank) were included in the phylogenetic analysis to determine whether they represented distinct sequence types. In our analysis, the sequence similarity of the full length 18S rRNA gene sequence of *Acanthamoeba* sp. UWC9 and *Acanthamoeba* sp. UWE39 was 98.2%, while *Acanthamoeba* sp. PN15 showed less than 92% sequence similarity to these two strains. Stothard *et al.* (1998) established the criterion that strains must be at least 5% different based on their 18S rRNA gene sequence to belong to different sequence types. Since *Acanthamoeba* sp. UWC9 and *Acanthamoeba* sp. UWE39 are less than 5% different and show less separation than some representatives of the sequence type T4, we conclude that *Acanthamoeba* sp. UWE39 should be allocated to the sequence type T13. The distinctiveness of sequence type T14, represented by the strain *Acanthamoeba* sp. PN15 (Gast 2001), is not in doubt. The new sequence type described in this study, corresponding to the species *A. jacobsi*, is therefore designated T15.

The position of *A. jacobsi* in Fig. 1 provides further evidence that the morphological groups II and III are not monophyletic. Beyond its affinity with sequence type T13 (not assigned to a morphological group), *A. jacobsi* (which has typical group III cyst morphology) shows the greatest affinity to the T3, T4 and T11 *Acanthamoeba* species, all of which belong to morphological group II. Therefore cyst morphology can provide criteria for preliminary sorting of strains without indicating their true affinity.

The 18S rRNA gene analysis presented here confirms the conclusion of the isozyme analysis, that *A. jacobsi* is a distinct genetic entity, widely distributed and relatively uniform (Flint *et al.* 2003). Since there is also strong concordance of sequence and isozyme identities for *A. culbersoni* (T10), *A. healyi* (T12), *A. lenticulata* (T5) and *A. palestinensis* (T2) (Flint *et*

al. 2003), we predict that other *Acanthamoeba* lineages recognised from isozyme criteria will prove to represent new sequence types.

REFERENCES

Flint J. A., Dobson P. J., Robinson B. S. (2003) Genetic analysis of forty isolates of *Acanthamoeba* group III by multilocus isoenzyme electrophoresis. *Acta Protozool.* **42:** 317-324

Gast R. J. (2001) Development of an *Acanthamoeba*-specific reverse dot-blot and the discovery of a new ribotype. *J. Eukaryot. Microbiol.* **48:** 609-615

Gast R. J., Ledee D. R., Fuerst P. A., Byers T. J. (1996) Subgenus systematics of *Acanthamoeba*: four nuclear 18S rDNA sequence types. *J. Eukaryot. Microbiol.* **43:** 498-504

Horn M., Fritsche T. R., Gautom R. K., Schleifer K. H., Wagner M. (1999) Novel bacterial endosymbionts of *Acanthamoeba* spp. related to the *Paramecium caudatum* symbiont *Caedibacter caryophilus*. *Environ. Microbiol.* **1:** 357-367

Kumar S., Tamura K., Jakobsen I., Nei M. (2000) Molecular Evolutionary Genetics Analysis. ver. 2b3

Pussard M., Pons R. (1977) Morphologie de la paroi kystique et taxonomie du genre *Acanthamoeba* (Protozoa, Amoebida). *Protistologica* **13:** 557-598

Sawyer T. K., Nerad T. A., Visvesvara G. S. (1992) *Acanthamoeba jacobsi* sp.n. (Protozoa: Acanthamoebidae) from sewage contaminated ocean sediments. *J. Helminthol. Soc. Wash.* **59:** 223-226

Schroeder J. M., Booton G. C., Hay J., Niszl I. A., Seal D. V., Markus M. B., Fuerst P. A., Byers T. J. (2001) Use of subgenic 18S ribosomal DNA PCR and sequencing for genus and genotype identification of Acanthamoebae from humans with keratitis and from sewage sludge. *J. Clin. Microbiol.* **39:** 1903-1911

Stothard D. R., Schroeder-Diedrich J. M., Awwad M. H., Gast R. J., Ledee D. R., Rodriguez-Zaragoza S., Dean C. L., Fuerst P. A., Byers T. J. (1998) The evolutionary history of the genus *Acanthamoeba* and the identification of eight new 18S rRNA gene sequence types. *J. Eukaryot. Microbiol.* **45:** 45-54

Swofford D. L. (1998) PAUP* Phylogenetic Analysis Using Parsimony (*and Other Methods). ver. 4. Sinauer Associates, Sunderland, Massachusetts

Thompson J. D., Gibson T. J., Plewniak F., Jeanmougin F., Higgins D. G. (1997) The CLUSTAL_X windows interface: flexible strategies for multiple sequence alignment aided by quality analysis tools. *Nucleic Acids Res.* **25:** 4876-4882

Todd M. K., Robinson B. S., Saint C. P. (2001) Molecular characterisation of bacterial endosymbionts of *Acanthamoeba* sp. In: IXth International Meeting on the Biology and Pathogenicity of Free-Living Amoebae Proceedings, (Eds. S. Billot-Bonef, P. A. Cabanes, F. Marciano-Cabral, P. Pernin, E. Pringuez). John Libbey Eurotext, Paris, 140-150

Received on 22nd May, 2003; accepted on August 27th, 2003

Acta Protozool. (2003) 42: 331 - 343

ACTA
PROTOZOOLOGICA

Pseudodidymium cryptomastigophorum gen. n., sp. n., a *Hyperamoeba* or a Slime Mould? A Combined Study on Morphology and 18S rDNA Sequence Data

Rolf MICHEL[1], Julia WALOCHNIK[2] and Horst ASPÖCK[2]

[1]Central Institute of the Armed Forces Medical Services, Koblenz, Germany; [2]Dept. of Med. Parasitology, Clin. Inst. of Hygiene and Med. Microbiology, University of Vienna, Vienna, Austria

Summary. The *Hyperamoeba*-like amoeboflagellate (Wi7/2-PE) has been isolated from a hydrotherapy pool inside a hospital at Wildbach/ Germany. Based on combined morphological and molecularbiological data we conclude that this isolate can neither be assigned to the genus *Hyperamoeba* nor to any of the myxogastrean slime moulds, which are the closest relatives of *Hyperamoeba*. We thus considered describing this isolate within a new genus, *Pseudodidymium*, as a new species, *Pseudodidymium cryptomastigophorum*. As observed by phase contrast microscopy the gross morphology and size of the three stages - trophozoite, cyst, and flagellate stage - is comparable to respective characters of *Hyperamoeba* as described by Karpov and Mylnikov (1997). However, in contrast to these characters they have in common with *Hyperamoeba*, the features of the flagellate stage shown by electron microscopy revealed marked differences to the previously described *Hyperamoeba*. In addition to the anterior flagellum responsible for the locomotion a second recurrent flagellum could be observed which is tightly attached to the cell membrane of the flagellate by a desmosome-like connection zone. Both flagellae are anchored to the tapered frontal part of the cell by kinetosomes with accessory structures located at an acute angle to each other. While the frontal flagellum is as long or even longer than the cell body the second one has a length of about one third of the cell and appears barren. This tight attachment of the inactive flagellum is the reason for its invisibility by means of light microscopy. All three stages possess mitochondria with a dense central core as known from *Hyperamoeba*, which are characteristic for myxogastrean slime moulds as well. However, various attempts to induce the formation of fruiting bodies in order to show a putative relationship to certain slime moulds remained unsuccessful. In 18S rDNA sequencing our isolate did not show highest identity to the only hitherto sequenced strain of *Hyperamoeba* sp., but, as also a undescribed strain of *Hyperamoeba*, to a strain of *Didymium nigripes*, a myxogastrean slime mould. However, this strain of *Didymium* shows an insertion, which our isolate does not have. In conclusion, it is neither possible to assign this *Hyperamoeba*-like isolate to the genus *Hyperamoeba* nor to the genus *Didymium* as it differs fundamentally from both genera in several aspects.

Key words: amoeboflagellates, *Hyperamoeba*, *Pseudodidymium cryptomastigophorum* sp. n., slime moulds, 18S rDNA, ultrastructure.

INTRODUCTION

The amoeboflagellate *Hyperamoeba flagellata* is a rarely isolated species. It was first isolated from an infusion of horse faeces and described by Alexeieff in 1923. In 1997 Karpov and Mylnikov redescribed a strain of this species by means of light and electron microscopy, which they had isolated from a pond in Russia. Later 9 strains of this species were isolated from 200 human faecal specimens from which a single isolate was investigated morphologically and on the molecular level (Zaman *et al.* 1999). The molecular investigation of the 18S rDNA showed that this *Hyperamoeba* isolate was closely related to the plasmodial slime mould *Physarum*

Address of correspondence: Rolf Michel, Central Institute of the Armed Forces Medical Services, Andernacher Str. 100, 56070 Kobenz, Germany; E-mail: rmichel@amoeba-net.de

polycephalum although it did not develop a plasmodium, which, however, is characteristic for *Physarum*. Since 1988 we isolated and collected 9 *Hyperamoeba*-like strains from different aquatic and terrestrial sources. As the genetic distance of our isolate Wi7/2-PE from the only hitherto sequenced and described *Hyperamoeba* (Zaman *et al*. 1999) was remarkably high we selected this strain as object for the present morphologic investigation in combination with studies on the molecular level as basis for a possible description of a novel species.

MATERIALS AND METHODS

Organism. The strain Wi7/2-PE was isolated from water samples of a physiotherapy bath of a hospital at Wildbad in Germany and maintained on NN-agar according to Page (1988) seeded with *Enterobacter cloacae* as food bacteria. With the aim to carry out the flagellate transformation test the amoebae from a 3-5 days old culture were suspended either in distilled water or in As-solution (amoeba-saline) according to Page (1988) and the transformation process was observed. Within 30 min 80-90 % of the amoebae had transformed to fully developed flagellate stages. In order to induce the formation of fruiting bodies amoebae from optimal cultures were transferred to agar plates prepared with either quarter strength Emerson-yps-medium (Schuster, personal comm.) or with sterilized oat flakes as they were made use of in the cultivation of plasmodia of *Physarum.*

Isolation of DNA. For isolation of DNA six parallel cultures were installed. Whole-cell DNA was isolated from actively growing (dividing) cultures. The trophozoites (~10^6 cells) were harvested from the plate cultures with a sterile cotton tipped applicator and washed 3x in sterile 0.9% NaCl by centrifugation 500 *g* for 7 min. For isolation of DNA a modified UNSET-procedure (Hugo *et al.* 1992) was used. Briefly, the cell-pellet was resuspended in 500 µl of UNSET-lysis buffer, overlaid with 500 µl phenol-chloroform-isoamylalcohol (PCI) and shaken gently for 5 h. After several rounds of PCI-extraction with an incubation period of 10 min the DNA was precipitated in alcohol at -20°C overnight. After centrifugation at 12000 *g* for 30 min at 4°C the DNA-pellet was washed in 70% ethanol, air-dried and resuspended in 30 µl of sterile double-distilled water.

PCR and sequencing. The 18S rDNA was amplified using the SSU1 and SSU2 primers (Gast *et al.* 1996), complementary to the strongly conserved ends of the eukaryotic 18S rRNA gene. Thirty PCR-cycles were run with 94°C 1 min, 52°C 2 min, 72°C 3 min. The amplification of the 18S rDNA was visualised with ethidium-bromide in an agarose-gel electrophoresis and the amplification product was purified using the GFX™ PCR-purification kit (Amersham, Pharmacia). The amplified 18S rDNA was sequenced stepwise by direct sequencing from the PCR-product and subsequent construction of complementary internal primers. Sequences were obtained from both strands. The sequencing PCR was run with 96°C 10 s, 50°C 5 s and 60°C 4 min using the ABI PRISM® BigDye sequencing kit (Applied Biosystems). Sequencing was carried out in a 310 ABI PRISM® automated sequencer (Applied Biosystems).

The obtained sequence fragments were aligned using the ClustalX program (Thompson *et al.* 1997) and processed with the GeneDoc sequence editor (Nicholas *et al.* 1997). The complete 18S rDNA sequence was compared to the ones of published strains using BLAST search (Altschul *et al.* 1990).

Cluster analysis. In order to proof the relatedness of our isolate to *Didymium* despite the *Hyperamoeba* morphology observed by light microscopy, we performed a cluster analysis for the myxogastrean slime moulds including other myxogastrean slime mould species. The cluster analysis was carried out using the PHYLIP (Felsenstein 1989) package. Primer sites, unique gaps, and inserts were rejected from the analysis. For evaluation of the statistic significance 1000 replicates of the nucleotide sequence alignment were generated using the SEQBOOT application. Distance matrices were calculated using DNADIST. Bootstrapped matrices were analyzed with the Neighbor joining application and a Kimura two parameter correction. A consensus tree was build from the resulting trees using CONSENSE and prepared as figure with the TREEVIEW (Page 1996) application. A strain of *Vannella anglica* (GenBank Ref. No. AF099101), a species presumed to be rather closely related to, but to branch clearly not within the slime moulds, possibly at the very base of the amoebozoa (Bolivar *et al.* 2001, Cavalier-Smith and Chao 2003), was used as an outgroup.

However, as the relationship between the dictyostelid and the myxogastrid slime moulds has not been wholly elucidated yet (Hendriks *et al.* 1991, Hinkle and Sogin 1993), a second, more large scale cluster analysis was performed in order to analyse the position of the genus *Hyperamoeba* within the amoebozoa. The phylogenetic position of *Hyperamoeba* was inferred with the maximum likelihood (ML) method using *Trypanosoma* and *Leishmania* (GenBank Ref. No. AF416562 and AF303938) as an outgroup. The choice of the outgroup was a critical matter. As in the past years it has become questionable, whether the diplomonads and parabasalids are actually early branching lineages and their phylogenetic position on the whole is rather unclear, we decided to use *Trypanosoma* and *Leishmania* as outgroup, as this has already been suggested by Dacks *et al*. (2002). With this outgroup long branch attraction, which can obscure other relationships, seems to play a minor role. Although also *Trypanosoma* might be a long branch, *Leishmania* seems to reduce its effects (Dacks *et al.* 2002). Data were also analyzed with NJ and maximum parsimony. Bootstrap values were processed with 100 (ML) and 1000 (NJ and maximum parsimony) replicates, respectively.

Sequence data reported in this paper are available at GenBank under the following accession number: AY207466.

The strain Wi7/2-PE was deposited as a typestrain at the "Culture Collection of Algae and Protozoa" at Ambleside, Cumbria under the CCAP-nr.: 1573/1.

Electron microscopy. Amoebae or flagellates obtained after transformation test mentioned above were harvested and centrifuged for 10 min at 2000 rpm. Pellets were fixed for 1 h with 3% glutaraldehyde, transferred to 0.1 M cacodylate buffer, postfixed in 1% osmium tetroxide and embedded in Spurr resin. Sections were stained with uranyl acetate and Reynold's lead citrate and examined using a Zeiss EM 10a electron microscope.

RESULTS

The strain Wi7/2-PE had been isolated from water samples from a physiotherapeutic bath in a hospital at Wildbad in Germany in the year 1988. The sample of

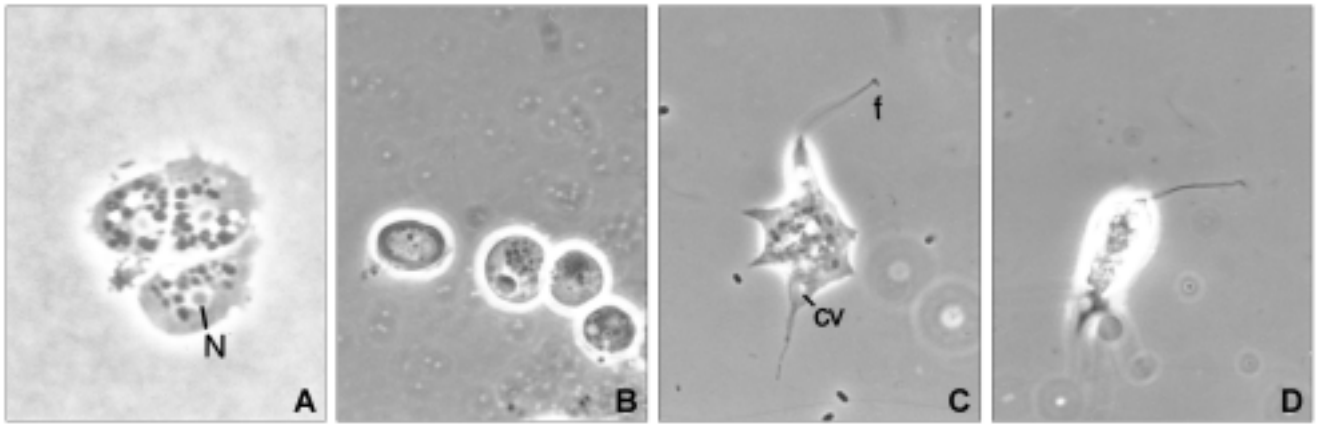

Figs 1 A-D. A - three trophozoites of Wi7/2-PE with short blunt pseudopodia. N - nucleus. Phase contrast, x1200; **B** - group of three cysts and one encysting stage (right side); **C** - transitory stage from trophozoite to flagellate stage with one frontal flagellum (f) still attached to the substratum, an uroidal filopodium visible. cv - contractile vacuole; **D** - mature flagellate with frontal flagellum and characteristic elongated body shape. Phase contrast, x1000.

100 ml was filtered through a membrane filter (Sartorius), which was then placed upside down onto NN-agar plates according to Page (1988) seeded with *Enterobacter cloacae* as food bacteria. After 48 h it was removed and the mixed population of amoebae was investigated. Since that time the strain Wi7/2-PE was maintained on the same agar plates, as it was not possible to establish axenic cultures of these amoeboflagellates. In order to exclude that the *Hyperamoeba*-like protists were not only stages of slime moulds with similar flagellate stages actively growing amoebae of Wi7/2-PE were transferred to media known to induce the formation of fruiting bodies of a number of true slime moulds. Neither the transfer to Emerson-yps-medium (Schuster, personal communication) nor to plates prepared with oat flakes made use of in cultivating *Physarum* plasmodia induced any fruiting bodies of the present strain.

Observations under phase contrast. The novel species is represented by three main stages comprising the trophozoite (Fig. 1A), the flagellate stage (Figs 1C, D) and the cyst (Fig. 1B). Only the uninucleate trophozoite ingests bacteria as food and multiplies by binary fission - in contrast to the flagellates, which represent a temporary stage without feeding and dividing.

The amoebae have a variable size from 15 to 18 µm. They produce blunt filopodia emanating from a frontal hyaline zone. Under phase contrast the nucleus, the contractile vacuole, and some ingested food bacteria can be observed. They sometimes exhibit a tendency to form small aggregates as shown in Fig. 1A. If transferred from the agar surface of the NN-agar plate into Assolution or distilled water a high percentage of the amoebae transform into the flagellated stage with a long single frontal flagellum within 30 min. The flagellate has an elongated shape looking somewhat like a sausage moving actively by gyration in the direction of the flagellum. The flagellate is 15-20 µm long - its fully developed flagellum is as long or even a little bit longer than the cell body. The anterior end of the cell is tapered whereas the posterior end is stouter and somewhat rounded. After retransfer of the flagellates to the agar surface of a fresh agar plate seeded with *Enterobacter cloacae* they attach to the substratum by their cell body and become amoeboid again slowly incorporate their anterior flagellae. Within a period of 8-12 min the retransformation to normal trophozoites is completed.

The inconspicuous cysts have a round or oval outline and range in their size from 6 to 9 µm. They cannot be distinguished from *Hartmannella* cysts by light microscopy.

Electron microscopy

Trophozoite. The investigation by electron microscopy showed trophozoites with an irregular shape containing a nucleus with a diameter of 2.3 µm, a prominent nucleolus of 1.15 µm in diameter, and heterochromatin granules scattered throughout the karyoplasm (Figs 2A, C). The nucleus is separated from the cytoplasm by a nuclear envelope composed of 2 membranes that can be best observed in Figs 2A and 2B. Conspicuous mitochondria with tubular cristae are characterized by a

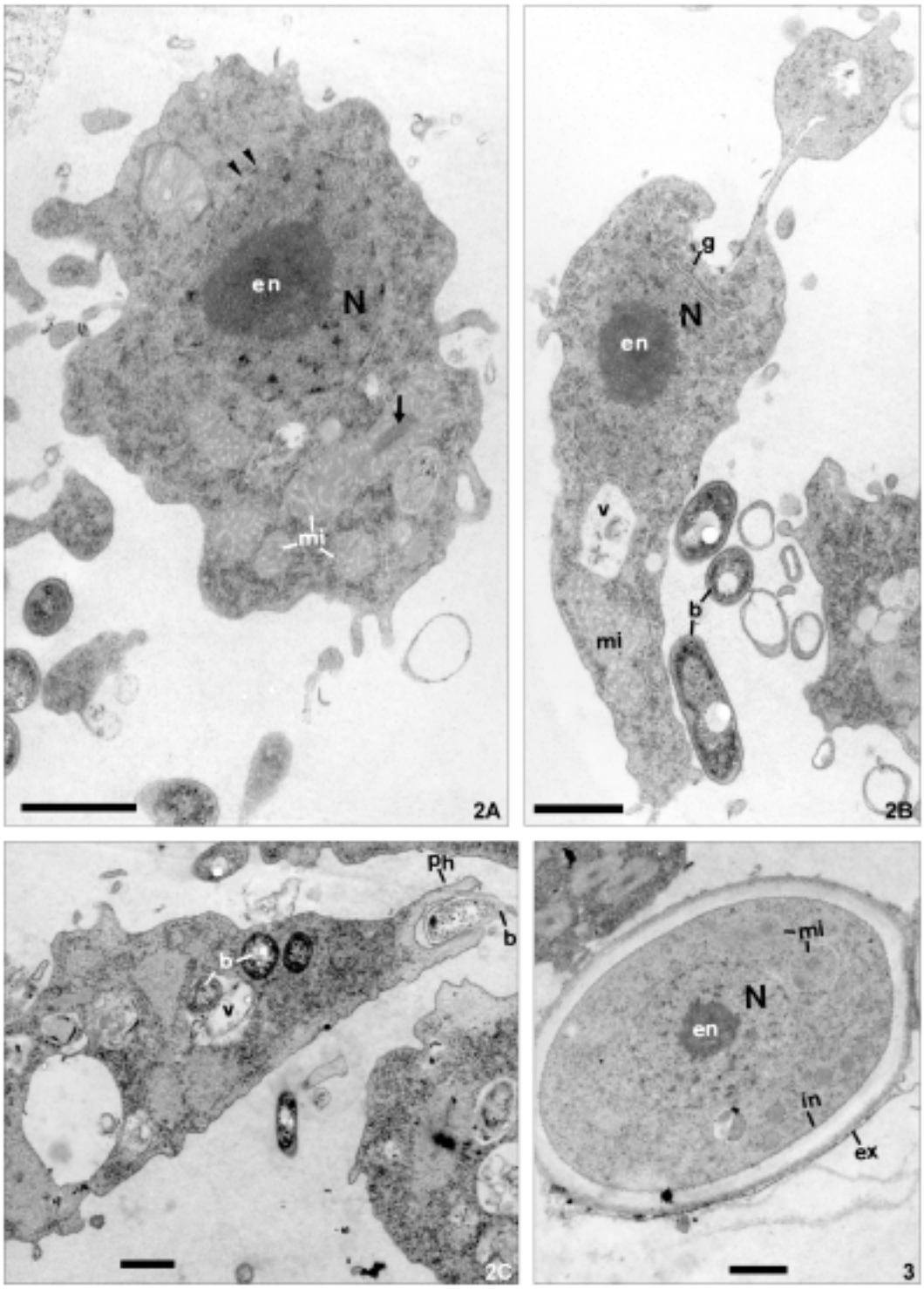

Figs 2 A-C. A - Wi7/2-PE-trophozoite with large nucleus (N) and prominent nucleolus or endosome (en) and heterochromatin granules. Irregular shape of the amoeba with subpseudopodia. Cytoplasm - containing ribosomes and glycogen-like granules - with conspicuous mitochondria containing tubular cristae (mi) characterized by the central electrondense core (arrow) typical for most slime moulds. Arrowheads - nuclear membrane; **B -** dividing of a trophozoite: Golgi zone (g) is located adjacent to the prominent nucleus (N). en - nucleolus, mi - mitochondrium, v - food vacoule; **C** - trophozoite of Wi7/2-PE ingesting *Enterobacter cloacae* as food bacterium (b) by forming a "food cup" that is surrounded by a hyaline zone produced by a meshwork of actin microfilaments (Ph). Food vacuoles (v) contain some bacteria too. Scale bars 1.0 µm.

Fig. 3. Cyst of strain Wi7/2-PE: the cyst wall is composed of a prominent ectocyst (ex - exine) separated by a wide empty space from the less pronounced endocyst (in - intine) attached closely to the cell membrane of the enclosed amoeba, mi - mitochondrium, N - nucleus with nucleolus (en). Scale bar 1.0 µm.

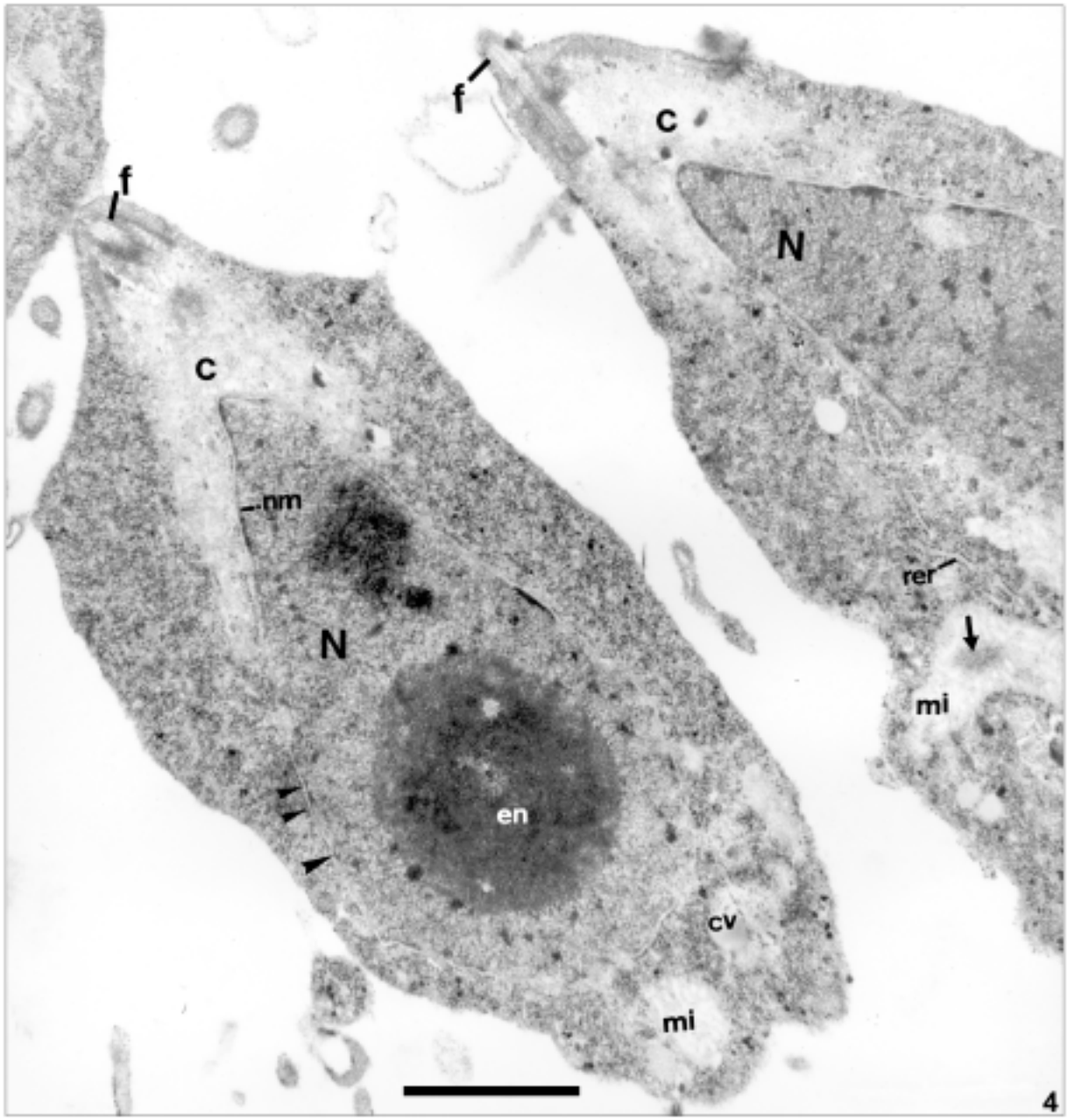

Fig. 4. Two flagellate stages of Wi7/2-PE with the anterior flagellum (f) discernible at the frontal tip of the cells. Nuclei (N) of both flagellates are tapering off in direction to the flagellar bases. They are enveloped by an electron lucent area representing "microtubular cones" (c). Nucleus of the left flagellate with most prominent nucleous (en), cv - contractile vacuole visible at the posterior end. arrow - electrondense core of mitochondrium, mi - mitochondrium, nm - nuclear membrane, rer - rough endoplasmatic reticulum. Scale bar 1.0 µm.

central electron dense core, which is located along the longitudinal axis of the mitochondrium as well known from flagellate stages of various myxogastrien slime moulds. The relative high optical density of the cytoplasm results from numerous ribosomes and glycogen granules. In addition it contains empty vacuoles or others filled with living bacteria and their remnants as a result of intracellular digestion (Figs 2B, C). One trophozoite in Fig. 2C exhibited food cup formation in order to ingest bacteria as prey. A putative dividing stage is presented in

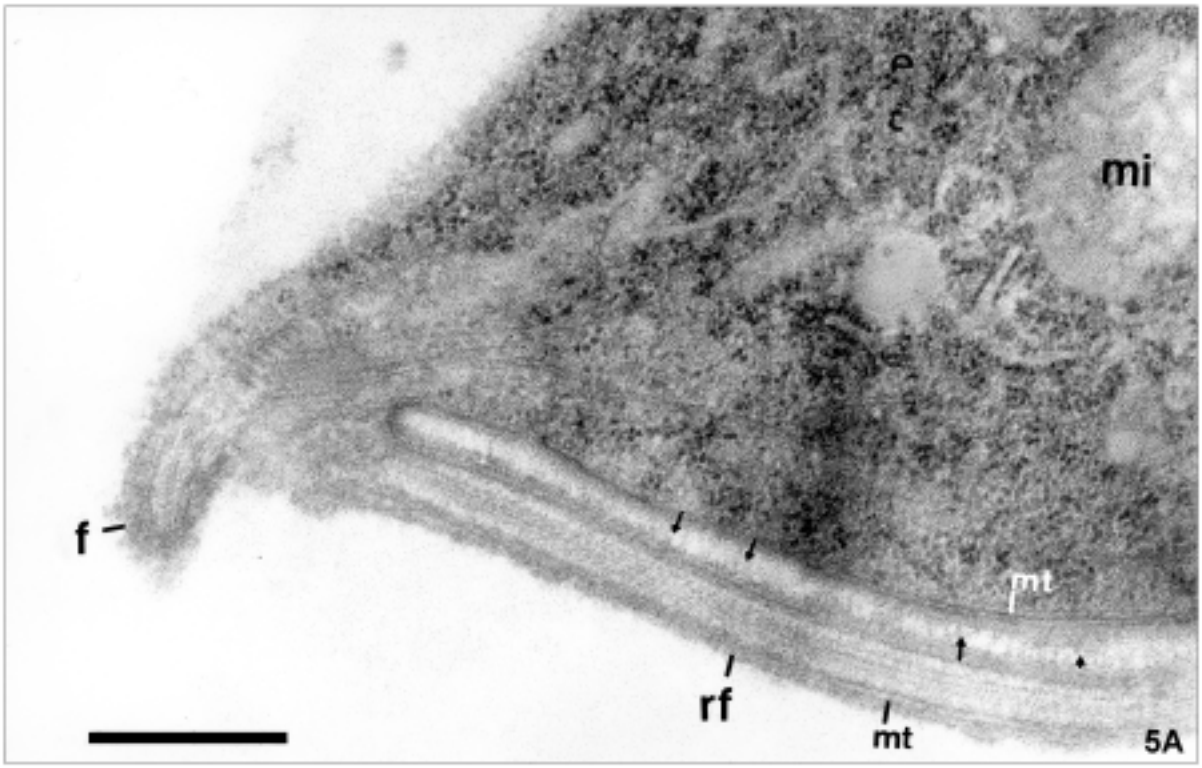
mi
f
mt
rf
mt
5A

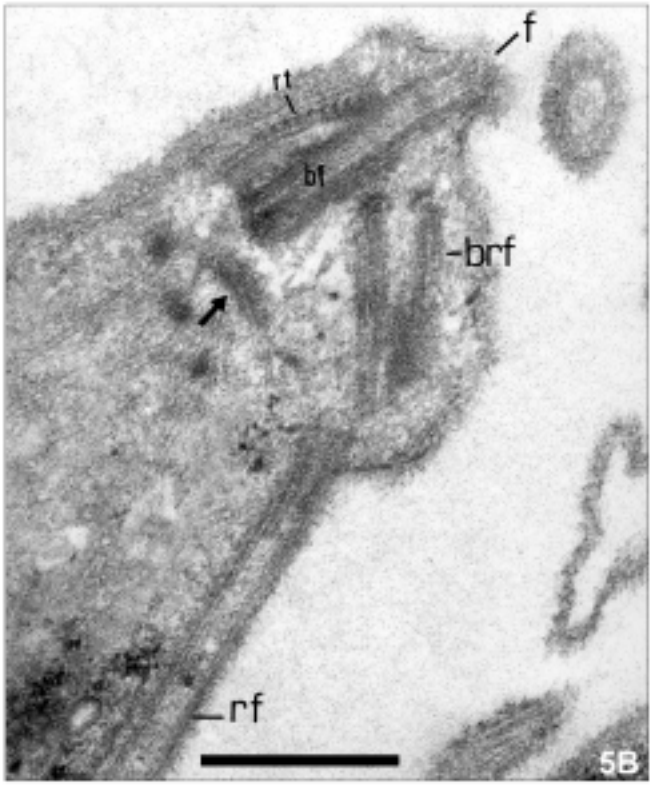
f
rt
bf
brf
rf
5B

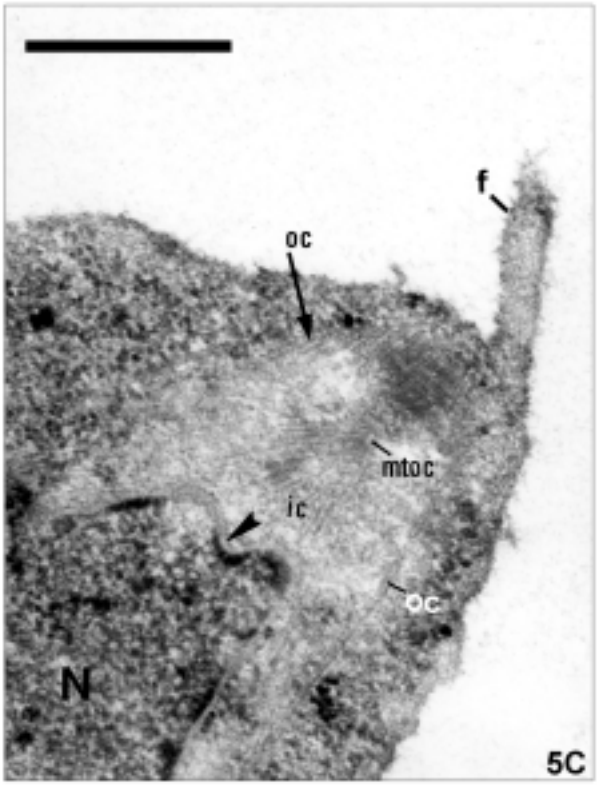
f
oc
mtoc
ic
oc
N
5C

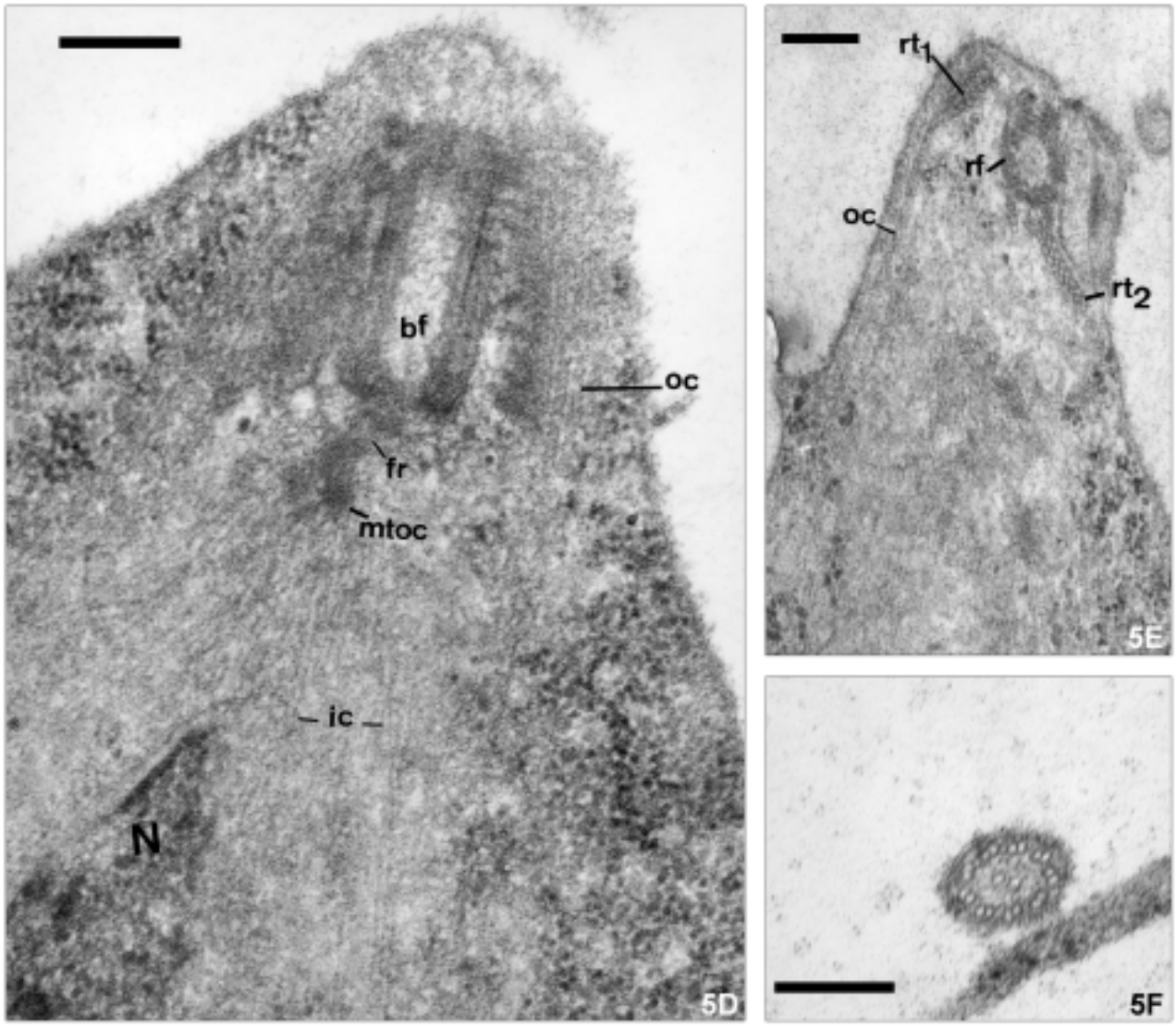

Figs 5 A-F. A - frontal part of a flagellate showing one frontal flagellum (f) and a second recurrent flagellate (rf) attached closely to the cell membrane of the flagellate stage by a desmosome-like connection containing fibrous filaments (arrows). mt - microtubules within the flagellum and beneath the cell membrane opposite to the recurrent flagellum (rf); mi - mitochondrium. **B** - a section through the anterior tip of a flagellate demonstrates both: the kinetosome of the frontal flagellum (bf) and of the recurring flagellum (brf) as well. The second flagellum (rf) appears tightly attached to the cell membrane. Arrow indicates the "microtubular organizing center" (mtoc) from which the inner cone of microtubules originates. rt - rootlet; **C** - anterior tip of a flagellate showing the microtubular organizing center (mtoc) with the origin of the inner cone (ic) surrounding the anterior part of the nucleus (N) that appears beaked (arrowhead) depending on the section plane. Microtubules forming the outer cone (oc) (arrow) are discernible too. f - flagellum; **D** - flagellar apparatus showing the kinetosom of the frontal flagellum (bf) surrounded by microtubules of the outer cone (oc). The kinetosome is connected with the microtubular organizing center (mtoc) by the "fibrillar rootlet" (fr) of the flagellar basal body. The inner microtubular cone (ic) arises from "mtoc". N - nucleus; **E** - anterior tip of the flagellate stage (Wi7/2-PE) reveals the position of the rootlets in relation to kinetosomes: the basal body of the recurrent flagellate (rf) cut obliquely is connected with its rootlet (rt_2) consisting of a double row of microtubules whereas the rootlet of the frontal flagellum (rt_1) consists of only a single row of microtubules. oc - microtubules of the outer cone; **F** - cross section through an anterior flagellum showing the characteristic 9 + 2 pattern of microtubules. Scale bars 0.5 µm (A-D), 0.2 µm (E, F).

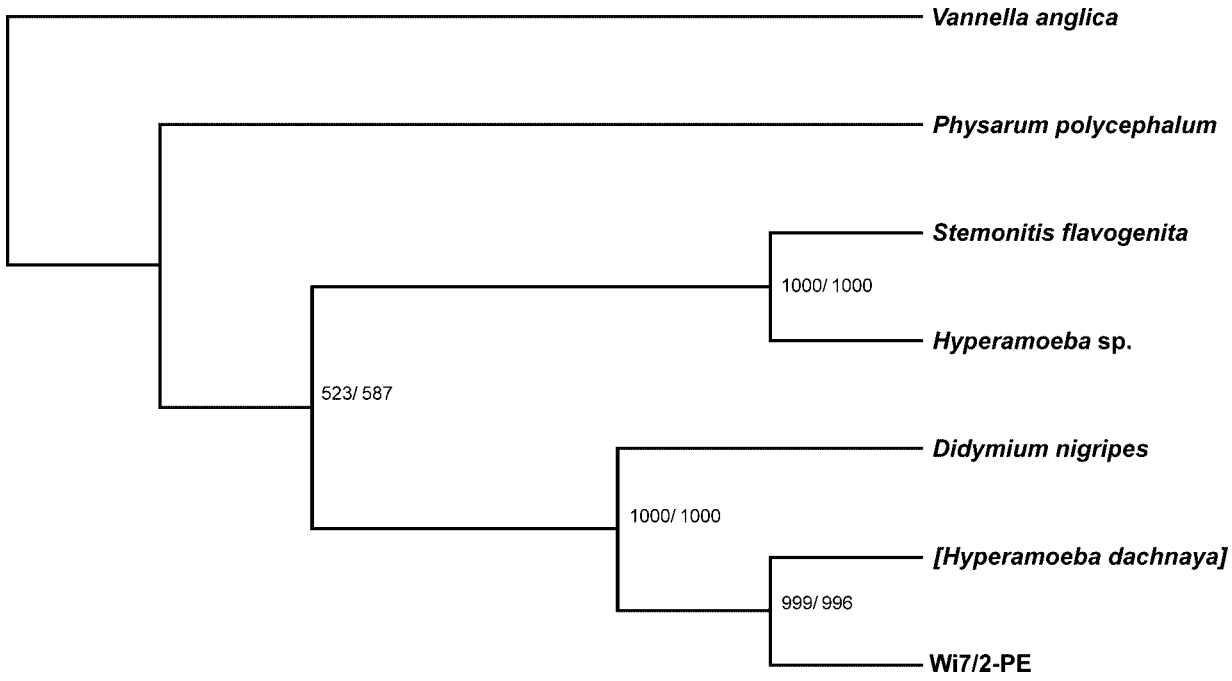

Fig. 6. 18S rDNA neighbour-joining cluster analysis of our isolate Wi7/2-PE, the *Hyperamoeba* sp. strain (GenBank accession number: AF093247), and several myxogastrean slime moulds using a strain of *Vannella anglica* (GenBank accession number AF099101) as outgroup. The still undescribed strain "*Hyperamoeba dachnaya"* was added to the alignment and used in brackets. The numbers at the nodes represent bootstrap values based on 1000 replicates. Bootstrap values of the maximum parsimony analyses are given behind the slash. Our isolate Wi7/2-PE clusters unambiguously with the "*Hyperamoeba dachnaya*" isolate together forming a cluster with the myxogastrean genus *Didymium* (strain *D. nigripes* GenBank accession number AF239230), while the described *Hyperamoeba* sp. strain forms a cluster with the myxogastrean genus *Stemonitis* (strain *S. flavogenita* GenBank accession number AF239229).

Fig. 2B with two daughter cells still connected by a thread-like cytoplasmic bridge. The lower division partner reveals also a conspicuous Golgi apparatus (dictyosome).

Cyst. Most cysts have a round or oval shape with a varying size from 6 to 9 µm (Fig. 3). The cyst wall is composed of a prominent ectocyst (0.1-0.2 µm thick) separated by a wide electron translucent space filled with thin fibrillar material of 0.28-0.38 µm from the delicate endocyst attached tightly to the enclosed amoeba. Within the latter the nucleus with nucleolus and persisting mitochondria are visible. Food vacuoles could not be observed but some lipid granules instead.

Flagellate stage. As the flagellate stages reveal more morphologic details than the trophozoites and cysts together increased attention has to be paid to this important developmental stage in the life cycle of these amoeboflagellates. As recognized by phase contrast microscopy the trophozoites transform *via* transitory stages to an elongated sausage-like form with a single visible flagellum emanating from the frontal tapered end of the cell (Figs 4, 5A-C). The flagellum is anchored by a basal body (kinetosome) with accessory structures in the anterior cytoplasm of the flagellate (Figs 4, 5B, D, E). Mature flagellates of Wi7/2-PE - as can be observed within a period of 30 min after suspension of the trophozoites in As-solution - had a defined sausage-like shape with a smooth and stable outline. Two sections of them can be recognized in Fig. 4, each of them with one anterior flagellum. The prominent nuclei of both are tapering off in direction to the basal bodies of the flagellum. They are enveloped by conical arrays of microtubules corresponding to the electron lucent area in Fig. 4. Mitochondria of the tubular cristae type showing a dense central core characteristic for certain slime moulds can be observed within the flagellates as well. A contractile vacuole - as seen by phase contrast - is located at the posterior end of the cell.

Since only one frontal flagellum can be recognized by means of phase contrast microscopy it was surprising to notice that a second recurrent flagellum was found, which was attached to the cell membrane of the flagel-

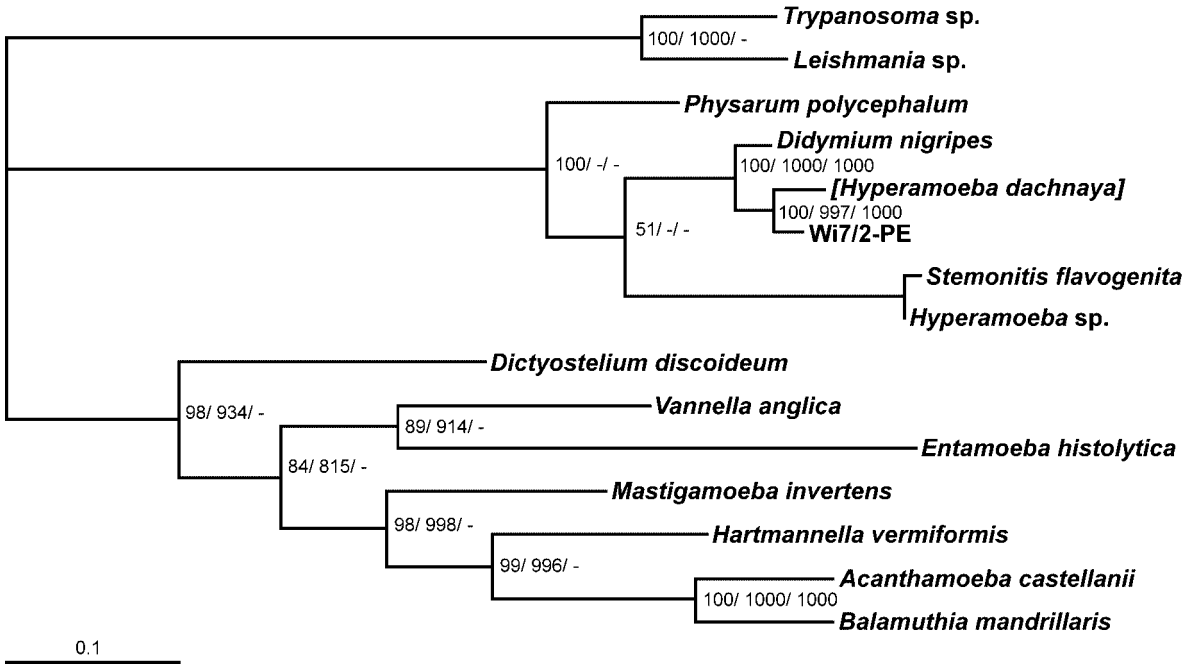

Fig. 7. 18S rDNA maximum likelihood analysis of the position of *Hyperamoeba* within the amoebozoa using *Leishmania* (GenBank accession number AF303938) and *Trypanosoma* (AF416562) as outgroup. Bootstrap values were calculated based on 100 (ML) and 1000 (distance and maximum parsimony) replicates, respectively. The bootstrap values are shown at the nodes (ML/ Distance/ P). The scale bar indicates the mean number of substitutions per site.

late stage by a desmosome-like connection zone containing fibrous filaments (Fig. 5A). Still more tightly attached appears the recurrent flagellum in Fig. 5B. This second hidden flagellum has a length of about one third of the cell body. The kinetosomes of both flagellae are shown in Fig. 5B, where they are located at an acute angel of about 45° to each other with the microtubular rootlet of the anterior flagellum. The organisation of the outer and inner microtubular cone both of which surround the frontal part of the nucleus like a double basket is discernible at Figs 5B-D. The inner cone emanates from the microtubular organisation center (mtoc), which is connected with the kinetosome of the frontal flagellum by the fibrillar rootlet (Fig. 5D). The outer basket is supposed to originate from the microtubular rootlet (Fig. 5E) as well known from *Hyperamoeba* (Karpov and Mylnikov 1997). The tip of the nucleus may appear beaked in some cases depending on the section plane. Rarely the rootlets of both basal bodies can be found in one section (Fig. 5E). The rootlet of the anterior flagellum is composed of a single row of microtubules whereas the rootlet of the second recurrent flagellum is composed of two rows of 7-8 microtubules each. Also a very short single row of 3-4 MT can be recognized in connection with this kinetosome.

Investigation on the molecular level

The 18S rRNA gene of the Wi7/2-PE strain of the *Hyperamoeba*-like amoeboflagellate shows a length of 1876 bp (with primer sites excluded), with a G+C content of 52.72%. It exhibits the highest sequence similarity, namely 94.78% to a strain of *Hyperamoeba dachnaya*, which has been submitted to the GenBank during the preparation of this manuscript, but which has not been described yet. The strain with the second highest sequence similarity (93.96% identity) is a strain of *Didymium nigripes* (GenBank AF239230). However, the strain of *Didymium* shows an insertion of 654 bp length after the 1726th bp. The sequence identity to the only published and described strain of *Hyperamoeba* is only 80.25%!

This closer relatedness of our isolate (and also of the hitherto undescribed "*Hyperamoeba dachnaya*") to *Didymium* than to the initially sequenced strain of

Hyperamoeba was proven by cluster analysis. As shown in Fig. 6 the strain Wi7/2-PE (together with "*Hyperamoeba dachnaya*") clusters with *Didymium*, while the described strain of *Hyperamoeba* clusters with *Stemonitis*. Groupings remained also in the same order when maximum parsimony was used and both analyses revealed high bootstrap values for these groupings.

However, the distinction from *Didymium* is clear, by the insertion this strain of *Didymium* has (all the other strains of the Myxogastria used in this study do not show any insert) and also when the insertion is excluded the identity is only 93.96%.

Altogether, the investigation on the molecular level corroborates the morphological data indicating that it is neither possible to assign this *Hyperamoeba*-like isolate to the genus *Hyperamoeba* nor to the genus *Didymium* as it differs fundamentally from both genera in several aspects. We thus considered to describe this isolate within a new genus, *Pseudodidymium*, as a new species, *Pseudodidymium cryptomastigophorum.*

In order to assess, whether these groupings are constant also in a more large scale investigation and also to reveal the position of *Hyperamoeba* within the amoebozoa a second cluster analysis was performed including several genera of the amoebozoa and using *Trypanosoma* and *Leishmania* as an outgroup. As shown in Fig. 7 the groupings of the different *Hyperamoeba* strains remained in the same order and these groupings also reveal high bootstrap values. However, whether the branch including *Didymium*, the "*Hyperamoeba dachnaya*" strain and our isolate clusters with the *Stemonitits* group or rather with *Physarum* is not well resolved. Interestingly, in this analysis *Dictyostelium* did not cluster together with the myxogastrid slime moulds, but together with *Mastigamoeba* and the lobosean amoebae.

DISCUSSION

As the isolate Wi7/2-PE, which had been isolated from a hydrotherapy pool of a hospital at Wildbach/ Germany could neither be assigned to the genus *Hyperamoeba* nor to any of the myxogastrean slime moulds, which are the closest relatives of *Hyperamoeba*, we considered to describe this isolate within a new genus, *Pseudodidymium*, as a new species, *Pseudodidymium cryptomastigophorum*.

In addition to the distinct genetic distance shown on the molecular level attention was focused to morphological differences on the ultrastructural level. The overall morphology of trophozoites, cysts, and flagellates is comparable to the features of *Hyperamoeba flagellata* (Karpov and Mylnikov 1997, Zaman *et al.* 1999) on one side and to myxogastrean slime mould stages on the other side.

Characteristic for both groups is the nucleus with a prominent nucleolus and dispersed particles of heterochromatine. Within the flagellate stage the frontal part of the nucleus is enveloped by a double conal array of MT emanating from the rootlets and from the "mtoc" respectively, which are located in relation to the basal bodies. Very important are the mitochondria of both vegetative stages exhibiting a dense central core that can be found within *Hyperamoeba* and also within slime moulds where this unique trait is confined to Myxogastrea in contrast to Protostelidae and the cellular slime moulds such as *Dictyostelium* where it is lacking (Schuster 1965, Aldrich 1968, Karpov and Mylnikov 1997).

Concerning solely the morphological similarities mentioned it becomes already evident that *Hyperamoeba* and the presently described new species are distinctly related to Myxogastrea with the main exception that they are unable to form fruiting bodies in the course of their life cycle. After stressing the common features of the organisms mentioned attention has now to be paid to differences between those species in question.

From the three stages differences in cyst shape can be observed at a first glimpse. The *Hyperamoeba* isolated by Zaman *et al.* (1999) from human faeces formed cysts with ectocysts, which greatly varied in thickness and contained clumps of Gram-negative bacteria whereas the ectocyst of our strain was of constant thickness and devoid of bacteria. It is comparable to the also uninuclear cysts of *Didymium nigripes* with inconspicuous ecto- and endocyst (Schuster 1965). One of the most conspicuous traits of Wi7/2-PE is the nucleus of the flagellates tapering off in frontal direction with its tip eventually beaked in some cases - in contrast to *Hyperamoeba* with a round at least moderately pointed nucleus within the flagellate stage (Karpov *et al.*1997) The elongated nucleus of Wi7/2-PE resembles the nucleus of the flagellated stages of *Stemonitis* (Ishigami 1977), *Physarum* (Wright *et al.* 1979), and *Didymium* (Schuster 1965) - the tip of the latter becoming blunt in older stages. However, the most striking difference of Wi7/2-PE from *Hyperamoeba* described so far is the

presence of a second recurrent flagellum in addition to the long frontal flagellum! *Hyperamoeba flagellata* was shown to possess only one functional frontal flagellum with its kinetosome and a second barren kinetosome being located with an acute angle in relation to the first one.

The recurrent flagellum of Wi7/2-PE does not contribute to the swimming locomotion, the force of which is generated solely by the long frontal flagellum. The tight attachment of the useless short flagellum to the cell surface by a desmosome-like connection is the reason why the fagellates appear ostensibly uniflagellate when examined under phase contrast. The possession of such a short second flagellum has Wi7/2-PE in common with various flagellate stages of Myxogastria such as *Didymium nigripes* (Schuster 1965), *Stemonitis* (Ishigami 1977), and *Physarum* (Aldrich 1968; Wright 1979). But in contrast to the situation in Wi7/2-PE these recurrent flagellae can be distinguished as a free however useless trailing flagellum of the flagellate stages in these slime moulds.

Those remarkable differences can be recognized without going into details of the very complex morphology of the flagellar apparatus described as far as possible from the micrographs. The organisation of the flagellar apparatus of Wi7/2-PE corresponds well to the general scheme of these structures at *Hyperamoeba* as presented by Karpov and Mylnikov (1997) - with one exception: The long one of the two rootlets anchoring the second kinetosome (rt2 in Fig. 5E) is composed of a single row of MT of two closely apposed layers of MT with a basal layer of fibrillar material in the case of our isolate resembling the three layered rootlet shown in *Physarum* flagellates (Wright *et al*. 1979).

We think that, as a result of the morphological examination alone a description of Wi7/2-PE as a novel species *Pseudodidymium cryptomastigophorum* is justified. The name *Pseudodidymium* refers to its relatedness to *Didymium* and the species name *cryptomastigophorum* was chosen because of its hidden second flagellum.

By comparison with *Hyperamoeba* on one side and the slime moulds on the other it becomes evident that this isolate has greatest morphologic affinities to the myxogastrean slime moulds. Since no formation of fruiting bodies could be observed by methods of induction mentioned above the discussion is open to the question whether it is a precursor protist or a secondarily derived form of a slime mould such as *Didymium* for instance, which has lost its capability to produce fruiting bodies. Similar considerations for the relationship of *Hyperamoeba* and slime moulds are known from Cavallier-Smith and Chao (1998).

In molecular biological investigations our strain showed highest affinity to "*Hyperamoeba dachnaya*" (GenBank AY062881). However, this strain has not been described yet, and both of these strains show significant higher sequence identity to *Didymium* (93.96% in case of Wi7/2-PE) than to the originally published *Hyperamoeba* strain (80.25%). As also shown in a more large scale analysis including various other amoebozoa, all three *Hyperamoeba* isolates constantly form a cluster with the myxogastrid slime moulds, however, our data indicate that the genus *Hyperamoeba* is not monophyletic. In fact the *Hyperamoeba* isolates are dispersed among the myxogastrid slime moulds.

Interestingly, *Dictyostelium* did not cluster with the myxogastrid slime moulds to form a monophyletic mycetozoan branch, but clustered together with *Mastigamoeba* and the lobosean amoebozoa. A close relationship of *Dictyostelium discoideum*, *Mastigamoeba balamuthi* and *Entamoeba histolytica* has already been observed by other authors (Arisue *et al.* 2002, Bapteste *et al.* 2002).

The phylogenetic position of the mycetozoa and whether they form a monophyletic group is still not wholly elucidated. Baldauf and Doolittle (1997) found evidence for a monophyletic group Mycetozoa standing within the crown of the eukaryote tree. Karpov (1997) assumed that the myxomycetes might be closely related to the cercomonads. And indeed these two groups share quite a few morphological features. However, some very recent papers indicate that the cercomonads might rather be related to the foraminifera, than to the slime moulds (Keeling 2001, Archibald *et al.* 2003). And finally Cavalier-Smith and Chao (2003) proposed to remove the amoebozoa including also the mycetozoa from the opisthokont branch and to place them rather at the base of the bikont clade. There is and has been a lot of regrouping within the protozoa and certainly the last word has not yet been spoken. In the case of the myxogastrid slime moulds it is clear that a lot more data are needed to place them correctly and to solve their relationship to the other mycetozoa. However, it was not the intention of our study to solve the phylogeny of the mycetozoa, but to analyse the position of *Hyperamoeba*

within the amoebozoa and to prove our findings that the genus *Hyperamoeba* at the present state seems to be polyphyletic.

Altogether, we think that it is neither possible to assign the *Hyperamoeba*-like isolate Wi7/2-PE to the genus *Hyperamoeba* nor to the genus *Didymium* as it differs fundamentally from both genera in several aspects, and that it is thus justified to describe it as a new species *Pseudodidymium cryptomastigophorum*, within a new genus.

The possible medical significance of *Hyperamoeba*-like strains is not yet known. The amoeboflagellate isolated from human nasal mucosa by Mascaro *et al.* (1986) was similar to the amoeboflagellates - described and mentioned here - by morphologic terms only. It was highly virulent in mice when introduced into the sinus cavity. Some mice were killed after invasion into the brain tissue - others developed chronic infections. All mice investigated had amoebae in their lungs. The *Hyperamoeba* strains isolated from human feces in Karatschi were shown to induce ulceration of the skin in mice after subcutaneous injection of the amoeboflagellates and were considered therefore to have a pathogenic potential (Zaman *et al*. 1999). These data from experimental animals suggest performing corresponding pathogenicity tests in future with cell cultures and eventually by inoculation tests with suited experimental animals.

***Pseudodidymium cryptomastigorum* gen. n., sp. n.**

Diagnosis: amoeboflagellate with three stages in its life cycle: trophozoite, flagellate stage and cyst. The uninucleate trophozoites of varying size and shape (15-18 µm). Blunt filopodia emanate from a frontal hyaline cytoplasm margin in locomotion. Vesicular nucleus (1.8-2.2 µm in diameter) is rounded or slightly oblong with a central rounded nucleolus (0.8-1.2 µm). Heterochromatin granules are scattered throughout the karyoplasm. Mitochondria with tubular cristae exhibit a central electron dense core well known from myxogastrean slime moulds. A Golgi apparatus is observable. The sausage like shaped flagellated stage shows a variable length of 15-20 µm. The single anterior flagellum is a long or ever a bit longer than cell body. The second recurrent flagellum has about one third of the cell length, is closely connected with the surface of the flagellate, and has no function. The prominent nucleus is tapering off in frontal direction and is partially surrounded by an outer and inner cone of mt emanating from the rootlet of the anterior flagellum and the mtoc, respectively. The rootlet of the anterior kinetosome consists of a single row of mt whereas that of the recurrent flagellum is composed of two rows of 7-8 mt each. The mitochondria are comparable to those of the trophozoite especially with the dense core and correspond as well to mitochondria from myxogastrea. The inconspicuous cyst has a double cyst wall separated by an empty space and has a diameter of 6-9 µm. The 18S rRNA gene of Wi7/2-PE shows a length of 1876 bp (with primer sites excluded), with a G+C content of 52.72%.

Differential diagnosis: *P. cryptomastigophorum* has morphological similarities to *Hyperamoeba flagellata* on one side and to myxogastrean slime moulds on the other. It differs from *Hyperamoeba* by its recurrent flagellum always present in the flagellate stage and by the possession of the distinct double row of mt in contrast to a single row described for *Hyperamoeba*. The possession of mitochondria with tubular cristae and the distinct electron dense core indicate - as in the case of *Hyperamoeba* - the relatedness to myxogastrean slime moulds. Protostelidae and cellular slime moulds do not have these mitochondrial traits. Also *Cercomonas* has normal mitochondria without that dense core indicating no close relationship with our isolate. The close relationship to Myxogastrea is supported by the pear shaped nucleus of the flagellate stage that tapers off in frontal direction as has been described from *Stemonitis Physarum,* and *Didymium*. In addition these myxogastrea have flagellate stages (zoospores) with a second recurrent but trailing flagellum. Despite these morphological similarities with slime moulds the novel species is characterized by its incapability to form fruiting bodies pertaining to these organisms. Wi7/2-PE exhibits 94.78% sequence similarity to a strain of "*Hyperamoeba dachnaya*", which has, however, not been described yet and both of these strains show significant higher sequence identity to *Didymium* (93.96%) than to the originally published *Hyperamoeba* strain (80.25%). This strain of *Didymium*, however, shows an insertion of 654 bp length after the 1726th bp, which Wi7/2-PE does not have.

Acknowledgement. We thank Gerhild Gmeiner (Laboratory for Electron Microscopy, CIFAFMS, Koblenz; Head: B. Hauröder) for excellent technical assistance.

REFERENCES

Aldrich H. C. (1968) The development of flagella in swarm cells of the myxomycete *Physarum flavicomum. J. Gen. Microbiol.* **50:** 217-222

Alexeieff A. G. (1923) *Hyperamoeba flagellata* n. gen. n. sp. *Archiv Russkogo Protistologicheskogo Obschestva* **2**: 280-288

Altschul S. F., Gish W., Miller W., Myers E. W., Lipman D. (1990) Basic local alignment search tool. *J. Mol. Biol.* **215:** 403-410

Archibald J. M., Longet D., Pawlowski J., Keeling P. J. (2003) A novel polyubiquitin structure in cercozoa and foraminifera: evidence for a new eukaryotic supergroup. *Mol. Biol. Evol.* **20:** 62-66

Arisue N., Hashimot T., Lee J. A., Moore D. V., Gordon P., Sensen C. W., Gaasterland T., Hasegawa M., Muller M. (2002) The phylogenetic position of the pelobiont *Mastigamoeba balamuthi* based on sequences of rDNA and translation elongation factors EF-1alpha and EF-2. *J. Eukaryot. Microbiol*. **49:** 1-10

Baldauf S. L., Doolittle W. F. (1997) Origin and evolution of the slime moulds (Mycetozoa). *Proc. Natl. Acad. Sci. USA.* **94:** 12007-12

Bapteste E., Brinkmann H., Lee J. A., Moore D. V., Sensen C. W., Gordon P., Durufle L., Gaasterland T., Lopez P., Muller M., Philippe H. (2002) The analysis of 100 genes supports the grouping of three highly divergent amoebae: Dictyostelium, Entamoeba, and Mastigamoeba. *Proc. Natl. Acad. Sci. USA.* **99:** 1414-9

Bolivar I., Fahrni J. F., Smirnov A., Pawlowski J. (2001) SSU rRNA-based phylogenetic position of the genera *Amoeba* and *Chaos* (Lobosea, Gymnamoebia): the origin of gymnamoebae revisited. *Mol. Biol. Evol.* **18:** 2306-2314

Cavalier-Smith T., Chao E. E. (1998) *Hyperamoeba* rRNA phylogeny and the classification of the phylum Amoebozoa. *J. Eukar. Microbiol.* The Society of Protozoologists, 51 st Annual Meeting, August 1-8

Cavalier-Smith T., Chao E. E. (2003) Phylogeny of choanozoa, apusozoa, and other protozoa and early eukaryote megaevolution. *J. Mol. Evol*. **56:** 540-63

Dacks J. B., Marinets A., Ford Doolittle W., Cavalier-Smith T., Logsdon J. M. Jr. (2002) Analyses of RNA Polymerase II genes from free-living protists: phylogeny, long branch attraction, and the eukaryotic big bang. *Mol. Biol. Evol.* **19:** 830-40

Felsenstein J. (1989) PHYLIP-phylogeny inference package, vers. 3.2. *Cladistics* **5:** 164-166

Gast R. J., Ledee D. R., Fuerst P. A., Byers T. J. (1996) Subgenus systematics of *Acanthamoeba*: four nuclear 18S rDNA sequence types. *J. Eukaryot. Microbiol*. **43:** 498-504

Hendriks L., De Baere R., Van de Peer Y., Neefs J., Goris A., De Wachter R. (1991) The evolutionary position of the rhodophyte *Porphyra umbilicalis* and the basidiomycete *Leucosporidium scottii* among other eukaryotes as deduced from complete sequences of small ribosomal subunit RNA. *J. Mol. Evol.* **32:** 167-177

Hinkle G., Sogin M. L. (1993). The evolution of the Vahlkampfiidae as deduced from 16S-like ribosomal RNA analysis. *J. Eukaryot. Microbiol.* **40:** 599-603

Hugo E. R., Stewart V. J., Gast R. J., Byers T. J. (1992) Purification of amoeba mtDNA using the UNSET procedure. In: Protocols in Protozoology, (Eds A. T. Soldo, J. J. Lee) Allen, Lawrence, Kansas, 7.1

Ishigami M. (1977) A light and electron microscopic study of the flagellate-to-ameba conversion in the myxomycete *Stemonitis pallida*. *Protoplasma* **91:** 31-54

Karpov S. A. (1997) Cercomonads and their relationship to the myxomycetes. *Arch. Protistenkd.* **148:** 297-307

Karpov S. A., Mylnikov A. P. (1997) Ultrastructure of the colorless flagellated *Hyperamoeba flagellata* with special reference to the flagellar apparatus. *Europ. J. Protistol.* **33:** 349-355

Keeling P. J. (2001) Foraminifera and Cercozoa are related in actin phylogeny: two orphans find a home? *Mol. Biol. Evol.* **18:** 1551-1557

Mascaro M. L., Mascaro M. C., Osuna A., Perez M. L., Gonzalez-Castro J. (1986) Study of an amoeboflagellate isolated from the nasal mucosa of man. *J. Protozool.* **53:** 89-93

Nicholas K. B., Nicholas H. B. Jr., Deerfield D. W. II. (1997) GeneDoc: Analysis and visualization of genetic variation. *Embnew. News*. **4:** 14

Page F. C. (1988) A new key to freshwater and soil Gymnamoebae. Freshwater Biological Association, The Ferry House, Ambleside, Cumbria

Page R. D. M. (1996) TREEVIEW: An application to display phylogenetic trees on personal computers. *Comput. Appl. Biosci.* **12:** 357-358

Thompson J. D., Gibson T. J., Plewniak F., Jeanmougin F., Higgins D. G. (1997) The ClustalX windows interface: flexible strategies for multiple sequence alignment aided by quality analysis tools. *Nucleic Acids Res.* **24:** 4876-4882

Schuster F. L. (1965) Ultrastructure and morphogenesis of solitary stages of true slime moulds. *Protistologica* **1:** 49-62

Walochnik J., Michel R., Aspöck H. (2002) Untersuchungen zur Phylogenie der Gattung Hyperamoeba 21. Jahrestagung der Deutschen Gesellschaft für Protozoologie, 27.02.-2.03.2002, Konstanz

Wright M., Moisand A., Mir L. (1979) The structure of the flagellar apparatus of the swarm cells of *Physarum polycephalum*. *Protoplasma* **100:** 231-250

Zaman V., Zaki M., Howe J., Ng M., Leipe D. D., Sogin M. L., Siberman J. D. (1999) *Hyperamoeba* isolated from human feces: Description and phylogenetic affinity. *Europ. J. Protistol.* **35:** 197-207

Received on 28th January, 2003; revised version on 1st July, 2003; accepted on 8th July, 2003

Acta Protozool. (2003) 42: 345 - 355

ACTA
PROTOZOOLOGICA

Redescription of Two Known Species, *Gastrocirrhus monilifer* (Ozaki et Yagiu, 1942) and *Gastrocirrhus stentoreus* Bullington, 1940, with Reconsideration of the Genera *Gastrocirrhus* and *Euplotidium*

Xiaozhong HU* and Weibo SONG

Laboratory of Protozoology, Ocean University of China, Qingdao, P. R. China

Summary. The living morphology and infraciliature of two poorly known planktonic ciliates, *Gastrocirrhus monilifer* (Ozaki et Yagiu, 1942) and *G. stentoreus* Bullington, 1940, collected from coastal mollusc-farming waters off Qingdao, P. R. China, were described based on observations of specimens *in vivo* and following protargol impregnation. Since no recent data deriving from silver staining methods on these two species are available, detailed redescriptions were presented. Based on the previous and current studies, improved redefinition for two hitherto confused genera *Gastrocirrhus* and *Euplotidium* are supplied. The diagnosis for *Gastrocirrhus*: marine planktonic Gastrocirrhidae, cells generally cup- or bell-shaped with anterior end truncated; oral field broad and opening anteriorly; adoral zone of membranelles dominant, terminated deeply near cytostome after spiraling around bell-edge in one turn; undulating membrane single-structured; frontoventral cirri arranged in two rows, which are formed by multi-anlagen during morphogenesis; 5 or more well-developed transverse cirri; marginal and caudal cirri absent. Diagnosis for the genus *Euplotidium*: marine Gastrocirrhidae, body shape cylindrical to dorso-ventrally flattened, buccal apparatus being of *Euplotes*-pattern; about 10 frontoventral cirri sparsely distributed but not in rows; *ca* 5 transverse and one or more left marginal cirri; no caudal cirri. Based on the new definition and the data available, 5 nominal species are recognized in the genus *Euplotidium*: *E. itoi* Ito, 1958; *E. psammophilius* (Vacelet, 1961) Borror, 1972 [basonym: *Euplotes psammophilius* Vacelet, 1961]; *E. arenarium* Magagnini et Nobili, 1964; *E. helgae* Hartwig, 1980 and *E. prosaltans* Tuffrau, 1985, and 5 in *Gastrocirrhus*: *G. intermedius* Lepsi, 1928; *G. stentoreus* Bullington, 1940; *G. monilifer* (Ozaki et Yagiu, 1942) Curds et Wu, 1983 [junior synonym: *G. adhaerens* Fauré-Fremiet, 1954; *G. trichocystus* Ito, 1958]; *G. agitatus* (Noland, 1937) comb. n. [basonym: *Euplotidium agitatum* Noland, 1937] and *G. smalli* (Lei Y., Choi J. K. et Xu K., 2002) comb. n. [basonym: *Euplotidum smalli* Lei Y., Choi J. K. et Xu K., 2002].

Key words: *Euplotidium*, *Gastrocirrhus*, infraciliature, morphology, new combination.

INTRODUCTION

As in many other little-known marine ciliates, much disarray remains in the plankton euplotids, *Gastrocirrhus-Euplotidium-Cirrhogaster*-complex in terms of their generic separation as well as species identification (Kahl 1932, Bullington 1940, Borror 1972, Hill 1980, Curds and Wu 1983, Borror and Hill 1995). This confusion derives from many forms having been described on the basis of insufficient living observations. Other reasons include: (1) some features (e.g. distribution or arrangement of frontoventral cirri, number of transverse cirri, presence/absence of the marginal cirrus) are likely variable or inconspicuous, and hence are easily overlooked in some

Address for correspondence: Weibo Song, Laboratory of Protozoology, Ocean University of China, Qingdao 266003, P. R. China; Fax: +86 532 203 2283; E-mail: wsong@ouc.edu.cn

* Present address: Faculty of Fisheries, Nagasaki University, Bunkyo-machi 1-14, Nagasaki 852-8521, Japan

cases but often, unfortunately, used as a reliable diagnostic character and (2) many authors paid insufficient attention to comparing their populations with previous studies. Therefore, morphological data based on modern techniques, especially the structure of oral and somatic ciliature for most congeners of these genera are extremely necessary for accurate species identification.

Recently, two *Gastrocirrhus* species were found in maricultural waters along the coasts of Qingdao, China. Subsequent studies demonstrate that they belong to two known but poorly described organisms. Based on the comparison of related taxa, the re-definition of the confused *Gastrocirrhus-Euplotidium-Cirrhogaster*-complex and relationships among them are reconsidered and outlined. In the present paper, redescriptions of living morphology and infraciliature of these two species as well as the redefinitions of the genera *Gastrocirrhus* and *Euplotidium* are documented here.

MATERIALS AND METHODS

Samples were collected from the molluscs culturing waters off the coast of Qingdao (Tsingtao, 36°08'N; 120°43'E), China in August 2000 and May 2001. Salinity was about 32‰, water temperature was about 25°C and 15°C for *Gastrocirrhus monilifer* and *G. stentoreus*, respectively, and pH was *ca* 8.2. After isolation, a pure culture was kept for a few days at room temperature (25°C or so) in boiled seawater, to which crushed rice grains were added as a food source for bacteria.

Ciliates were examined with an Olympus microscope with bright field and differential interference contrast equipment. The protargol silver staining method according to Wilbert (1975) was used to reveal the infraciliature. All drawings on prepared specimens were performed at a magnification of x1250 with the help of a camera lucida. Measurements were made with an ocular micrometer.

RESULTS

Reconsideration of the genus *Gastrocirrhus* Lepsi, 1928

Syn. *Cirrhogaster* Ozaki et Yagiu, 1942

Since only very few studies on the *Gastrocirrhus-Euplotidium*-complex have been performed using silver staining or other modern methods, there is still some confusion in separation at the generic level considering their diagnosis and description on the patterns of infraciliature. Morphologically, however, the genus *Gastrocirrhus* could be clearly outlined, in our opinion, due to the features of non-differentiated frontoventral cirri, absence of marginal cirri, body shape, highly developed transverse cirri and the buccal apparatus (Lepsi 1928, Fauré-Fremiet 1954, Curds and Wu 1983, Dragesco and Dragesco-Kernéis 1986). Based on previous descriptions and the present data, we supply here an improved diagnosis for the genus *Gastrocirrhus*.

Diagnosis of the genus *Gastrocirrhus*: marine planktonic Gastrocirrhidae, cells generally cup- or bell-shaped with anterior end truncated; oral field broad and opening anteriorly; adoral zone of membranelles dominant, terminated deeply near cytostome after spiraling around bell-edge in one turn; undulating membrane single-structured; frontoventral cirri arranged in two rows, which are formed by multi-anlagen during morphogenesis; 5 or more transverse well-developed cirri; marginal and caudal cirri absent.

Remarks: as revealed recently, the morphogenesis of this genus is of the pattern of multi-anlagen (non-5-anlagen) considering the origin of the frontoventral cirri (Lei *et al.* 2002), which is thus clearly different from that of most "typical" euplotids (i.e. *Euplotes, Diophrys, Uronychia, Aspidisca*) (Deroux and Tuffrau 1965; Diller 1966; Song and Packroff 1993; Song 1995, 2003). This indicates that *Gastrocirrhus* might represent a "lower" and isolated group among "traditional" hypotrichs (Corliss 1979; Hill 1980, 1981; Curds and Wu 1983; Tuffrau and Fleury 1994; Lynn and Small 2000).

We agree with Curds and Wu (1983) that the genus *Cirrogaster* Ozaki et Yagiu, 1942 should be synonymized with *Gastrocirrhus.*

In 1937, Noland described a new marine form, *Euplotidium agitatum,* using it as the type species, and he established a monotypic genus, *Euplotidium*. Unfortunately, the infraciliature of this species remains hitherto unknown. Based on the living morphology and the arrangement of cirri in original description, nevertheless, it is reasonable to identify it as a member of *Gastrocirrhus*. Hence, we suggest a new combination, *G. agitatus* (Noland, 1937) comb. n. It differs from the "true" *Euplotidium* in the non-differentiated frontoventral cirri and absence of marginal cirri (see also below).

Recently, Lei *et al.* (2002) described a new form under the name of *Euplotidium smalli.* Considering the body shape and ciliary pattern, this species should be clearly assigned - as a new combination - to *Gastrocirrhus*: *G. smalli* (Lei Y., Choi J. K. et Xu K., 2002) comb. n.

Recognized species in the genus *Gastrocirrhus*: totally, 5 morphospecies are involved in this genus: *G. intermedius* Lepsi, 1928; *G. stentoreus* Bullington,

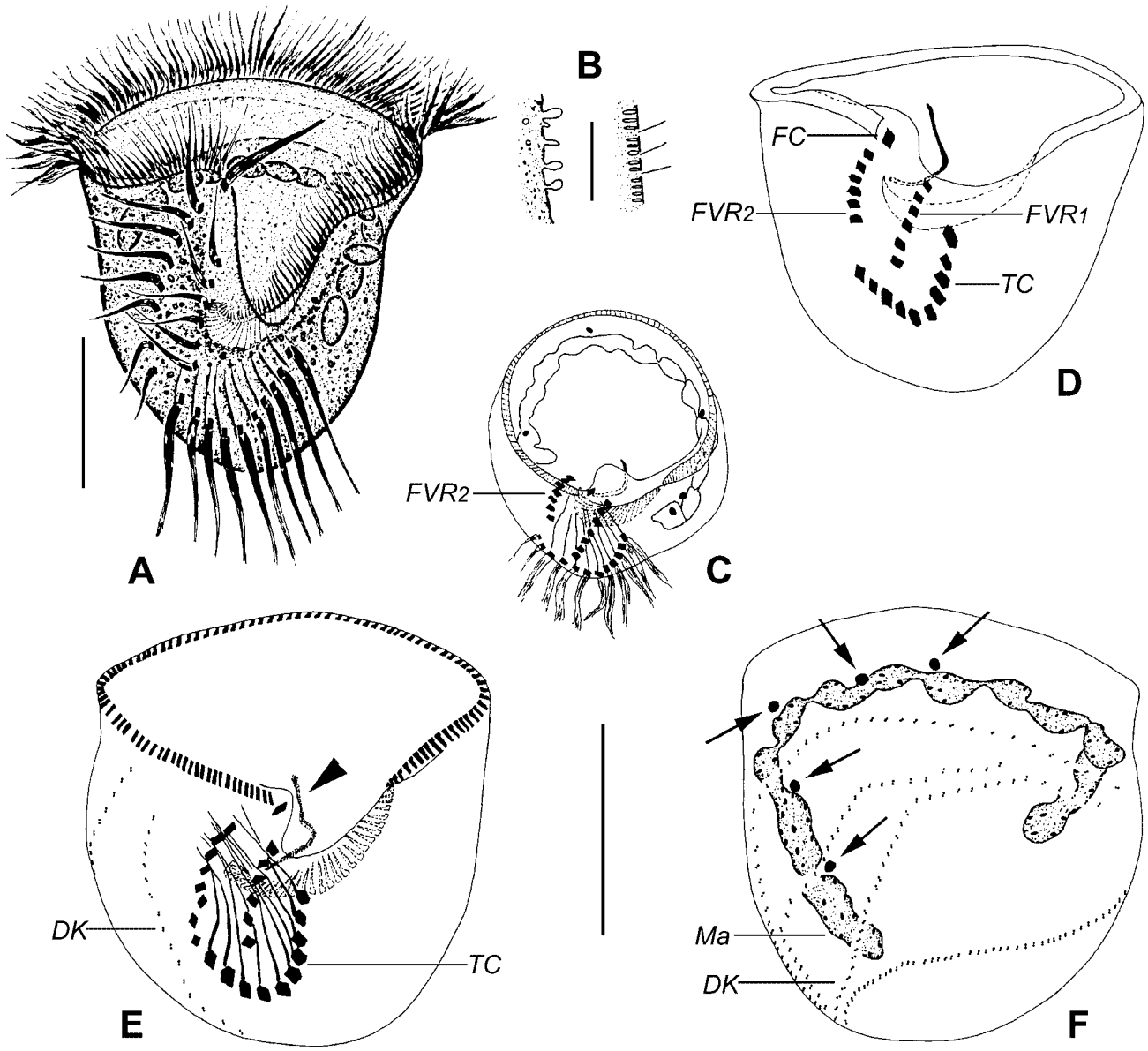

Fig. 1. Morphology of *Gastrocirrhus monilifer* from life (A, B) and after protargol impregnation (C-F). **A** - ventral view *in vivo*; **B** - pellicular structure; **C** - apical view, note infraciliature and nuclear apparatus; **D, E, F**- ventral (D,E) and dorsal (F) views of infraciliature, arrowhead-paroral membrane, arrows-micronuclei. DK - dorsal kineties, $FVR_{1,2}$ - left and right fronto-ventral row, Ma - macronucleus, TC - transverse cirri. Scale bars 50 µm (A, E, F); 10 µm (B).

1940; *G. monilifer* (Ozaki et Yagiu, 1942) Curds et Wu, 1983 [junior synonym: *G. adhaerens* Fauré-Fremiet, 1954; *G. trichocystus* Ito, 1958]; *G. agitatus* (Noland, 1937) comb. n. [basonym: *Euplotidium agitatum* Noland, 1937] and *G. smalli* (Lei Y., Choi J. K. et Xu K., 2002) comb. n. [basonym: *Euplotidum smalli* Lei Y., Choi J. K. et Xu K., 2002].

Redefinition of the genus *Euplotidium* Noland, 1937

Syn. *Paraeuplotidium* Lei, Choi et Xu, 2002

Similar to *Gastrocirrhus*, this genus is also insufficiently described considering its diagnosis and separation and no clear definition has been given though a "typical" *Euplotidium* might be more *Euplotes*-like as noticed by

Table 1. Morphometric data on *Gastrocirrhus monilifer* (first line) and *Gastrocirrhus stentoreus* (second line). All data based on protargol-impregnated specimens. Measurements in µm.

Character	Min	Max	Mean	SD	SE	CV	n
Body, length	80	136	101.4	15.01	3.64	14.8	17
	84	112	97.9	8.93	2.23	9.1	16
Body, width	80	118	93.6	9.78	2.37	10.4	17
	66	82	75.4	5.11	1.28	6.8	16
Adoral zone of membranelles, length	44	80	59.8	11.12	2.70	18.6	17
	50	71	61.4	6.09	1.52	9.9	16
Number of adoral membranelles	105	134	120.2	8.95	2.17	7.4	17
	73	91	83.4	6.18	1.55	7.4	16
Number of frontal cirri	1	1	1	0	0	0	17
	1	1	1	0	0	0	16
Number of cirri in fronto-ventral row (left row) 1	6	8	6.8	0.66	0.16	9.8	17
	5	6	5.1	0.25	0.06	4.9	16
Number of cirri in fronto-ventral row 2* (right row)	6	11	8.8	1.15	0.28	14.8	17
	8	10	8.6	0.62	0.15	8.1	16
Number of transverse cirri	10	10	10	0	0	0	17
	7	8	7.1	0.26	0.07	3.7	15
Number of macronuclear segments	10	14	-	-	-	-	-
	1	1	1	0	0	0	16
Macronucleus length of each segment	12	20	16.6	2.53	0.68	15.3	14
	-	-	-	-	-	-	-
Macronucleus width	5	12	8.5	1.79	0.48	21.0	14
	-	-	-	-	-	-	-
Number of micronuclei	4	9	5.4	1.22	0.30	22.8	17
	2	2	2	0	0	0	16
Micronucleus diameter	2.5	3	-	-	-	-	16
	4	4	4	0	0	0	16
Number of dorsal kineties	5	5	5	0	0	0	12
	5	5	5	0	0	0	16

* Including frontal cirrus

previous authors (Noland 1937, Ito 1958, Magagnini and Bobili 1964, Curds and Wu 1983, Lei *et al.* 2002). As a result deduced from the data obtained, the following diagnostic characters for this taxon can be summarized:

Diagnosis of the genus *Euplotidium*: marine Gastrocirrhidae, body shape cylindrical to dorso-ventrally flattened with buccal apparatus being of *Euplotes*-pattern; about 10 frontoventral cirri sparsely distributed; *ca* 5 transverse and one or more left marginal cirri; no caudal cirri.

Remarks: this genus was established by Noland (1937) with a monotype *Euplotidium agitatum.* Afterward several nominal species were added to this genus, which share, with the exception of the type species *E. agitatum* (see above), the same ciliary pattern (Ito 1958, Vacelet 1961, Magagnini and Bobili 1964, Hartwig 1980). According to the new definition, this taxon differs from the similar genus *Gastrocirrhus* in the presence of left marginal cirri and the fronto-ventral cirri being (basically) distributed in a sparse pattern (*vs.* in two-rowed pattern in the latter) (the pattern in *E. itoi* might be very likely misinterpreted). In addition, though morphogenetic data is still lacking, the frontoventral cirri of this genus possibly develop from 5-anlagen during divisional process, i.e. like most typical euplotids.

Lei *et al.* (2002) established a new genus, *Paraeuplotidium* to involve formerly *Euplotidium*-forms, which have single left marginal cirrus and (seemingly) sparsely distributed frontoventral cirri. We disagree with this arrangement because the genus *Euplotidium* is well known for a long time with several relatively clearly outlined morphotypes. Hence, we suggest a redefinition for this genus for the sake of stability and treat *Paraeuplotidium* as a junior synonym.

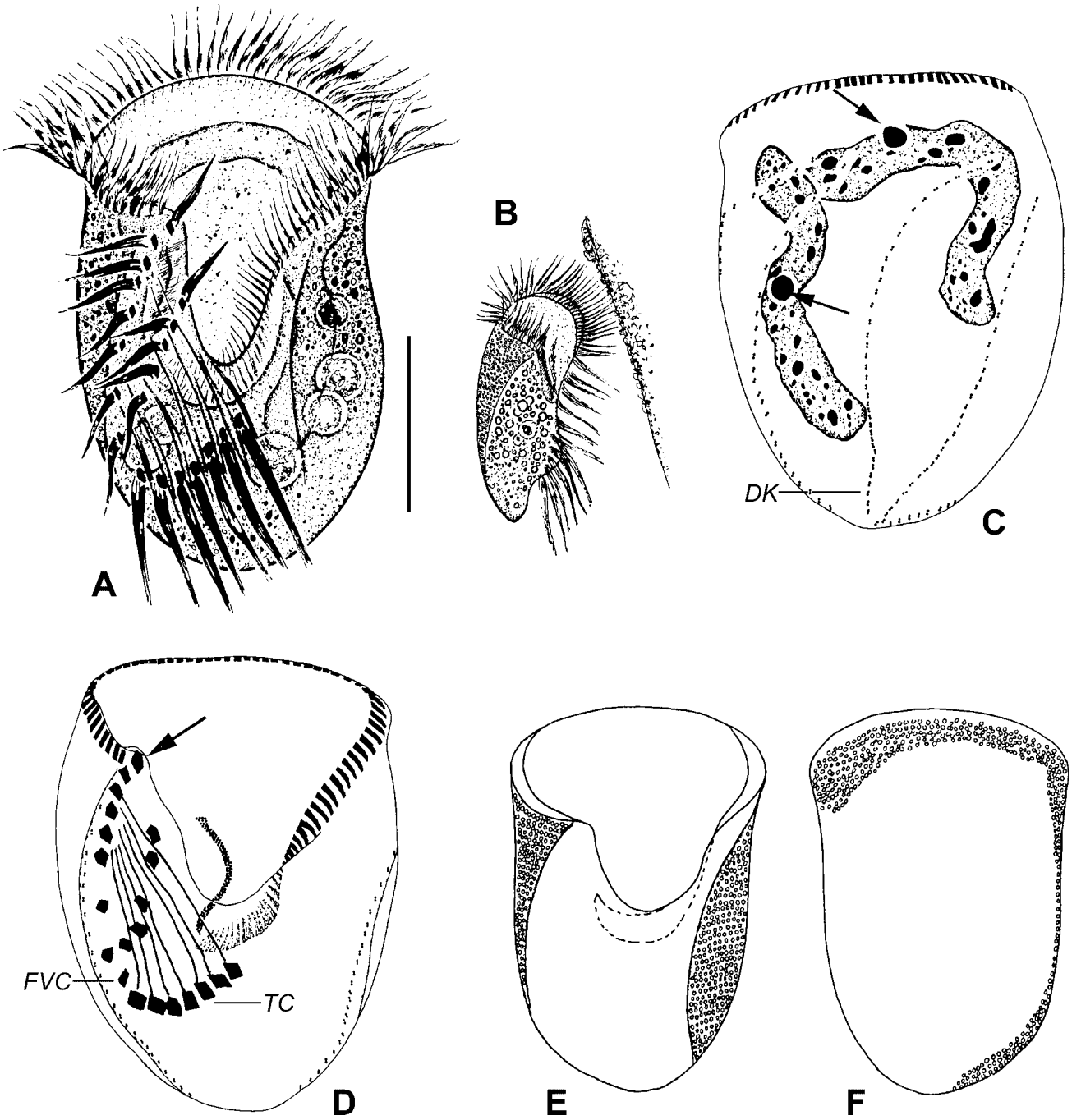

Fig. 2. Morphology of *Gastrocirrhus stentoreus* from life (A, B, E, F) and after protargol impregnation (C, D). **A** - ventral view *in vivo*; **B** - individual attaching to substrate when feeding; **C, D** - ventral and dorsal views of infraciliature, arrows in C - micronuclei, arrow in D - frontal cirrus; **E, F** - ventral and dorsal views, note the arrangement of trichocysts. DK - dorsal kineties, FVC - fronto-ventral cirri, TC - transverse cirri. Scale bar 40 μm.

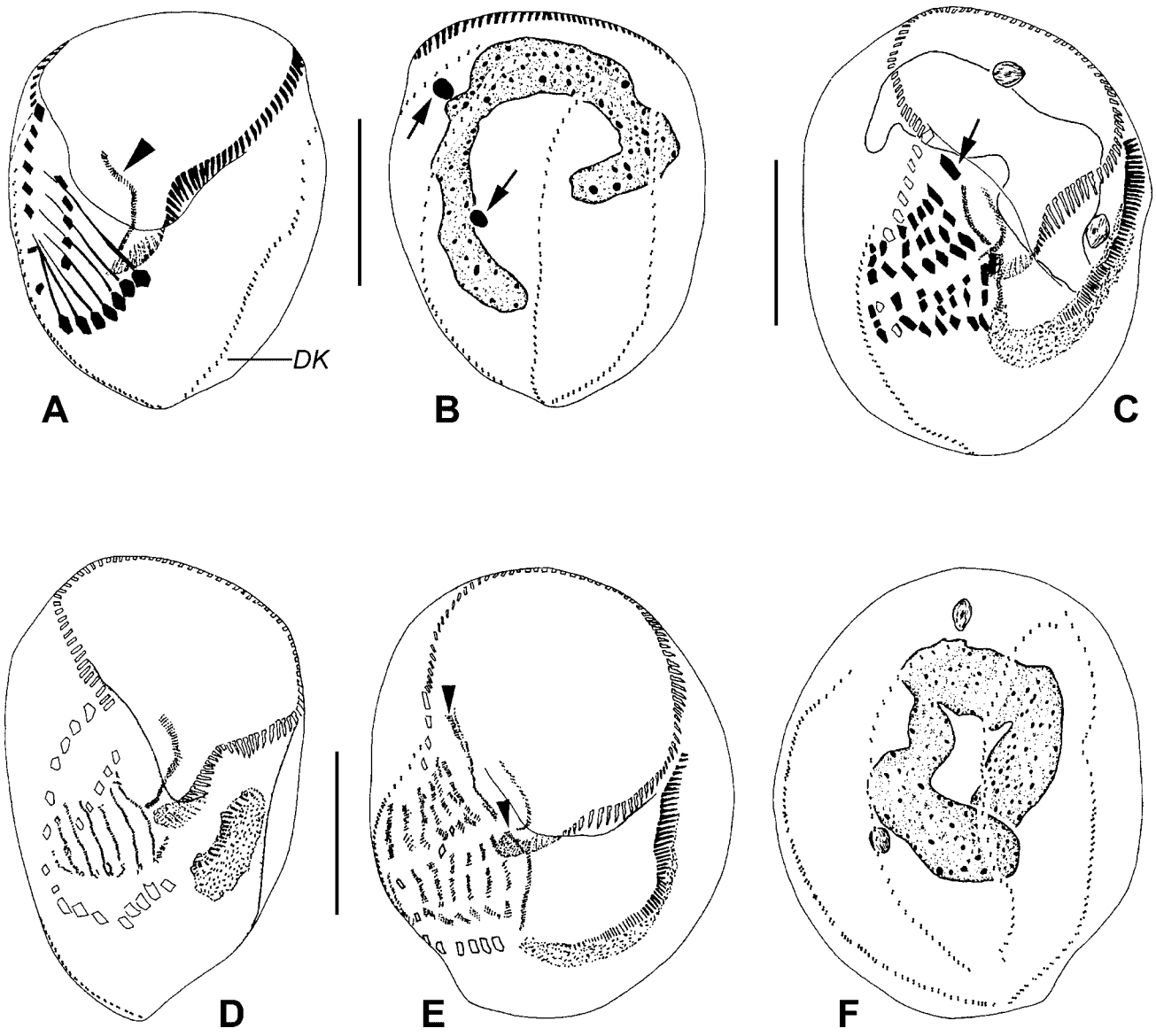

Fig. 3. Infraciliature (A, B) and morphogenesis (C-F) of *Gastrocirrrhus stentoreus* after protargol impregnation. **A, B** - ventral and dorsal views of infraciliature, arrowhead-paroral membrane, arrows-micronuclei; **C** - ventral view, note the formation of the new cirri and the development of the oral primordia, arrow-frontal cirrus; **D** - ventral view, the appearance of the oral primordia and the cirral anlagen; **E, F**- ventral and dorsal, arrowheads-the anlage for frontal cirrus. DK - dorsal kineties. Scale bars 40 μm.

Since the original type species, *Euplotidium agitatum* Noland, 1937 is transferred into the genus *Gastrocirrhus* (see above), according to ICZN (1999), article 70.3, a new type species is fixed:

Type species: *Euplotidium itoi* Ito, 1958

Recognized species in the genus *Euplotidium*: Based on the new understanding, this genus presently comprises the following five species: *E. itoi* Ito, 1958; *E. psammophilius* (Vacelet, 1961) Borror, 1972 [basonym: *Euplotes psammophilius* Vacelet, 1961]; *E. arenarium* Magagnini et Nobili, 1964; *E. helgae* Hartwig, 1980 and *E. prosaltans* Tuffrau, 1985.

Redescription of two known *Gastrocirrhus* species

Both species described below are known for a long time but no data concerning their infraciliature is avail-

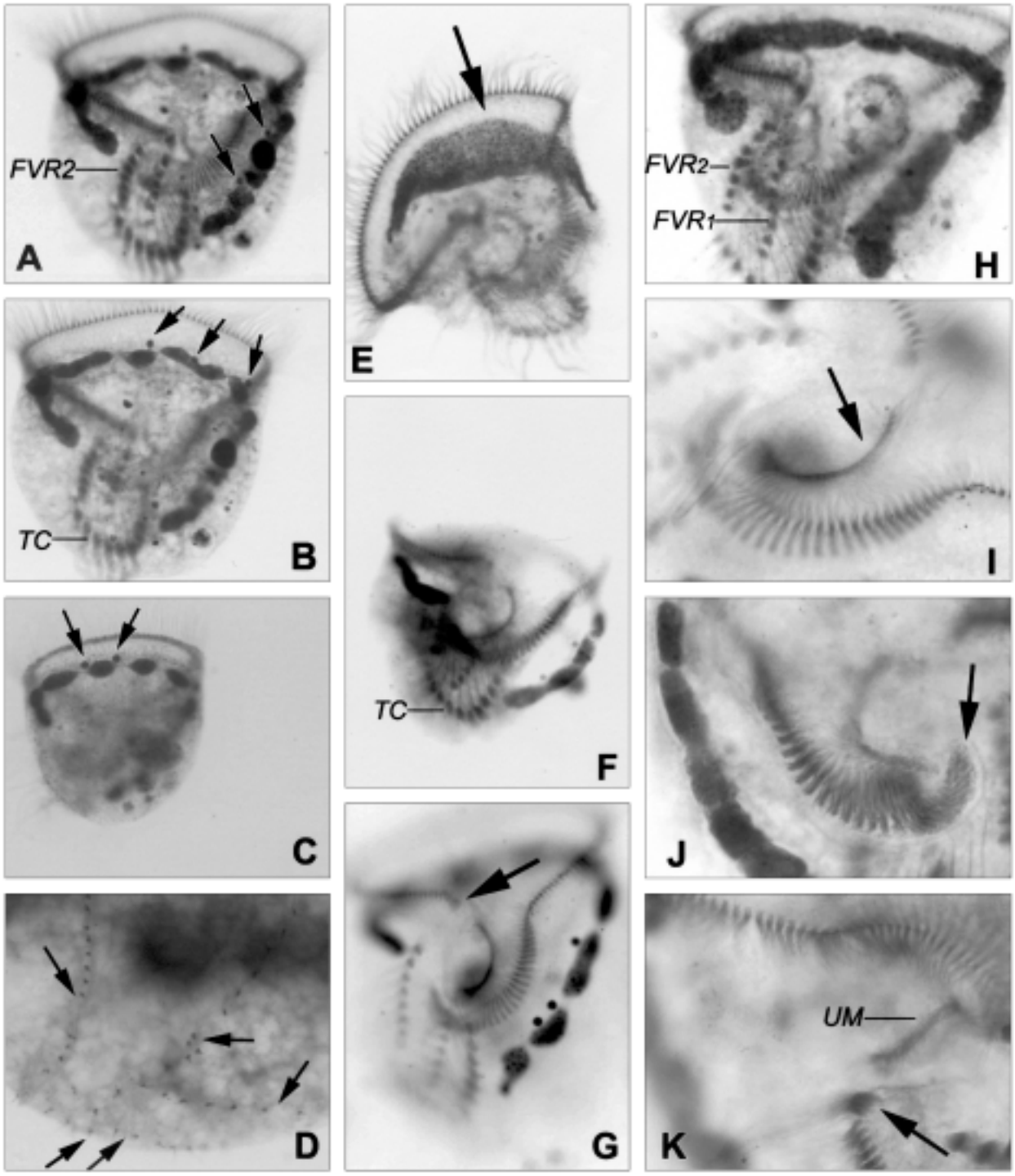

Fig. 4. Photomicrographs of morphology of *Gastrocirrhus monilifer* after protargol impregnation. **A, B, F-H, K** - ventral views of infraciliature, arrows in A, B - micronuclei, arrow in G, K - frontal cirrus; **C** - dorsal view, arrows - micronuclei; **D** - dorsal view, arrows - dorsal kineties; **E** - ventral view, arrow to show macronucleus just after division; **I** - ventral view, arrow to show undulating membrane; **J** - arrow - curvation at the posterior end of adoral zone of membranelles. $FVR_{1,2}$ - left and right fronto-ventral rows, TC - transverse cirri, UM - undulating membrane.

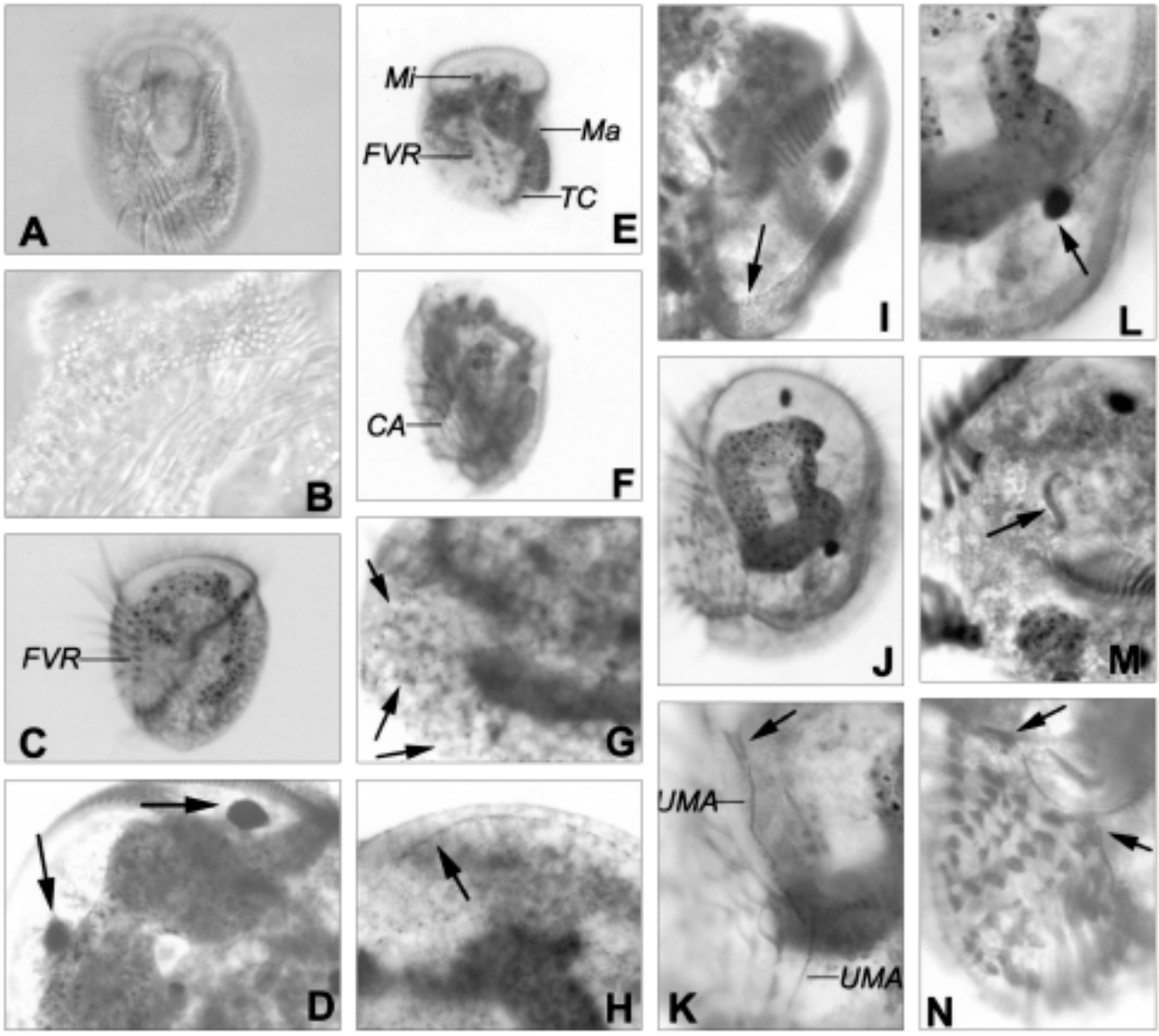

Fig. 5. Photomicrographs of morphology and morphogenesis of *Gastrocirrrhus stentoreus* from life (A, B) and after protargol impregnation (C-N). **A** - ventral view *in vivo*; **B** - trichocysts; **C, E** - infraciliature on ventral side; **D, L** - arrows-micronuclei; **F, J** - ventral view, note infraciliature in morphogenesis; **G** - dorsal view, arrows-dorsal kineties; **H** - arrow-dorsal kineties anlage; **I** - arrow-oral primordium in the opisthe; **K** - arrow-anlage for frontal cirrus; **M** - arrow-undulating membrane; **N** - ventral view, note the development of cirral anlagen, arrow -new frontal cirrus. CA - cirral anlagen, FVR - fronto-ventral rows, Ma - macronucleus, Mi - micronucleus, TC - transverse cirri, UMA - undulation membrane anlage.

able, hence their identification remains questionary. Based on the Qingdao populations we isolated recently, detailed redescriptions on both living morphology and infraciliature are supplied here.

***Gastrocirrhus monilifer* (Ozaki et Yagiu, 1942) (Figs 1, 4; Table 1)**

Syn. *Cirrhogaster monilifer* Ozaki et Yagiu, 1942
Gastrocirrhus adhaerens Fauré-Fremiet, 1954
Gastrocirrhus trichocystus Ito, 1958

This species was originally reported by Ozaki et Yagiu (1942) as *Cirrhogaster monilifer*. Thereafter no redescription was made on it until Curds et Wu (1983) in their revision paper transferred it to the genus *Gastrocirrhus* though the data about infraciliature on dorsal side are still lacking (Dragesco and Dragesco- Kernéis 1986; under the name of *Cirrhogaster adhaerens* Fauré-Fremiet, 1954). With reference to the living morphology (e.g. body size, shape, locomotion, and the general arrangement of the cirri), the Qingdao population corresponds

Table 2. Morphological comparison among the known *Gastrocirrhus*-species.

Species name	body length in µm	FVC, number*	TC, number	Ma, shape	MS, number	Reference
Gastrocirrhus intermedius	68	9	7	oval	1	Lepsi 1928
Gastrocirrhus monilifer Called *Cirrhogaster monilifer*	95-105	10	12	moniliform	11-15	Ozaki and Yagiu 1942
Gastrocirrhus monilifer Called *G. adhaerens*	100	16	12	moniliform	*ca* 12	Fauré-Fremiet 1954
Gastrocirrhus monilifer	95-103	18	13	moniliform	10-12	Ito 1958
Gastrocirrhus monilifer Called *Cirrhogaster adhaerens*	*ca* 100	16	12	bead-like	-	Dragesco and Dragesco-Kernéis 1986
Gastrocirrhus stentoreus	104	11	5	-	-	Bullington 1940
Gastrocirrhus smalli comb. n. Called *Euplotidium smalli*	100-140	13-14	7	C-shaped	2	Lei *et al.* 2002
Gastrocirrhus monilifer	100-140	12-19	10	moniliform	10-14	this study
Gastrocirrhus stentoreus	80-130	*ca* 13	7-8	ribbon-like	1	this study

* Including frontal cirrus; - No data available
FVC - fronto-ventral cirri; Ma - macronucleus; MS - macronuclear segments; TC - transverse cirri.

well with populations reported previously. Hence, the identification is rather certain.

Based on this study, a new diagnosis for this species is supplied here:

Diagnosis for *Gastrocirrhus monilifer*: *in vivo* about 100-140 µm long; macronucleus beaded with about 10-14 segments and 4-9 micronuclei; *ca* 120 membranelles; 6-8 frontoventral cirri in left row and 6-11 in right one; 10 transverse cirri; 5 dorsal kineties.

Morphology and infraciliature: body inverted-bell-shaped, *in vivo ca* 100-140 µm long. Oral field broad, opening anteriorly and concaved at middle-posterior portion, funnel-like (Fig. 1A). A well-developed adoral zone of membranelles (AZM) borders the C-shaped anterior body edge and winds clockwise down the left of the peristome, cilia of membranelles about 25 µm long; two oblique frontoventral rows, located to right of peristome (Figs 1C, D; 4A), of which frontal cirrus is rather thick, about 35 µm long and distributed anterior-most and near the distal end of AZM (FC - Figs1A, D; 4G, K, arrow). Transverse cirri situated along the posterior border, arranged in U-shaped (Figs 1D, E; 4B, F). Several ridges evidently occur between transverse cirri. Dorsal cilia about 4 µm long. Pellicle thin, sensitive to disturbance; cortical granules oval, *ca* 2 µm long, located vertical to pellicle (Fig. 1B). Endoplasm contains numerous granular inclusions, which render body dark at low magnification. Macronucleus moniliform, consisting of 10-14 pieces; 4-9 spherical micronuclei located adjacent to macronucleus (Figs 1C, F, arrows; 4A-C, arrows).

Locomotion by crawling on substrate or on bottom of Petri dish for most of the time, occasionally by jumping or swimming quickly for a short while.

Infraciliature as shown in Figs 1D-F and 4A-K. AZM composed of 105-134 membranelles; undulating membrane (UM) as a single structure, which is composed of rows of kinetosomes with 2-4 basal bodies each (Figs 1E, arrowhead; 4I, arrow, K). Eleven to eighteen frontoventral cirri in two rows (6-8 in left and 6-11 in right row); consistently 10 transverse cirri (n=17). Five dorsal kineties spiraled and converged at posterior end, of which the leftmost one is evidently longer than the others, with its anterior part transversely arranged, and the basal bodies in the fourth kinety (counted from left to right) are more densely packed (Figs 1E, F; 4D, arrows).

Comparison and discussion: this species can be clearly separated from its congeners by the following combined characters: the number of membranelles and the somatic cirri, as well as the presence of beaded macronucleus (Table 2).

Gastrocirrhus trichocystus Ito, 1958 is very possibly a junior synonym of *G. monilifer,* though the number of frontoventral cirri, as depicted in original report (Ito 1958) is higher than that in the latter. We consider them conspecific because this character is variable as well among individuals of our samples and we believe that this is a population-dependent feature.

In 1954, Fauré-Fremiet described a new species, *Gastrocirrhus adhaerens* without noticing the work by

Ozaki et Yagiu (1942), of which the infraciliature was (partly) studied by Dragesco and Dragesco-Kernéis (1986). Due to the great similarity to *G. monilifer*, in all aspects, i.e. the body size/shape, basic pattern of the ciliary organelles and the nuclear apparatus, both forms should be considered being conspecific (Dragesco, 1965). Hence, *Gastrocirrhus adhaerens* is synonymized with the former.

Gastrocirrhus stentoreus Bullington, 1940 (Figs 2, 3, 5; Table 1)

Since Bullington reported this species from Tortugas with no information about either the ciliature or the nuclear apparatus (Bullington 1940), no further studies have been carried out and hence its definition remains unclear. We identified our Qingdao-population basically because, compared with the original descriptions, our form possesses extremely similar size, body shape, general living appearances, as well as the number of frontoventral and transverse cirri. Based on the Qingdao population, we give here an improved diagnosis for this poorly studied species:

Diagnosis for *Gastrocirrhus stentoreus*: *in vivo* about 80-130 μm in length with long and ribbon-like macronucleus, 2 micronuclei; *ca* 80 membranelles; 5-6 frontoventral cirri in left fronto-ventral row and 8-10 in right one; 7-8 transverse cirri; 5 dorsal kineties.

Morphology and infraciliature: Cell likes the species described above, cup-shaped, *in vivo ca* 80-130 μm long (Figs 2A, 5A). A well developed adoral zone of membranelles (AZM) borders anterior cell edge and winds clockwise down the left of the peristome, cilia of membranelles about 25 μm long; two oblique frontoventral rows, located right to peristome (Figs 2D; 3A; 5C, E), of which frontal cirrus (FC - Fig. 2D, arrow) is evidently thick and distributed anterior-most, near the distal end of AZM, about 35 μm long. Transverse cirri situated posterior to cytostome, arranged in J-shape; and several ridges occur between transverse cirri. Dorsal kineties densely ciliated, cilia about 4 μm long. Trichocysts arranged in patches (Figs 2E, F; 5B). Endoplasm colorless to grayish, containing numerous granular inclusions and several large food vacuoles, which render cell opaque. Macronucleus ribbon-like, constantly two micronuclei attached to macronucleus (Figs 2C; 3B, arrows; 5D, L, arrows).

Movement modestly fast, by crawling on substrate or jumping back and forth; sometimes recognized with adoral membranelles sticking to substrate or surface of other substance when feeding (Fig. 2B).

Infraciliature as shown in Figs 2C, D; 3A-F and 5C-N: AZM composed of 73-91 membranelles; undulating membrane like in *Gastrocirrhus monilifer*, composed of rows of kinetosomes (Figs 3A, arrowhead; 5M, arrow). On average 5 cirri in left and 9 in right frontoventral row, in which the posterior 2-3 cirri of the right row are always far away from the others; 7-8 transverse cirri. Consistently 5 dorsal kineties aligned spirally and converged at posterior extremity (Figs 3A, B; 5G, arrows).

Several morphogenetic stages have been observed, which indicate the following features (Figs 3C-F; 5F, H-L, N): (1) Oral primordium appears on the surface of the cortex posterior to cytostome in the opisthe, which then develops into new membranelles posteriad and finally makes new adoral zone of membranelles (Figs 3C, D; 5I, arrow); (2) Fronto-ventral transverse cirral anlagen in both dividers are derived from the breaking of 7 streaks of primary primordia, which occur as a ladder-like structure in the middle part of the cell (Fig. 3D). Each anlage subsequently fragments and evolves into new cirri (Figs 3C, E); (3) The old AZM is possibly inherited by the proter; (4) The undulating membrane comes from the newly-formed anlage in both dividers, from which single frontal cirrus is also derived at the anterior end (Figs 3C, E, arrow and arrowheads; 5K, N, arrows); (5) The renewal of dorsal kineties occurs within the old structures (Fig. 5H, arrow).

Comparison and discussion: in terms of the body size, shape, the number of transverse cirri and dorsal kineties, *Gastrocirrhus stentoreus* is very similar to *G. smalli* (Lei Y., Choi J. K. et Xu K., 2002). However, both organisms can be separated by the feature of the macronuclear apparatus (single and ribbon-like in *G. stentoreus vs.* two segments in the latter) (Lei *et al.* 2002).

Different from other nominal congeners, *Gastrocirrhus stentoreus* can be recognized by combined features of number of frontoventral and transverse cirri and the number of macronuclear segments (Table 2) (Ozaki and Yagiu 1942, Fauré-Fremiet 1954, Curds and Wu 1983, Lei *et al.* 2002).

Acknowledgements. This work was supported by the "Natural Science Foundation of China" (project number: 30170114) awarded to WS, and by "JSPS Postdoctoral Fellowship for Foreign Researcher" awarded to XH. Many thanks are also due to Dr. Toshikazu Suzuki, Faculty of Fisheries, Nagasaki University, Japan for technical support during the preparation of this manuscript.

REFERENCES

Borror A. (1972) Revision of the order Hypotrichida (Ciliophora, Protozoa). *J. Protozool.* **19:** 1-23

Borror A. C., Hill B. F. (1995) The order Euplotida (Ciliophora): taxonomy, with division of *Euplotes* into several genera. *J. Euk. Microbiol.* **42:** 457-466

Bullington W. E. (1940) Some ciliates from Tortugas. *Pap. Tortugas Lab.* **32:** 179-222

Corliss J. O. (1979) The Ciliated Protozoa: Characterization, Classification and Guide to the Literature. 2nd ed. Pergamon Press, Oxford

Curds C. R., Wu C. H. (1983) A review of the Euplotidae (Hypotrichida, Ciliophora). *Bull. Bri. Mus. nat. Hist. (Zool.)* **44:** 191-247

Deroux G., Tuffrau M. (1965) *Aspidisca orthopogon* n. sp. Révision de certains mécanismes de la morphogenèse a l'aide d'une modification de la technique au protargol. *Cah. Biol. Mar.* **6:** 293-310

Diller W. F. (1966) Correlation of ciliary and nuclear development in the life cycle of *Euplotes*. *J. Protozool.* **13:** 43-54.

Dragesco J. (1965) Compléments à la connaissance de *Swedmarkia arenicola* et *Discocephalus ehrenbergi* ciliés hypotriches. *Ann. biol.* **4:** 187-204

Dragesco J., Dragesco-Kernéis A. (1986) Ciliés libres de l'Afrique intertropicale. *Faune Tropicale* **26:** 1-559

Fauré-Fremiet E. (1954) *Gastrocirrhus adhaerens* n. sp. *An. Acad. Bras. Cienc.* **26:** 163-168

Hartwig E. (1980) The interstitial ciliates of Bermuda with notes on their geographical distribution and habitat. *Cah. Biol. mar.* **21:** 409-441

Hill B. F. (1980) Classification phylogeny in the suborder Euplotina (Ciliophora, Hypotrichida). Ph. D. Diss., University of New Hampshire, Durham

Hill B. F. (1981) *Uronychia transfuga* (O. F. Müller, 1786) Stein, 1859 (Ciliophora, Hypotrichia, Uronychiidae): cortical structure and morphogenesis during division. *J. Protozool.* **37:** 99-107

Ito S. (1958) Two new species of marine ciliates *Euplotidium itoi* sp. nov. and *Gastrocirrhus trichocystus* sp. nov. *Zool. Mag. Tokyo* **67:** 184-187

ICZN (The International Commission on Zoological Nomenclature) (1999) International Code of Zoological Nomenclature. 4th ed. Tipografia la Garangola, Padova

Kahl A. (1932) Urtiere oder Protozoa. I: Wimpertiere oder Ciliata (Infusoria), 3. Spirotricha. *Tierwelt Dtl.* **25:** 399-650

Lei Y., Choi J. K., Xu K. (2002) Morphology and infraciliature of a new marine ciliate *Euplotidium smalli* n. sp. with description of a new genus *Paraeuplotidium* n. g. (Ciliophora, Euplotida). *J. Eukar. Microbiol.* **49:** 402-406

Lepsi J. (1928) Un nouveau protozoaire marin; *Gastrocirrhus intermedius*. *Annls Protist.* **1:** 195-197

Lynn D. H., Small E. B. (2000) Phylum Ciliophora Doflein, 1901. In: The Illustrated Guide to the Protozoa, (Eds. J. J. Lee, G. F. Leedale and P. Bradbury), 2nd ed, 371-656. Society of Protozoologists, Lawrence, Kansas

Magagnini G., Nobili R. (1964) Su *Euplotes woodruffi* Gaw e su *Euplotidium arenarium* n. sp. (Ciliatea Hypotrichida). *Monit. Zool. Ital.* **72:** 128-202

Noland L. E. (1937) Observations on marine ciliates of the gulf coast of Florida. *Trans. Am. Microsc. Soc.* **56:** 160-171

Ozaki Y., Yagiu R. (1942) A new marine ciliate *Cirrhogaster monilifer* n. g. n. sp. *Ann. Zool. Jap.* **21:** 79-81

Song W. (1995) Morphogenetic studies on *Uronychia uncinata* (Protozoa, Ciliophora) during its asexual division. *Acta Oceanol. Sin.* **15:** 93-99

Song W. (2003) Reconsideration of the morphogenesis in the marine hypotrichous ciliate, *Aspidisca leptaspis* Fresenius, 1865 (Protozoa, Ciliophora). *Europ. J. Protistol.* **39:** 53-62

Song W., Packroff G. (1993) Beitrag zur Morphogenese des marinen Ciliaten *Diophrys scutum* (Dujardin, 1841). *Zool. Jb. Anat.* **123:** 85-95

Tuffrau M. (1985) Une nouvelle espèce du genre *Euplotidium* Noland 1937: *Euplotidium prosaltans* n. sp. (Cilié hypotriche). *Cah. Biol. mar.* **26:** 53-62

Tuffrau M., Fleury A. (1994) Classe des Hypotrichea Stein, 1859. *Traité de Zoologie* **2(2):** 83-151

Vacelet E. (1961) La faune infusorienne des «Sables à Amphioxus» des environs de Marseille. *Bull. Inst. Oceanogr. Monaco* **3:**1-12

Wilbert N. (1975) Eine verbesserte Technik der Protargolimprägnation für Ciliaten. *Mikrokosmos* **64:** 171-179

Received on 2nd February, 2003; revised version on 25th June, 2003; accepted on 9th July, 2003

Acta Protozool. (2003) 42: 357 - 360

ACTA
PROTOZOOLOGICA

Short Communication

Strains of *Paramecium quadecaurelia* from Namibia, Africa; Genetic and Molecular Studies

Ewa PRZYBOŚ[1], Manabu HORI[2] and Sergei I. FOKIN[3]

[1]Institute of Systematics and Evolution of Animals, Polish Academy of Sciences, Kraków, Poland; [2]Biological Institute, Yamaguchi University, Yoshida, Japan; [3]Biological Institute of St. Petersburg State University, Old Peterhof, Russia

Summary. New strains of *Paramecium quadecaurelia* were found in Namibia, Africa. Previously, this species from the *P. aurelia* complex was known only from Australia, Emily Gap. Namibian strains were identified by mating reaction; their relationship with the Australian strain was studied by classical strain crosses (survival in F1 and F2 generations) and by comparison of cytosol-type *hsp70* gene sequences. Phylogenetic trees of the Namibian and Australian strains of *P. quadecaurelia* and the other species of the *P. aurelia* complex were generated based on the maximum-likelihood method.

Key words: breeding system, genetic relationships, geographical distribution, *hsp70* gene sequences, *Paramecium, Paramecium aurelia* species complex, phylogenetic tree of the *P. aurelia* spp. complex.

INTRODUCTION

Among 15 known species of the *Paramecium aurelia* complex (14th characterized by Sonneborn, 1975 and 15th - *P. sonneborni* by Aufderheide *et al*. 1983), *P. quadecaurelia* was presented as a species, which "has been found only once, at Emily Gap, Australia" (Sonneborn 1975). The mentioned strain, designated 328 is a reference (standard) strain of the species. *P. quadecaurelia* according Sonneborn (1975) "is characterized by its inability to react or conjugate with any other species". Mating type inheritance is by the caryonidal system. The species is distinguished from the other *P. aurelia* spp. complex electrophoretically examined by two cathodal bands and no anodal bands for esterase C (Allen *et al.* 1973). The species belongs to the group of the largest ones in the *P. aurelia* complex: length of the cells reaches 175 μm.

The paper presents new strains of the species, found in Africa in Namibia.

Address for correspondence: Ewa Przyboś, Institute of Systematics and Evolution of Animals, Polish Academy of Sciences, Sławkowska 17, 31-016 Kraków, Poland; Fax: (048 12) 422 42 94; E-mail: przybos@isez.pan.krakow.pl

MATERIALS AND METHODS

Strains. The strains were established from the water sample collected by Dr S. Dobretzov in 2001 in Vindhoek, capital of Namibia, from pond in a park.

The strains were designated AN1-1, AN1-2, AN1-3, and AN1-6. The strain AN1-2 was identified as *Paramecium multimicronucleatum*,

the others as species of the *P. aurelia* complex, by the type and number of micronuclei (Vivier 1974). The preparations were stained by acetocarmine (Sonneborn 1970) and by Giemsa's stain and Feulgen reaction (after fixation and hydrolysis, Przyboś 1978).

Strain cultivation and identification by mating reaction. Cultivation and identification of the established strains of the *Paramecium aurelia* spp. were carried out according to Sonneborn (1950, 1970). The species was identified by mating the investigated strains with the mating types of the standard strains of known species of the *P. aurelia* complex. The following standard strains were used: strain 90 of *P. primaurelia*; the Rieff strain, Scotland, of *P. biaurelia*; strain 324 of *P. triaurelia*; strain 159 of *P. sexaurelia*; strain 325 of *P. septaurelia*; strain 138 of *P. octaurelia*; strain 510 of *P. novaurelia*; strain 223 of *P. decaurelia*; strain 219 of *P. undecaurelia*; strains 321 and 209 of *P. tredecaurelia*, and strain 328 of *P. quadecaurelia*.

The paramecia were cultivated on a lettuce medium inoculated with *Enterobacter aerogenes* (Sonneborn 1970).

Strain crosses. In the intra- and inter-strain crosses, F1 generation was received by conjugation and F2 by autogamy (by the method of daily isolation lines). The occurrence of the desired stage of autogamy (specimens in the stage of two macronuclear anlagen) was examined on preparations stained with acetocarmine. Survival of 100 clones in both generations was estimated after 72 h after separation of partners of conjugation or postautogamous caryonids (cf Chen 1956).

The percentage of surviving hybrid clones in the inter-strain crosses (Namibian strains x Australian strain) was compared. Methods were described in details by Przyboś (1975).

Cell cultivation in molecular studies. *Paramecium* strains were in cultivated in 1.25% (w/v) lettuce juice in modified Dryl' s solution (Dryl 1959), in which KH_2PO_4 was replaced with $NaH_2PO_4 \cdot 2H_2O$, and inoculated with a nonpathogenic strain of *Klebsiella pneumoniae* at 25°C, as described previously (Fujishima *et al*. 1990).

Strains used in molecular studies: strain HV15-1 of *P. primaurelia*, strain 51 of *P. tetraurelia*, strain 87 of *P. pentaurelia*, strain 91 YB 1-3 of *P. novaurelia*, strain 321 of *P. tredecaurelia*, strain G3 from Japan of *P. caudatum*.

Amplification of the cytosol-type *hsp70* gene and sequencing. Cells of each strain in stationary phase were washed with modified Dryl' s solution. Ten to twenty cells were used as a template after boiling for 10 min at 95°C. The amplification protocol consisted of denaturation at 94°C for 2 min, followed by 30 cycles of denaturation at 94°C for 45 s, annealing at 50°C for 60 s, and extension at 72°C for 60 s, with final extension at 72°C for 5 min. To isolate the cytosol-type *hsp70* gene, we utilized the specific nucleotide primers, 5-GAGGAGAAGATTTCGATAAC-3 (sense, corresponding to the amino acid sequence GEDFDN) and 5-GCTTCATCTGGGTTGATTGA-3 (antisense, corresponding to the amino acid sequence SINPDE), which yielded a PCR product of 416 bp.

PCR products were cloned into the T/A plasmid vector pGEM-T easy (Promega Biotech). Plasmids were purified with Wizard Plus SV Minipreps DNA Purification system (Promega Biotech). Genomic clones were sequenced on both strands with the dideoxy termination methods using a Thermo Sequenase Cycle Sequencing Kit (Amersham Pharmacia Biotech Inc). The resulting nucleotide sequences were analyzed with the GENETYX-SV/RC 9.0 program (Genetyx Corp.).

Phylogenetic analysis. The *hsp70* sequences determined in this study were aligned by the GENETYX-SV/RC 9.0 program. Phylogenetic trees were generated using the nucML of molphy program package version 2.3 based on the maximum-likelihood method (Felsenstein 1981, Adachi *et al*. 1996).

To investigate the relationships within the *P. aurelia* spp. complex and other *Paramecium* species, we used cytosol type *hsp70* sequences of *Paramecium caudatum* (AB048692), *P. primaurelia* (AB100846), *P. tetraurelia* (AB100847), *P. pentaurelia* (AB100848), *P. novaurelia* (AB100851), *P. tredecaurelia* (AB100852) and *P. quadecaurelia* (AB106336).

RESULTS AND DISCUSSION

The strains AN1-1, AN1-3, and AN1-6, three clones in each strain, were identified as *P. quadecaurelia* by mating reaction with the reference specimens of the strain 328 from Australia and by checking vitality of the inter-strain hybrid clones in F1 and F2.

A very strong conjugation (95 - 100% of conjugating pairs) was observed after mixing the complementary mating types of the studied strains and the appropriate standard ones.

Conjugation appeared within the strains from Namibia and within the strain from Australia on 6th and 7th days of culturing clones in 24°C.

Autogamy was observed in the Namibian strains, the Australian strain, and inter-strain hybrids after 15 - 18 fissions (the growth rate of cultures was 3 fissions per day) in the daily isolation lines cultivated at 24°C (5 to 6 days).

A high viability was observed in both generations in inter-strain crosses (Table 1). The results of crosses between strain from Australia and strains from Africa of *Paramecium quadecaurelia* show that in those species exists a type of breeding system, which can be called moderate inbreeding. This means inbreeding with high fertility in crosses of geographically distant populations. There is probability of gene flow among populations, which are not genetically isolated.

The investigations carried out on *P. triaurelia* and *P. sexaurelia* (Stoeck *et al*. 1998) and later on *P. pentaurelia* and *P. novaurelia* (Stoeck *et al*. 2000) in which combination of classical strain crosses and molecular technique (RAPD-PCR) was used, showed that those species differ in their degree of inbreeding. The species of the *P. aurelia* can be arranged in some order as far as degree of inbreeding is concerned, from

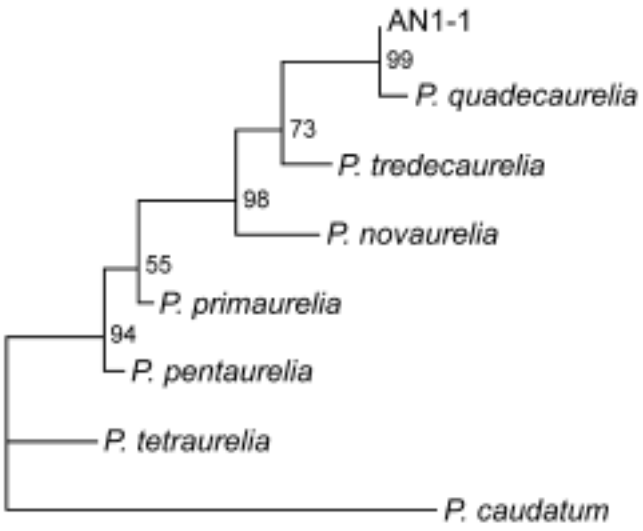

Fig. 1. Phylogeny of the *Paramecium aurelia* spp. complex, based on the comparison of cytosol type hsp70 sequences. Bootstrap probabilities are given as percentages near the individual nodes.

extreme inbreeders (*P. tetraurelia*, *P. sexaurelia* and to some extent *P. primaurelia*), moderate inbreeders (*P. novaurelia*, *P. triaurelia*), and at the other end, weak inbreeders (*P. pentaurelia*). It is based on the mentioned studies (Stoeck *et al*. 1998, 2000).

Inbreeding which is generally characterising for species of the *P. aurelia* complex (Landis 1986) is leading to a molecular differentiation of local populations showed by karyological, antigenic (cf Przyboś 1986) and molecular studies (Stoeck *et al*. 1998, 2000). Strains, however, maintain a similar morphology and possibility to cross and produce lively offspring.

It is interesting to mention that the electrokaryotype of the strain AN1-6 (Potekhin *et al*. 2002), obtained by pulsed-field gel electrophoresis (PFGE) of macronuclear DNA, differed from PFGE profiles characteristic for the previously studied strains of the *P. aurelia* complex (Rautian and Potekhin 2002). The dominant high molecular weight band (2000kb) and specific banding of the molecular spectrum were the special features for the strain AN1-6 (Potekhin *et al*. 2002), identified presently as *P. quadecaurelia*.

The strain AN1-1, AN1-3 and AN1-6 have the same base sequence for the cytosol type *hsp70* gene. The Genbank accession number for An1-1 is AB106337; AN1-3 and An1-6 have not been registered because their sequences are the same. The base sequence of these strains was 99.2% identical to the cytosol type *hsp70* gene of the Australian (328) strain of *P. quadecaurelia* (AB106336). The sequences of the

Table 1. Percentage of surviving clones in *Paramecium quadecaurelia* strain, crosses in F1 and F2 generations

Strain	F1 by conjugation	F2 by autogamy
328 (Australia) x 328	100	96
AN1-1 x AN1-1 (Africa, Namibia)	100	98
AN1-3 x AN1-3 (Africa, Namibia)	100	100
AN1-6 x AN1-6 (Africa, Namibia)	100	100
AN1-1 x 328 (Namibian x Australian)	100	96
AN1-3 x 328 (Namibian x Australian)	98	98
AN1-6 x 328 (Namibian x Australian)	100	100

Namibian and Australian strains of *P. quadecaurelia* were compared with those of *P. primaurelia* (AB100846), *P. tetraurelia* (AB100847), *P. pentaurelia* (AB100848) and *P. tredecaurelia* (AB100852), however, the homology was 93.7, 89.9, 92.9 and 96.0 %, respectively. Furthermore, phylogenetic tree suggests that the strains from Namibia belong to *P. quadecaurelia* (Fig.1).

Investigations concerning occurrence of species of the *P. aurelia* complex carried out in Africa are very rare. From that continent only *P. sexaurelia* from Kenya and *P. octaurelia* from Uganda (Sonneborn 1975) were previously known. Sonneborn (1975), however, supposed "Further sampling elsewhere may not only yield new species but modify presently known ranges of the 14 species. Present knowledge of geographical distribution is thus of limited value". It was written many years ago, since that time several studies were carried out in Europe and Asia (cf Przyboś and Fokin 2000) but investigations in Africa still are very limited.

It is also very interesting that both localities in which *P. quadecaurelia* was recorded, the one in Australia (Emily Gap situated 15 km east from Alice Springs) and the other one in Africa (Namibia, Vindhoek), are situated in the neighbourhood of the tropic of Capricorn, in the similar geographical latitude. Again Sonneborn's (1957) opinion turned out to be true that climatic zones are the main factor limiting appearance of species of the *P. aurelia* complex.

Acknowledgements. E. Przyboś thanks Ms Marta Surmacz for excellent technical assistance.

REFERENCES

Adachi J., Hasegawa M. (1996) MOLPHY version 2.3: Programs for molecular phylogenetics, based on maximum likelihood. *Computer Sciences Monographs* **28:** 5-150

Allen S. L., Farrow S. W., Golembiewski P .A. (1973) Esterases variations between 14 syngens of *Paramecium aurelia* under axenic growth. *Genetics* **18:** 518-525

Aufderheide K. J., Daggett P-M., Nerad T. A. (1983) *Paramecium sonneborni* n. sp., a new member of the *Paramecium aurelia* species-complex. *J. Protozool*. **30:** 128-131

Chen T. T. (1956) Varieties and mating types in *Paramecium bursaria*. II. Variety and mating types found in China. *J. exp. Zool*. **132:** 255-268

Dryl S. (1959) Antigenic transformation in *Paramecium aurelia* after homologous antiserum treatment during autogamy and conjugation. *J. Protozool*. **6:** 25

Felsenstein J. (1981) Evolutionary trees from DNA sequences: a maximum likelihood approach. *J. Mol. Evol.* **17:** 368-376

Fujishima M., Sawabe H., Iwatsuki K. (1990) Scanning electron microscopic observation of differentiation from the reproductive short form to the infectious long form of *Holospora obtusa*. *J. Protozool*. **37:** 123-128

Landis W.G. (1986) The interplay among ecology, breeding systems, and genetics in the *Paramecium aurelia* and *Paramecium bursaria* complexes. *Progress in Protist* **1:** 287-307

Potekhin A., Przyboś E., Rautian M. (2002) Identification of the ciliates of genus *Paramecium* by electrokaryotyping. XIV All Russian Symposium "Cell Nucleus Structure and Functions", July 15-17, 2002, Saint-Petersburg, Russia. *Cytology* (*Russian*) **44:** 901 (in Russian)

Przyboś E. (1975) Genetic studies of *Paramecium jenningsi* strains (Diller & Earl, 1958). *Folia Biol.* (*Kraków*) **23:** 425-471

Przyboś E. (1978) Cytological and karyological studies of *Paramecium jenningsi*. *Folia biol.* (*Kraków*) **26:** 25-29

Przyboś E. (1986) Species structure in ciliates. *Folia Biol.* (*Kraków*) **34:** 103-132

Przyboś E., Fokin S. (2000) Data on the occurrence of species of the *Paramecium aurelia* complex world-wide. *Protistology* **1:** 179-184

Rautian M. S., Potekhin A.(2002) Electrokaryotypes of macronuclei of several *Paramecium* species. *J. Eukaryot. Microbiol*. **49:** 296-304

Sonneborn T.M. (1950) Methods in the general biology and genetics of *Paramecium aurelia*. *J. Exp. Zool.* **13:** 87-148

Sonneborn T. M. (1957) Breeding systems, reproductive methods, and species problems in Protozoa. In: The Species Problem, (Ed. E. Mayr). AAAS, Washington, 155-324

Sonneborn T. M. (1970) Methods in *Paramecium* research. In: Methods in Cell Biology, (Ed. D. M. Prescott), Academic Press, New York, **4:** 241-339

Sonneborn T. M. (1975) The *Paramecium aurelia* complex of fourteen sibling species. *Trans. Am. Microsc. Soc.* **94:** 155-178

Stoeck T., Przyboś E., Schmidt H. J. (1998) A combination of genetics with inter- and intra-strain crosses and RAPD-fingerprints reveals different population structures within the *Paramecium aurelia* species complex. *Europ. J. Protistol*. **34:** 348-355

Stoeck T., Przyboś E., Kusch J., Schmidt H. J. (2000) Intra-species differentiation and level of inbreeding of different sibling species of the *Paramecium aurelia* complex. *Acta Protozool*. **39:** 15-22

Vivier E. (1974) Morphology, taxonomy and general biology of the genus *Paramecium* In: *Paramecium*, A Current Survey, (Ed. W. I. van Wagtendonk). Elsevier, Amsterdam, 1-89

Received on 7th April, 2003; revised version on 14th July, 2003; accepted on 16th July 2003

INSTRUCTIONS FOR AUTHORS

ACTA PROTOZOOLOGICA publishes original papers on experimental or theoretical research in all fields of protistology with the exception of faunistic notices of local character and purely clinical reports. Short communications, as well as longer review articles may also be submitted. Contributions should be written in English. Submission of a manuscript to ACTA PROTOZOOLOGICA implies that the contents are original and have not been published previously, and are not under consideration or accepted for publication elsewhere. There are no page charges except colour illustration. Names and addresses of suggested reviewers will be appreciated. In case of any question please do not hesitate to contact Editor. Authors should submit papers to:

Mrs Małgorzata Woronowicz-Rymaszewska
Managing Editor of ACTA PROTOZOOLOGICA
Nencki Institute of Experimental Biology,
ul. Pasteura 3
02-093 Warszawa, Poland
Fax: (4822) 822 53 42
E-mail: jurek@ameba.nencki.gov.pl

Extensive information on ACTA PROTOZOOLOGICA is now available *via* internet. The address is: **http://www.nencki.gov.pl/ap.htm**

Organization of Manuscripts

Submissions

Please enclose three copies of the text, one set of original of line drawings (without lettering!) and three sets of copies with lettering, four sets of photographs (one without lettering). In case of photographs arranged in the form of plate, please submit one set of original photographs unmounted and without lettering, and three sets of plates with lettering.

The ACTA PROTOZOOLOGICA prefers to use the author's word-processor disks (format IBM or IBM compatible, and MacIntosh 6 or 7 system on 3.5" 1.44 MB disk only) of the manuscripts instead of rekeying articles. If available, please send a copy of the disk with your manuscript. Preferable programs are Word or WordPerfect for Windows. Disks will be returned with galley proof of accepted article at the same time. Please observe the following instructions:

1. Label the disk with your name: the word processor/computer used, e.g. IBM; the printer used, e.g. Laserwriter; the name of the program, e.g. Word for Windows.
2. Send the manuscript as a single file; do not split it into smaller files.
3. Give the file a name which is no longer than 8 characters.
4. If necessary, use only italic, bold, underline, subscript and superscript. Multiple font, style or ruler changes, or graphics inserted the text, reduce the usefulness of the disc.
5. Do not right-justify and use of hyphen at the end of line.
6. Avoid the use of footnotes.
7. Distinguish the numerals 0 and 1 from the letters O and l.

Text (three copies)

The text must be typewritten, double-spaced, with numbered pages. The manuscript should be organized into Summary, Key words, Abbreviations used, Introduction, Materials and Methods, Results, Discussion, Acknowledgements, References, Tables and Figure Legends. The Title Page should include the full title of the article, first name(s) in full and surname(s) of author(s), the address(es) where the work was carried out, page heading of up to 40 characters. The present address for correspondence, Fax, and E-mail should also be given.

Each table must be on a separate page. Figure legends must be in a single series at the end of the manuscript. References must be listed alphabetically, abbreviated according to the World List of Scientific Periodicals, 4th ed. (1963). Nomenclature of genera and species names must agree with the International Code of Zoological Nomenclature, third edition, London (1985) or International Code of Botanical Nomenclature, adopted by XIV International Botanical Congress, Berlin, 1987. SI units are preferred.

Examples for bibliographic arrangement of references:

Journals:

Häder D-P., Reinecke E. (1991) Phototactic and polarotactic responses of the photosynthetic flagellate, *Euglena gracilis*. *Acta Protozool.* **30:** 13-18

Books:

Wichterman R. (1986) The Biology of *Paramecium*. 2 ed. Plenum Press, New York

Articles from books:

Allen R. D. (1988) Cytology. In: *Paramecium*, (Ed. H.-D. Görtz). Springer-Verlag, Berlin, Heidelberg, 4-40

Zeuthen E., Rasmussen L. (1972) Synchronized cell division in protozoa. In: Research in Protozoology, (Ed. T. T. Chen). Pergamon Press, Oxford, **4:** 9-145

Illustrations

All line drawings and photographs should be labelled, with the first author's name written on the back. The figures should be numbered in the text as Arabic numerals (e.g. Fig. 1). Illustrations must fit within either one column (86 x 231 mm) or the full width and length of the page (177 x 231 mm). Figures and legends should fit on the same page. Lettering will be inserted by the printers and should be indicated on a tracing-paper overlay or a duplicate copy.

Line drawings (three copies + one copy without lettering)

Line drawings should preferably be drawn about twice in size, suitable for reproduction in the form of well-defined line drawings and should have a white background. Avoid fine stippling or shading. Computer printouts of laser printer quality may be accepted, however *.TIF, *.PSD, *.CDR graphic formats (**Grayscale and Color - 600 dpi, Art line - 1200 dpi**) on CD are preferred.

Photographs (three copies + one copy without lettering)

Photographs at final size should be sharp, with a glossy finish, bromide prints. Photographs grouped as plates (in size not exceeding 177 x 231 mm including legend) must be trimmed at right angles accurately mounted and with edges touching and mounted on firm board. The engraver will then cut a fine line of separation between figures. Magnification should be indicated. Colour illustration (charged) on positive media (slides 60 x 45 mm, 60 x 60 mm, transparency or photographs) is preferred.

Proof sheets and offprints

Authors will receive one set of page proofs for correction and are asked to return these to the Editor within 48-hours. Fifty reprints will be furnished free of charge. Orders for additional reprints have to be submitted with the proofs.

Indexed in: Current Contents, Biosis, Elsevier Biobase, Science Citation Index, Chemical Abstracts Service, Librex-Agen, Protozoological Abstracts, Polish Scientific Journals Contents - Agric. & Biol. Sci. at http://ciuw.warman.net.pl/alf/psjc/, Microbes.info "Spotlight" at http://www.microbes.info/, and at Nencki Institute of Experimental Biology website http://www.nencki.gov.pl/ap.htm

ACTA
PROTOZOOLOGICA

ORIGINAL ARTICLES

SHORT COMMUNICATION

2003 NOVEMBER
VOLUME 42 NUMBER 4